DISSERTATIONES SCHOLA DOCTORALIS SCIENTIAE CIRCUMIECTALIS,
ALIMENTARIAE, BIOLOGICAE. UNIVERSITATIS HELSINKIENSIS

20/2016

JAANA KUUSKERI

Genomics and Systematics of the White-Rot Fungus *Phlebia radiata*: Special Emphasis on Wood-Promoted Transcriptome and Proteome

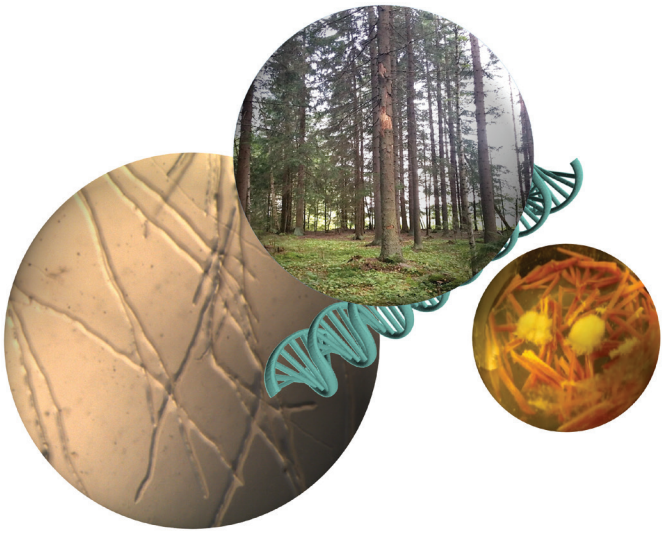

DIVISION OF MICROBIOLOGY AND BIOTECHNOLOGY
DEPARTMENT OF FOOD AND ENVIRONMENTAL SCIENCES
FACULTY OF AGRICULTURE AND FORESTRY
DOCTORAL PROGRAMME IN MICROBIOLOGY AND BIOTECHNOLOGY
UNIVERSITY OF HELSINKI

Genomics and systematics of the white-rot fungus *Phlebia radiata*: special emphasis on wood-promoted transcriptome and proteome

JAANA KUUSKERI

Division of Microbiology and Biotechnology
Department of Food and Environmental Sciences
Faculty of Agriculture and Forestry and
Doctoral Programme in Microbiology and Biotechnology
University of Helsinki, Finland

ACADEMIC DISSERTATION

To be presented, with the permission of the Faculty of Agriculture and Forestry of the University of Helsinki, for public examination in auditorium 1041, Biocenter 2, Viikinkaari 5, on October 7th 2016, at 12 o'clock noon.

Helsinki 2016

Supervisor: Docent Taina Lundell
Department of Food and Environmental Sciences, University of Helsinki, Finland

Co-supervisors: Dr. Miia Mäkelä
Department of Food and Environmental Sciences, University of Helsinki, Finland

Docent Ilona Oksanen
Department of Food and Environmental Sciences, University of Helsinki, Finland

Pre-examiners: Professor Jarkko Hantula
Natural Resources Institute Finland (Luke), Vantaa Research Centre, Finland

Associate Professor Tomas Johansson
Department of Biology, Lund University, Sweden

Opponent: Professor David Hibbett,
Department of Biology, Clark University, MA, USA

Custos: Professor Kaarina Sivonen,
Department of Food and Environmental Sciences, University of Helsinki, Finland

Dissertationes Schola Doctoralis Scientiae Circumiectalis, Alimentariae, Biologicae

Cover: Hyphae of *Phlebiopsis gigantea* (FBCC0315) on malt extract agar (left). Mixed forest with Norway spruce (*Picea abies*) and birch (*Betula* sp.) (upp). Solid-state cultivation of *Phlebia radiata* isolate 79 on spruce wood sticks after three weeks (right). The double helix of DNA is in the middle.

ISSN 2342-5423 (print)
ISSN 2342-5431 (online)
ISBN 978-951-51-2419-7 (paperback)
ISBN 978-951-51-2420-3 (PDF)

Hansaprint
Turenki 2016

Contents

List of original publications

This thesis is based on the following publications:

I **Kuuskeri J.**, Mäkelä M. R., Isotalo J., Oksanen I., Lundell T. 2015. Lignocellulose-converting enzyme activity profiles correlate with molecular systematics and phylogeny grouping in the incoherent genus *Phlebia* (Polyporales, Basidiomycota). BMC Microbiology, 15:217. doi:10.1186/s12866-015-0538-x.

II Salavirta H., Oksanen I., **Kuuskeri J.**, Mäkelä M., Laine P., Paulin L., Lundell T. 2014. Mitochondrial genome of *Phlebia radiata* is the second largest (156 kbp) among fungi and features signs of genome flexibility and recent recombination events. PLoS ONE, 9(5): e97141. doi:10.1371/journal.pone.0097141.

III **Kuuskeri J.**, Häkkinen M., Laine P., Smolander O.-P., Tamene F., Miettinen S., Nousiainen P., Kemell M., Auvinen P., Lundell T. 2016. Time-scale dynamics of proteome and transcriptome of the white-rot fungus *Phlebia radiata*: growth on spruce wood and decay effect on lignocellulose. Biotechnology for Biofuels, 9:192. doi:10.1186/s13068-016-0608-9.

The publications are referred to in the text by their roman numerals.
The contribution of the author to the publications:

I Jaana Kuuskeri participated in the planning of the study and carried out the experiments. She performed the phylogenetic analyses and analyses of enzyme activity. She collaborated in statistical analyses, wrote the first version of the manuscript, and was the corresponding author.

II Jaana Kuuskeri participated in planning of the experiments, and performed the fungal cultivations and DNA extractions. She also participated in interpretation of the data and writing of the manuscript together with the co-authors.

III Jaana Kuuskeri participated in the design of the study, performed the wood cultivations, DNA, RNA and protein extractions, mRNA purification, part of the lignin analysis and sample preparations for microscoping. She analysed and interpreted the proteomic and genomic data together with the co-authors, wrote the manuscript, and collaborated in the submission process.

Abbreviations

AA	Auxiliary activity
AFTOL	Assembling the fungal tree of life project
ATP	Adenosine triphosphate
CAZy, CAZyme	Carbohydrate-active enzyme
CBH	Cellobiohydrolase
CDH	Cellobiose dehydrogenase
CE	Carbohydrate esterase
CRO	Copper radical oxidase
DyP	Dye-decolorizing peroxidase
FBCC	Fungal biotechnology culture collection
FE-SEM	Field emission scanning electron microscope
GH	Glycoside hydrolase
GLOX	Glyoxal oxidase
GMC oxidoreductase	Glucose–methanol–choline oxidoreductase
HE	Homing endonuclease
HTP	Hemethiolate peroxidase
ITS	Internal transcribed spacer
Lacc	Laccase
LC-MS/MS	Liquid chromatography–tandem mass spectrometry
LiP	Lignin peroxidase
LPMO	Lytic polysaccharide monooxygenase
MnP	Manganese peroxidase
mtDNA, mitogenome	Mitochondrial genome
ORF	Open reading frame
PL	Polysaccharide lyase
Pyrolysis-GC-MS	Pyrolysis–gas chromatography–mass spectrometry
rRNA	Ribosomal ribonucleic acid
tRNA	Transfer ribonucleic acid
UPO	Unspecific peroxygenase
VP	Versatile peroxidase

Abstract

The wood-decaying white-rot fungi have the profound ability to completely degrade lignocelluloses and all wood components. These fungi and their enzymes have evolved to modify the various lignocellulose feedstocks in nature, and thereby, they are important organisms for bioconversions as well as in fundamental research on fungal biology. The enzymes have many potential applications in biotechnology and industrial purposes including bioenergy production. Evolutionary background of the fungal species and their organelles thus requires deeper understanding to aid in elucidating the relationship of the species to their lifestyles.

This PhD study concentrated on the white-rot fungal species *Phlebia radiata*, Finnish isolate number 79 (FBCC0043). The phylogenetic studies confirmed positioning of *P. radiata* species in the systematic class Agaricomycetes of Basidiomycota, and in the phlebioid clade of the order Polyporales. The sequenced and annotated mitochondrial genome of *P. radiata* was discovered to have features that indicate evolutionary pressure and structural diversity in fungal mitogenomes, not being as stable and compact entities than was previously believed. In this study, *P. radiata* together with species like *Phlebia acerina* and *Phlebia brevispora* was demonstrated to form a *Phlebia sensu stricto* group which consists of efficient producers of lignin-modifying enzymes. The results pinpointed that there is a species-level connection of fungal molecular systematics to the efficiency in the production of wood-decaying enzymes and activities.

Norway spruce (*Picea abies*) is a common tree species in the boreal forests providing an important source of biomass for forest-based industry. Therefore, *P. radiata* was cultivated on Norway spruce wood under conditions mimicking natural solid-wood colonization, up to six weeks of growth, and the dynamics of fungal enzyme production and gene expression was studied. The lignin-modifying class-II peroxidases (LiPs and various MnPs) were produced, especially in the beginning of fungal growth and colonization of wood, thus indicating the essence of class-II peroxidase as the primary enzymes to function against coniferous wood lignin. Moreover, these extracellular oxidoreductases enhance the accessibility of lignocellulose carbohydrates and thereby, they promote fungal growth in wood. Simultaneously, lytic polysaccharide monooxygenases and several CAZyme glycoside hydrolases attacking cellulose, hemicellulose and pectin were produced, which demonstrates ongoing depolymerization of the polysaccharides to monomers and oligomers. Electron microscopic examination of fungal-colonized wood after six weeks of growth indicated that the decay of wood cell walls was initiated at the tracheid lumen side apparently proceeding towards the middle lamellae. Furthermore,

degradation of spruce wood lignin was detected by pyrolysis-GC/MS as decrease in the amount of phenylpropane units with concomitant increase in the number of smaller fragmented products from these lignin units.

Thus, the previously observed unique and strong ability of *P. radiata* to degrade wood lignin and lignin-like aromatic compounds was confirmed. According to the results of this PhD study, *P. radiata* produces the white-rot type of decay of wood components when growing on Norway spruce. This is due to the efficient ability of the fungus to express and produce a versatile enzyme repertoire for degradation of wood lignocellulose, and in consequence, to generate diverse reactions and bioconversions important for carbon cycling in the forest ecosystems.

Tiivistelmä

Valkolahoa tuottavat sienet hajottavat tehokkaasti lignoselluloosaa ja puuaineksen biopolymeerejä, kuten selluloosaa, hemiselluloosaa ja ligniiniä. Valkolahottavat sienet ovat evoluution myötä kehittyneet tuottamaan erilaisia entsyymejä, jotka kykenevät muokkaamaan ja pilkkomaan monimutkaisia raaka-aineita. Tämän vuoksi valkolahottajat ovat kiinnostavia tutkimuskohteita niin teollisesti kuin perustutkimuksenkin näkökulmasta. Sienten tuottamia entsyymejä voidaan hyödyntää bioteknisissä ja teollisissa sovelluksissa, kuten biopolttoaineiden ja uusien biomateriaalien tuotannossa. Puunlahottajien ja niiden mitokondrioiden pitkän evoluutiohistorian selvittäminen on tärkeää, jotta sienilajien ja niiden elintapojen välisiä suhteita voidaan ymmärtää.

Tässä väitöskirjatutkimuksessa oli keskeisessä roolissa Suomesta eristetty rusorypykän (*Phlebia radiata*) sienikanta 79 (FBCC0043). Fylogeneettinen monigeenitarkastelu vahvisti rusorypykän ja lajin muiden edustajien kuuluvan kantasienten Agaricomycetes-luokan Polyporales-lahkoon, ja siinä edelleen niin kutsuttuun phlebioid-sukuryhmään. Rusorypykän mitokondrion genomin sekvensointi osoitti, että tumallisten eliöiden mitogenomit eivät ole niin vakaita ja yhteneviä yksikköjä kuin aikaisemmin on uskottu. Sienten mitogenomit ovat monimuotoisia ja jatkuvan evolutiivisen paineen alla. Laajempi *Phlebia*-suvun lajien ja isolaattien fylogeneettinen tutkimus osoitti, että rusorypykkä muodostaa yhdessä lajien *Phlebia acerina* ja *P. brevispora* kanssa *Phlebia sensu stricto* -ryhmän, jonka jäsenet tuottavat tehokkaasti ligniiniä hajottavia hapetus-pelkistysentsyymeitä. Tässä tutkimuksessa huomattiin myös, että molekyylisystematiikan perusteella arvioidut lajien väliset geneettiset suhteet ovat yhteydessä puuta sisältävällä alustalla tuotettaviin entsyymiaktiivisuuksiin ja lajien entsyymiprofiileihin.

Kuusi (metsäkuusi, *Picea abies*) on yksi pohjoisen havumetsävyöhykkeen tärkeimmistä raaka-aineista. Tästä syystä rusorypykän isolaattia 79 kasvatettiin kuusipuuaineksella sienirihmaston luonnollisia kasvuolosuhteita jäljittelevissä oloissa kuuden viikon ajan lahoentsyymien tuoton ja niitä koodaavien geenien ilmentymisen muutosten seuraamiseksi. Rusorypykkä tuotti ligniiniä muokkaavia hapetus-pelkistysentsyymeitä, kuten ligniini- ja mangaaniperoksidaaseja, runsaasti jo ensimmäisellä kasvuviikolla. Havainnot osoittivat näiden peroksidaasientsyymien tärkeyden havupuuligniinin hajotuksen alkuvaiheessa sekä merkityksen hiilihydraattipolymeerien saatavuuden ja sienirihmaston kasvun edistämisessä. Samanaikaisesti kun ligniiniä hajotettiin, rusorypykkä tuotti tasaisemmin lyyttisiä polysakkaridi-mono-oksygenaaseja sekä useita selluloosaa, hemiselluloosaa ja pektiiniä hajottavia glykosidihydrolaaseja, jotka pilkkovat hiilihydraattipolymeerejä

helpommin hyödynnettäviksi mono- ja oligomeereiksi. Elektronimikroskopia osoitti, että kuusipuuaineksen hajotus alkoi puusolujen soluonteloista ja ilmeisesti eteni paksuihin puusoluseiniin ja kohti välilamelleja. Lisäksi massaspektrometrinen analyysi (pyrolyysi-GC/MS) osoitti, että ligniinin hajotusta oli tapahtunut kuuden viikon seuranta-aikana. Nämä havainnot vahvistavat aikaisempia tuloksia rusorypykän erinomaisesta kyvystä hajottaa puuainesta sekä muokata ja pilkkoa ligniiniä sekä ligniinin kaltaisia aromaattisia yhdisteitä. Tulosten perusteella voidaan todeta, että rusorypykkä *P. radiata* tuottaa valkolahottajille tyypillisen entsyymikirjon ja hyödyntää monipuolisia biokemiallisia reaktioita kierrättääkseen lignoselluloosan hiiltä kasvuympäristössään.

1 Introduction

Lignocellulose, which is plant cell wall biomass found in e.g. trees and grasses, is Earth's largest organic renewable resource being constantly produced contrary to the limited availability of fossil fuels. It is estimated that globally there are three trillion trees and the world's forests store 650 billion tonnes of carbon (Crowther et al., 2015; Popkin, 2015). Carbon in lignocellulose is challenging to recycle, because of the recalcitrant nature of the organic polymers that are present in the plant cell walls. In the forest ecosystems, saprotrophic fungi have an important role in performing biological decomposition of dead wood and thereby, in nutrient recycling. Because of the great diversity and long evolutionary history of these fungi, they are a key resource to study lignocellulose decay. Modification of lignocellulose is also essential for example in the production of biofuels and other valuable biochemicals.

In this doctoral thesis, genetic and enzymatic characteristics of the white-rot Basidiomycota fungus *Phlebia radiata* isolate 79 were widely studied. *P. radiata* 79 is a biotechnologically versatile organism which produces an array of lignocellulose-acting enzymes, being able to act on lignin and hazardous xenobiotics, and demonstrates robustness and stability in decomposition of diverse plant biomasses (Hatakka, 1994). In this work, special emphasis was given on how expression of genes and production of proteins are affected when the fungus is growing on solid spruce wood. In addition, evaluation of the genotypic and enzyme phenotypic properties of other species and isolates of *Phlebia* are described. The results of these studies contribute to knowledge on fungal wood-decaying strategies and comparative genomic analyses.

1.1 Wood-decay in Basidiomycota

The wood-decomposing fungi have previously been divided into white-rot and brown-rot fungi based on their visually observable decay types. Their genomes also encode different repertoires of enzymes for plant biomass decomposition (Eastwood et al., 2011; Floudas et al., 2012; Lundell et al., 2014). Recently, whole-genome sequencing of ecologically divergent fungi has revealed that the described classification is not as clear as previously thought. Wood-decay mechanisms are demonstrated to be more diverse and additional soft rot-like decay types have been proposed (Floudas et al., 2015; Nagy et al., 2015; Riley et al., 2014). Briefly, during the evolution transitions from white-rot to brown-rot lifestyles have occurred several times among Agaricomycotina and possibly in several stages. Due to this, some fungi show intermediate characteristics of wood-decay (Floudas et al., 2015). This PhD thesis

concentrates on wood-decay of the classic white-rot fungi and the model species of the study, *P. radiata,* is a typical representative of this group.

White-rot fungi are traditionally described as wood-colonizing polyporoid Basidiomycota able to attack all wood components including lignin, but this classification may also include soil litter-decomposing and mushroom-forming species as well as a few species of Ascomycota (Hatakka, 2001; Lundell et al., 2014; Nagy et al., 2015). Phylum Basidiomycota contains 32% of the described fungal species (Kirk et al., 2008).

Despite the findings on more diverse enzyme machineries for plant biomass degradation, fungi that produce lignin-modifying class-II peroxidases and have enzymes capable of degrading crystalline cellulose are defined as white-rot fungi (Floudas et al., 2012; Riley et al., 2014). Additionally, white-rot fungi degrade cellulose mainly with their enzyme machinery while brown-rot fungi employ also non-enzymatic oxidative Fenton mechanism which produce higly reactive hydroxyl radicals ($H_2O_2 + Fe^{2+} \rightarrow {}^{\cdot}OH + OH^- + Fe^{3+}$) (Arantes et al., 2012; Eastwood et al., 2011; Martinez et al., 2009). The role of the white-rot fungi is significant because of their ability to decompose all polymeric components of wood lignocellulose including lignin, cellulose and hemicellulose. These fungi have also been estimated to comprise the great majority (over 90%) of wood-decaying Basidiomycota species (Gilbertson, 1980).

Usually white-rot species can be found to colonize angiosperm wood although substrate preferences may occur. As these fungi are able to degrade lignin, they leave white or yellowish, soft and fiber-like cellulose-containing remains of the decayed wood. Although white-rot fungi have mainly adopted saprotrophic lifestyle, this wide group includes also severe tree pathogenic species of the genera *Heterobasidion* and *Ganoderma* inhabiting a diverse array of host tree species (Korhonen and Stenlid, 1998; Kües et al., 2015).

1.1.1 Phlebioid clade of Polyporales

Polyporales is a diverse order in the Basidiomycota systematic class Agaricomycetes (Figure 1) which includes efficient wood-decaying species (Binder et al., 2013). The phlebioid clade of Polyporales is a diverse group of corticioid and polyporoid basidiocarp-forming species. It is a sister clade to the clade containing the polyporoid, antrodia and gelatoporia clades (Binder et al., 2013). Core polyporoid clade and small gelatoporia lineage comprise efficient white-rot decayer genera while the antrodia clade comprises brown-rot wood-decaying species (Binder et al., 2013). As previously presented, there have been several transitions between polyporoid and corticioid fruiting body forms during evolution of the phlebioid clade (Floudas and Hibbett,

2015). Hymenophore morphologies are not constant across evolution of phlebioid fungi (Binder et al., 2005; Floudas and Hibbett, 2015). Thus, it is obvious that the visible fruiting body is not a reliable classification criterion for these fungi. As well as macro-morphologies, microscopic characters are also variable among the phlebioids (Binder et al., 2013). Generally in Fungi, many morphological characters are actually result of convergent evolution and do not reveal the evolutionary relationships (Hibbett, 2007; Liu and Hall, 2004).

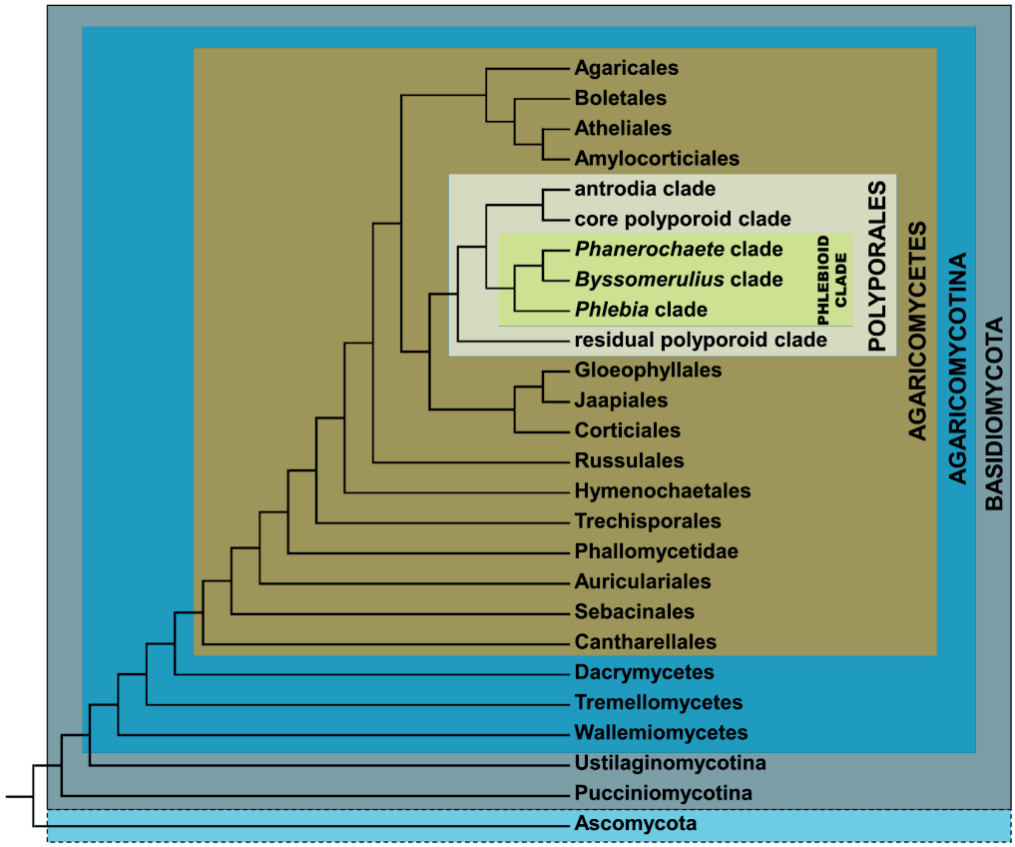

Figure 1. Higher-level phylogenetic relationships illustrating the positioning of phlebioid clade of Polyporales in the Basidiomycota systematic class Agaricomycetes. The tree topology is based on phylogenetic studies on Agaricomycetes (Hibbett et al., 2014; Nagy et al., 2015), Polyporales (Binder et al., 2013) and phlebioid clade (Floudas & Hibbett, 2015; **Publication I**).

All of the species addressed to phlebioid clade produce white-rot in wood and plant biomass except one species, *Leptoporus mollis*. It has been stated that this species appears to show an independent origin of brown-rot mode of wood-decay outside of

the antrodia clade of Polyporales (Binder et al., 2013; Floudas and Hibbett, 2015). Further analyses of the genotype and phenotype of *L. mollis* will tell more about its wood-decay mode. This type of isolated lineage of brown-rot within a clade having white-rot fungal decay type is not unusual, since similar lifestyle and decay type divergence has also been observed in the order Agaricales (Floudas et al., 2015).

The species inside the phlebioid clade can be divided into several minor groups according to their phylogenetic positioning, of which *Phlebia*, *Byssomerulius* and *Phanerochaete* clades receive the best phylogenetic support (**Publication I**; Floudas and Hibbett, 2015). *Phlebia* clade includes so far two genome-sequenced species: *P. radiata* (**Publication III**, genome to be published) and *Phlebia brevispora* (Binder et al., 2013). *Byssomerulius* clade has only one genome available for *Trametopsis cervina* (JGI MycoCosm: http://genome.jgi.doe.gov/programs/fungi/index.jsf; Grigoriev et al., 2011). The *Phanerochaete* clade includes sequenced genomes of the species *Phanerochaete chrysosporium* (Martinez et al., 2004; Ohm et al., 2014), *Phanerochaete carnosa* (Suzuki et al., 2012), *Bjerkandera adusta* (Binder et al., 2013) and *Phlebiopsis gigantea* (Hori et al., 2014b). *P. chrysosporium* has traditionally been the model species for investigating the physiology and genetics of lignin degradation (Vanden Wymelenberg et al., 2006), and the species was the first filamentous Basidiomycota that was genome sequenced already in 2002 (Martinez et al., 2004).

1.1.2 *Phlebia radiata* and other *Phlebia* species

Despite the obvious role of *P. chrysosporium* as the most studied white-rot fungal species, *P. radiata* has as well been widely studied due to its applicability as a model organism to be cultivated and studied under laboratory conditions, its efficient production of lignin-modifying enzymes, and capability to degrade lignin and other aromatic compounds. Overall, 300 publications according to Web of Science search (May 12th, 2016) on the topic "*Phlebia radiata*" have been published (compared to over 6 000 hits to *Phanerochaete chrysosporium*).

P. radiata Fr. is the type species of the genus *Phlebia,* and the species owes wide geographical distribution throughout North America and Europe (Nakasone and Burdsall, 1984; Nakasone and Sytsma, 1993). *P. radiata* has a monomitic hyphal system with clamp connections, which are typical for dikaryotic Basidiomycota filaments (Figure 2). Lignin degradation of this fungus has been studied on coniferous wood (softwood) (Fackler et al., 2006; Hakala et al., 2004) and on deciduous wood (hardwood) (Hatakka and Uusi-Rauva, 1983). Lignin peroxidase (LiP3) from *P. radiata* isolate 79 (FBCC0043, ATCC64658) is able to oxidize and cleave dimeric lignin model compounds (Lundell et al., 1993a, 1993b) and a short-type manganese peroxidase (MnP3) of *P. radiata* has been shown to convert milled pine wood in connection to lipid-peroxidation (see Chapter 1.3.4.1) (Hofrichter et al., 2001). The

fungus has been applied for degradation of wheat straw (Bule et al., 2016; Vares et al., 1995) and is able to degrade and mineralize ^{14}C-labelled synthetic lignin and lignin-like compounds to carbon dioxide (Hatakka et al., 1991; Hofrichter et al., 1999; Kapich et al., 1999; Lundell et al., 1990; Moilanen et al., 1996; Niemenmaa et al., 2006; Tuomela et al., 2002).

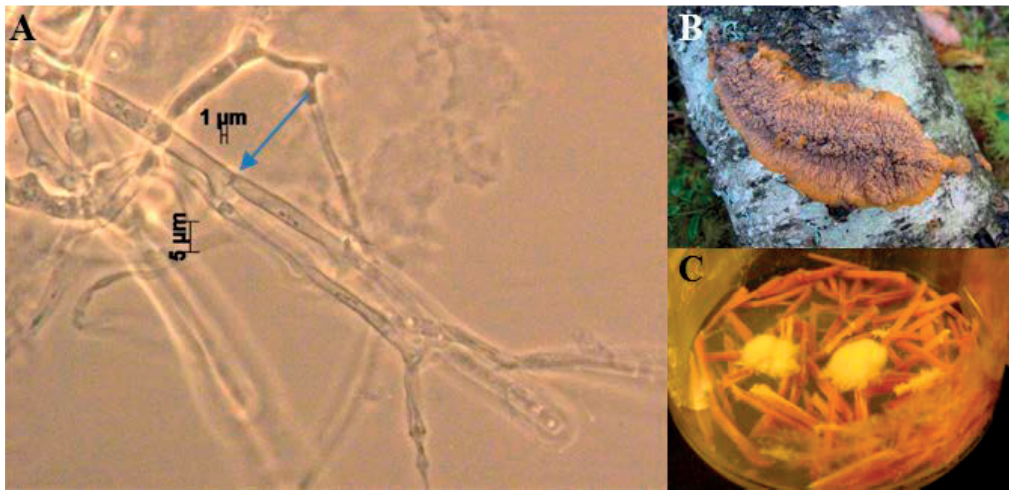

Figure 2. Hyphae, fruiting body and hyphal growth on wood of *Phlebia radiata.* A) Hyphae of the isolate 79 after six weeks of cultivation on malt extract agar. Arrow indicates a clamp connection which is characteristic of dikaryotic hyphae of Basidiomycota. B) Fruiting body of *P. radiata* on a birch log (Photo: Matti J. Koivula). C) Solid-state cultivation of isolate 79 on spruce wood sticks after three weeks. Photos A) and C) by the author.

Prior to the genome sequencing era, the genes encoding three class-II lignin peroxidase enzymes (Hildén et al., 2006), two MnPs (Hildén et al., 2005), and two laccases (Mäkelä et al., 2006; Saloheimo et al., 1991) were cloned and characterized. In addition, corresponding enzymes and H_2O_2-producing glyoxal oxidase (GLOX) have been characterized and studied under variable culture conditions (Karhunen et al., 1990; Lundell and Hatakka, 1994; Lundell et al., 1993b; Moilanen et al., 1996; Mäkelä et al., 2013; Niku-Paavola et al., 1988; Vares et al., 1995).

In addition to the lignin-modifying enzymes, previous studies have described extracellular cellulolytic enzyme activities in cultures of *P. radiata*, including β-1,4-endoglucanase, β-1,4-exoglucanase (cellobiohydrolase) and β-1,4-glucosidase activity (Rogalski et al., 1993b). Besides these, also enzyme activities of hemicellulolytic β-1,4-endomannanase and debranching acetyl-esterase, α-L-arabinofuranosidase and feruloyl esterase have been measured in the cultures of *P. radiata* (Rogalski et al., 1993a). In addition, some plant-polysaccharide-degrading enzymes from *P. radiata* have been biochemically characterized including hemicellulases such as β-1,4-

mannosidase (Prendecka et al., 2007), β-1,4-xylosidase and β-1,4-endoxylanase (Rogalski et al., 2001) as well as polysaccharide debranching enzymes including α-glucuronidase (Mierzwa et al., 2005) and α-galactosidase (Prendecka et al., 2003). These studies indicate the abilities of the fungus to decompose all components of plant cell wall.

In addition to the type species *P. radiata*, the genus *Phlebia* include numerous other species (Binder et al., 2013; Floudas and Hibbett, 2015) with hundreds of recorded taxons in fungal databases (MycoBank: http://www.mycobank.org/, Index Fungorum: http://www.indexfungorum.org). However, the physiology and potential for lignocellulose degration of only a few species of the genus have been studied, including *P. floridensis, P. brevispora*, *Phlebia lindtneri, Phlebia tremellosa*, and *Phlebia ochraceofulva* (Arora and Sharma, 2011; Sharma and Arora, 2011; Sulej et al., 2013; Vares et al., 1994, 1993). These species, except *P. ochraceofulva* belong to *Phlebia sensu stricto* group (**Publication I,** Chapter 4.1.1). This group also includes two *Phlebia* sp. isolates with yet non-defined taxon identity (b19 and the hypersaline tolerant MG60) whose MnP enzymes were previously studied together with cloning of the respective genes (Hildén et al., 2008; Hofrichter et al., 1999; Kamei et al., 2008).

Phlebia species are tolerant against environmental contaminants and produce high amounts of extracellular lignin-modifying enzymes (class-II peroxidases and laccases) that have low substrate specifities, which makes these fungi and their enzymes well fitted for bioremediation studies. Briefly, the biological machinery to degrade such a recalcitrant substrate as lignin is capable to degrade a large range of recalcitrant aromatic pollutants (Tuomela and Hatakka, 2011). *Phlebia* species have been shown to degrade phthalates (Yeo et al., 2008), trichloroanisole (Campoy et al., 2009), dieldrin (Xiao et al., 2011a), dichlorodiphenyltrichloroethane (DDT) (Xiao et al., 2011b), heptachlor (Xiao et al., 2011c), polychlorinated dibenzo-*p*-dioxin (PCDD) (Kamei et al., 2005), decabromodiphenyl ether (Xu and Wang, 2014), polycyclic aromatic hydrocarbons (PAHs) (Mori et al., 2003) and trinitrotoluene (Van Aken et al., 1997). Taken together, genus *Phlebia* is regarded to comprise several biotechnologically interesting and applicable fungal species and isolates.

1.2 Chemical and structural composition of spruce wood

In this PhD thesis, Norway spruce (*Picea abies*) softwood was used as growth material for *P. radiata* and other studied fungi. In Finland, Norway spruce is the second most common tree species, and it is an important renewable raw material for the Finnish forest industry (Peltola, 2014). The xylem of *P. abies* has typical coniferous softwood structure composed of tracheids and ray parenchyma cells (Figures 3A and 3C) that strengthen the sapwood and take part in water transport for the tree (Eriksson et al.,

1990). The long tracheids (wood cells) of softwood are connected through bordered pits (Figure 3B). In contrast, angiosperm hardwood tree species have a more complex structure of xylem including variable sizes of shorter tracheids and for example vessels. In general, the wood cell wall of tracheids is composed of secondary and primary cell walls, in addition to middle lamellae that bind the individual cells together (Eriksson et al., 1990). The secondary cell wall has three layers, namely S_1, S_2 and S_3 (Eriksson et al., 1990). Each cell layer is comprised of a combination of amorphous and aromatic lignin polymers orientated next to the polysaccharides, specifically hemicelluloses and the linear cellulose microfibrils. Cellulose microfibrils dominate the secondary cell walls, and they are differentially orientated in different layers of the cell walls. The proportion of these biopolymers and overall chemical components can vary between various wood cell types, cell wall layers, xylem locations, tree age and species (Eriksson et al., 1990).

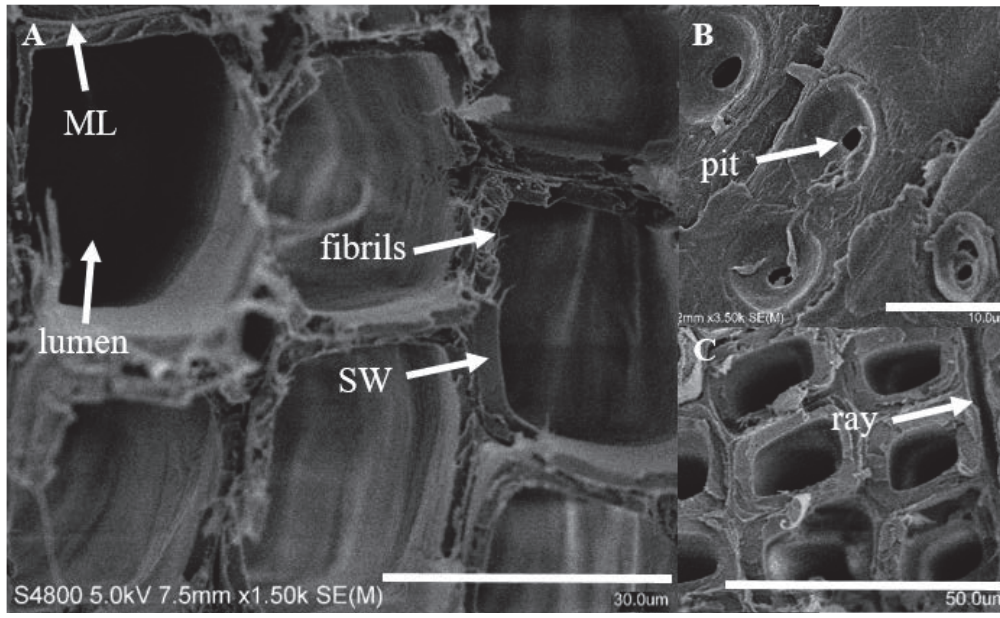

Figure 3. Field emission scanning electron microscope (FE-SEM) images of Norway spruce (*Picea abies*) xylem showing structural composition of the tracheid cell wall. A) Cross section of sapwood showing middle lamellae (ML), which also includes the primary cell wall layer and S_1 layers. Other arrows point to empty cell lumen, secondary wall (SW, mainly S_2 layer) and cellulose microfibrils. B) Longitudinal section with the tracheid bordered pits pointed with arrow. C) Cross section with ray cell pointed with arrow. Scale bars are A) 30 µm, B) 10 µm and C) 50 µm in length. Pictures are taken by M. Kemell.

Cellulose is a long unbranched chain of glucose units linked by β-1,4-glycosidic bonds. The molecules are arranged through hydrogen bonding into microfibrils (Figure 3A), each containing about 40 cellulose chains (Cullen, 2013). Rigid microfibrils are differentially oriented in the plant cell wall layers and occur embedded by a hemicellulose-lignin matrix. Hemicellulose is a heteropolymer with β-1,4-linked backbone of glucose, mannose or xylose decorated with short branches (Scheller and Ulvskov, 2010). These branches comprise of different sugar, sugar acid, acetylated sugar or sugar acid ester units (Cullen, 2013). The structure of hemicelluloses of various wood types differ in their mannose and xylose content. Hardwoods contain mainly glucuronoxylan whereas galactoglucomannan is the main hemicellulose of softwood (Eriksson et al., 1990; Sjöström and Westermark, 1998). The third main polymer of wood, lignin, is partially covalently bonded via ether and benzyl ester linkages to the carboxyl groups of hemicellulose, while hemicellulose and cellulose are connected through hydrogen bonding.

Lignin is a complex high-molecular weight biopolymer composed of phenylpropanoid residues with variable linkage types including carbon-carbon and ether bonds (Boerjan et al., 2003). There are three types of aromatic subunits in lignin: *p*-hydroxyphenyl, guaiacyl and syringyl rings. The subunits are formed from respective phenylpropanoid monolignol precursors: *p*-coumaryl, coniferyl and sinapyl alcohols (Boerjan et al., 2003). Lignin has a significant role in the rigidity and toughness of woody cell walls. Lignin gives strength to the plant stem as well as resistance to chemical and enzymatic degradation of wood. It also facilitates transport of water and dissolved solutes from roots to other parts of the plant by waterproofing the xylem (Halpin, 2013).

The complexicity and challenges in lignin decomposition arise from the various interlinkages, sidegroups and covalent linkages to hemicelluloses. Lignin occurs in all cell wall layers of wood while most of the lignin polymers are situated in the secondary cell wall layers, and middle lamellae have the highest lignin content (Eriksson et al., 1990). Gymnosperm wood (softwood) includes more lignin than angiosperm wood (hardwood) and the type of lignin also differs between plant species. Hardwoods vary with their syringyl *versus* guaiacyl lignin unit composition, while softwoods have mainly guaicyl type of lignin (Eriksson et al., 1990).

Besides the main biopolymers, wood cell wall contains some minor compounds such as extractives, proteins, inorganic compounds and pectin. Precisely, Norway spruce xylem consists of glucomannan (16.3%) and glucuronoxylan (8.6%) hemicelluloses, together with cellulose (41.7%), lignin (27.4%), extractives (1.7%), other polysaccharides (3.4%) and residual constituents (0.9%) (Sjöström, 1981). Pectic polysaccharides, detected mainly as galacturonic acid and rhamnose monomers, are crosslinked to hemicellulose and lignin in the primary cell walls and middle lamellae of Norway spruce xylem (Bertaud and Holmbom, 2004; Caffall and Mohnen, 2009).

Taken together, wood is a complex and demanding growth substrate for fungi. Unique enzyme systems together with non-enzymatic mechanisms have evolved in white-rot fungi which enables them to gain access to the organic carbon sources of wood.

1.3 Enzymatic conversion of lignocellulose by white-rot fungi

White-rot fungi produce a wide variety of extracellular enzymes that are able to modify lignocellulose. These enzymes include both carbohydrate-active enzymes and oxidoreductases which are currently classified in the Carbohydrate-Active enZYme (CAZy) database according to their structural similarity (Lombard et al., 2014, www.cazy.org). Fungi use cellulose and hemicelluloses as carbon and energy sources while lignin is only depolymerized with the aim of gaining access to these sources. Genome sequencing of the white-rot fungi has widened our knowledge about the various enzyme types and gene numbers that these fungi have evolved for wood degradation (Table 1). However, the overall fungal wood-decay mechanisms are networks of enzymatic and chemical reactions targetting the wood polymeric components.

Table 1. Sequenced white-rot fungal genomes including both litter-decomposing and wood-decaying species: systematic order and selected gene numbers of enzymes important in wood cell wall degradation and possible enzyme substrates.

	Order	Ag	Ag	Ag	Po	Po	Po	Po	Po	Po	Po	Po	Po	Po	Co	Ru	Ru	Hy	Au
		Species																	
Substrate	CAZy family and other proteins	*Pleurotus ostreatus*	*Galerina marginata*	*Agaricus bisporus* var bisporus	*Dichomitus squalens*	*Trametes versicolor*	*Pycnoporus cinnabarinus*	*Gelatoporia subvermispora*	*Phanerochaete carnosa*	*Phanerochaete chrysosporium*	*Phlebiopsis gigantea*	*Bjerkandera adusta*	*Phlebia brevispora*	*Phlebia radiata*	*Punctularia strigosozonata*	*Stereum hirsutum*	*Heterobasidion irregulare*	*Fomitoporia mediterranea*	*Auricularia subglabra*
L	AA1_1 Lacc	10	8	12	12	7	5	7	0	0	0	0	5	5	12	15	16	10	7
L	AA2 MnP	6	16	2	9	13	3	13	7	5	7	6	10	6	10	5	6	16	6
L	AA2 VP	3	1	0	3	3	2	0	0	0	0	1	0	0	0	0	0	0	0
L	AA2 LiP	0	4	0	0	10	4	2	4	10	3	12	5	4	0	0	0	0	0
C	AA3_1 CDH	1	1	1	1	1	1	1	1	1	1	1	1	1	1	1	2	1	1
L	AA5_1 GLOX+ CRO	16	16	9	9	9	7	3	6	7	6	7	8	4	9	8	5	4	7
C H	AA9 LPMO	29	19	11	15	18	15	9	11	15	15	28	12	13	14	16	10	13	20
L	DyP	4	5	0	1	2	0	0	0	0	4	10	2	1	5	2	1	3	11
L	HTP	3	24	24	4	3	2	9	3	3	4	4	2	5	8	10	5	4	16
C H	GH1	3	5	1	4	2	1	3	2	2	2	2	2	2	1	3	2	5	1
H P	GH2	3	3	2	4	5	3	4	2	2	3	3	2	3	4	3	3	2	7
C H P	GH3	13	11	8	8	13	7	6	11	11	9	9	8	11	14	17	12	8	14
C H	GH5	21	40	19	19	22	17	18	24	19	19	19	23	24	18	20	16	20	43
C	GH6	3	3	1	1	1	1	1	1	1	1	1	1	1	1	1	1	2	2
C	GH7	16	8	1	4	4	3	3	5	9	5	5	4	7	5	3	1	2	8
C	GH9	1	1	1	0	1	1	0	1	1	1	1	1	1	1	1	1	1	0
H	GH10	3	9	2	5	6	2	6	5	6	4	4	8	8	5	6	2	4	4
H	GH11	2	8	2	0	0	0	1	1	1	2	0	0	1	1	1	0	0	3
C H	GH12	2	4	2	3	5	3	2	3	2	3	2	2	2	2	5	4	3	1
H	GH27	7	8	4	6	4	1	4	3	3	3	3	2	2	5	5	4	4	5
P	GH28	6	20	6	7	11	4	6	4	4	10	6	5	7	13	17	8	17	14
H	GH29	0	1	1	0	0	0	0	0	0	0	0	1	1	1	4	2	0	3
H	GH31	8	4	6	6	5	5	5	8	6	6	4	5	4	8	8	10	5	11
H P	GH35	4	10	1	3	2	2	1	4	3	2	4	4	3	4	7	4	2	6
H P	GH43	8	6	4	7	3	2	2	4	4	7	6	2	2	7	12	4	7	28
C	GH44	1	2	1	1	0	0	0	0	0	0	0	2	1	1	1	0	0	1
C	GH45	2	2	1	2	2	1	2	1	2	1	1	3	3	1	1	2	0	2
H P	GH51	3	5	1	2	2	0	2	2	2	2	2	1	1	3	3	1	1	3
H	GH74	3	2	1	1	1	1	1	2	4	2	2	1	2	2	2	1	4	1
H	GH95	1	2	1	1	1	1	1	1	1	0	1	3	1	1	1	1	2	1
P	GH105	2	1	2	1	1	0	0	0	0	0	1	0	3	2	2	2	1	3
H P	GH115	1	1	2	2	2	2	2	1	1	1	2	2	1	1	2	1	3	2
C	GH131	2	4	0	3	3	5	1	2	3	2	0	2	2	2	3	2	2	2
H P	CE1	2	2	1	0	3	3	2	2	4	2	1	1	2	2	1	1	0	4
H	CE5	0	6	6	0	0	0	0	0	0	0	0	1	0	1	1	0	0	3
P	CE8	2	3	2	3	2	1	2	2	2	3	2	3	2	6	5	3	3	2
P	CE12	2	4	3	2	0	1	0	0	0	1	1	0	0	0	3	2	2	1
H	CE15	1	1	1	2	2	2	2	3	3	1	2	2	2	2	1	1	1	6
H	CE16	9	10	11	13	8	6	5	5	1	6	15	8	11	12	14	6	6	12
P	PL4	2	0	1	1	1	1	0	0	0	0	1	1	1	3	3	1	0	1

Abbreviations of substrates: C = cellulose, H = hemicellulose, P = pectin, L = lignin. Abbreviations of fungal orders: Au = Auriculariales, Ag = Agaricales, Co = Corticiales, Hy = Hymenochaetales, Po = Polyporales, Ru = Russulales. This data set was derived from Hori et al., 2014b; Levasseur et al., 2014; Lundell et al., 2014; Riley et al., 2014 and references therein. Gene numbers of *P. radiata* are from **Publication III**.

1.3.1 Fungal decomposition of cellulose

In order to hydrolyse cellulose to glucose, white-rot fungi need to produce several carbohydrate-active enzymes, specifically cellulases. The most important CAZy families, including glycoside hydrolases (GH) and auxiliary activities (AA), that are important for attacking cellulose are indicated in Table 1. Secreted cellulases include both endo- and exo-acting enzymes which synergistically degrade cellulose (Kostylev and Wilson, 2012). Amorphous region of cellulose is hydrolysed by β-1,4-endoglucanases (for example CAZy families GH5, GH9, GH12, GH44, GH45) at random positions and thereby, cellulose chain ends are produced. Cellobiohydrolases (CBH) attack chain ends unidirectionally proceeding either from the reducing (CAZy family GH7) or non-reducing (GH6) ends of the cellulose polymer. The resulting oligo- and disaccharides (cellobiose) are hydrolysed to monomers (glucose) by β-1,4-glucosidases (GH1 and GH3) (Medie et al., 2012). In addition, cellobiose dehydrogenase (CDH, AA3_1) can bind to cellulose and oxidize the oligo- and disaccharides to corresponding lactones (Henriksson et al., 2000).

The above mentioned enzyme, CDH is classified to oxidoreductive enzymes and it includes both a cytochrome and a flavin-containing domain (Ludwig et al., 2010). CDH has uncertain biological function. However, it has been shown to play a variable role in lignocellulose modification, and in addition to using cellulose as substrate, it can participate in decomposition of hemicellulose and lignin (Henriksson et al., 2000). The versatility of this enzyme is possible due to its ablity to promote iron reduction to Fe^{2+} ions and production of hydrogen peroxide, thus fostering Fenton reaction and generation of hydroxyl radicals (Ludwig et al., 2010).

Electrons produced by action of CDH and various other electron-transferring proteins can be utilized by another oxidoreductive enzyme, namely the lytic polysaccharide monooxygenase (LPMO, AA9) (Beeson et al., 2014; Langston et al., 2011). LPMOs directly act on cellulose chains at the β-1,4-linkages which leads to hydroxylation and cleavage of the glycosidic bond and thus provides new chain ends for cellulolytic hydrolases (Beeson et al., 2014; Vaaje-Kolstad et al., 2010). As being numerously present in fungal genomes (9-29 copies in Agaricomycetes, Table 1) and taking into account its oxidoreductive and oxygen activating mechanism, it is not suprising that recent studies have shown that some LPMOs may act on certain hemicelluloses as well as polysaccharides with α-glycosidic bonds (like in starch) (Agger et al., 2014; Vu et al., 2014).

Briefly, the catalytic mechanism of LPMOs include oxygen activation with the help of external electron donor. The donors may be CDH, proteins with heme domain fused to cellulose-binding modules (cytochrome b562-CBM1), or lignocellulose-derived or fungal-produced diphenols (Courtade et al., 2016; Kracher et al., 2016). In addition, these diphenols/quinones may work as redox mediators between LPMO and

glucose–methanol–choline (GMC) oxidoreductases (AA3), such as glucose oxidase and pyranose dehydrogenase enzymes (Kracher et al., 2016).

1.3.2 Fungal decomposition of hemicellulose

Due to the heterogeneous chemical structure of hemicelluloses, these polysaccharides are degraded by an array of fungal CAZymes including glycoside hydrolases (GHs), carbohydrate esterases (CEs), and the above mentioned oxidoreductases (AA9, AA3_1). Hemicellulose specific GHs and AA9 LPMOs cleave glycosidic bonds in the hemicellulose chains and CEs hydrolyze ester linkages of side groups (Table 1).

Briefly, mannanases act on hemicelluloses which are composed of the main sugar monomer mannose, and xylanases degrade hemicelluloses composed of xylan units (reviewed by Rytioja et al., 2014). Mannanases include β-1,4-endomannanases (GH5 and GH26), which cleave mannan backbone into mannooligosaccharides. These are hydrolysed by β-1,4-mannosidases (GH2) into monosaccharides. Xylanases include β-1,4-endoxylanases (GH10 and GH11) which hydrolyze the xylan backbone into xylo-oligosaccharides. These are further hydrolysed by β-1,4-xylosidases (GH3 and GH43) to monosaccharides. The classical hydrolytic cellulases including endoglucanases, cellobiohydrolases (GH6 and GH7) and β-glucosidases are usually also able to act on different hemicelluloses including xyloglucans and β-glucan.

Despite the main-chain-depolymerizing hemicellulases, also several debranching enzymes are needed to fully decompose hemicelluloses. These include β-1,4-galactosidases (GH2 and GH35), α-1,4-galactosidases (GH27 and GH36), α-arabinofuranosidases (GH51 and GH54), galactomannan acetyl esterases, α-xylosidases (GH31), α-fucosidases (GH29 and GH95), α-glucuronidases (GH67 and GH115), acetyl xylan esterases (CE1 and CE5) and feruloyl esterases (CE1) (reviewed by de Vries et al., 2001; Rytioja et al., 2014).

1.3.3 Fungal decomposition of pectin

Pectin heteropolysaccharides in plant biomass are degraded by CAZymes belonging to GHs, CEs and polysaccharide lyases (PLs). The corresponding genes are well represented in white-rot fungal genomes (Table 1). Pectinases include a wide array of enzymes acting on the smooth and hairy region of pectin backbones of homogalacturonan, xylogalacturonan, rhamnogalacturonan I, and rhamnogalacturonan II, as well as various debranching enzymes attacking poly- and oligosaccharide side chains (Rytioja et al., 2014). For example, endo- and exopolygalacturonases cleave D-galacturonic acid from the homogalacturonan backbone whereas endo- and exorhamnogalacturonases act on rhamnogalacturonan

backbone. All of these enzymes belong to CAZy family GH28 (Benoit et al., 2012). PLs cleave carbohydrate polymers containing uronic acid, which are common in pectins (Lombard et al., 2010).

Despite the fact that pectin content of wood is low, white-rot fungi produce pectinases during growth on wood (**Publication III**, Couturier et al., 2015; MacDonald et al., 2011) and the white-rot fungi have several genes encoding these enzymes (Table 1). Pectinases are considered important in wood degradation because pectins are present in the middle lamellae of tracheid cell walls, in the centers of bordered pits uniting the tracheids, and in the ray parenchyma cells, which are strategic positions in the xylem tissue during fungal colonization of wood (Green et al., 1996). Additional role of pectinases in fungal wood colonization may be the release of calcium ions that are chelated by the pectin. This has been suggested to occur by synergistic action of fungal-secreted pectinases with production of oxalic acid (Dutton and Evans, 1996). The release of calcium-ion introduces suitable linkages for polygalacturonases to act (Green et al., 1996).

The long evolutionary history implicates the importance of pectinases in fungi despite the loss of pectinase-encoding genes in some fungal lineages. Chang et al. (2015) studied evolutionary aspects of fungal pectinase-encoding genes and provided knowledge of gene duplications in early ancestors of terrestrial fungi, which were living in semi-aquatic slime environments. The slimy environments were prevalent before the association of fungi with the earliest land plants and prior to the start of lignin biosynthesis in plants.

1.3.4 Fungal modification of lignin

As already mentioned, fungi are able to hydrolyze cellulose into glucose monomers, if the surrounding lignin units are degraded or otherwise bypassed. Because lignin is a complex structure with variable chemical linkages, lignin-modifying enzymes need to cover wide substrate specificities (Janusz et al., 2013). Many of these metal-containing oxidoreductase enzymes belong to AA families of CAZy classification and are characteristic to white-rot fungi (Table 1).

1.3.4.1 Class-II peroxidases

Class-II peroxidases (AA2) are critical enzymes in lignin conversion by white-rot fungi (Lundell et al., 2010). These enzymes include manganese peroxidases (MnPs), lignin peroxidases (LiPs) and versatile peroxidases (VPs) and they are regarded as high-redox potential peroxidases due to their ability to act on even non-phenolic aromatic compounds and lignin substructures of redox potential over 1 eV (Hofrichter et al., 2010; Ruiz-Dueñas et al., 2009; Schoemaker et al., 1994).

Class-II peroxidases catalyse oxidative reactions using hydrogen peroxide as electron acceptor with concurrent release of two water molecules and two-electron transfer oxidations of their substrates (Lundell et al., 1993a; Mäkelä et al., 2015). The active electron transfer center of class-II peroxidases is the iron-containing heme (protoporphyrin IX) which may bind hydrogen peroxide or organic peroxides (Hofrichter et al., 2010). Each of the class-II peroxidases comprises specific catalytic sites for binding of their reducing substrates. MnPs have a Mn-binding site near the heme propionates, LiPs have a surface-exposed tryptophan radical center, and VPs have both the Mn-binding site and exposed tryptophan (Hofrichter et al., 2010; Lundell et al., 2010; Ruiz-Dueñas et al., 2009).

The ligninolytic ability of MnPs is based on their ability to oxidize Mn^{2+} to Mn^{3+} which form chelated complexes with dicarboxylic acid anions, for example oxalate or malonate (Hofrichter, 2002; Hofrichter et al., 2010; Wariishi et al., 1992). Chelated Mn^{3+} ions penetrate into the wood cell wall and begin the decay process by oxidizing phenolic rings of lignin which further allows the invasion of enzyme molecules into wood (Blanchette et al., 1997). As the majority of lignin subunits in wood are non-phenolic, MnPs apparently oxidize these structures by mediator molecules such as syringyl-type phenols (Nousiainen et al., 2014). Another mechanism by which MnPs can oxidize non-phenolic lignin subunits is lipid peroxidation (Jensen et al., 1996; Kapich et al., 1999). It has been demonstrated that the oxidative activity of fungal MnP may be promoted even towards solid wood and lignin substrates by addition of lipids to the reaction mixtures (Hofrichter et al., 2001), and that lipid peroxyls and reactive oxygen species are generated in the reactions (Kapich et al., 2005). The fatty acids used in the lipid peroxidation has been suggested to be derived from the fungus or generated from wood extractives during the degradation processes (Gutiérrez et al., 2002).

LiPs catalyze direct oxidative cleavage of C-C and ether bonds in aromatic non-phenolic lignin subunits, and is able to oxidize veratryl alcohol, which is a secondary metabolite produced by fungi (Hammel et al., 1993; Hammel and Cullen, 2008; Lundell et al., 1993b; Tien and Kirk, 1984). The reactions catalyzed by LiP result with formation of organic radicals, either phenoxyl or aryl-cation radicals, which lead to a variety of unspecific radical and oxygen incorporation reactions (Hammel et al., 1993; Lundell et al., 1993a). The third lignin-modifying high-redox potential peroxidase, VP combines the catalytic properties of MnP and LiP (Ruiz-Dueñas et al., 2009). VPs may oxidize Mn^{2+} ions and additionally, non-phenolic substrates like veratryl alcohol, without addition of Mn (Mester and Field, 1998).

As being the main determinator of eco-physiological grouping of the wood-decaying white-rot fungi, the evolutionary roots of these fungi are connected to the appearance of class-II peroxidase-encoding genes. Evolutionary reconstruction and comparative genomic studies have shown that these enzymes have a non-ligninolytic

peroxidase ancestor which was further evolved presumably to MnP-encoding genes in the common ancestor of Agaricomycetes (Floudas et al., 2012). Duplications of the genes, possibly as a part of genome-size expansion, have occurred after the appearance of the first white-rot species (Nagy et al., 2015) and the evolutionary process has continued to appearance of several subfamilies of these enzymes (VPs, LiPs, long-MnPs, short-MnPs, atypical MnPs, atypical VPs) with specific functions especially in the white-rot Polyporales (Ruiz-Dueñas et al., 2013).

The evolution of class-II peroxidases had gone through several stages in Polyporales: first from ancestral MnP to long and short-MnPs, followed by gaining the catalytic tryptophan at the protein surface, thus generating VP enzymes, and leading to the loss of Mn-binding site resulting with evolution of LiP enzymes (Ruiz-Dueñas et al., 2013). MnPs are widely distributed among white-rot fungal species while LiPs are mainly present in the order Polyporales (Table 1). However, several atypical LiP genes together with MnP and VP genes were found in the genome of Agaricales species *Galerina marginata* (Kohler et al., 2015). Some correlation of fungal colonization of softwood in nature and favouring MnP-encoding genes over LiP (or tendency to a loss of class-II peroxidase-encoding genes) has been observed but the connection remains to be further studied (Couturier et al., 2015; Ruiz-Dueñas et al., 2013). Additionally, the white-rot species *Ceriporiopsis subvermispora* has two unique class-II peroxidases named as VP-LiP transitional enzymes based on their intermediate phylogenetical and catalytic properties (Fernández-Fueyo et al., 2012). With the expanding fungal genomic data, variants of MnP and VP enzymes (atypical-short-MnPs, atypical VPs) with modifications of the amino-acid residues at Mn-binding site are depicted in Agaricomycetes, ranging from ectomycorrhizal species to litter-decomposing and wood-decaying Polyporales species (Floudas et al., 2012; Hildén et al., 2014; Kohler et al., 2015; Ruiz-Dueñas et al., 2013).

1.3.4.2 Other lignin-modifying peroxidases

In addition to class-II peroxidases, also two other secreted heme-containing peroxidase families are of special interest, namely the dye-decolorizing peroxidases (DyP) and hemethiolate peroxidases (HTP) (Hofrichter et al., 2010; Linde et al., 2015). DyPs are produced by a few species of litter-decomposing and wood-decaying Agaricomycetes (Hofrichter et al., 2010). The fungal DyPs are most likely a result of horizontal gene transfer from cyanobacterial ancestors (Zámocký et al., 2015). These peroxidases are biotechnically interesting because of their ability to degrade recalcitrant compounds including phenolic compounds (Liers et al., 2014) as well as various textile dyes (Kim and Shoda, 1999; Sugano, 2009). The physiological roles of DyPs are presumably diverse and the enzymes have been shown to slowly oxidize non-phenolic lignin model dimers (Liers et al., 2010), wheat straw and veratryl alcohol (Salvachúa et al., 2013b).

However, the redox-potential of DyP is lower compared to LiP (Linde et al., 2015), which questions the biological role of DyP as a lignin-modifying enzyme. Despite this, analyses of fungal genomes have shown that DyPs are unevenly spread among the white-rot Agaricomycetes (Table 1). For example, DyP enzymes have been detected in the secretome of *Pleurotus ostreatus* during growth on poplar (*Populus alba*) wood and wheat straw (Fernández-Fueyo et al., 2016) as well as in the wheat straw secretome of *Irpex lacteus* (Salvachúa et al., 2013a). It seems probable that DyPs take part in the fungal oxidation of lignin-derived compounds and phenolic residues of lignin (Linde et al., 2015).

HTPs form a superfamily including unspecific peroxygenases (UPOs) and chloroperoxidases (Hofrichter et al., 2010). Actually, HTPs are phylogenetically distant from both class-II peroxidases and DyPs (Hofrichter et al., 2010). Characteristic for the enzymes of this family is the ability to catalyze extensive reactions including oxidation of both aromatic and aliphatic compounds (Gutiérrez et al., 2011; Ullrich and Hofrichter, 2005). The evolutionary history of HTPs is obviously long since HTP-encoding genes were included in the genomes of early diverging fungi (Zámocký et al., 2015). High numbers of HTP-encoding genes (from 2 to 24) may exist in white-rot Agaricomycetes (Table 1). The UPO enzyme from *Agrocybe aegerita* has been shown to oxidize veratryl alcohol (Ullrich et al., 2004) and cleave lignin model compounds (Kinne et al., 2011). Instead of direct lignin polymer degradation, HTPs propably contribute to modification by oxygenating compounds originating from lignin or other aromatic compounds, including plant extractives (Kinne et al., 2011).

1.3.4.3 Laccases

Besides peroxidases, also the four-copper-containing phenol oxidases, laccases (AA1_1), are produced by white-rot fungal species. The role of laccases in lignin modification has been much debated (reviewed by Munk et al., 2015). Laccases are phenol oxidases which use oxygen as the final electron acceptor (Giardina et al., 2010). The substrate range of these enzymes is wide including phenols, aromatic amines and heterocyclic compounds. Furthermore, it can be even wider in reactions boosted by a laccase-mediator system. These include chain of electron transfers wherein enzyme oxidizes a compound and the electron deficient (oxidized) form mediates the oxidation of a substrate (Christopher et al., 2014). All in all, laccases are not able to directly depolymerize lignin but can unspecifically affect phenolic lignin structures and also non-phenolic structures with the help of mediators (Hatakka and Hammel, 2010). In addition, laccases have long evolutionary history, diversity in substrates and functional roles in fungi (Baldrian, 2006; Hoegger et al., 2006; Lundell et al., 2010). There is also a high variability of laccase-encoding genes in white-rot fungi (Table 1).

1.3.4.4 Copper radical oxidases and GMC superfamily oxidoreductases

Fungal lignin modification is also enhanced by production of variety of hydrogen-peroxide producing oxidoreductases, namely copper radical oxidases (CROs, AA5) and GMC superfamily oxidoreductases (AA3). Genes encoding all these enzymes are varyingly present in the white-rot fungal genomes (Table 1). Hydrogen peroxide (H_2O_2) is needed for peroxidase-catalyzed reactions as well as for Fenton reactions (Martinez et al., 2009). These oxidases and dehydrogenases may also be seen as acessory enzymes due to the generation of H_2O_2, but not being able to attack lignin structures directly.

Glyoxal oxidases (GLOXs), which belong to CROs, are probably the best studied H_2O_2-producing enzymes in wood-decaying Agaricomycetes. GLOX oxidize various small aldehydes to corresponding carboxylic acids (Kersten and Cullen, 2014; Whittaker, 2005). GLOX-encoding genes are present in many Agaricomycetes genomes that contain class-II peroxidases which makes them characteristic among wood-decay white-rot fungi (Table 1). Besides GLOXs, the other CROs have wide distribution in Agaricomycetes (Cullen, 2013). CROs have differences in their physiological roles and actually their substrate specificities are unknown (Kersten and Cullen, 2014).

The GMC oxidoreductase enzymes are flavoproteins, and they vary from alcohol oxidases to sugar oxidases and dehydrogenases. GMC superfamily includes aryl-alcohol oxidase, glucose oxidase, pyranose dehydrogenase, pyranose oxidase, alcohol oxidase and already mentioned CDH activities (Ferreira et al., 2015). Aryl-alcohol oxidase-encoding genes have frequently been identified in the white-rot fungal genomes together with other GMC oxidoreductases. As highlighted in the evolutionary study of Polyporales species, their ancestor apparently had a variety of GMC oxidoreductase genes, which makes it likely that diversification of these genes occurred earlier at a more ancestral stage of fungal evolution (Ferreira et al., 2015).

1.4 Fungal low molecular weight compounds in wood decay

The fungal extracellular enzymes are too large in size to be able to penetrate into the wood cell wall layers. Therefore, fungal conversion and attack on lignocellulose progresses at the distance from hyphae with the help of small diffusible oxidants and secreted metabolites (Blanchette et al., 1997; Eriksson et al., 1990). In order to enhance lignocellulose degration, wood-decay fungi secrete low molecular weight compounds and organic acids. These small compounds are thought to be important in the beginning

of wood-decay because of their small size in comparison to lignin-modifying enzymes, and due to their diffusibility into the wood cell wall (Blanchette et al., 1997). Fungal low molecular weight compounds may be oxidized as substrates by lignin-modifying enzymes. This oxidation may result in the formation of diffusible free radicals.

For example, veratryl (3,4-dimethoxybenzyl) alcohol has been detected in culture liquids of *P. radiata* and it has been proposed that this metabolite may take part in LiP-mediated oxidation and modification of lignin (Hatakka et al., 1991; Lundell et al., 1993b; Schoemaker et al., 1994). Alternatively, the compound may act as a substrate for fungal aryl-alcohol oxidases thus promoting hydrogen peroxide (H_2O_2) production (Ferreira et al., 2005). In addition to veratryl alcohol, unsaturated fatty acids produced by the fungi are involved in the MnP-catalyzed lipid peroxidation reactions which produce reactive oxygen species (ROS) that can oxidize lignin (Chapter 1.3.4.1, Gutiérrez et al., 2002; Kapich et al., 1999).

In addition, both white-rot and brown-rot fungi are able to produce peptides and phenolate-derivative compounds as low molecular weight Fe^{3+}-reductants (Arantes et al., 2011). These reductants may take part in Fenton chemistry because of their capability to reduce Fe^{3+} back to Fe^{2+} and to maintain hydroxyl radical generation (Arantes et al., 2011).

Fungal secreted carboxylic acids such as oxalic acid have various roles in biodegradation of lignocellulose and plant biomass. Oxalic acid acts for example in extracellular pH controlling and acting as a chelator for unstable Mn^{3+} ions as well as in solubilization of Ca^{2+} ions from wood cell walls and middle lamellae (reviewed by Mäkelä et al., 2010). Accumulation of oxalic acid and presence of calcium oxalate crystals have been detected in cultures of *P. radiata* on solid lignocellulose substrates (Daniel et al., 2004; Galkin et al., 1998).

1.5 Genomics as a tool to study fungi

Innovations in high-throughput genome sequencing technologies have enabled numerous microbial whole-genome sequencing projects and gained a multitude of information about the biology and evolution of fungi. Until now, 41 Polyporales genomes and totally 173 genomes of the Agaricomycetes class have been sequenced at JGI (situation on May 29th, 2016), and are available at the MycoCosm database in connection to the 1000 Fungal Genomes Project (Grigoriev et al., 2011, 2014). Comparative genomics of fungi has provided important molecular-level information on for example fungal strategies of plant biomass decay and degradation of lignocellulose as discussed earlier. Information on the evolutionary history of the organisms and their organelles has also been gained. In addition, genome sequencing

has enabled mass spectrometric identification of proteins and the whole field of functional genomics.

1.5.1 Mitochondrial genomes

Mitochondria are membrane-bound cell organelles of eukaryotes (Figure 4). Typically, they contain outer and inner membranes, and an isolated middle space (matrix). The inner membrane is highly folded into cristae (Chan, 2006). Mitochondria are vital for the majority of eukaryotic organisms due to their massive role in respiratory metabolism producing energy by adenosine triphosphate (ATP) formation from energy-rich compounds. This process is called oxidative phosphorylation and it is coupled to proton transfer across the inner mitochondrial membrane. During oxidative phosphorylation dioxygen receives electrons via several redox reactions through the membrane bound electron-transfer chain proteins and as a result, water is generated. During the process, respiratory complexes I, III and IV pump protons from the matrix through the mitochondrial inner membrane, and energy is stored as membrane potential. Finally, ATP is synthesized via complex V (ATP synthase) after which the protons return to the mitochondrial matrix. Mitochondria also contribute to several cellular processes such as regulating calcium levels, signalling, cell aging and death, cell differentiation, control of cell growth and cell cycle, and take part in iron metabolism (Antico Arciuch et al., 2012; Chan, 2006; Contreras et al., 2010; Richardson et al., 2010).

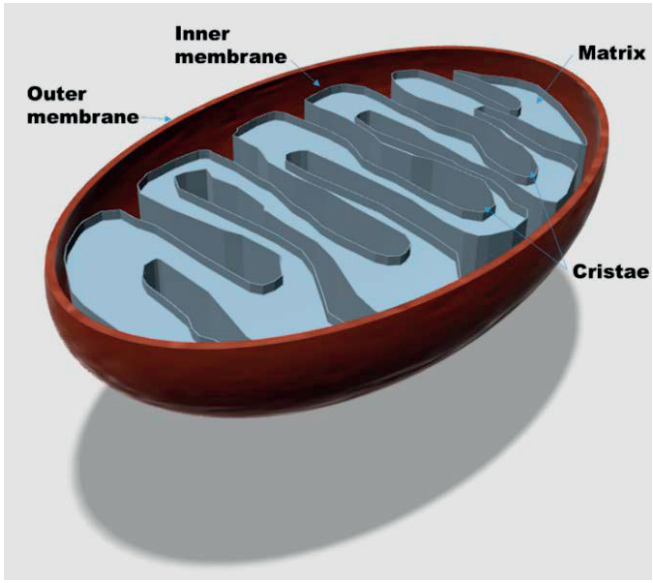

Figure 4. The structure of mitochondrion. Schematic picture made by the author.

According to the endosymbiont theory, mitochondria originated from ancestors of planktonic marine α-proteobacteria, most probably from the SAR11 clade (pelagibacteria) in the Rickettsiales (Thrash et al., 2011). Recent studies have shown that about 2 x 10^9 years ago an archaeal host cell may have acquired the mitochondrial endosymbiont thus leading to emergence of an ancestor of eukaryotes (Spang et al., 2015; Williams et al., 2013). During the co-evolution with the host cells, mitochondrial genome (mitogenome, mtDNA) has lost its capability to provide most of the proteins encoded by the bacterial ancestors. During adaptation to the host organism, the mitochondria gained many new functions like cell signalling, and thus became a fundamental regulator of the host cell (Antico Arciuch et al., 2012). Many of the lost ancestral mitochondrial genes have relocated to the host organism's nucleus. These genes have functional roles in the mitochondrial processes or have evolved to control cellular processes and thereby, reduction of the size of the mitogenome occurred, but all in all, essential functions have remained (Bullerwell and Lang, 2005; Timmis et al., 2004). This has lead to significant dependence on the host cell nuclear genome.

Fungal mitogenomes are not as widely studied as animal and plant mitogenomes, but they also provide sights into evolution of organelles and species, population genetics and biology of fungi. The majority (~99%) of the mitochondrial proteome is encoded by the nuclear genome and the proteins are produced by cytosolic ribosomes, and then processed and imported into mitochondria to specific locations. Fungal mtDNA generally include 30-40 genes which are involved in certain processes such as electron transporting, oxidative phosphorylation, mitochondrial protein synthesis and RNA processing (Bullerwell and Lang, 2005). Generally, only 12-14 conserved protein-encoding genes are present (**Publication II**). One mitochondrion encloses several mtDNA molecules which are packed into dynamic nucleoproteins called mt nucleids (Basse, 2010).

Overall, the fungal mitogenomes have conserved gene contents but their sizes, structures, intron contents and gene orders show flexibility between and within fungal phyla (**Publication II**; Bullerwell and Lang, 2005; Paquin et al., 1997). Until today, over 200 fungal mitogenomes from six phyla have been sequenced, and the data is deposited in the NCBI database (NCBI Organelle Genome Resources, http://www.ncbi.nlm.nih.gov/genome/organelle). A vast majority of the sequenced mitogenomes are from Ascomycota. The two major phyla, Ascomycota and Basidiomycota, have differences in gene loci and orientation regarding the mitogenome DNA strands. Most of Ascomycota mitogenome open reading frames (ORFs) are located on one mtDNA strand while in Basidiomycota, genes are variably encoded on either of the two mtDNA strands (Aguileta et al., 2014). Fungal mitogenomes may have extensive intergenic regions which are comprised of a variable number and length of introns and sequence repeats (**Publication II**; Aguileta et al., 2014).

Introns in the fungal mitogenome genes may be divided into group I and group II self-splicing introns based on their secondary structure and splicing mechanism (Pelin et al., 2012). Some of them may also be mobile via a mechanism called intron homing (Lang, 2007). Intron homing thus leads to multiplication of these gene intervening sequences into previously intronless genes. Intron homing is facilitated by homing endonuclease (HE) enzymes whose ORF sequences are found in the intronic regions (Stoddard, 2011). HEs generate double strand breaks at specific sites of mtDNA, and their collaboration with self-splicing introns even allows invasions into conserved genomic regions in the host DNA, thus sometimes leading to functional disruption of the target gene (Stoddard, 2011). HEs are partly responsible of the genetic variability and adaptive responses of mitogenomes which are not prone to allelic recombination due to the generally uniparental inheritance of mtDNA and mitochondria (Basse, 2010).

A few genes that are conserved in fungal mitogenomes have been useful markers for molecular systematics, such as *atp6* gene, and the small and large subunit rRNA-encoding genes (Table 2) (Binder et al., 2005; Lutzoni et al., 2004; McLaughlin et al., 2009). The studies on fungal mitogenomes are not only useful tools for research on fungal molecular systematics and evolution, but may as well promote research on diseases which are results of mitochondrial dysfunction, such as Mitochondrial encephalomyopathy, lactic acidosis, and stroke-like episodes (MELAS) affecting human brain, heart and muscle cells (Wallace, 2010). Mitogenome sequencing may be an alternative to nuclear genome sequencing, if the aim is to study evolution or population structures or identify species, because fungal mtDNAs are relatively small and thus, remarkably easier and more economical to sequence and assemble (Joardar et al., 2012; Santamaria et al., 2009).

Table 2. Molecular markers used in fungal phylogenetical studies.

Characteristics of loci	Molecular marker	Abbreviation	Reference[1]
Ribosomal loci	ITS region of nuclear ribosomal RNA gene	*ITS*	Gardes and Bruns, 1993; White et al., 1990
	18S nuclear ribosomal small subunit rRNA gene	*SSU*	White et al., 1990
	28S nuclear ribosomal large subunit rRNA gene	*LSU*	Hopple and Vilgalys, 1999
	mitochondrial small subunit rRNA gene	*mt-ssu*	White et al., 1990
	mitochondrial large subunit rRNA gene	*mt-lsu*	White et al., 1990
Non-ribosomal loci	ATP synthase F_o subunit 6 (mitochondrial)	*atp6*	Kretzer and Bruns, 1999
	cytochrome c oxidase subunit 3 (mitochondrial)	*cox3*	Kretzer and Bruns, 1999
	glyceraldehyde phosphate dehydrogenase	*gapdh*	**Publication I**; Kreuzinger et al., 1996
	the largest subunit of RNA polymerase II	*rpb1*	Matheny et al., 2002
	the second largest subunit of RNA polymerase II	*rpb2*	Liu et al., 1999; Matheny et al., 2007
	translation elongation factor 1-α	*tef1*	Donnell et al., 2001
	β-tubulin	*β-tub*	Keeling, 2003
	minichromosome maintenance protein, DNA replication licensing factor	*MCM7*	Schmitt et al., 2009

[1]References are examples of studies describing the locus-specific primer sequences.

1.5.2 Molecular markers in phylogenetics and determination of fungal species

The ultimate aim of fungal taxonomy is to uncover and characterize all fungal species. This is a huge task when it is estimated that fungal diversity on Earth is up to 5.1×10^6 species (Blackwell, 2011), although this value may be a vast overestimation (Tedersoo et al., 2014). Fungal taxonomy classifies species on the basis of phylogenetic relationships together with morphological, ecological and physiological characters (Hibbett et al., 2011). Until now, the requirements for description of a new fungal species were the deposition of a collected type specimen and marker DNA sequences in a fungal culture collection and in a publicly available nucleotide sequence database, respectively (Blackwell, 2011). Earlier, fungal species were described purely based on

their morphological (such as fruiting body macro- and micro-morphologies) features and phenotype characteristics (biological species recognition). However, studying the genotype characteristics (genealogical concordance and phylogenetic species recognition) has revealed more species in the fungal kingdom than was previously realized (Blackwell, 2011; Taylor et al., 2000).

Nowadays there are approximately 100 000 described fungal species (Blackwell, 2011; Taylor et al., 2000). The genealogical concordance method forms the gold standard for species determination in fungi, and it is performed by using multiple unlinked gene loci to evaluate the limits of recombination (Taylor et al., 2000). This research area has now evolved from single locus trees of nuclear rRNA-encoding sequences into multilocus phylogenies based on both protein-encoding and non-protein-encoding sequences (James et al., 2006; Lutzoni et al., 2004; Matheny et al., 2007; McLaughlin et al., 2009), and including also mitogenome located genes (Table 2, Chapter 1.5.1). 'Assembling the Fungal Tree of Life' (AFTOL) and the preceding Deep Hypha project were specimen-based projects and acted as major forces towards multilocus phylogenetic analyses, enlightening the deep relations of fungi (Blackwell et al., 2007; Hibbett et al., 2007; Lutzoni et al., 2004).

During the molecular revolution in fungal taxonomy discussions have been ongoing on which molecular markers should be used for species identification and in systematics. The main idea behind several markers are that when resolving older nodes in the phylogenetic trees, markers with slower evolutionary rates should be used, and following this, markers with faster evolutionary rates should be selected for younger nodes (Stajich, 2015). Both types of molecular markers should be used for proper phylogenetic analysis of species. Besides AFTOL, several other projects have contributed to searching the optimal barcodes for fungal species, for example the 'International Barcode of Life' (www.ibol.org) project.

The nuclear genome-located ribosomal RNA-encoding gene regions, including 18S, 5.8S and 28S rRNA genes as well as the two internal transcribed spacers ITS1 and ITS2 surrounding the 5.8S rRNA gene, is widely used in phylogenetics and global meta-barcoding studies (Schoch et al., 2012; Tedersoo et al., 2014). At this point, it seems that the ITS region (including ITS1 and ITS2) is selected for fungal barcoding and identification due to the suitability of this nucleotide sequence region to resolve closely related species, and applicability to use universal primers for PCR, thereby giving excellent sequencing degree in the kingdom of Fungi (Schoch et al., 2012). Nevertheless, additional markers are still needed for a deeper understanding of species delimitation in many fungal groups.

New rapid and efficient DNA-sequencing methodologies have dramatically changed the abilities to uncover new species, and we are transforming into a situation in which molecular ecologists discover new taxons faster than the traditional taxonomists are able to identify (Hibbett et al., 2011). This reform has caused pressure

towards sequence-based taxonomy with omitted cultivation and morphological analysis of fungi (Hibbett and Taylor, 2013). Environmental sequences are still offering some problems before being able to fully resolve species delimitations according to the above mentioned gold standard of fungal species description (the genealogical concordance method). These problems include the use of single loci, intra-genomic heterogeneity in tandemly repeated ribosomal RNA genes, sequencing errors, and the conflict of gene trees versus species trees (Hibbett and Taylor, 2013). Despite the problems, the new sequencing-based taxonomic categorization is proposed for environmental sampling and sequencing in order to help the integration into specimen-based taxons (Hibbett et al., 2011; Hibbett and Taylor, 2013).

As data from whole genome sequencing increases constantly, it is possible to compare conserved single-copy genes and study the evolution of the complete fungal kingdom by computing methods known as phylogenomics. Phylogenomics enables multigene phylogeny with concatenated supermatrix datasets, as well as improved resolution and support for higher-level relationships of fungal groups (Hibbett et al., 2014; McLaughlin et al., 2009). Recent studies have, however, shown that when fungal phylogeny is studied in the context of wide taxon sampling, various drawbacks may occur. One of these is the lack of information on individual gene content which arises from the early splits in fungal evolution (Chang et al., 2015). On the other hand, when the aim is to improve support and resolution of fungal phylogeny, the number of genes in the phylogenetic analyses is more important than the number of taxa included (Binder et al., 2013). Taken together, new genomes and orthologous gene sequences of especially early diverging fungal taxa are needed. However, this does not remove the importance in selecting suitable genes to make reliable phylogenetic analyses.

Despite the great possibilities (*e.g.* lower costs, more rapid analysis times, less computing time and efficiency needed) in low-coverage genome sequencing, the alternative phylogenetic method is called high-throughput phylogenomics that will allow studying hundreds of different loci (genes, amplicons) from a wide repertoir of species (Lemmon et al., 2012). It utilizes probes that can be designed based on single-copy genes and hybrid enrichment methods (Faircloth et al., 2012; Lemmon et al., 2012; Li et al., 2013). These probes capture target genes which can be then sequenced with modern sequencing technologies (Lemmon et al., 2012). At this point, these methods have been applied mainly in vertebrate phylogenetics (Brandley et al., 2015), but in future the hybrid enrichment method will most probably be successfully adopted for studies on fungal phylogenetics.

2 Aims of the study

The purpose of this PhD research was to study the molecular systematics and wood-decay enzyme production of species and isolates of the divergent fungal genus *Phlebia*, in respect to the known characteristics of the type species *P. radiata*. Additional aims were to initiate genome sequencing of *P. radiata* isolate 79, starting with characterization and gene annotation of its mitochondrial genome, and performing detailed research on its transcriptome and proteome upon six weeks of growth on solid spruce wood. The latter study was also designed to contribute to our knowledge on the specific features of wood-decay strategies of the white-rot Polyporales phlebioid fungi.

Although improvements in genomics, transcriptomics and proteomics have revolutionized the research in the field of fungal biology, the total variety of fungal genomes and wood-decay mechanisms has not been fully elucidated. Especially long-term time-dependent changes in the expression of wood-decay enzymes and corresponding genes on natural-like growth conditions are not yet thoroughly studied. For that reason, special attention was given to the dynamics of expression and production of the wood-decay machinery, studied in the total proteome and transcriptome when *P. radiata* 79 was growing in solid-state cultures on Norway spruce wood.

The specific aims in studies (**I-III**) were as follows:

- To study the genetic and physiological versatility of the fungal genus *Phlebia*, and to enhance phylogenetic knowledge of the phlebioid clade in the order Polyporales (**I-II**).
- To compare whether the species and isolates of *Phlebia* have significant differences in their abilities to produce lignocellulose-converting enzyme activities (**I**).
- To sequence and characterize the mitochondrial genome of the model species *P. radiata* in order to add up our knowledge on fungal mitogenomes and their genes (**II**).
- To analyze the proteome and transcriptome of *P. radiata* grown on spruce wood with special emphasis on plant-cell-wall degrading enzymes (**III**).
- To evaluate the dynamic changes in protein production of *P. radiata* upon six weeks of growth on wood (**III**).
- To elucidate the enzyme repertoire associated with the white-rot type of decay and biological mechanisms of coniferous wood degradation of *P. radiata* (**III**).

3 Summary of materials and methods

The experimental setup as well as detailed descriptions of the analytical methods are explained in the publications (**I-III**), and are indicated in Table 3. Fungal isolates used in the study are presented in Table 4. The isolates originate from the HAMBI-FBCC Fungal Biotechnology Culture Collection of the University of Helsinki, which is maintained at the Division of Microbiology and Biotechnology, Department of Food and Environmental Sciences. The main results of the studies will be introduced and discussed in the next chapter.

Table 3. Methods used in this PhD study.

Method	Described and used in
Fungal cultivations	
on agar plates for hyphal growth rate determination	I
liquid cultures	I, II, III
semi-solid wood cultures	I
solid-state wood cultures	III
Extraction of fungal DNA	I, II
PCR amplification	I, II
Enzyme activity measurements	I, III
PCR-product sequencing and analyses	I
Genomic DNA sequencing	II
Extraction of RNA from wood cultures	III
mRNA purification	III
RNA-sequencing	III
Transcriptome assembly and analyses	III
Gene annotation	II, III
Extraction of proteome on wood	III
Peptide LC-MS/MS	III
Protein concentration measurements	III
Microscopy of wood; FE-SEM	III
Klason and acid soluble lignin	III
Pyrolysis-GC-MS	III
Bioinformatic sequence analyses	I, II, III
Phylogenetic analyses	I, II
Statistical analyses with R and SPSS programs	I, II, III

Table 4. Fungal isolates studied in the experiments. Abbreviations of natural substrates: C = Coniferous wood, D = Deciduous wood.

HAMBI-FBCC identifier	Species identity	Site of origin	Natural substrate	Studied in publication no.
43	*Phlebia radiata*	Finland; Vantaa	D	I, II, III
297	*Phlebia rufa*	Sweden		I
125	*Phlebia radiata*	Finland; Lieksa	D	I
149	*Phlebia radiata*	Finland; Ruovesi	D	I
179	*Phlebia radiata*	Finland; Lammi	D	I
194	*Phlebia radiata*	Finland; Sodankylä	D	I
226	*Phlebia radiata*	Finland; Kolari		I
279	*Phlebia radiata*	Sweden		I
443	*Phlebia radiata*	UK	D	I
444	*Phlebia radiata*	France		I
750	*Phlebia radiata*	Finland; Lammi		I
790	*Phlebia radiata*	Finland; Ruovesi	D	I
791	*Phlebia radiata*	Finland; Ruovesi	D	I
792	*Phlebia radiata*	Finland; Ruovesi	D	I
794	*Phlebia radiata*	Finland; Ruovesi	D	I
1374	*Phlebia radiata*	Finland; Lammi	D	I
1375	*Phlebia radiata*	Finland; Ruovesi	D	I
1376	*Phlebia radiata*	unknown		I
1377	*Phlebia radiata*	unknown		I
4	*Phlebia acerina*	unknown		I
345	*Phlebia acerina*	Russia		I
464	*Phlebia* sp.	Argentina; Bariloche	D	I
1463	*Phlebia brevispora*	USA; Florida		I
82	*Phlebia tremellosa*	Finland; Salo	D	I
91	*Phlebia tremellosa*	Finland; Perniö	D	I
294	*Phlebia tremellosa*	Canada	D	I
362	*Phlebia tremellosa*	Russia; Kavalerovo	D	I
446	*Phlebia tremellosa*	Netherlands		I
278	*Phlebia tremellosa*	Sweden		I
937	*Phlebia livida*	Finland; Lammi	C	I
1283	*Phlebia livida*	Norway; Telemark	C	I

HAMBI-FBCC identifier	Species identity	Site of origin	Natural substrate	Studied in publication no.
423	*Phlebia (Scopuloides) hydnoides*	Belgium; Bois de Matignolle	D	I
422	*Phlebia (Scopuloides) hydnoides*	France; Haute Savoie		I
307	*Phlebia chrysocreas*	unknown		I
309	*Phlebia chrysocreas*	unknown		I
295	*Phlebia ochraceofulva*	Sweden		I
360	*Phlebia ochraceofulva*	Sweden		I
207	*Phlebia centrifuga*	Finland; Kolari	C	I
213	*Phlebia centrifuga*	Finland; Aakenus	C	I
195	*Phlebia centrifuga*	Finland; Sodankylä	C	I
359	*Phlebia centrifuga*	Sweden		I
692	*Phlebia centrifuga*	Finland; Sodankylä	C	I
947	*Phlebia centrifuga*	Finland; Kolari	C	I
1252	*Phlebia centrifuga*	Bulgaria; Rila mountains		I
1253	*Phlebia centrifuga*	Bulgaria; Rila mountains		I
1264	*Phlebia centrifuga*	Bulgaria; Rila mountains		I
421	*Phlebia centrifuga*	USA; Idaho	C	I
426	*Phlebia subserialis*	France		I
427	*Phlebia* sp.	France; Rhône		I
296	*Phlebia* sp.	Sweden		I
315	*Phlebiopsis gigantea*	Sweden		I
316	*Phlebiopsis gigantea*	Sweden		I
318	*Phlebiopsis gigantea*	Sweden		I
986	*Phlebiopsis gigantea*	Finland; Kolari	C	I

4 Results and discussion

4.1 Systematics of *Phlebia* species (I, II)

In order to confirm the taxonomic positioning of *P. radiata*, various molecular systematic analyses were performed including both single gene and multiple gene comparisons. This study also confirmed the identity of many *Phlebia* isolates which were earlier mainly morphologically identified.

4.1.1 ITS phylogeny

As a starting point, phylogenetic analyses based on ITS sequence dataset of the Polyporales phlebioid clade were conducted. This ribosomal RNA-encoding gene region was selected because of the widest availability of reference sequences in nucleotide sequence databases. In total, 481 ITS sequences (including ITS1, 5.8S and ITS2 regions) were used in the alignment (54 produced in this study) and for maximum likelihood evolutionary analysis (Figure 1A in **Publication I**). The main finding of the analysis was that the phlebioid clade can be further divided into three lineages. These lineages were named as *Phlebia, Byssomerulius* and *Phanerochaete* clades in regard to family level resolvance and to be comparable with a previous study (Floudas and Hibbett, 2015). The *Phanerochaete* clade seemingly comprises also the *Phlebiopsis* clade. All these four clades included fungi with species name *Phlebia*. Previously, it has been shown that outside of the phlebioid clade, in the 'residual polyporoid clade' of Polyporales, there are species named as *Phlebia bresadolae* and *Phlebia queletii* (Binder et al., 2013; Parmasto and Hallenberg, 2000). These results confirmed the polyphyletic nature of genus *Phlebia* and the earlier observations that the genus is a group of unrelated taxa having some equal morphological features (Binder et al., 2005; de Koker et al., 2003; Dresler-Nurmi et al., 1999; Wu et al., 2010).

However, a majority of *Phlebia* species were positioned in *Phlebia* clade (Figure 5) which also included fungal isolates from the genera *Ceriporiopsis, Scopuloides, Climacodon, Phlebiopsis, Ceriporia* and *Hydnophlebia*. The sequence phylogeny analyses of this study confirmed the existence of the *Phlebia sensu stricto* group, in which the following species were proposed as members: *P. radiata, Phlebia rufa, Phlebia acerina, P. floridensis, P. brevispora, P. lindtneri, Phlebia setulosa, Phlebia serialis*, *Phlebia leptospermi* and *P. tremellosa* (**Publication I**). The number of species is higher than studied by Floudas and Hibbett (2015) but lower in comparison to the earlier systematic study of Parmasto and Hallenberg (2000). Although supported by ITS-phylogeny (Figure 5), *P. centrifuga* was not included in the *Phlebia sensu stricto* since the other phylogenetic analyses done in this study together with two other studies

(Binder et al., 2013; Wu et al., 2010) on Polyporales and phlebioid species were not supporting the positioning. Together with *P. centrifuga*, many species of the genera *Phlebia* are left outside of the *Phlebia sensu stricto* clade (**Publication I**). For example, *Phlebia livida, Phlebia hydnoides, P. ochraceofulva* and *Phlebia chrysocreas* fall outside of the clade and thus, should be taxonomically re-positioned with genus-level re-naming. Some of the re-classifications may be possible because of the availability of specimen-based reference sequences, and in fact, the grouping of *P. hydnoides* into *Scopuloides* clade (Floudas and Hibbett, 2015) is well supported. *P. ochraceofulva* in turn produced a separated lineage without reference sequences and was clustered together with *Phlebia* spp. species distant from *Phlebia sensu stricto* group. Similar taxonomically narrower concept of genus *Phlebia* has been suggested earlier, but the *sensu stricto* concept would not yet result with the group of similar morphological characters (Floudas and Hibbett, 2015; Parmasto and Hallenberg, 2000).

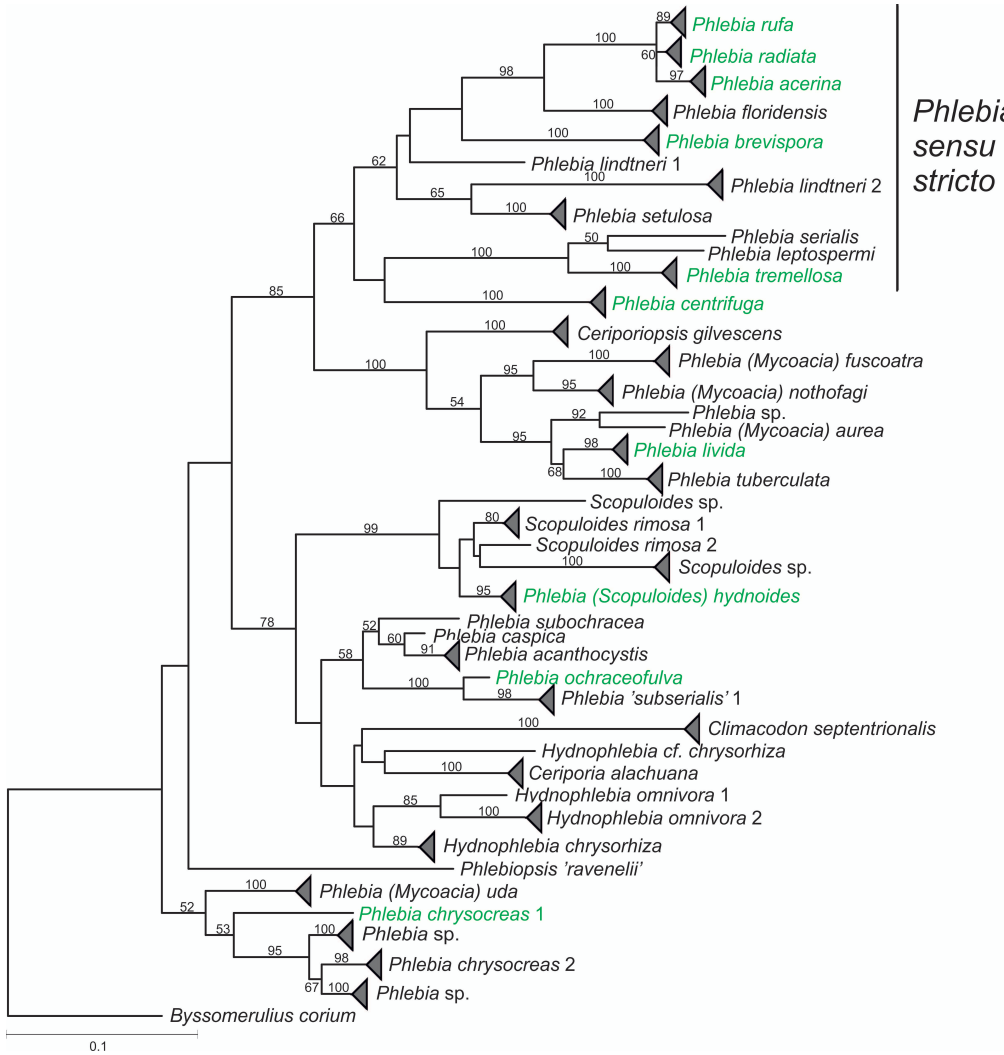

Figure 5. Phylogeny of the *Phlebia* clade of Polyporales. Tree is derived from ITS1-5.8S-ITS2 sequences using maximum likelihood analysis. Nodes with several isolates were collapsed and marked with triangle. The fungal species including the studied isolates are marked in green (ITS accession numbers are presented in Table 1 in **Publication I**). Other taxons are represented with sequences retrieved from NCBI database. Bootstrap values (100 replications) ≥ 50% are marked at the nodes. *Byssomerulius corium* was used as outgroup. Scale bar corresponds to 0.01 nucleotide substitutions per position. (**Publication I**)

The close relationship of the three species *P. radiata*, *P. acerina* and *P. rufa,* which formed a distinct branch (bootstrap value 100) in ITS analysis, was distinguishable. It was also shown that several isolates, represented by reference sequences and isolates of this study, were incorrectly named inside group of *P. radiata*, *P. acerina* and *P. rufa*. This genetic similarity and evolutionary close speciation is in line with the reports on their similarity in basidiocarp (basidiomal) and hymenial macro-structure and micro-morphology (Nakasone and Sytsma, 1993).

More complicated is the finding that several ITS sequences under the same taxon identity were divided into at least two separate branches and numbers were given as identifiers after the names (Figure 5). Inside the *Phlebia* clade this kind of deviations were seen for species *P. lindtneri, Scopuloides rimosa, Hydnophlebia omnivora, P. chrysocreas* and *Phlebia subserialis.* The ITS sequences of *P. subserialis* were the most diversified. One lineage (number 1) was included in the main *Phlebia* clade (Figure 5), but the second clustered to the *Phanerochaete* clade (number 2). In addition, a third lineage was demonstrated by Floudas and Hibbett (2015) to group with the members of the *Phlebia* clade, but this reference sequence (Parmasto and Hallenberg, 2000) was excluded from present study due to lack of ITS1 region.

Furthermore, the *P. subserialis* clade number 2 was divided into two lineages (Additional file 2: Figure S1A in **Publication I**). The first lineage comprised one isolate of this study, FBCC0426, and one reference sequence while the second lineage, including four reference sequences, was tentatively named as *Phanerochaete krikophora* by Floudas and Hibbett (2015). This suggests that there are at least four lineages all named as *P. subserialis* which explains the variation in taxonomic positioning of the species in other studies depending on the reference sequences used (Binder et al., 2013; de Koker et al., 2003; Greslebin et al., 2004; Moreno et al., 2011; Parmasto and Hallenberg, 2000; Tomsovsky et al., 2010; Wu et al., 2010).

4.1.2 Multigene phylogeny

In order to study the genetic diversity of *Phlebia* isolates of this study and to confirm the phylogenetic positioning explained above, a study adopting rRNA-encoding (SSU and LSU) and two cellular core protein-encoding genes - glyceraldehyde phosphate dehydrogenase (*gapdh*) and nuclear RNA polymerase II (*rpb2*) - was conducted. This analysis resulted in a well-supported maximum likelihood phylogram, which divided *Phlebia* isolates into ten phylogroups (Figure 6). Similar grouping was observed in all evolutionary analyses based on individual or concatenated gene sequences. It was also shown that at least the isolates of *P. radiata, P. tremellosa* and *P. centrifuga* diverged at the species level but no clear connection to biogeographic origin or host tree of these species were observed. Further analysis with wider isolate sampling is needed to address this issue more deeply. Based on the phylogroups, their enzyme-phenotype profiles were analysed (Chapter 4.3).

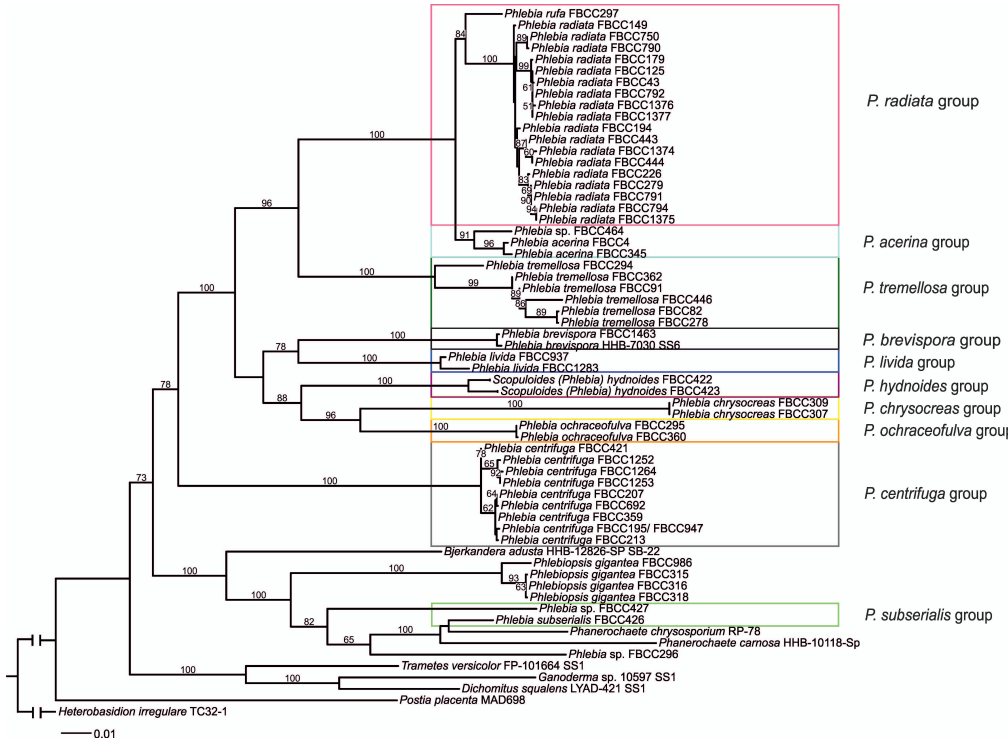

Figure 6. Maximum likelihood phylogeny of the *Phlebia* isolates and the phylogroups based on concatenated sequences of 5.8S, partial LSU, and partial sequences from two protein-encoding genes (*gapdh, rpb2*). The aligned sequences were subjected to phylogenetic analysis using RAxML v. 7.2.8. and with 100x bootstrapping. The sequences from isolates with FBCC-identifier are produced in the present study. The concatenated sequence from *Heterobasidion irregulare* was used as outgroup. Only bootstrap values >50 are indicated and scale bar represents 0.01 nucleotide substitutions per position. (**Publication I**)

To study the phylogenetic positioning of *P. radiata* at phylum level, Bayesian inference and maximum likelihood phylogenetic analyses based on concatenated mitogenome-encoded proteomes were used (**Publication II**). The resulted well-supported trees showed grouping of *P. radiata* near other Agaricomycotina species (Basidiomycota) including white-rot decay producing Polyporales species *Ganoderma* spp. and *Trametes cingulata* (Figure 7). Similar grouping into the subphylum Agaricomycotina was observed in the evolutionary analysis based on the ORF codon usage of the mitogenome proteome (Figure 4 in **Publication II**). These results are in agreement with the current fungal evolutionary taxonomy (Hibbett et al., 2007; Stajich et al., 2009) and indicate that the Basidiomycota and their mitogenomes have single common origin. Further description of the mitochondrial genome of *P. radiata* is presented in the next chapter.

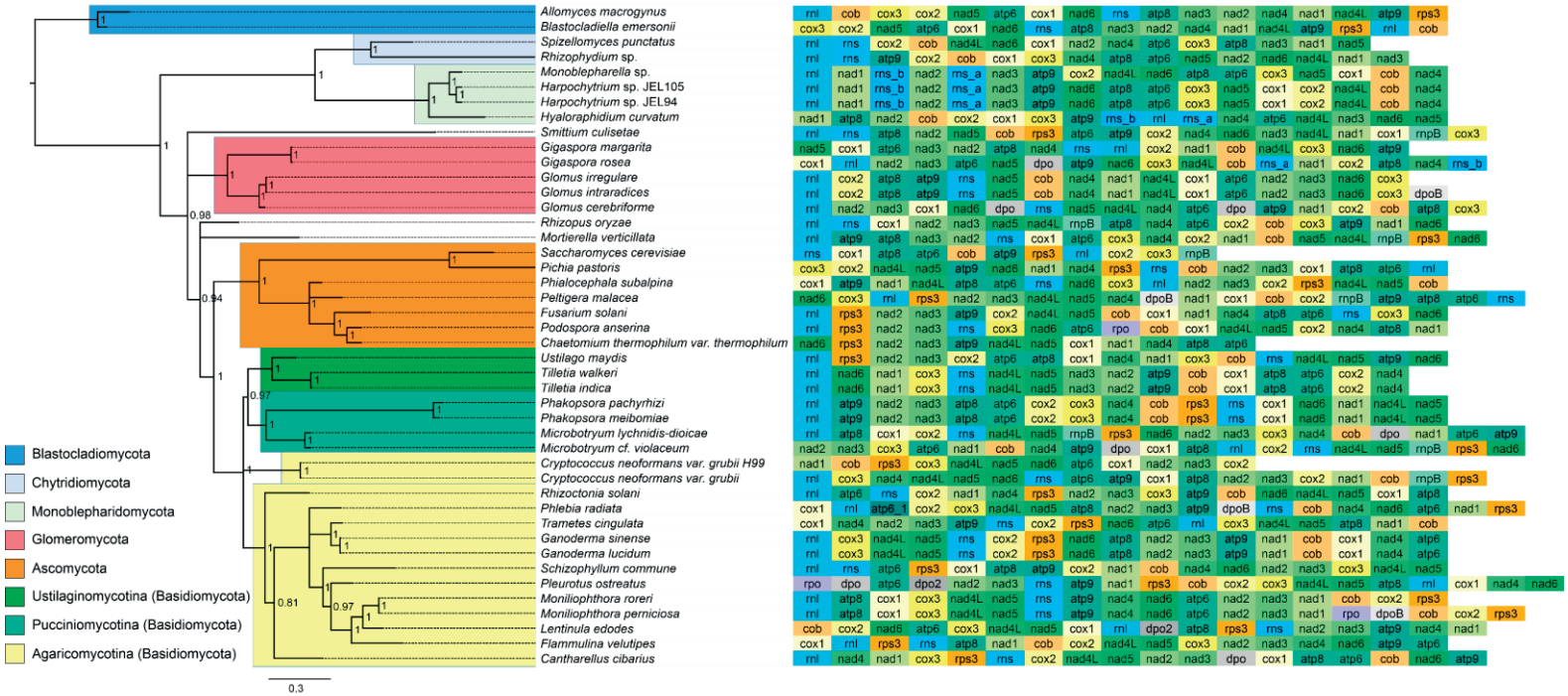

Figure 7. The phylogenetical tree derived by Bayesian inference from a multi-gene alignment of mitogenome-encoded proteins (2 019 amino acid (aa) positions) from 44 species. Colours in the tree refer to phyla or sub-phyla. The numbers presented are branch support values (posterior probabilities from Bayesian inference) and nodes with support lower than 0.8 were collapsed into polytomies. Mid-point rooting was used and scale bar correspond to 0.3 aa substitutions per site. The series of coloured boxes on the right represent gene order in mt-genomes derived from GenBank annotations (excluding tRNAs and intronic and unidentified ORFs). Futher information of the species and their mtDNA accessions are presented in Table 5 in **Publication II**. The abbreviations of genes are as follow: rns, rns_a, rns_b, rnl: ribosomal RNAs; rps3: ribosomal protein; cox1, cox2, cox3: Cytochrome c oxidase subunits; cob: Apocytochrome b; nad1-6, nad4L: NADH dehydrogenase subunits; atp6, atp8-9: ATP synthase subunits; rpo: DNA dependent RNA polymerase; dpoB, dpo, dpo2: DNA directed DNA polymerase; rnpB: ribonuclease P RNA.

4.2 Mitochondrial genome of *P. radiata* (II)

The sequencing and assembly of *P. radiata* mtDNA resulted with one of the largest mitogenomes described for fungi, in total 156 348 bp. The mitogenome contains 16 protein-encoding core genes (15 unique), 28 tRNA genes (26 unique) and genes for large and small RNAs of the mitochondrial ribosome (*rnl* and *rns*, respectively) (Figure 1 in **Publication II**). Overall, the core genes were those typically present in most of the fungal mitogenomes (Figure 7) including genes encoding proteins for the mitochondrial inner membrane complexes I, III, IV and V of the respiratory chain. These are genes encoding protein subunits of NADH dehydrogenase complex (I) (*nad1, 2, 3, 4, 4L, 5, 6*), cytochrome bc1 complex (III) (*cob*), cytochrome c oxidase complex (IV) (*cox1, 2, 3*), and F_0 subunits of the ATP synthase complex (V) (*atp6* (two identical copies)*, 8, 9*), to be precise. The presence of all these genes was expected since even the compact mitogenomes from *Harpochytrium* spp. (19-24 kbp) of the phylum Chytridiomycota have all these proteins (Figure 7). Still, there are variations in the gene content among fungi since for example the yeast *Saccharomyces cerevisiae* mitogenome lacks genes encoding membrane complex I proteins (Foury, 1998) but as an alternative, it has genome-encoded NADH dehydrogenases (Luttik et al., 1998). The core mitoproteome of *P. radiata* also included small ribosomal subunit protein S3 (*rps3*) which is required in ribosome assembly but is not observed in all fungal mitogenomes (Figure 7). Actually, during the fungal evolution, *atp9* has once been lost and transferred to the nucleus among euascomycetes whereas the genes *rps3* and *rnpB* (the latter encodes RNA component of RNAse P, not included in *P. radiata* mitogenome) have been lost several times (Adams and Palmer, 2003; Bullerwell and Lang, 2005).

4.2.1 Variation in the fungal mitogenome size and gene order

Despite the highly conserved core gene content of fungal mitogenomes, the mtDNA sizes vary considerably, and a trend for larger mitogenomes in the Basidiomycota subphylum Agaricomycotina as well as among the filamentous Ascomycota has been observed (Table 5 in **Publication II**). The large size of *P. radiata* mitogenome was further studied and it could be demonstrated that genes encoding proteins, rRNAs and tRNAs, cover 56% of the *P. radiata* mt-genome while the rest of the mtDNA is intergenic regions (Figure 8). Protein-encoding genes have also frequent splicing by long introns (average 1 500 bp, Table 3 in **Publication II**) and short exons. In fact, inconsistency in mitogenome sizes is mainly due to the variations in length and organization of the intergenic regions, or intron number and length. For example, the Agaricomycetes species *Schizophyllum commune* mitogenome lacks introns (Paquin

et al., 1997), whereas the intronic and intergenic non-coding proportion of *P. radiata* mitogenome is 80%.

In addition, the inverted duplication of a 6.1 kbp region in *P. radiata* mitogenome increases the size of the genome. Similar type of duplications, although composed of different sets of genes, have been observed in the mitogenome of another Agaricomycetes species *Agaricus bisporus* as well as Ascomycota species *Candida albicans* and, for instance, plants like cucumber (Férandon et al., 2013; Gerhold et al., 2010; Sloan et al., 2012).

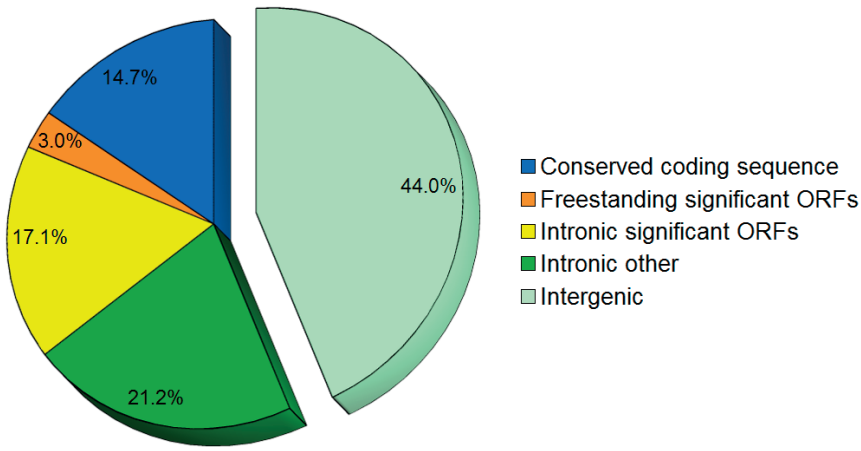

Figure 8. Composition of *P. radiata* mitogenome. The conserved fungal mitoproteome ORFs, and rRNAs and tRNAs are included in the conserved coding sequence. The significant ORFs include additional identified and hypothetical protein-coding sequences (E-value = 0.001 in blastP search). Freestanding refers to genes without introns. Intronic significant ORFs comprise HEs, also exon-to-exon-fused ORFs, excluding intergenic open reading frame HE-encoding genes. (**Publication II**)

As can be observed from Figure 7, the gene order is variable among fungal mitogenomes and especially within Basidiomycota, and the phenomenon is thoroughly reported in the study of Aguileta et al. (2014). The gene order changes are probably occurring due to intramolecular recombination events (Aguileta et al., 2014), because allelic recombination does not occur in the uniparentally inherited mitogenomes (Basse, 2010). Actually, nonhomologous recombination has been proved to occur in nature for fungal mitogenomes, and is proposed to be a repair mechanism to restore mitochondrial function (van Diepeningen et al., 2010).

In the comparative analysis, tRNA distribution and intergenic repetitive sequences were shown to promote the variation in mitogenome gene order (Aguileta et al., 2014).

The characteristics of *P. radiata* mitogenome are the high amount of repetitive sequences especially in intergenic regions as well as the scattered distribution of tRNA-encoding genes. Especially at certain location of the mitogenome (nucleotide positions from 90 000 to 110 000) both of these features are accumulated. The tRNAs are able to change location in genomes (Perseke et al., 2008) and DNA repeats may mediate recombination events (Bi and Liu, 1996), both changes affecting the order of genes, thus promoting the flexibility of the mitogenome.

Additionally, putative plasmid-originated reverse transcriptase and two DNA polymerase B-encoding (*dpoB*) genes were annotated in *P. radiata* mitogenome. Adding even more possible contributors for the gene order changes, the existence of reverse transcriptase genes together with horizontal gene transfer (from bacteria) may both function in promoting mitogenome dynamics. The plasmid-derived genes belong to the group of exchangeable genes which also includes HEs and non-conserved ORFs, all of which additionally have an effect on the size of mitogenome (Himmelstrand et al., 2014). All these features influence to the fact that the large size and different gene order of *P. radiata* mitogenome is divergent from most of the so far sequenced fungal mitogenomes. However, the *P. radiata* mitogenome is so far the only representative characterized among the phlebioid species of Polyporales.

4.2.2 Role of homing endonucleases in *P. radiata* mitogenome

P. radiata mitogenome includes high amount of mobile DNA elements which were identified as type I and II self-splicing introns, which harness the homing endonuclease (HE) domain-encoding ORFs. It was shown that 11 intron-containing conserved genes included HE domains and in total 57 HE domain-encoding ORFs were identified (Tables 3 and 4 in **Publication II**). The HEs were shown to belong to three structural families, i.e. LAGLIDADG subtypes 1 and 2, and GIY-YIG, and the majority of the HE-encoding genes were located within group I type introns.

Surprisingly, there is no strong correlation between gene order changes in mitogenomes and HEs (Aguileta et al., 2014), although HEs are able to insert copies of their respective genetic elements in different locations of the host DNA. Despite that, it was observed that the mitogenome of *P. radiata* included two genes - *atp6* and *cox2* - demonstrating HE-transmitted introns and alternative coding sequences in their C-terminus (Figures 3A and 3B in **Publication II**), which is similar to the variations recorded for *atp6* gene of the Blastocladiomycota species *Allomyces macrogynus* (Paquin et al., 1994). These findings indicate that the typical role of HEs are to interrupt and introduce introns and intronic HE-domains in their target sites (Stoddard, 2011).

HEs have also maturase activity which allows them to take part in splicing of intron-including RNA by assisting in folding and formation of secondary structures in

the intron sequences (Stoddard, 2011). As the core genes of *P. radiata* mt-genome included a high number of group I introns and HE domains, it is expected that they could aid in splicing and regulating transcription of their target genes. These genes have been shown to be transcriptionally active in the Ascomycota species *Ophiocordyceps sinensis* which possesses a large mitogenome (157.5 kbp) (Li et al., 2015) that is similar in size to *P. radiata* mitogenome. This indicates that HEs may have an active role in increasing the intron number and expanding the mitogenome size. In conclusion, mitochondrial genomes seem to allow continuos and adaptive modifications and should not be considered as stable and compact units as has been previously suggested.

4.3 Lignocellulose-converting enzyme activity profiles of *Phlebia* species (I)

While increasing number of wood-decaying fungal genomes is available, the functional studies on lignocelluloses and plant biomasses are quite limited, especially concerning protein production, enzyme secretion and biochemical reactions on solid substrates. In regard to degradation of wood, secreted fungal CAZyme activities need to be confirmed in studies based on both proteomics and biochemical activity assays.

Additionally, relatively little was known about the production and activities of wood-decay enzymes of *Phlebia* species other than *P. radiata*. Therefore, this study included the lignocellulose-converting enzyme activity profiling of 49 *Phlebia* species on semi-solid liquid medium with milled spruce as sole carbon source for 21 days. The isolates were divided into ten phylogroups based on their phylogenetic profiling excluding the species *P. brevispora* which was only represented by one isolate (Chapter 4.1). This study revealed that there are significant differences in the production of lignocellulose-converting oxidoreductase and cellulolytic enzyme activities among the *Phlebia* phylogroups when the data was analysed with the generalized estimating equations (GEE) procedure for generation of regression model with correlated data. The enzyme activities measured included CAZy lignin-modifying oxidoreductases (laccase and MnP) together with cellulolytic activities (CBH, endoglucanase and β-glucosidase). During the cultivation period, all isolates produced lignocellulose-converting enzyme activities periodically as can be observed from the fitted values of enzyme activities of each phylogroup (Figure 9). The highest activities of laccase and MnP were produced by *P. radiata* species group.

In future, with more genomes available from *Phlebia* species, it will be possible to study if the species-level phylogrouping reflects recent evolution of, not only enzyme-encoding genes, but of regulatory differences for certain gene families. Differences in the production of enzyme activities, which is due to regulatory variation, have been

shown to occur in Ascomycota in nearly related *Aspergillus* species, which share fairly similar CAZyme gene numbers and even similar identified regulators for gene expression (Benoit et al., 2015). The regulatory protein-encoding genes in the wood-decaying Basidiomycota is much less studied compared to Ascomycota (Todd et al., 2014) and will need careful genomic and functional studies.

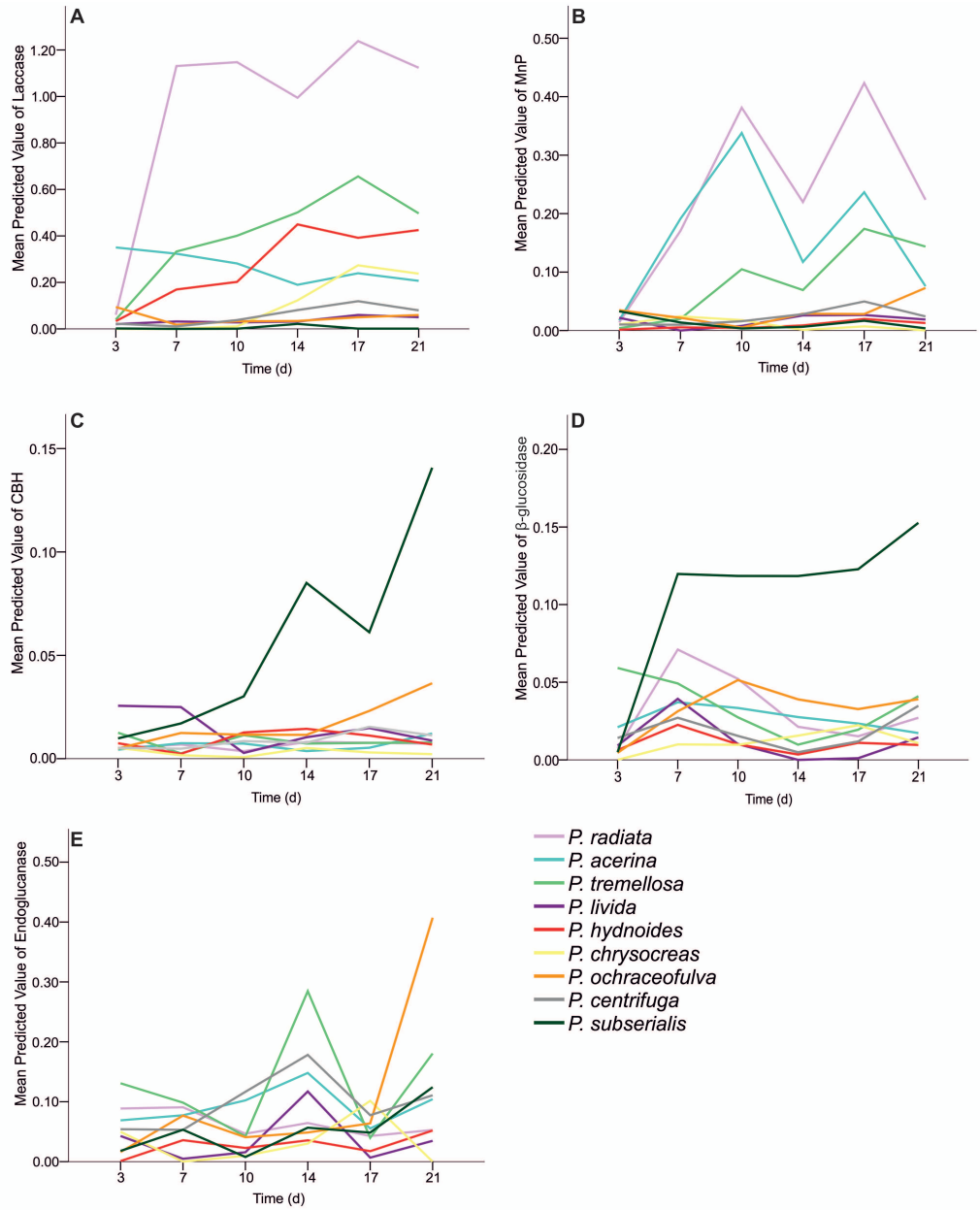

Figure 9. Mean predicted values (based on enzyme activity values) of A) laccase B) MnP C) CBH D) β-glucosidase and E) endoglucanase activities of nine phylogenetic groups of the genus *Phlebia* during 21 days of cultivation in semi-solid milled spruce cultures (**Publication I**).

4.3.1 Laccase and manganese peroxidase activities

Taking into account the importance of MnP enzymes in the white-rot type of wood-decay, it was expected that all *Phlebia* isolates would have produced MnP activities on spruce wood. In this study, it was shown that the *Phlebia sensu stricto* species *P. radiata, P. acerina* and *P. tremellosa* had a cyclic pattern of production of MnP (activity peaking on 10th and 17th days of cultivation; Figure 9), whereas the rest of the species groups produced low levels of MnP activity.

In accordance with these results, and as described in Chapter 1.1.2, divergent MnP genes and enzymes have been characterized from *Phlebia sensu stricto*. Of the other *Phlebia* species, MnP activity has been measured in liquid cultures of *P. subserialis* isolate RLG-6074-sp (Bonnarme and Jeffries, 1990). Surprisingly, no LiP activity was detected in any of the cultivations in the present study, which is contradictory to the well-known production of LiP by *P. radiata* isolate 79 (Lundell et al., 1993b; Vares et al., 1995) and other species of *Phlebia sensu stricto* like *P. tremellosa* (Vares et al., 1994), and to the presence and expression of four LiP-encoding genes of *P. radiata* (Hildén et al., 2006; **Publication III**; genome to be published). The inability to detect LiP activity in the culture fluids is probably due to the the veratryl alcohol and Azure B assay methods which are disturbed by coloured, apparently phenolic compounds that were present in the culture liquids and originated from the wood substrate. Similar inhibition of LiP activity by plant biomass and lignocelluloses has also been experienced earlier in fungal cultures (Lundell and Hatakka, 1994; Vares et al., 1995).

The laccase activity production was another clearly distinctive feature between the phylogroups. The *P. radiata*, *P. tremellosa* and *P. hydnoides* species groups produced relatively high amounts of laccase activity while *P. centrifuga* species group produced moderate laccase activities although a couple of the isolates attained higher activity levels similar to the *P. radiata* phylogroup (Figure 4 in **Publication I**). The production of laccase activity among phlebioid fungi of Polyporales is interesting because of the clear absence of laccase activity and laccase *sensu stricto* encoding genes of *P. carnosa, P. chrysosporium* and *P. gigantea* (Hori et al., 2014b; Suzuki et al., 2012). However, several laccase-encoding genes are identified in the two recently sequenced *Phlebia* genomes, that is in *P. radiata* (5 genes; Mäkelä et al., 2013; genome to be published) and *P. brevispora* (5 genes; Binder et al., 2013). The role of laccases in wood-decay by *P. radiata* is discussed in Chapter 4.4.4.1.

4.3.2 Cellulolytic enzyme activities

On the contrary to the lignin-modifying oxidoreductases, the hydrolytic CAZymes were moderately produced in all *Phlebia* species groups, and less evident differences were observed between the phylogroups. The majority of previous studies have

concentrated on lignin-modifying (ligninolytic) enzymes of the genus *Phlebia* and less is known about the hydrolytic CAZyme production. In this study (**Publication I**), one of the phylogroups, that is the phylogenetically most distant and incoherent *P. subserialis* species group, was shown to produce the highest CBH and β-glucosidase activities. This result is furthermore supported by the closer evolutionary relationship of *P. subserialis* to genus *Phanerochaete* than to *Phlebia sensu stricto*. Moreover, species of *Phanerochaete* (*P. chrysosporium, P. carnosa, P. sordida*) are efficient producers of cellulolytic enzymes on wood and lignocelluloses, with several CAZymes and respective genes characterized (Adav et al., 2012; Diorio et al., 2009; MacDonald et al., 2011; Vanden Wymelenberg et al., 2009). In addition, white-rot Polyporales species outside the phlebioid clade have been demonstrated to express relatively notable cellulose-degrading enzyme activities on lignocellulose containing culture media (Manavalan et al., 2012; Zhu et al., 2016). In this respect, it may be concluded that the *Phlebia sensu stricto* species have a more controlled production of cellulolytic enzymes.

The endoglucanase (e.g. CAZy family GH5) activity was produced in cycles in the wood-containing cultures (**Publication I**), and two distinguishable activity peaks were observed, which were those produced by *P. tremellosa* species group on day 14, and *P. ochraceofulva* species group on day 21 (Figure 9). In accordance with this study, the observed endoglucanase activities produced by *P. radiata* on crystalline cellulose (Avicel) have been shown to be higher than activities of CBH or β-glucosidase (Rogalski et al., 1993b). In previous bioreactor cultivation of *P. radiata* 79 on Norway spruce, with glucose as primary carbon source, CBH or endoglucanase activities could not be detected (Niku-Paavola et al., 1990). This result is probably due to glucose repression, together with difficult access of fungal mycelium onto solid wood pieces in the bioreactor design (Niku-Paavola et al., 1990). However, low endoglucanase activities on wood cultures of *P. tremellosa* and *P. radiata* isolates have been reported (Ander and Eriksson, 1977). One possible explanation for the low cellulolytic enzyme activities may be the same as observed in studies on enzymatic hydrolysis of lignocellulose: lignin surfaces may adsorb cellulolytic enzyme proteins, and smaller molecular size degradation products of lignin may in turn inhibit the activity of cellulases (Berlin et al., 2006; Rahikainen et al., 2013; Yang et al., 2012).

4.3.3 Enzyme phenotype clusters of *Phlebia*

In addition to comparison of the phylogroups, the plant-biomass degrading enzyme activities of each fungal isolate on day 14 of cultivation were compared and visualized (Figures 4 and 5 in **Publication I**). Based on the enzyme activity production, three enzyme phenotype clusters resulted with two enzyme production patterns: fungal isolates showing high activities of the oxidoreductases (laccase and MnP) and isolates

producing high activities of cellulose-degrading enzymes (endoglucanase, CBH, β-glucosidase). The hierarchial clustering analysis showed that inside the species-level phylogroups, there were also intra-species variation (variation within species). Especially, intra-species variation was observed for cellulolytic enzyme activities, which may be related to isolate-level differences in the hyphal growth rates, or efficiency in e.g. intake of the wood-decay products, such as released sugars. In the study on populations of the species *Heterobasidion parviporum*, the age of the fungal isolate (years since isolation of each fungal strain) has been demonstrated to affect respiration rates (CO_2 accumulation) of the isolates on wood cultures (Müller et al., 2015), which may also be one of the factors introducing phenotypical changes in the isolates used in the present study.

4.4 Wood-decaying strategy of *P. radiata* (III)

The ligninolytic system of *P. radiata* has been extensively studied during the past years and recently some studies on wood-decay fungal secretomes and transcriptomes of other Agaricomycetes species have been carried out (Couturier et al., 2015; Fernández-Fueyo et al., 2016; Floudas et al., 2012; Gaskell et al., 2014; Hori et al., 2014a, 2014b, 2013; Korripally et al., 2015). However, this study allowed revision and completion of the previous work of *P. radiata* and because of the available genome and on-going gene annotation, especially polysaccharide degradation of *P. radiata* was studied in more detail and total lignocellulose degradation was possible to study in a broader view. A majority of previous studies have been done in liquid cultures supplemented with lignocellulose. In order to approach the situation reflecting more natural solid-wood colonization, *P. radiata* was cultivated on spruce wood sticks up to six weeks. By using this method, it was possible to analyse the total fungal proteome including intracellular, extracellular and membrane-bound proteins of the fungus. A more wider range of proteins was gained compared to studying only the secretome, which is the share of secreted extracellular proteins of the total proteome. Wood as solid and complex organic growth substrate offered a great analytical challenge to receive sufficient amount of proteins and RNA, but the complexity and sample variation were overcome by introducing several biological replicate cultures together with the extended cultivation period.

The label-free quantification of proteins important for wood-decay resulted with over 1 300 mass-spectrometer identified proteins. Simultaneously, transcriptomes from spruce wood cultivation at days 14 and 28 were studied and compared to malt-extract transcriptome from day 14 to support the proteome study and provide details of gene expression on wood. In contrast to transcriptome studies, proteome analysis reports the abundancy of the expressed translated (and therefore possibly also active) proteins although the LC-MS/MS analysis may fail to detect proteins without trypsin

cleavage site, proteins with fast turnover rate, low molecular weight proteins or proteins that remain attached to wood (Hori et al., 2014a). However, the presence of proteins or the regulation and expression of the corresponding transcripts does not confirm the activity of enzymes underscoring the importance of enzyme activity measurements.

Briefly, the results of this study (**Publication III**) showed that *P. radiata* produces a wide repertoire of plant-polysaccharide degrading and lignin-modifying enzymes, and the respective genes displayed significantly higher expression on spruce wood than on malt extract medium suggesting that they are important in wood-decay. In this PhD thesis, the wood-decay enzymes are grouped based on their potential substrates in plant cell walls. However, since carbohydrate and lignin polymers are connected and structurally ordered in the plant cell walls, the strict division of cellulolysis, hemicellulolysis, pectinolysis and ligninolysis is actually non-natural. Especially, these limits are not clear in reactions involving non-specific oxidative species. Despite that, next chapters will describe the produced proteins and transcribed genes of *P. radiata* for degradation of the major components of wood. The metabolism of the minor wood components like extractives were left to be studied in the future.

4.4.1 Cellulose decomposition

During the six weeks of growth on spruce wood, *P. radiata* produced CAZy GH7 and GH6 cellobiohydrolases (Figure 10). Besides these exoglucanases also several putative endoglucanases were produced such as proteins from CAZy families GH5, GH12 and GH44 as well as transcripts of GH9 and GH45. Several β-glucosidases (families GH1 and GH3) were detected as proteins and transcripts. In accordance to protein and transcript abundances, all these cellulolytic activities were assayed in wood culture protein extracts (**Publication III**). The above mentioned CAZy families are typical for white-rot Agaricomycetes and more expanded than in brown-rot species (Riley et al., 2014).

Cellulolytic CAZymes are present in white-rot fungal transcriptomes and secretomes on various lignocelluloses containing culture media (Hori et al., 2014a, 2014b; MacDonald et al., 2011; Rytioja et al., 2014; Sato et al., 2009; Vanden Wymelenberg et al., 2009; Zhu et al., 2016). The only exception is family GH44 which is not presented in every white-rot Agaricomycetes genome (Riley et al., 2014) and as proteins, these enzymes were reported once in the secretome of *P. brevispora* (Hori et al., 2013).

P. radiata produced also two putative GH131 proteins with transcripts up-regulated on wood. CAZy family GH131 includes proteins with β-glucanase activities which may have also β-1,4-endoglucanase activity as was demonstrated in the Ascomycota species *Podospora anserina* (Lafond et al., 2012). GH131 transcripts

were up-regulated with proteins identified in the Agaricomycetes species *Pycnoporus coccineus* cultivated on pine and aspen wood (Couturier et al., 2015). For *P. radiata* GH131 proteins, their specific enzyme activities remain to be studied.

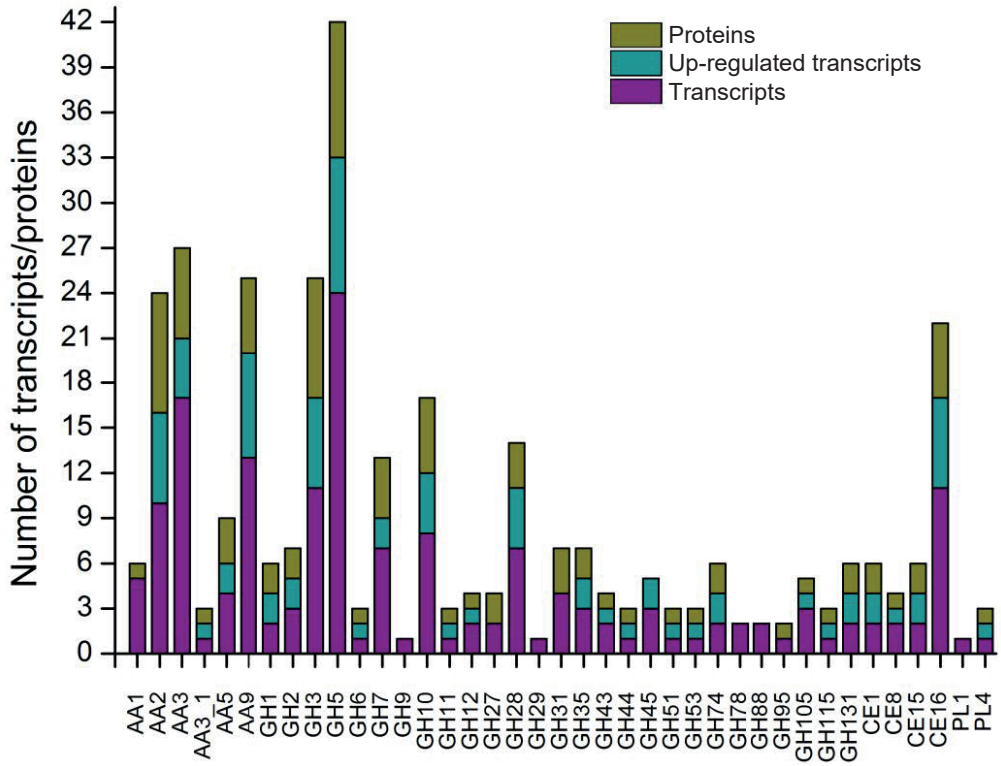

Figure 10. Number of *P. radiata* CAZy auxiliary activity oxidoreductase (AA), glycoside hydrolase (GH), carbohydrate esterase (CE) and polysaccharide lyase (PL) encoding genes important in wood-decay detected as proteins and transcripts, and up-regulated on spruce wood. Values include all proteins identified with with at least two unique peptides mapping per protein. Up-regulated transcripts have a significantly higher level of expression (p-value < 0.05 and $\log_2$-fold change ≥ 1) on wood in both time points (2-week and 4-week) as compared to the malt-extract cultivations. (**Publication III**)

In addition to the GH hydrolases, several proteins of the oxidative cellulose-acting LPMOs (AA9) were produced by *P. radiata* together with one putative CDH (AA3_1) (Figure 10). LPMOs were among the highest up-regulated transcripts on spruce wood. In total, seven of the twelve annotated LPMO-encoding genes were significantly upregulated on wood, whereas five of these were identified as peptides in the proteome. Presence of both CAZy GHs and AAs in the transcriptome and proteome of

P. radiata confirms the importance of a wide array of cellulolytic enzymes, both hydrolytic and oxidative, for complete degradation of wood cellulose. Expression of LPMOs and CDH in wood cultivations is reported for white-rot Agaricomycetes Polyporales species like *C. subvermispora* (Hori et al., 2014a)*, Dichomitus squalens* (Rytioja et al., 2014), *P. gigantea* (Hori et al., 2014b), and *P. coccineus* (Couturier et al., 2015) but not for the order Agaricales species *P. ostreatus* (Fernández-Fueyo et al., 2016). Noticeably, the wood-decay secretomes of Agaricomycetes brown-rot species *Coniophora puteana* (order Boletales) and *Gloeophyllum trabeum* (order Gloeophyllales) (Floudas et al., 2012) include both LPMOs and CDHs, indicating importance of these oxidoreductase enzymes in plant cell wall degradation of Agaricomycetes species with different lifestyles.

When abundances of cellulolytic proteins were studied, it was shown that many cellulose attacking proteins (GH3, GH5, GH6, GH7, CDH) were among the most abundant CAZymes (average abundance) produced (Table 3 in **Publication III**) during the cultivation on spruce wood. Cellulolytic enzymes (net abundances) were constantly produced and were already present in the malt extract inoculum culture (Figure 11) and especially GH3 proteins were highly present. These β-glucosidases may be important in utilizing sugars from malt-extract medium or as pointed out earlier, they may also hydrolyze other substrates intracellularly (Lundell et al., 2014). Although detected as peptides at each time point, the enzymatic activity of CBH was measured on wood starting on week three while β-glucosidase activity was assayed one week earlier (Additional file 3: Figure S2 in **Publication III**) and the levels were correspondent to spruce-supplemented liquid culture values (**Publication I)**. These results indicate active and versatile utilization of wood cellulose by *P. radiata*.

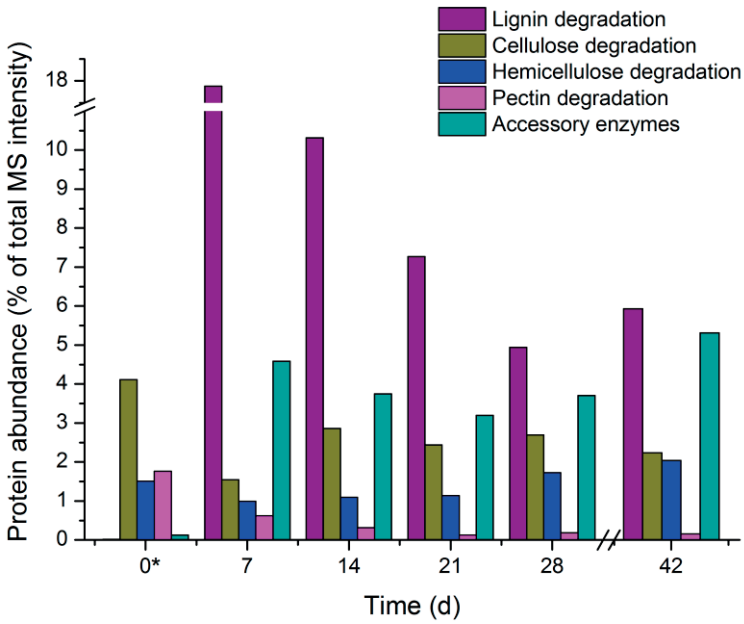

Figure 11. Net abundances of proteins (% of total MS intensity) of *P. radiata* involved in the degradation of various wood components, and H_2O_2-generating accessory enzymes at each time point on spruce wood. *The total proteome at cultivation time point zero is from the inoculum culture on malt extract liquid, and contained approximately 1/10 of the number and amount of proteins detected at later time points. (**Publication III**)

4.4.2 Hemicellulose decomposition

P. radiata produced a great variety of proteins and transcripts putatively important in degrading hemicellulose chains of wood. The activities against the main chain of hemicellulose included proteins and transcripts from CAZy families GH2, GH3, GH5, GH10, GH11 and GH74 (Figure 10). These families include β-1,4-mannosidase, β-1,4-xylosidase, β-1,4-endomannanase, β-1,4-endoxylanase and xyloglucan β-1,4-endoglucanase activities. In addition, several hemicellulose debranching proteins and corresponding transcripts from CAZy families GH27, GH35, GH51, GH95, GH115, CE1, CE15 and CE16 were identified. These families include α-1,4-galactosidase, β-1,4-galactosidase, α-arabinofuranosidase, α-fucosidase, α-glucuronidase, acetyl xylan esterase, glucuronoyl esterase and acetylesterase activities. In addition, members of GH12 (including xyloglucan-specific endoglucanase activities), GH29 (including α-fucosidase activities) and GH43 (including β-1,4-xylosidase activities) were identified from the transcriptome but none of them were up-regulated or found as peptides in the proteome analyses.

Almost all of the above mentioned hemicellulases are identified in secretomes of *P. chrysosporium* on various lignocelluloses (Hori et al., 2011; Manavalan et al., 2011;

Sato et al., 2007; Vanden Wymelenberg et al., 2011, 2009, 2005; Zhu et al., 2016). Only exceptions were the members of families GH29, GH115 and CE16, with no proteins detected although transcripts of *P. chrysosporium* GH115 and CE16 have been identified on spruce wood cultures (Korripally et al., 2015). The only putative GH29 gene detected from *P. radiata* transcriptome is an interesting candidate for future studies, because the annotated genome of *P. chrysosporium* does not include this gene, and the nearest protein homolog (best blastP hit) is from a predicted *H. irregulare* GH29 gene, which has been proposed to be important in colonizing fresh wood (Olson et al., 2012). Another gene present and expressed in *P. radiata* but absent from some of the genomes of white-rot Agaricomycetes and from all brown-rot genomes, is a gene encoding a putative GH11 enzyme, which may present β-1,4-endoxylanase activity (Rytioja et al., 2014).

From hemicellulose-attacking activities, only CE16 and GH10 proteins were among the most abundant CAZy enzymes during the six week period on wood (Table 3 in **Publication III**). In a previous secretome study of *P. ostreatus*, a CE16 acetylesterase was shown to be highly overproduced in lignocellulose-containing cultures (Fernández-Fueyo et al., 2016). The relative abundances of all hemicellulose-degrading enzymes increased during the active growth of *P. radiata* on spruce wood (Figure 11). Although enzymes important in xylan degradation such as GH10 and GH11 proteins were detected as peptides from week one to six, xylanase activity was detected only at time points of one, four and six weeks (Additional file 3: Figure S2 in **Publication III**). Similar cyclic xylanolytic enzyme activity has been measured for *P. radiata* on wheat bran lignocellulose medium (Rogalski et al., 2001).

These results confirmed the wide hemicellulase repertoire utilized by *P. radiata* as suggested by the earlier enzyme activity and protein purification studies on this organism (Mierzwa et al., 2005; Prendecka et al., 2007, 2003, Rogalski et al., 2001, 1993a). During the six weeks on wood, *P. radiata* actively produced enzymes to degrade potential ester and covalent bonds between hemicellulose and lignin units, and against the hemicellulose polymers. Since an array of CAZymes against both glucomannan and xylan-type of hemicelluloses were produced it seems that *P. radiata* is adapted to grow on various types of hemicellulose-containing substrates.

4.4.3 Pectin decomposition

During the cultivation on wood, *P. radiata* produced few proteins putatively important in pectin decomposition of CAZy families GH28, GH53, GH105, CE8 and PL4 (Figure 10). These families include polygalacturonase, β-1,4-endogalactanase, rhamnogalacturonan hydrolase, pectin methyl esterase and rhamnogalacturonan lyase enzyme activities (Rytioja et al., 2014). The overall abundance of these proteins was low and the abundance decreased during the cultivation showing the importance of

pectin degradation at the beginning (Figure 11). This is in agreement with the suggested role of pectinases in promoting the initial phase of fungal wood-decay and assisting in hyphal colonization of wood (Green et al., 1996). In the present study, especially the GH28 transcripts were significantly differentially expressed (p-value < 0.01 and $\log_2$-fold change ≥ 2) on wood compared to malt extract, illustrating their importance at least in degradation of coniferous softwood. Previous studies have shown divergent results on change in GH28 gene expression in fungal cultures on softwood versus hardwood. In studies of the white-rot phlebioid species *P. carnosa* (MacDonald et al., 2011) and Agaricomycetes polyporoid brown-rot species *Postia placenta* (Vanden Wymelenberg et al., 2011) which both colonize softwood in nature, higher expression of GH28 transcripts on softwood than hardwood was demonstrated. Although expression was induced in wood substrates, no change was observed in the study of the white-rot species *P. coccineus* (Couturier et al., 2015).

4.4.4 Lignin modification

4.4.4.1 Lignin-modifying enzymes expressed on spruce

During the six week cultivation *P. radiata* produced several class-II peroxidases belonging to CAZy family AA2 (Figure 10). The proteome included four LiPs (LiP1-4) together with three long-MnPs (MnP1-2, 6) and one short-MnP (MnP3). Trancriptome study was able to detect two additional short-MnPs (MnP4-5). From these ten genome annotated class-II peroxidase-encoding genes, three LiPs (LiP1-3) and three MnPs (MnP1-3) were up-regulated on both time-points (two and four weeks) on spruce wood. Actually, these were the same isoenzymes as detected from previous cultivations of *P. radiata* (Lundell and Hatakka, 1994; Moilanen et al., 1996; Niku-Paavola et al., 1988). These proteins were also the most abundant on spruce wood and therefore seemingly the main enzymes used by the fungus for lignin degradation.

With the help of genome and transcriptome sequencing, it was possible to detect the LiP2 transcripts for the first time adding up to the protein that was previously identified on liquid medium and lignocellulose cultivations (Lundell and Hatakka, 1994; Niku-Paavola et al., 1988; Vares et al., 1995). Similar to long-MnP1, long-MnP6 and the short-MnP4-5 transcripts and gene sequences were the first time identified in the present study. Of these, MnP1 (previously MnPx) was most likely previously purified from glucose containing cultures (Lundell and Hatakka, 1994; Moilanen et al., 1996).

The MnP enzyme activities were detected in every time point and the activity levels were similar as in **Publication I** (Additional file 3: Figure S2 in **Publication III**). Previous studies of *P. radiata* grown in various semi-solid cultivations indicate that production of the lignin-modifying peroxidases is promoted

on wood (Mäkelä et al., 2013). The role of these peroxidases was significant also in the present study since several MnPs and LiPs proteins were included in the list of most abundant proteins and were highly up-regulated as transcripts. Abundance of these peroxidases was at high levels after one week of growth on wood but in the course of the cultivation the abundances were decreasing (Figure 11) mainly due to the sharper decline in LiP abundances, similarly to as was observed in *P. carnosa* (MacDonald and Master, 2012). From the lignin peroxidases, only LiP1 peptides were detected at the last time point on week six. In addition, compared to proteins taking part in polysaccharide degradation, the lignin-modifying peroxidases were not highly abundant in the malt-extract inoculum of *P. radiata* (Figure 11) thus further illustrating that expression and production of the AA2 peroxidases was promoted on wood.

The several MnP enzymes were more constantly produced or present as proteins in the course of the six week's growth on wood, and the abundance of one long-MnP (MnP2) was even increasing during the cultivation. The long-MnPs and LiPs are restricted to the genomes of Polyporales species, while short-MnPs are more widely spread in the Agaricomycetes (Floudas et al., 2012; Ruiz-Dueñas et al., 2013). The short-MnPs have shorter C-terminal tail than the traditional MnPs first described from *P. chrysosporium* (Hildén et al., 2005; Sundaramoorthy et al., 2005). According to the results of this study, especially the long-MnPs and LiPs seem to be highly produced on spruce wood. In addition, one short-MnP (MnP3) was highly abundant after the first week on wood but in the course of the cultivation, the abundance was decreasing similarly to LiPs. Moreover, short-MnP3 possesses some Mn-independent (together with Mn^{2+}-oxidizing) ability to oxidize phenols and dyes but inability to oxidize veratryl alcohol (Lundell et al., 2016). Since no VP-encoding genes were identified in the genome of *P. radiata* (to be published elsewhere) or *P. brevispora* (Ruiz-Dueñas et al., 2013), the short-MnPs like MnP3 may be complementary to VPs. The evolutionary path of VPs from short-MnPs is evident and they share a very high degree of protein and gene homology (Ruiz-Dueñas et al., 2013). The results suggest also that MnP3 has a different role in wood-decay compared to the other short-MnPs of *P. radiata*.

4.4.4.2 Additional enzymes involved in lignin-modification

In addition to the class-II peroxidases recognized in *P. radiata*, one DyP transcript was detected. The DyP-encoding gene was up-regulated on wood at the two week time point but no corresponding peptides were detected in the proteome. High production of DyP-proteins and transcripts by another species of the phlebioid clade, *Phlebiopsis gigantea*, was detected on pine wood (Hori et al., 2014b). However, class-II peroxidases were absent in the wood-cultivation secretome of *P. gigantea* suggesting fairly different strategy to colonize wood and bypass the lignin barrier compared to

P. radiata. This implies that various strategies for wood and lignocellulose degradation exist among the different clades among phlebioid fungi.

On the contrary to the coherence of existence and expression of majority of the ten class-II peroxidases in both the transcriptome and proteome of *P. radiata*, laccase gene responses were very different. Transcriptome analysis of *P. radiata* detected five distinct laccase genes transcribed on spruce wood but none of the genes were up-regulated, and only one of them (Lacc1) was found as peptides in the proteome samples. Similarly laccase activity was detected in every time points. In the previous cultivations of *P. radiata* in liquid media and on solid lignocellulose, Lacc1 was identified as the main secreted laccase protein (Lundell and Hatakka, 1994; Lundell et al., 1990; Mäkelä et al., 2013; Mäkelä et al., 2006; Niku-Paavola et al., 1988; Vares et al., 1995). Thus, Lacc1 seems to be part of *P. radiata* secretome regardless of the culture medium and carbon source, indicating constant gene expression.

The accessory enzymes belonging to CROs and GMC oxidoreductases were providing H_2O_2 mainly for the peroxidases during the wood cultivation (Figure 11). The main protein of this group was a glyoxal oxidase (AA5_1) which was one of the most abundant proteins identified in the proteome samples. CRO-encoding genes of *P. radiata* were previously unknown. Corresponding proteins with GLOX-like activity were purified from cultivations on wheat straw (Vares et al., 1995), and on glucose with high Mn^{2+} supplementation (Moilanen et al., 1996). Taken together, the combined expression of H_2O_2-producing enzymes together with H_2O_2-consuming peroxidase proteins is similar as suggested for *P. chrysosporium* (Hammel et al., 1994; Kersten, 1990).

In addition, GMC aryl-alcohol oxidases (AA3) were detected as transcripts and proteins confirming the previous enzyme activity results from a different isolate of *P. radiata* than 79 grown on beech wood (Liers et al., 2011). In accordance, several putative transcripts of other GMC oxidoreductases including an aryl-alcohol dehydrogenase and various alcohol oxidases were detected. These results suggest that besides a strong ability for extracellular enzymatic production of H_2O_2, active intracellular transformation of lignin-derived compounds is on-going in *P. radiata* hyphae likewise is indicated for *P. chrysosporium* on wood (Korripally et al., 2015). The recycling of lignin-derived compounds may also be connected to synergistic oxidoreductase action for electron transfer to LPMOs thereby enhancing degradation of cellulose and hemicellulose as is currently suggested by Kracher et al. (2016).

4.4.4.3 Changes in spruce wood structure and lignin composition

It appears that during the six weeks of growth on spruce wood, the up-regulated expression of a versatile repertoire of the CAZy extracellular enzymes of *P. radiata* degrade wood cell walls (Figure 12) and modify the wood components. Particular

attention was addressed to changes in lignin composition because of the known ability of *P. radiata* to effectively oxidize and degrade lignin and lignin model compounds. However, after six weeks, no apparent release of lignin decomposition products were detected since the Klason lignin content and total yield of aromatic compounds released by pyrolysis were not critically affected (**Publication III**). One explanation for this may be that more evident decrease of total lignin could have been detected after even more prolonged cultivation since earlier studies on the same fungus demonstrate delignification after ten weeks of cultivation on spruce (Hakala et al., 2004). Lignin substructures are nevertheless affected by *P. radiata* 79 which is seen as decrease of the amount of phenylpropane units and increase in the number of oligomeric and monomeric phenols together with phenolic compounds such as coniferyl aldehyde and vanillin. These results suggest that non-phenolic structures in spruce lignin are affected and that due to this and concomitant protein existence, most probably, the several LiPs of *P. radiata* have an important role in the degradation processes.

The term 'selective white-rot' has been presented in several studies, and it refers to a specific type of white-rot fungal decay of wood in which hemicellulose and lignin are degraded preferentially, leaving most of wood cell wall cellulose intact. Another decay type is 'simultaneous white-rot' where all wood cell -wall polymers are degraded somewhat simultaneously in the course of fungal growth in wood (Blanchette, 1984; Eriksson et al., 1990). A few Agaricomycetes species of the Polyporales order such as *C. subvermispora, Obba (Physisporinus) rivulosa* and *D. squalens* are referred as selective wood-decayers (Fackler et al., 2006; Hakala et al., 2004; Hatakka and Hammel, 2010).

P. radiata has also been suggested to belong to the selective white-rot group of fungi (Ander and Eriksson, 1977; Fackler et al., 2006). In the present study, the microscopic changes of spruce wood after six weeks of hyphal growth of *P. radiata* were studied. The wood-decay of *P. radiata* proceeded from the inside cell lumen towards middle lamellae since thinning and increased porosity of wood cell walls was observed (Figure 12A). The fungal hyphae were observed to be attached to the wood cell walls from the lumen side (Figure 12B). These results suggest that *P. radiata* utilizes a simultaneous degradation pattern of wood polymers when growing on spruce wood. Selectivity in fungal wood-decay may also depend upon the cultivation time, growth temperature and tree species (Hatakka and Hammel, 2010).

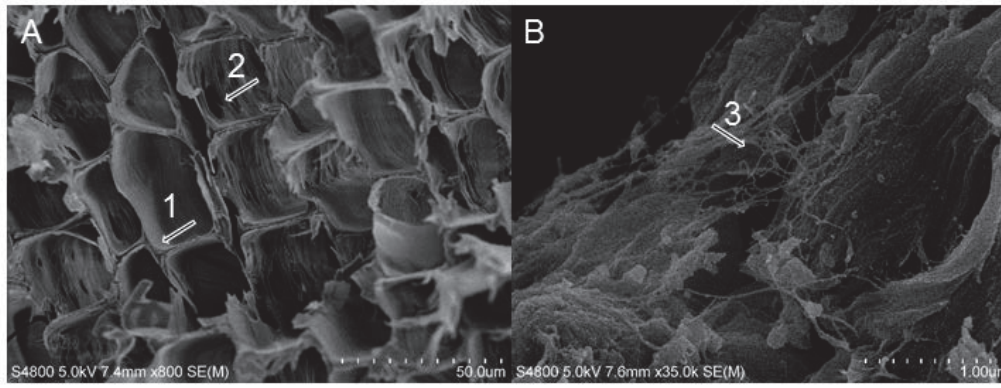

Figure 12. FE-SEM images of Norway spruce wood after six weeks of growth of *P. radiata*. A) Transverse section of wood with arrows pointing 1) thinned secondary wall and 2) enlarged pit. B) Transverse section pointing to 3) hyphae inside the trancheids. Pictures are taken by M. Kemell.

5 Conclusions

In this PhD thesis, the taxonomic positioning of *P. radiata* in the phlebioid clade of the fungal systematic order Polyporales was confirmed, and the fungal species composition of *Phlebia sensu stricto* group was proposed. In addition, it was confirmed that fungi with species name *Phlebia* are found in most of the currently recognized lineages of the phlebioid clade demonstrating the need for additional isolate sampling and possible nomenclatural changes.

After studying the enzyme production of several species-level groups of *Phlebia* and phlebioid fungi, it was demonstrated that the lignocellulose-converting enzyme phenotypes were different. The *Phlebia* isolates were clustered in several different enzyme production patterns which may be a result of variations in enzyme production efficiencies in nature and predict differences in their strategies to degrade various types of lignocelluloses.

In the semi-solid spruce wood cultivations, it was observed that *P. radiata* species group produced the highest lignin-modifying oxidoreductase activities while cellulolytic enzyme activities were low. Similar enzyme production pattern was observed while *P. radiata* 79 was cultivated as solid-state cultures on spruce wood. On spruce wood, there is a clear pattern on timing for CAZy enzyme expression: at first on wood, *P. radiata* expresses a set of lignin-attacking class-II peroxidases together with hydrogen peroxide producing glyoxal oxidases and aryl-alcohol oxidases, together with lytic polysaccharide mono-oxygenases. The oxidative pattern is then followed with expression of a wide array of hydrolytic CAZys, and the oxidoreductases and hydrolytic enzymes are expressed and operating in collaboration for several weeks. Moreover, lignin-modifying enzymes were abundant in the proteome and lignin substructures were affected, which implies more lignin-attacking fungal activity in the initiation stage of wood colonization. In addition, the microscopic investigation suggested simultaneous degradation of wood cell walls indicating that secreted enzymes are actively degrading their substrates.

It can be concluded that white-rot fungal wood-decay includes complex and synergistic enzyme production. As *P. radiata* and other white-rot fungal species colonize variable host species with different compositions of cellulose, hemicellulose, lignin and pectin in nature, they need to produce wide array of enzymes and efficient degradation is dependent of the right combination.

The genome sequencing of *P. radiata* included sequencing and characterizing of mitochondrial genome. Although having conserved core gene content, the mitochondrial genomes were shown to have variation in size and gene order. The results of this study contributed to demonstrating the mitochondrial genome enlargement of Agaricomycotina which is mainly result of expansion of non-coding

proportion. Similarly, mitogenomes were shown to allow continuous and adaptive modifications.

The results of this PhD thesis, the mitochondrial genome, the on-going annotation of the nuclear genome and availability of CAZy genes of *P. radiata* will facilitate further studies on fungal physiology and wood-decay mechanisms. In addition, the transcripts encoding core metabolic proteins and the detected proteins with unknown functions are potential targets for future studies. Moreover, the 152 new fungal systematic marker sequences of culture collection isolates will aid in understanding the fungal diversity in various habitats in environmental studies.

6 Acknowledgements

This thesis work was carried out at the Division of Microbiology and Biotechnology, Department of Food and Environmental Sciences, University of Helsinki. The financial support provided by Academy of Finland Ox-Red research project (grant 138331), The Doctoral Programme in Microbiology and Biotechnology (MBDP), The Niemi Foundation and University of Helsinki is greatly appreciated. The Viikki Graduate School in Molecular Biosciences (VGSB) is thanked for the 'Matching Funds' position.

I wish to thank my supervisors for providing valuable scientific advices, support and encouragement during this study. I sincerely thank my main supervisor docent Taina Lundell for giving me the opportunity to work in her group. I appreciate the trust you gave me during this study and all the inspiring discussions we have had. I am grateful to Dr. Miia Mäkelä for guiding me in writing and in the lab. I thank docent Ilona Oksanen, your knowledge on phylogeny has been of great help.

I warmly thank my other coauthors, Petri Auvinen, Jarkko Isotalo, Marianna Kemell, Pia Laine, Sini Miettinen, Mari Mäkinen née Häkkinen, Paula Nousiainen, Lars Paulin, Heikki Salavirta, Olli-Pekka Smolander and Fitsum Tamene, for their contribution. Especially, I would like to thank Dr. Mari Mäkinen for all the help in the finalizing step of this study.

Prof. Jarkko Hantula and Assoc. Prof. Tomas Johansson are thanked for their valuable suggestions to improve this thesis. I thank Prof. Annele Hatakka and docent Petri Auvinen for the helpful comments and suggestions during my thesis committee meetings.

I am very thankful to all present and former members of the Lignin group, other members of MIB division and the members of TL group. During these years, I have been fortunate to work with wonderful people. I would especially like to thank Johanna, Suvi, Minna, Outi, Anu, Mari, Grit and Mila for their friendship and support during my studies.

This journey could not have been possible without my family and friends. I thank my mother, brother, sisters and their families for all their love, understanding and believing in me. I also warmly thank my other family in Merikarvia. My deepest thanks belong to my husband Risto for endless encouragement and for always being there for me. Finally, my little Valtteri, thank you for your supportive warm hugs and for filling my life with joy and happiness.

Jaana

Helsinki, August 2016

7 References

Adams, K.L., Palmer, J.D., 2003. Evolution of mitochondrial gene content: Gene loss and transfer to the nucleus. Mol. Phylogenet. Evol. 29, 380–395.

Adav, S.S., Ravindran, A., Sze, S.K., 2012. Quantitative proteomic analysis of lignocellulolytic enzymes by *Phanerochaete chrysosporium* on different lignocellulosic biomass. J. Proteomics 75, 1493–1504.

Agger, J.W., Isaksen, T., Várnai, A., Vidal-Melgosa, S., Willats, W.G.T., Ludwig, R., Horn, S.J., et al., 2014. Discovery of LPMO activity on hemicelluloses shows the importance of oxidative processes in plant cell wall degradation. Proc. Natl. Acad. Sci. U. S. A. 111, 6287–6292.

Aguileta, G., De Vienne, D.M., Ross, O.N., Hood, M.E., Giraud, T., Petit, E., Gabaldón, T., 2014. High variability of mitochondrial gene order among fungi. Genome Biol. Evol. 6, 451–465.

Ander, P., Eriksson, K.-E., 1977. Selective degradation of wood components by white-rot fungi. Physiol. Plant. 41, 239–248.

Antico Arciuch, V.G., Elguero, M.E., Poderoso, J.J., Carreras, M.C., 2012. Mitochondrial regulation of cell cycle and proliferation. Antioxid. Redox Signal. 16, 1150–1180.

Arantes, V., Jellison, J., Goodell, B., 2012. Peculiarities of brown-rot fungi and biochemical Fenton reaction with regard to their potential as a model for bioprocessing biomass. Appl. Microbiol. Biotechnol. 94, 323–338.

Arantes, V., Milagres, A.M.F., Filley, T.R., Goodell, B., 2011. Lignocellulosic polysaccharides and lignin degradation by wood decay dungi: the relevance of nonenzymatic Fenton-based reactions. J. Ind. Microbiol. Biotechnol. 38, 541–555.

Arora, D.S., Sharma, R.K., 2011. Effect of different supplements on bioprocessing of wheat straw by *Phlebia brevispora*: changes in its chemical composition, in vitro digestibility and nutritional properties. Bioresour. Technol. 102, 8085–8091.

Baldrian, P., 2006. Fungal laccases-occurrence and properties. FEMS Microbiol. Rev. 30, 215–242.

Basse, C.W., 2010. Mitochondrial inheritance in fungi. Curr. Opin. Microbiol. 13, 712–719.

Beeson, W.T., Vu, V.V., Span, E.A., Phillips, C.M., Marletta, M.A., 2014. Cellulose degradation by polysaccharide monooxygenases. Annu. Rev. Biochem. 84, 150317182619002.

Benoit, I., Coutinho, P.M., Schols, H.A, Gerlach, J.P., Henrissat, B., de Vries, R.P., 2012. Degradation of different pectins by fungi: correlations and contrasts between the pectinolytic enzyme sets identified in genomes and the growth on pectins of different origin. BMC Genomics 13, 321.

Benoit, I., Culleton, H., Zhou, M., DiFalco, M., Aguilar-Osorio, G., Battaglia, E., Bouzid, O., et al., 2015. Closely related fungi employ diverse enzymatic strategies to degrade plant biomass. Biotechnol. Biofuels 8, 107.

Berlin, A., Balakshin, M., Gilkes, N., Kadla, J., Maximenko, V., Kubo, S., Saddler, J., 2006. Inhibition of cellulase, xylanase and β-glucosidase activities by softwood lignin preparations. J. Biotechnol. 125, 198–209.

Bertaud, F., Holmbom, B., 2004. Chemical composition of earlywood and latewood in Norway spruce heartwood, sapwood and transition zone wood. Wood Sci. Technol. 38, 245–256.

Bi, X., Liu, L.F., 1996. DNA rearrangement mediated by inverted repeats. Proc. Natl. Acad. Sci. 93, 819–823.

Binder, M., Hibbett, D.S., Larsson, K.-H., Larsson, E., Langer, E., Langer, G., 2005. The phylogenetic distribution of resupinate forms across the major clades of mushroom-forming fungi (Homobasidiomycetes). Syst. Biodivers. 3, 113–157.

Binder, M., Justo, A., Riley, R., Salamov, A., Lopez-Giraldez, F., Sjökvist, E., Copeland, A., et al., 2013. Phylogenetic and phylogenomic overview of the Polyporales. Mycologia 105, 1350–1373.

Blackwell, M., 2011. The fungi: 1, 2, 3 ... 5.1 million species? Am. J. Bot. 98, 426–438.

Blackwell, M., Hibbett, D.S., Taylor, J.W., Spatafora, J.W., 2007. Research coordination networks: a phylogeny for kingdom Fungi (Deep Hypha). Mycologia 98, 829–837.

Blanchette, R.A., 1984. Screening wood decayed by white rot fungi for preferential lignin degradation. Appl. Environ. Microbiol. 48, 647–653.

Blanchette, R., Krueger, E., Haight, J., 1997. Cell wall alterations in loblolly pine wood decayed by the white-rot fungus, *Ceriporiopsis subvermispora*. J. Biotechnol. 53, 203–213.

Boerjan, W., Ralph, J., Baucher, M., 2003. Lignin biosynthesis. Annu. Rev. Plant Biol. 54, 519–546.

Bonnarme, P., Jeffries, T.W., 1990. Mn(II) regulation of lignin peroxidases and manganese-dependent peroxidases from lignin-degrading white rot fungi. Appl. Environ. Microbiol. 56, 210–217.

Brandley, M.C., Bragg, J.G., Singhal, S., Chapple, D.G., Jennings, C.K., Lemmon, A.R., Lemmon, E.M.,et al., 2015. Evaluating the performance of anchored hybrid enrichment at the tips of the tree of life: a phylogenetic analysis of Australian Eugongylus group scincid lizards. BMC Evol. Biol. 15, 62.

Bule, M.V., Chaudhary, I., Gao, A.H., Chen, S., 2016. Effects of extracellular proteome on wheat straw pretreatment during solid-state fermentation of *Phlebia radiata* ATCC 64658. Int. Biodeterior. Biodegradation 109, 36–44.

Bullerwell, C.E., Lang, B.F., 2005. Fungal evolution: the case of the vanishing mitochondrion. Curr. Opin. Microbiol. 8, 362–369.

Caffall, K.H., Mohnen, D., 2009. The structure, function, and biosynthesis of plant cell wall pectic polysaccharides. Carbohydr. Res. 344, 1879–1900.

Campoy, S., Alvarez-Rodríguez, M.L., Recio, E., Rumbero, A., Coque, J.-J.R., 2009. Biodegradation of 2,4,6-TCA by the white-rot fungus *Phlebia radiata* is initiated by a phase I (O-demethylation)-phase II (O-conjugation) reactions system: implications for the chlorine cycle. Environ. Microbiol. 11, 99–110.

Chan, D.C., 2006. Mitochondria: Dynamic Organelles in Disease, Aging, and Development. Cell 125, 1241–1252.

Chang, Y., Wang, S., Sekimoto, S., Aerts, A.L., Choi, C., Clum, A., LaButti, K.M., et al., 2015. Phylogenomic analyses indicate that early Fungi evolved digesting cell walls of algal ancestors of land plants. Genome Biol. Evol. 7, 1590–1601.

Christopher, L.P., Yao, B., Ji, Y., 2014. Lignin biodegradation with laccase-mediator systems. Front. Energy Res. 2, 1–13.

Contreras, L., Drago, I., Zampese, E., Pozzan, T., 2010. Mitochondria: The calcium connection. Biochim. Biophys. Acta 1797, 607–618.

Courtade, G., Wimmer, R., Røhr, Å.K., Preims, M., Felice, A.K.G., Dimarogona, M., Vaaje-Kolstad, G., et al., 2016. Interactions of a fungal lytic polysaccharide monooxygenase with β-glucan substrates and cellobiose dehydrogenase. Proc. Natl. Acad. Sci. 113, 5922-5927.

Couturier, M., Navarro, D., Chevret, D., Henrissat, B., Piumi, F., Ruiz-Dueñas, F.J., Martinez, A.T., et al., 2015. Enhanced degradation of softwood versus hardwood by the white-rot fungus *Pycnoporus coccineus*. Biotechnol. Biofuels 8, 216.

Crowther, T.W., Glick, H.B., Covey, K.R., Bettigole, C., Maynard, D.S., Thomas, S.M., Smith, J.R., et al., 2015. Mapping tree density at a global scale. Nature 525, 201–205.
Cullen, D., 2013. Wood decay, in: Martin, F. (Ed.), The ecological genomics of fungi. John Wiley & Sons, Inc, Hoboken, NJ, USA, pp. 43–62.
Daniel, G., Volc, J., Niku-Paavola, M.-L., 2004. Cryo-FE-SEM & TEM immuno-techniques reveal new details for understanding white-rot decay of lignocellulose. C. R. Biol. 327, 861–871.
de Koker, T.H., Nakasone, K.K., Haarhof, J., Burdsall, H.H., Janse, B.J.H., 2003. Phylogenetic relationships of the genus *Phanerochaete* inferred from the internal transcribed spacer region. Mycol. Res. 107, 1032–1040.
de Vries, R.P., Visser, J., 2001. *Aspergillus* enzymes involved in degradation of plant cell wall polysaccharides. Microbiol. Mol. Biol. Rev. 65, 497–522.
Diorio, L., Galati, B., García, M.A., Papinutti, L., 2009. Degradation of pruning wastes by *Phanerochaete sordida* growing in SSF: Ultrastructural, chemical, and enzymatic studies. Int. Biodeterior. Biodegradation 63, 19–23.
Dresler-Nurmi, A., Kaijalainen, S., Lindström, K., Hatakka, A., 1999. Grouping of lignin degrading corticioid fungi based on RFLP analysis of 18S rDNA and ITS regions. Mycol. Res. 103, 990–996.
Dutton, M. V., Evans, C.S., 1996. Oxalate production by fungi: its role in pathogenicity and ecology in the soil environment. Can. J. Microbiol. 42, 881–895.
Eastwood, D.C., Floudas, D., Binder, M., Majcherczyk, A., Schneider, P., Aerts, A., Asiegbu, F.O., et al., 2011. The plant cell wall-decomposing machinery underlies the functional diversity of forest fungi. Science 333, 762–765.
Eriksson, K.-E., Blanchette, R.A., Ander, P., 1990. Microbial and enzymatic degradation of wood and wood components. Springer-Verlag, Berlin, Germany. 407 p.
Fackler, K., Gradinger, C., Hinterstoisser, B., Messner, K., Schwanninger, M., 2006. Lignin degradation by white rot fungi on spruce wood shavings during short-time solid-state fermentations monitored by near infrared spectroscopy. Enzyme Microb. Technol. 39, 1476–1483.
Faircloth, B.C., McCormack, J.E., Crawford, N.G., Harvey, M.G., Brumfield, R.T., Glenn, T.C., 2012. Ultraconserved elements anchor thousands of genetic markers spanning multiple evolutionary timescales. Syst. Biol. 61, 717–726.
Férandon, C., Xu, J., Barroso, G., 2013. The 135 kbp mitochondrial genome of *Agaricus bisporus* is the largest known eukaryotic reservoir of group I introns and plasmid-related sequences. Fungal Genet. Biol. 55, 85–91.
Fernández-Fueyo, E., Ruiz-Dueñas, F.J., López-Lucendo, M.F., Pérez-Boada, M., Rencoret, J., Gutiérrez, A., Pisabarro, A.G., et al., 2016. A secretomic view of woody and nonwoody lignocellulose degradation by *Pleurotus ostreatus*. Biotechnol. Biofuels 9, 49.
Fernández-Fueyo, E., Ruiz-Dueñas, F.J., Miki, Y., Martínez, M.J., Hammel, K.E., Martínez, A.T., 2012. Lignin-degrading peroxidases from genome of selective ligninolytic fungus *Ceriporiopsis subvermispora*. J. Biol. Chem. 287, 16903–16916.
Ferreira, P., Carro, J., Serrano, A., Martínez, A.T., 2015. A survey of genes encoding H_2O_2-producing GMC oxidoreductases in 10 Polyporales genomes. Mycol. 107, 1105–1119.
Ferreira, P., Medina, M., Guillén, F., Martínez, M.J., Van Berkel, W.J.H., Martínez, A.T., 2005. Spectral and catalytic properties of aryl-alcohol oxidase, a fungal flavoenzyme acting on polyunsaturated alcohols. Biochem. J. 389, 731–738.
Floudas, D., Binder, M., Riley, R., Barry, K., Blanchette, R.A., Henrissat, B., Martínez, A.T., et al., 2012. The Paleozoic origin of enzymatic lignin decomposition reconstructed from 31 fungal genomes. Science 336, 1715–1719.

Floudas, D., Held, B.W., Riley, R., Nagy, L.G., Koehler, G., Ransdell, A.S., Younus, H., et al., 2015. Evolution of novel wood decay mechanisms in Agaricales revealed by the genome sequences of *Fistulina hepatica* and *Cylindrobasidium torrendii*. Fungal Genet. Biol. 76, 78–92.

Floudas, D., Hibbett, D.S., 2015. Revisiting the taxonomy of *Phanerochaete* (Polyporales, Basidiomycota) using a four gene dataset and extensive ITS sampling. Fungal Biol. 119, 679–719.

Foury, F., 1998. The complete sequence of the mitochondrial genome of *Saccharomyces cerevisiae*. FEBS Lett. 440, 325–331.

Galkin, S., Vares, T., Kalsi, M., Hatakka, A., 1998. Production of organic acids by different white-rot fungi as detected using capillary zone electrophoresis. Biotechnol. Tech. 12, 267–271.

Gardes, M., Bruns, T.D., 1993. ITS primers with enhanced specificity for basidiomycetes, application to the identification of mycorrihiza and rusts. Mol. Ecol. 2, 113-118.

Gaskell, J., Marty, A., Mozuch, M., Kersten, P.J., Splinter BonDurant, S., Sabat, G., Azarpira, A., et al., 2014. Influence of *Populus* genotype on gene expression by the wood decay fungus *Phanerochaete chrysosporium*. Appl. Environ. Microbiol. 80, 5828–5835.

Gerhold, J.M., Aun, A., Sedman, T., Joers, P., Sedman, J., 2010. Strand invasion structures in the inverted repeat of *Candida albicans* mitochondrial DNA reveal a role for homologous recombination in replication. Mol. Cell 39, 851–861.

Giardina, P., Faraco, V., Pezzella, C., Piscitelli, A., Vanhulle, S., Sannia, G., 2010. Laccases: A never-ending story. Cell. Mol. Life Sci. 67, 369–385.

Gilbertson, R.R., 1980. Wood-rotting fungi of North America. Mycologia 72, 1–49.

Green, F., Kuster, T.A., Highley, T.L., 1996. Pectin degradation during colonization of wood by brown-rot fungi. Recent Res. Dev. Plant Pathol. 1, 83–93.

Greslebin, A., Nakasone, K.K., Rajchenberg, M., 2004. *Rhizochaete*, a new genus of phanerochaetoid fungi. Mycologia 96, 260–271.

Grigoriev, I. V., Cullen, D., Goodwin, S.B., Hibbett, D., Jeffries, T.W., Kubicek, C.P., Kuske, C., et al., 2011. Fueling the future with fungal genomics. Mycol. An Int. J. fungal Biol. 2, 192–209.

Grigoriev, I. V, Nikitin, R., Haridas, S., Kuo, A., Ohm, R., Otillar, R., Riley, R., et al., 2014. MycoCosm portal: gearing up for 1000 fungal genomes. Nucleic Acids Res. 42, 699–704.

Gutiérrez, A., Babot, E.D., Ullrich, R., Hofrichter, M., Martínez, A.T., del Río, J.C., 2011. Regioselective oxygenation of fatty acids, fatty alcohols and other aliphatic compounds by a basidiomycete heme-thiolate peroxidase. Arch. Biochem. Biophys. 514, 33–43.

Gutiérrez, A., del Río, J.C., Martínez-íñigo, M.J., Martínez, M.J., Martínez, A.T., 2002. Production of new unsaturated lipids during wood decay by ligninolytic Basidiomycetes. Appl. Environ. Microbiol. 68, 1344–1350.

Hakala, T.K., Maijala, P., Konn, J., Hatakka, A., 2004. Evaluation of novel wood-rotting polypores and corticioid fungi for the decay and biopulping of Norway spruce (*Picea abies*) wood. Enzyme Microb. Technol. 34, 255–263.

Halpin, C., 2013. Cell biology: Up against the wall. Curr. Biol. 23, 1048–1050.

Hammel, K., Mozuch, M.D., Jensen, K.A., Kersten, P.J., 1994. Recycling during oxidation of the arylglycerol *p*-aryl ether lignin structure. Biochemistry 33, 13349–13354.

Hammel, K.E., Cullen, D., 2008. Role of fungal peroxidases in biological ligninolysis. Curr. Opin. Plant Biol. 11, 349–355.

Hammel, K.E., Jensen, K.A., Mozuch, M.D., Landucci, L.L., Tien, M., Pease, E.A., 1993. Ligninolysis by a purified lignin peroxidase. J. Biol. Chem. 268, 12274–12281.

Hatakka, A., 1994. Lignin-modifying enzymes from selected white-rot fungi: Production and role in lignin degradation. FEMS Microbiol. Rev. 13, 125–135.

Hatakka, A., 2001. Biodegradation of lignin. Can. J. Bot. 73, 1011–1018.
Hatakka, A., Hammel, K.E., 2010. Fungal biodegradation of lignocelluloses, in: Hofrichter, M. (Ed.), Industrial applications, 2nd edn. The Mycota X. Springer, Berlin, Germany, pp. 319–340.
Hatakka, A.I., Lundell, T.K., Tervila-Wilo, A.L.M., Brunow, G., 1991. Metabolism of non-phenolic β-O-4 lignin model compounds by the white-rot fungus *Phlebia radiata*. Appl. Microbiol. Biotechnol. 36, 270–277.
Hatakka, A.I., Uusi-Rauva, A.K., 1983. Degradation of ^{14}C-labelled poplar wood lignin by selected white-rot fungi. Appl. Microbiol. Biotechnol. 17, 235–242.
Henriksson, G., Johansson, G., Pettersson, G., 2000. A critical review of cellobiose dehydrogenases. J. Biotechnol. 78, 93–113.
Hibbett, D.S., 2007. After the gold rush, or before the flood? Evolutionary morphology of mushroom-forming fungi (Agaricomycetes) in the early 21st century. Mycol. Res. 111, 1001–1018.
Hibbett, D.S., Bauer, R., Binder, M., Gianchini, A.J., Hosaka, K., Justo, A., Larsson, E.,et al., 2014. Agaricomycetes, in: McLaughlin, D.J., Spatafora, J.W. (Eds.), The mycota VII systematics and evolution Part A. Springer-Verlag, Berlin, Germany, pp. 373–447.
Hibbett, D.S., Binder, M., Bischoff, J.F., Blackwell, M., Cannon, P.F., Eriksson, O.E., Huhndorf, S., et al., 2007. A higher-level phylogenetic classification of the Fungi. Mycol. Res. 111, 509–547.
Hibbett, D.S., Ohman, A., Glotzer, D., Nuhn, M., Kirk, P., Nilsson, R.H., 2011. Progress in molecular and morphological taxon discovery in Fungi and options for formal classification of environmental sequences. Fungal Biol. Rev. 25, 38–47.
Hibbett, D.S., Taylor, J.W., 2013. Fungal systematics: is a new age of enlightenment at hand? Nat. Rev. Microbiol. 11, 129–133.
Hildén, K., Martinez, A.T., Hatakka, A., Lundell, T., 2005. The two manganese peroxidases Pr-MnP2 and Pr-MnP3 of *Phlebia radiata*, a lignin-degrading basidiomycete, are phylogenetically and structurally divergent. Fungal Genet. Biol. 42, 403–419.
Hildén, K., Mäkelä, M.R., Steffen, K.T., Hofrichter, M., Hatakka, A., Archer, D.B., Lundell, T.K., 2014. Biochemical and molecular characterization of an atypical manganese peroxidase of the litter-decomposing fungus *Agrocybe praecox*. Fungal Genet. Biol. 72, 131–136.
Hildén, K.S., Bortfeldt, R., Hofrichter, M., Hatakka, A., Lundell, T.K., 2008. Molecular characterization of the basidiomycete isolate *Nematoloma frowardii* b19 and its manganese peroxidase places the fungus in the corticioid genus *Phlebia*. Microbiology 154, 2371–2379.
Hildén, K.S., Mäkelä, M.R., Hakala, T.K., Hatakka, A., Lundell, T., 2006. Expression on wood, molecular cloning and characterization of three lignin peroxidase (LiP) encoding genes of the white rot fungus *Phlebia radiata*. Curr. Genet. 49, 97–105.
Himmelstrand, K., Olson, Å., Brandström Durling, M., Karlsson, M., Stenlid, J., 2014. Intronic and plasmid-derived regions contribute to the large mitochondrial genome sizes of Agaricomycetes. Curr. Genet. 60, 303–313.
Hoegger, P.J., Kilaru, S., James, T.Y., Thacker, J.R., Kües, U., 2006. Phylogenetic comparison and classification of laccase and related multicopper oxidase protein sequences. FEBS J. 273, 2308–2326.
Hofrichter, M., 2002. Review: Lignin conversion by manganese peroxidase (MnP). Enzyme Microb. Technol. 30, 454–466.
Hofrichter, M., Lundell, T., Hatakka, A., 2001. Conversion of milled pine wood by manganese peroxidase from *Phlebia radiata*. Appl. Environ. Microbiol. 67, 4588–4593.

Hofrichter, M., Ullrich, R., Pecyna, M.J., Liers, C., Lundell, T., 2010. New and classic families of secreted fungal heme peroxidases. Appl. Microbiol. Biotechnol. 87, 871–897.

Hofrichter, M., Vares, K., Scheibner, K., Galkin, S., Sipilä, J., Hatakka, A., 1999. Mineralization and solubilization of synthetic lignin by manganese peroxidases from *Nematoloma frowardii* and *Phlebia radiata*. J. Biotechnol. 67, 217–228.

Hopple, J.S., Vilgalys, R., 1999. Phylogenetic relationships in the mushroom genus Coprinus and dark-spored allies based on sequence data from the nuclear gene coding for the large ribosomal subunit RNA: divergent domains, outgroups, and monophyly. Mol. Phylogenet. Evol. 13, 1–19.

Hori, C., Gaskell, J., Igarashi, K., Kersten, P., Mozuch, M., Samejima, M., Cullen, D., 2014a. Temporal alterations in the secretome of the selective ligninolytic fungus *Ceriporiopsis subvermispora* during growth on aspen wood reveal this organism's strategy for degrading lignocellulose. Appl. Environ. Microbiol. 80, 2062–2070.

Hori, C., Gaskell, J., Igarashi, K., Samejima, M., Hibbett, D., Henrissat, B., Cullen, D., 2013. Genomewide analysis of polysaccharides degrading enzymes in 11 white- and brown-rot Polyporales provides insight into mechanisms of wood decay. Mycologia 105, 1412–1427.

Hori, C., Igarashi, K., Katayama, A., Samejima, M., 2011. Effects of xylan and starch on secretome of the basidiomycete *Phanerochaete chrysosporium* grown on cellulose. FEMS Microbiol. Lett. 321, 14–23.

Hori, C., Ishida, T., Igarashi, K., Samejima, M., Suzuki, H., Master, E., Ferreira, P., et al., 2014b. Analysis of the *Phlebiopsis gigantea* genome, transcriptome and secretome provides insight into its pioneer colonization strategies of wood. PLoS Genet. 10, e1004759.

James, T.Y., Kauff, F., Schoch, C.L., Matheny, P.B., Hofstetter, V., Cox, C.J., Celio, G., et al. 2006. Reconstructing the early evolution of Fungi using a six-gene phylogeny. Nature 443, 818–822.

Janusz, G., Kucharzyk, K.H., Pawlik, A., Staszczak, M., Paszczynski, A.J., 2013. Fungal laccase, manganese peroxidase and lignin peroxidase: Gene expression and regulation. Enzyme Microb. Technol. 52, 1–12.

Jensen, K.A., Bao, W., Kawai, S., Srebotnik, E., Hammel, K.E., 1996. Manganese-dependent cleavage of nonphenolic lignin structures by *Ceriporiopsis subvermispora* in the absence of lignin peroxidase. Appl. Environ. Microbiol. 62, 3679–3686.

Joardar, V., Abrams, N.F., Hostetler, J., Paukstelis, P.J., Pakala, S., Pakala, S.B., Zafar, N., et al., 2012. Sequencing of mitochondrial genomes of nine *Aspergillus* and *Penicillium* species identifies mobile introns and accessory genes as main sources of genome size variability. BMC Genomics 13, 698.

Kamei, I., Daikoku, C., Tsutsumi, Y., Kondo, R., 2008. Saline-dependent regulation of manganese peroxidase genes in the hypersaline-tolerant white rot fungus *Phlebia* sp. strain MG-60. Appl. Environ. Microbiol. 74, 2709–2716.

Kamei, I., Suhara, H., Kondo, R., 2005. Phylogenetical approach to isolation of white-rot fungi capable of degrading polychlorinated dibenzo-p-dioxin. Appl. Microbiol. Biotechnol. 69, 358–366.

Kapich, A, Hofrichter, M., Vares, T., Hatakka, A, 1999. Coupling of manganese peroxidase-mediated lipid peroxidation with destruction of nonphenolic lignin model compounds and ^{14}C-labeled lignins. Biochem. Biophys. Res. Commun. 259, 212–219.

Kapich, A.N., Prior, B.A., Lundell, T., Hatakka, A., 2005. A rapid method to quantify pro-oxidant activity in cultures of wood-decaying white-rot fungi. J. Microbiol. Methods 61, 261–271.

Karhunen, E., Kantelinen, A., Niku-Paavola, M.-L., 1990. Mn-dependent peroxidase from the lignin-degrading white rot fungus *Phlebia radiata*. Arch. Biochem. Biophys. 279, 25–31.
Keeling, P.J., 2003. Congruent evidence from α-tubulin and β-tubulin gene phylogenies for a zygomycete origin of microsporidia. Fungal Genet. Biol. 38, 298–309.
Kersten, P., Cullen, D., 2014. Copper radical oxidases and related extracellular oxidoreductases of wood-decay Agaricomycetes. Fungal Genet. Biol. 72, 124–130.
Kersten, P.J., 1990. Glyoxal oxidase of *Phanerochaete chrysosporium*: its characterization and activation by lignin peroxidase. Proc. Natl. Acad. Sci. U. S. A. 87, 2936–2940.
Kim, S.J.U.N., Shoda, M., 1999. Purification and characterization of a novel peroxidase from *Geotrichum candidum* Dec 1 involved in decolorization of dyes. Appl. Environ. Microbiol. 65, 1029–1035.
Kinne, M., Poraj-Kobielska, M., Ullrich, R., Nousiainen, P., Sipilä, J., Scheibner, K., Hammel, K.E., et al., 2011. Oxidative cleavage of non-phenolic β-O-4 lignin model dimmers by an extracellular aromatic peroxygenase. Holzforschung 65, 673–679.
Kirk, P.M., Cannon, P.F., Minter, D.W., Stalpers, J.A. (Eds.), 2008. Dictionary of the fungi, 10th edn. CABI, Wallingford, UK. 640 p.
Kohler, A., Kuo, A., Nagy, L.G., Morin, E., Barry, K.W., Buscot, F., Canbäck, B., et al., 2015. Convergent losses of decay mechanisms and rapid turnover of symbiosis genes in mycorrhizal mutualists. Nat. Genet. 47, 410–415.
Korhonen, K., Stenlid, J., 1998. Biology of *Heterobasidion annosum*, in: Woodward, S., Stenlid, J., Karjalainen, R., Hüttermann, A. (Eds.), *Heterobasidion annosum*: Biology, ecology, impact and control. CAB International, Wallingford, UK, pp. 43–104.
Korripally, P., Hunt, C.G., Houtman, C.J., Jones, D.C., Kitin, P.J., Cullen, D., Hammel, E., 2015. Regulation of gene expression during the onset of ligninolytic oxidation by *Phanerochaete chrysosporium* on spruce wood 81, 7802–7812.
Kostylev, M., Wilson, D., 2012. Synergistic interactions in cellulose hydrolysis. Biofuels 3, 61–70.
Kracher, D., Scheiblbrandner, S., Felice, A.K.G., Breslmayr, E., Preims, M., Haltrich, D., Eijsink, V.G.H., et al., 2016. Extracellular electron transfer systems fuel cellulose oxidative degradation. Science 3165, 1–13.
Kretzer, A.M., Bruns, T.D., 1999. Use of atp6 in fungal phylogenetics: an example from the boletales. Mol. Phylogenet. Evol. 13, 483–492.
Kreuzinger, N., Podeu, R., Gruber, F., Göbl, F., Kubicek, C.P., 1996. Identification of some ectomycorrhizal basidiomycetes by PCR amplification of their gpd (glyceraldehyde-3-phosphate dehydrogenase) genes. Appl. Environ. Microbiol. 62, 3432–3438.
Kües, U., Nelson, D.R., Liu, C., Yu, G.-J., Zhang, J., Li, J., Wang, X.-C.et al., 2015. Genome analysis of medicinal *Ganoderma* spp. with plant-pathogenic and saprotrophic life-styles. Phytochemistry. 114, 18-37.
Lafond, M., Navarro, D., Haon, M., Couturier, M., Berrin, J.G., 2012. Characterization of a broad-specificity β-glucanase acting on β-(1,3)-, β-(1,4)-, and β-(1,6)-glucans that defines a new glycoside hydrolase family. Appl. Environ. Microbiol. 78, 8540–8546.
Lang, B.F., 2007. Mitochondrial introns: a critical view. Trends Genet. 23, 119–125.
Langston, J.A., Shaghasi, T., Abbate, E., Xu, F., Vlasenko, E., Sweeney, M.D., 2011. Oxidoreductive cellulose depolymerization by the enzymes cellobiose dehydrogenase and glycoside hydrolase 61. Appl. Environ. Microbiol. 77, 7007–7015.
Lemmon, A.R., Emme, S.A., Lemmon, E.M., 2012. Anchored hybrid enrichment for massively high-throughput phylogenomics. Syst. Biol. 61, 727–744.
Levasseur, A., Lomascolo, A., Chabrol, O., Ruiz-Dueñas, F.J., Boukhris-Uzan, E., Piumi, F., Kües, U., et al., 2014. The genome of the white-rot fungus *Pycnoporus cinnabarinus*: a

basidiomycete model with a versatile arsenal for lignocellulosic biomass breakdown. BMC Genomics 15, 486.
Li, C., Hofreiter, M., Straube, N., Corrigan, S., Naylor, G.J.P., 2013. Capturing protein-coding genes across highly divergent species. Biotechniques 54, 321–326.
Li, Y., Hu, X.-D., Yang, R.-H., Hsiang, T., Wang, K., Liang, D.-Q., Liang, F., et al., 2015. Complete mitochondrial genome of the medicinal fungus *Ophiocordyceps sinensis*. Sci. Rep. 5, 13892.
Liers, C., Aranda, E., Strittmatter, E., Piontek, K., Plattner, D.A., Zorn, H., Ullrich, R., et al., 2014. Phenol oxidation by DyP-type peroxidases in comparison to fungal and plant peroxidases. J. Mol. Catal. B Enzym. 103, 41–46.
Liers, C., Arnstadt, T., Ullrich, R., Hofrichter, M., 2011. Patterns of lignin degradation and oxidative enzyme secretion by different wood- and litter-colonizing Basidiomycetes and Ascomycetes grown on beech-wood. FEMS Microbiol. Ecol. 78, 91–102.
Liers, C., Bobeth, C., Pecyna, M., Ullrich, R., Hofrichter, M., 2010. DyP-like peroxidases of the jelly fungus Auricularia auricula-judae oxidize nonphenolic lignin model compounds and high-redox potential dyes. Appl. Microbiol. Biotechnol. 85, 1869–1879.
Linde, D., Ruiz-Dueñas, F.J., Fernández-Fueyo, E., Guallar, V., Hammel, K.E., Pogni, R., Martínez, A.T., 2015. Basidiomycete DyPs: Genomic diversity, structural-functional aspects, reaction mechanism and environmental significance. Arch. Biochem. Biophys. 574, 66-74.
Liu, Y.J., Hall, B.D., 2004. Body plan evolution of ascomycetes, as inferred from an RNA polymerase II phylogeny. Proc. Natl. Acad. Sci. U. S. A. 101, 4507–4512.
Liu, Y.J., Whelen, S., Hall, B.D., 1999. Phylogenetic relationships among ascomycetes: evidence from an RNA polymerase II subunit. Mol. Biol. Evol. 16, 1799–1808.
Lombard, V., Bernard, T., Rancurel, C., Brumer, H., Coutinho, P.M., Henrissat, B., 2010. A hierarchical classification of polysaccharide lyases for glycogenomics. Biochem. J. 432, 437–444.
Lombard, V., Golaconda Ramulu, H., Drula, E., Coutinho, P.M., Henrissat, B., 2014. The carbohydrate-active enzymes database (CAZy) in 2013. Nucleic Acids Res. 42, 490–495.
Ludwig, R., Harreither, W., Tasca, F., Gorton, L., 2010. Cellobiose dehydrogenase: A versatile catalyst for electrochemical applications. Chem. Phys. Chem. 11, 2674–2697.
Lundell, T., Bentley, E., Hildén, K., Rytioja, J., Kuuskeri, J., Ufot, U.F., Nousiainen, P., et al., 2016. Engineering towards catalytic use of fungal class-II peroxidases for dye-decolorizing and conversion of lignin model compounds. Curr. Biotechnol. doi:10.2174/2211550105666160520120101.
Lundell, T., Hatakka, A., 1994. Participation of Mn(II) in the catalysis of laccase, manganese peroxidase and lignin peroxidase from *Phlebia radiata*. FEBS Lett. 348, 291–296.
Lundell, T., Leonowicz, A., Rogalski, J., Hatakka, A., 1990. Formation and action of lignin-modifying enzymes in cultures of *Phlebia radiata* supplemented with veratric acid. Appl. Environ. Microbiol. 56, 2623–2629.
Lundell, T., Schoemaker, H., Hatakka, A., Brunow, G., 1993a. New mechanism of the C-α-C-β cleavage in nonphenolic arylglycerol β-aryl ether lignin substructures catalyzed by lignin peroxidase. Holzforsch. Int. J. Biol. Chem. Phys. Technol. Wood 47, 219–224.
Lundell, T., Wever, R., Floris, R., Harvey, P., Hatakka, A., Brunow, G., Schoemaker, H., 1993b. Lignin peroxidase L3 from *Phlebia radiata*. Pre-steady-state and steady-state studies with veratryl alcohol and a non-phenolic lignin model compound 1-(3,4-dimethoxyphenyl)-2-(2-methoxyphenoxy)propane-1,3-diol. Eur. J. Biochem. 211, 391–402.

Lundell, T.K., Mäkelä, M.R., Hílden, K., 2010. Lignin-modifying enzymes in filamentous basidiomycetes--ecological, functional and phylogenetic review. J. Basic Microbiol. 50, 5–20.

Lundell, T.K., Mäkelä, M.R., de Vries, R.P., Hildén, K.S., 2014. Genomics, lifestyles and future prospects of wood-decay and litter-decomposing basidiomycota, in: Francis M.M. (Ed.), Advances in botanical research, Vol 70, Fungi. Academic, London, UK, pp. 329–370.

Luttik, M.A.H., Overkamp, K.M., Kötter, P., De Vries, S., Van Dijken, J.P., Pronk, J.T., 1998. The *Saccharomyces cerevisiae* NDE1 and NDE2 genes encode separate mitochondrial NADH dehydrogenases catalyzing the oxidation of cytosolic NADH. J. Biol. Chem. 273, 24529–24534.

Lutzoni, F., Kauff, F., Cox, C.J., McLaughlin, D., Celio, G., Dentinger, C., Padamsee, M., et al., 2004. Assembling the fungal tree of life: Progress, classification, and evolution of subcellular traits. Am. J. Bot. 91, 1446–1480.

MacDonald, J., Doering, M., Canam, T., Gong, Y., Guttman, D.S., Campbell, M.M., Master, E.R., 2011. Transcriptomic responses of the softwood-degrading white-rot fungus *Phanerochaete carnosa* during growth on coniferous and deciduous wood, Applied and Environmental Microbiology. 77, 3211-3218.

MacDonald, J., Master, E.R., 2012. Time-dependent profiles of transcripts encoding lignocellulose-modifying enzymes of the white rot fungus *Phanerochaete carnosa* grown on multiple wood substrates. Appl. Environ. Microbiol. 78, 1596–1600.

Manavalan, A., Adav, S.S., Sze, S.K., 2011. ITRAQ-based quantitative secretome analysis of *Phanerochaete chrysosporium*. J. Proteomics 75, 642–654.

Manavalan, T., Manavalan, A., Thangavelu, K.P., Heese, K., 2012. Secretome analysis of *Ganoderma lucidum* cultivated in sugarcane bagasse. J. Proteomics 77, 298–309.

Martinez, D., Challacombe, J., Morgenstern, I., Hibbett, D., Schmoll, M., Kubicek, C.P., Ferreira, P., et al., 2009. Genome, transcriptome, and secretome analysis of wood decay fungus *Postia placenta* supports unique mechanisms of lignocellulose conversion. Proc. Natl. Acad. Sci. U. S. A. 106, 1954–1959.

Martinez, D., Larrondo, L.F., Putnam, N., Gelpke, M.D.S., Huang, K., Chapman, J., Helfenbein, K.G., et al.., 2004. Genome sequence of the lignocellulose degrading fungus *Phanerochaete chrysosporium* strain RP78. Nat. Biotechnol. 22, 695–700.

Matheny, P.B., Liu, Y.J., Ammirati, J.F., Hall, B.D., 2002. Using RPB1 sequences to improve phylogenetic inference among mushrooms (Inocybe, Agaricales). Am. J. Bot. 89, 688–698.

Matheny, P.B., Wang, Z., Binder, M., Curtis, J.M., Lim, Y.W., Nilsson, H.R., Hughes, K.W., et al., 2007. Contributions of rpb2 and tef1 to the phylogeny of mushrooms and allies (Basidiomycota, Fungi). Mol. Phylogenet. Evol. 43, 430–451.

McLaughlin, D.J., Hibbett, D.S., Lutzoni, F., Spatafora, J.W., Vilgalys, R., 2009. The search for the fungal tree of life. Trends Microbiol. 17, 488–497.

Medie, F.M., Davies, G.J., Drancourt, M., Henrissat, B., 2012. Genome analyses highlight the different biological roles of cellulases. Nat. Rev. Microbiol. 10, 227–234.

Mester, T., Field, J.A., 1998. Characterization of a novel manganese peroxidase-lignin peroxidase hybrid isozyme produced by *Bjerkandera* species strain BOS55 in the absence of manganese. J. Biol. Chem. 273, 15412–15417.

Mierzwa, M., Tokarzewska-Zadora, J., Deptuła, T., Rogalski, J., Szczodrak, J., 2005. Purification and characterization of an extracellular α-D-glucuronidase from *Phlebia radiata*. Prep. Biochem. Biotechnol. 35, 243–256.

Moilanen, A.M., Lundell, T., Vares, T., Hatakka, A., 1996. Manganese and malonate are individual regulators for the production of lignin and manganese peroxidase isozymes and

in the degradation of lignin by *Phlebia radiata*. Appl. Microbiol. Biotechnol. 45, 792–799.
Moreno, G., Blanco, M.-N., Checa, J., Platas, G., Peláez, F., 2011. Taxonomic and phylogenetic revision of three rare irpicoid species within the Meruliaceae. Mycol. Prog. 10, 481–491.
Mori, T., Kitano, S., Kondo, R., 2003. Biodegradation of chloronaphthalenes and polycyclic aromatic hydrocarbons by the white-rot fungus *Phlebia lindtneri*. Appl. Microbiol. Biotechnol. 61, 380–383.
Munk, L., Sitarz, A.K., Kalyani, D.C., Mikkelsen, J.D., Meyer, A.S., 2015. Can laccases catalyze bond cleavage in lignin? Biotechnol. Adv. 33, 13–24.
Müller, M.M., Hamberg, L., Kuuskeri, J., LaPorta, N., Pavlov, I., Korhonen, K., 2015. Respiration rate determinations suggest *Heterobasidion parviporum* subpopulations have potential to adapt to global warming. For. Pathol. 45, 515-524.
Mäkelä, M.R., Hildén, K., Lundell, T.K., 2010. Oxalate decarboxylase: Biotechnological update and prevalence of the enzyme in filamentous fungi. Appl. Microbiol. Biotechnol. 87, 801–814.
Mäkelä, M.R., Hildén, K.S., Hakala, T.K., Hatakka, A., Lundell, T.K., 2006. Expression and molecular properties of a new laccase of the white rot fungus *Phlebia radiata* grown on wood. Curr. Genet. 50, 323–333.
Mäkelä, M.R., Lundell, T., Hatakka, A., Hildén, K., 2013. Effect of copper, nutrient nitrogen, and wood-supplement on the production of lignin-modifying enzymes by the white-rot fungus *Phlebia radiata*. Fungal Biol. 117, 62–70.
Mäkelä, M.R., Marinović, M., Nousiainen, P., Liwanag, A.J.M., Benoit, I., Sipilä, J., Hatakka, A., et al., 2015. Aromatic metabolism of filamentous fungi in relation to the presence of aromatic compounds in plant biomass. Adv. Appl. Microbiol. 91, 63–137.
Nagy, L.G., Riley, R., Tritt, A., Adam, C., Daum, C., Floudas, D., Sun, H., et al., 2015. Comparative genomics of early-diverging mushroom-forming fungi provides knsights into the origins of lignocellulose decay capabilities. Mol. Biol. Evol. 33, 959-970.
Nakasone, K.K., Burdsall, H.H., 1984. *Merulius*, a synonym of *Phlebia*. Mycotaxon 21, 241–246.
Nakasone, K.K., Sytsma, K.J., 1993. Biosystematic studies on *Phlebia acerina, P. rufa,* and *P. radiata* in North America. Mycologia 85, 996-1016.
Niemenmaa, O., Uusi-Rauva, A., Hatakka, A., 2006. Wood stimulates the demethoxylation of [$O^{14}CH_3$]-labeled lignin model compounds by the white-rot fungi *Phanerochaete chrysosporium* and *Phlebia radiata*. Arch. Microbiol. 185, 307–315.
Niku-Paavola, M.-L., Karhunen, E., Kantelinen, A., Viikari, L., Lundell, T. et al., 1990. The effect of culture conditions on the production of lignin modifying enzymes by the white-rot fungus *Phlebia radiata*. J. Biotechnol. 13, 211–221.
Niku-Paavola, M.L., Karhunen, E., Salola, P., Raunio, V., 1988. Ligninolytic enzymes of the white-rot fungus *Phlebia radiata*. Biochem. J. 254, 877–884.
Nousiainen, P., Kontro, J., Manner, H., Annele, H., Sipilä, J., 2014. Phenolic mediators enhance the manganese peroxidase catalyzed oxidation of recalcitrant lignin model compounds and synthetic lignin. Fungal Genet. Biol. 72, 137–149.
O'Donnell, K., Lutzoni, F.M., Ward, T.J., Benny, G.L., Donnell, K.O., Ward, T.J., 2001. Evolutionary relationships among mucoralean fungi (Zygomycota): Evidence for family polyphyly on a large scale. Mycologia 93, 286–297.
Ohm, R.A., Riley, R., Salamov, A., Min, B., Choi, I.G., Grigoriev, I. V., 2014. Genomics of wood-degrading fungi. Fungal Genet. Biol. 72, 82–90.
Olson, A., Aerts, A., Asiegbu, F., Belbahri, L., Bouzid, O., Broberg, A., Canbäck, B., et al., 2012. Insight into trade-off between wood decay and parasitism from the genome of a fungal forest pathogen. New Phytol. 194, 1001–1013.

Paquin, B., Laforest, M.J., Forget, L., Roewer, I., Wang, Z., Longcore, J., Lang, B.F., 1997. The fungal mitochondrial genome project: evolution of fungal mitochondrial genomes and their gene expression. Curr. Genet. 31, 380–395.

Paquin, B., Laforest, M.J., Lang, B.F., 1994. Interspecific transfer of mitochondrial genes in fungi and creation of a homologous hybrid gene. Proc. Natl. Acad. Sci. U. S. A. 91, 11807–11810.

Parmasto, E., Hallenberg, N., 2000. A taxonomic study of phlebioid fungi (Basidiomycota). Nord. J. Bot. 20, 105–118.

Pelin, A., Pombert, J.-F., Salvioli, A., Bonen, L., Bonfante, P., Corradi, N., 2012. The mitochondrial genome of the arbuscular mycorrhizal fungus *Gigaspora margarita* reveals two unsuspected trans-splicing events of group I introns. New Phytol. 194, 836–845.

Peltola A (editor), 2014. Finnish statistical yearbook of forestry. Finnish forest research institute. Tammerprint Oy, Tampere, Finland. 426 p.

Perseke, M., Fritzsch, G., Ramsch, K., Bernt, M., Merkle, D., Middendorf, M., Bernhard, D., et al., 2008. Evolution of mitochondrial gene orders in echinoderms. Mol. Phylogenet. Evol. 47, 855–864.

Popkin, G., 2015. Weighing the world's trees. Nature 523, 20–22.

Prendecka, M., Buczyńska, A., Rogalski, J., 2007. Purification and characterization of β-mannosidases from white rot fungus *Phlebia radiata*. Polish J. Microbiol. 56, 139–147.

Prendecka, M., Szyjka, K., Rogalski, J., 2003. Purification and properties of α-galactosidase isosymes from *Phlebia radiata*. Acta Microbiol. Pol. 52, 25–33.

Rahikainen, J.L., Evans, J.D., Mikander, S., Kalliola, A., Puranen, T., Tamminen, T., Marjamaa, K., et al., 2013. Cellulase-lignin interactions-The role of carbohydrate-binding module and pH in non-productive binding. Enzyme Microb. Technol. 53, 315–321.

Richardson, D.R., Lane, D.J., Becker, E.M., Huang, M.L., Whitnall, M., Suryo Rahmanto, Y., Sheftel, A.D., et al., 2010. Mitochondrial iron trafficking and the integration of iron metabolism between the mitochondrion and cytosol. Proc. Natl. Acad. Sci. U. S. A. 107, 10775–10782.

Riley, R., Salamov, A.A., Brown, D.W., Nagy, L.G., Floudas, D., Held, B.W., Levasseur, A.,et al., 2014. Extensive sampling of basidiomycete genomes demonstrates inadequacy of the white-rot/brown-rot paradigm for wood decay fungi. Proc. Natl. Acad. Sci. U. S. A. 111, 9923–9928.

Rogalski, J., Hatakka, A., Longa, B., Wojtas-Wasilewska, M., 1993a. Hemicellulolytic enzymes of the ligninolytic white-rot fungus *Phlebia radiata*. Influence of phenolic compounds on the synthesis of hemicellulolytic enzymes. Acta Biotechnol. 13, 53–57.

Rogalski, J., Hatakka, A., Wojtas-Wasilewska, M., Leonowicz, A., 1993b. Cellulolytic enzymes of the ligninolytic white-rot fungus *Phlebia radiata*. Acta Biotechnol. 13, 41–45.

Rogalski, J., Oleszek, M., Tokarzewska-Zadora, J., 2001. Purification and characterization of two endo-1,4-β-xylanases and a β-xylosidase from *Phlebia radiata*. Acta Microbiol. Pol. 50, 117–128.

Ruiz-Dueñas, F.J., Lundell, T., Floudas, D., Nagy, L.G., Barrasa, J.M., Hibbett, D.S., Martínez, A.T., 2013. Lignin-degrading peroxidases in Polyporales: an evolutionary survey based on 10 sequenced genomes. Mycologia 105, 1428–1444.

Ruiz-Dueñas, F.J., Morales, M., García, E., Miki, Y., Martínez, M.J., Martínez, A.T., 2009. Substrate oxidation sites in versatile peroxidase and other basidiomycete peroxidases. J. Exp. Bot. 60, 441–452.

Rytioja, J., Hildén, K., Hatakka, A., Mäkelä, M.R., 2014. Transcriptional analysis of selected cellulose-acting enzymes encoding genes of the white-rot fungus *Dichomitus squalens* on spruce wood and microcrystalline cellulose. Fungal Genet. Biol. 72, 91–98.

Rytioja, J., Hildén, K., Yuzon, J., Hatakka, A., de Vries, R.P., Mäkelä, M.R., 2014. Plant-polysaccharide-degrading enzymes from Basidiomycetes. Microbiol. Mol. Biol. Rev. 78, 614–649.

Saloheimo, M., Niku-Paavola, M.-L., Knowles, J.K., 1991. Isolation and structural analysis of the laccase gene from the lignin-degrading fungus *Phlebia radiata*. J. Gen. Microbiol. 137, 1537–1544.

Salvachúa, D., Martínez, A.T., Tien, M., López-Lucendo, M.F., García, F., de Los Ríos, V., Martínez, M.J., et al., 2013a. Differential proteomic analysis of the secretome *of Irpex lacteus* and other white-rot fungi during wheat straw pretreatment. Biotechnol. Biofuels 6, 115.

Salvachúa, D., Prieto, A., Martínez, Á.T., Martínez, M.J., 2013b. Characterization of a novel dye-decolorizing peroxidase (DyP)-type enzyme from *Irpex lacteus* and its application in enzymatic hydrolysis of wheat straw. Appl. Environ. Microbiol. 79, 4316–4324.

Santamaria, M., Vicario, S., Pappadà, G., Scioscia, G., Scazzocchio, C., Saccone, C., 2009. Towards barcode markers in Fungi: an intron map of Ascomycota mitochondria. BMC Bioinformatics 10, S15.

Sato, S., Feltus, F.A., Iyer, P., Tien, M., 2009. The first genome-level transcriptome of the wood-degrading fungus *Phanerochaete chrysosporium* grown on red oak. Curr. Genet. 55, 273–286.

Sato, S., Liu, F., Koc, H., Tien, M., 2007. Expression analysis of extracellular proteins from *Phanerochaete chrysosporium* grown on different liquid and solid substrates. Microbiology 153, 3023–3033.

Scheller, H.V., Ulvskov, P., 2010. Hemicelluloses. Annu. Rev. Plant Biol. 61, 263–289.

Schmitt, I., Crespo, A., Divakar, P.K., Fankhauser, J.D., Herman-Sackett, E., Kalb, K., Nelsen, M.P., et al., 2009. New primers for promising single-copy genes in fungal phylogenetics and systematics. Persoonia 23, 35–40.

Schoch, C.L., Seifert, K.A., Huhndorf, S., Robert, V., Spouge, J.L., Levesque, C.A., Chen, W.,et al., 2012. Nuclear ribosomal internal transcribed spacer (ITS) region as a universal DNA barcode marker for Fungi. Proc. Natl. Acad. Sci. U. S. A. 109, 6241–6246.

Schoemaker, H.E., Lundell, T.K., Hatakka, A.I., Piontek, K., 1994. The oxidation of veratryl alcohol, dimeric lignin models and lignin by lignin peroxidase: The redox cycle revisited. FEMS Microbiol. Rev. 13, 321–331.

Sharma, R.K., Arora, D.S., 2011. Solid state degradation of paddy straw by *Phlebia floridensis* in the presence of different supplements for improving its nutritive status. Int. Biodeterior. Biodegradation 65, 990–996.

Sjöström, E., 1981. Wood chemistry. Academic Press, London, UK. 293 p.

Sjöström, E., Westermark, U., 1998. Chemical composition of wood and pulps: Basic components and their distribution, in: Sjöström, E., Alén, R. (Eds.), Analytical methods in wood chemistry, pulping, and papermaking. Springer-Verlag, Berlin, Germany, pp. 1–19.

Sloan, D.B., Alverson, A.J., Chuckalovcak, J.P., Wu, M., McCauley, D.E., Palmer, J.D., Taylor, D.R., 2012. Rapid evolution of enormous, multichromosomal genomes in flowering plant mitochondria with exceptionally high mutation rates. PLoS Biol. 10, e1001241.

Spang, A., Saw, J.H., Jørgensen, S.L., Zaremba-Niedzwiedzka, K., Martijn, J., Lind, A.E., van Eijk, R., et al., 2015. Complex archaea that bridge the gap between prokaryotes and eukaryotes. Nature 521, 173–179.

Stajich, J., Berbee, M.L., Blackwell, M., Hibbett, D.S., James, T.Y., Spatafora, J.W., Taylor, J.W., 2009. The Fungi. Curr. Biol. 19, 840–845.

Stajich, J.E., 2015. Phylogenomics enabling genome-based mycology, in: McLaughlin, D.J., Spatafora, J.W. (Eds.), The Mycota VII Systematics and evolution Part B. Springer-Verlag, Berlin, Germany, pp. 279–294.

Stoddard, B.L., 2011. Homing endonucleases: from microbial genetic invaders to reagents for targeted DNA modification. Structure 19, 7–15.

Sugano, Y., 2009. DyP-type peroxidases comprise a novel heme peroxidase family. Cell. Mol. Life Sci. 66, 1387–1403.

Sulej, J., Janusz, G., Mazur, A., Żuber, K., Żebracka, A., Rogalski, J., 2013. Cellobiose dehydrogenase from the ligninolytic basidiomycete *Phlebia lindtneri*. Process Biochem. 48, 1715–1723.

Sundaramoorthy, M., Youngs, H., Gold, M.H., Poulos, T.L., 2005. High-resolution crystal structure of manganese peroxidase: substrate and inhibitor complexes. Biochemistry 44, 6463–6470.

Suzuki, H., MacDonald, J., Syed, K., Salamov, A., Hori, C., Aerts, A., Henrissat, B., et al., 2012. Comparative genomics of the white-rot fungi, *Phanerochaete carnosa* and *P. chrysosporium*, to elucidate the genetic basis of the distinct wood types they colonize. BMC Genomics 13, 444.

Taylor, J.W., Jacobson, D.J., Kroken, S., Kasuga, T., Geiser, D.M., Hibbett, D.S., Fisher, M.C., 2000. Phylogenetic species recognition and species concepts in fungi. Fungal Genet. Biol. 31, 21–32.

Tedersoo, L., Bahram, M., Põlme, S., Kõljalg, U., Yorou, N.S., Wijesundera, R., Ruiz, L.V., et al., 2014. Global diversity and geography of soil fungi. Science 346, 1256688.

Thrash, J.C., Boyd, A., Huggett, M.J., Grote, J., Carini, P., Yoder, R.J., Robbertse, B., et al., 2011. Phylogenomic evidence for a common ancestor of mitochondria and the SAR11 clade. Sci. Rep. 1, 13.

Tien, M., Kirk, T.K., 1984. Lignin-degrading enzyme from *Phanerochaete chrysosporium*: Purification, characterization, and catalytic properties of a unique H_2O_2-requiring oxygenase. Proc. Natl. Acad. Sci. U. S. A. 81, 2280–2284.

Timmis, J.N., Ayliffe, M.A., Huang, C.Y., Martin, W., 2004. Endosymbiotic gene transfer: organelle genomes forge eukaryotic chromosomes. Nat. Rev. 5, 123–135.

Todd, R.B., Zhou, M., Ohm, R.A., Leeggangers, H.A.C.F., Visser, L., de Vries, R.P., 2014. Prevalence of transcription factors in ascomycete and basidiomycete fungi. BMC Genomics 15, 214.

Tomsovsky, M., Menkis, A., Vasaitis, R., 2010. Phylogenetic relationships in European *Ceriporiopsis* species inferred from nuclear and mitochondrial ribosomal DNA sequences. Fungal Biol. 114, 350–358.

Tuomela, M., Hatakka, A., 2011. Oxidative fungal enzymes for bioremediation, in: Moo-Young, M., Agathos, S., (Eds.), Comprehensive biotechnology, vol 6, Environmental biotechnology and safety. Elsevier, London, UK, 183-196.

Tuomela, M., Oivanen, P., Hatakka, A., 2002. Degradation of synthetic ^{14}C-lignin by various white-rot fungi in soil. Soil Biol. Biochem. 34, 1613–1620.

Ullrich, R., Hofrichter, M., 2005. The haloperoxidase of the agaric fungus *Agrocybe aegerita* hydroxylates toluene and naphthalene. FEBS Lett. 579, 6247–6250.

Ullrich, R., Nüske, J., Scheibner, K., Spantzel, J., Hofrichter, M., 2004. Novel haloperoxidase from the agaric basidiomycete *Agrocybe aegerita* oxidizes aryl alcohols and aldehydes. Appl. Environ. Microbiol. 70, 4575–4581.

Vaaje-Kolstad, G., Westereng, B., Horn, S.J., Liu, Z., Zhai, H., Sørlie, M., Eijsink, V.G.H., 2010. An oxidative enzyme boosting the enzymatic conversion of recalcitrant polysaccharides. Science 330, 219–222.

Wallace, D.C., 2010. Mitochondrial DNA mutations in disease and aging. Environ. Mol. Mutagen. 51, 440–450.

Van Aken, B., Skubisz, K., Naveau, H., Agathos, S.N., 1997. Biodegradation of 2,4,6-trinitrotoluene (TNT) by the white-rot basidiomycete *Phlebia radiata*. Biotechnol. Lett. 19, 813–817.

van Diepeningen, A.D., Goedbloed, D.J., Slakhorst, S.M., Koopmanschap, A.B., Maas, M.F.P.M., Hoekstra, R.F., Debets, A.J.M., 2010. Mitochondrial recombination increases with age in *Podospora anserina*. Mech. Ageing Dev. 131, 315–322.

Vanden Wymelenberg, A., Gaskell, J., Mozuch, M., BonDurant, S.S., Sabat, G., Ralph, J., Skyba, O., et al., 2011. Significant alteration of gene expression in wood decay fungi *Postia placenta* and *Phanerochaete chrysosporium* by plant species. Appl. Environ. Microbiol. 77, 4499–4507.

Vanden Wymelenberg, A., Gaskell, J., Mozuch, M., Kersten, P., Sabat, G., Martinez, D., Cullen, D., 2009. Transcriptome and secretome analyses of *Phanerochaete chrysosporium* reveal complex patterns of gene expression. Appl. Environ. Microbiol. 75, 4058–4068.

Vanden Wymelenberg, A., Minges, P., Sabat, G., Martinez, D., Aerts, A., Salamov, A., Grigoriev, I., et al., 2006. Computational analysis of the *Phanerochaete chrysosporium* v2.0 genome database and mass spectrometry identification of peptides in ligninolytic cultures reveal complex mixtures of secreted proteins. Fungal Genet. Biol. 43, 343–356.

Vanden Wymelenberg, A., Sabat, G., Martinez, D., Rajangam, A.S., Teeri, T.T., Gaskell, J., Kersten, P.J., et al., 2005. The *Phanerochaete chrysosporium* secretome: Database predictions and initial mass spectrometry peptide identifications in cellulose-grown medium. J. Biotechnol. 118, 17–34.

Vares, T., Kalsi, M., Hatakka, A., 1995. Lignin peroxidases, manganese peroxidases, and other ligninolytic enzymes produced by *Phlebia radiata* during solid-state fermentation of wheat straw. Appl. Environ. Microbiol. 61, 3515–3520.

Vares, T., Lundell, T.K., Hatakka, A.I., 1993. Production of multiple lignin peroxidases by the white-rot fungus *Phlebia ochraceofulva*. Enzyme Microb. Technol. 15, 664–669.

Vares, T., Niemenmaa, O., Hatakka, A., 1994. Secretion of ligninolytic enzymes and mineralization of ^{14}C-ring-labelled synthetic lignin by three *Phlebia tremellosa* strains. Appl. Environ. Microbiol. 60, 569–575.

Wariishi, H., Valli, K., Gold, M.H., 1992. Manganese(II) oxidation by manganese peroxidase from the basidiomycete *Phanerochaete chrysosporium*. Kinetic mechanism and role of chelators. J. Biol. Chem. 267, 23688–23695.

White, T.J., Bruns, T., Lee, S., Taylor, J.W., 1990. Amplification and direct sequencing of fungal ribosomal RNA genes for phylogenetics, in: Innis, M.A., Gelfand, D.H., Sninsky, J.J., White, T.J. (Eds.), PCR Protocols: A guide to methods and applications. Academic Press Inc, New York, pp. 315–322.

Whittaker, J.W., 2005. The radical chemistry of galactose oxidase. Arch. Biochem. Biophys. 433, 227–239.

Williams, T.A., Foster, P.G., Cox, C.J., Embley, T.M., 2013. An archaeal origin of eukaryotes supports only two primary domains of life. Nature 504, 231–236.

Vu, V.V, Beeson, W.T., Span, E.A., Farquhar, E.R., Marletta, M.A., 2014. A family of starch-active polysaccharide monooxygenases. Proc. Natl. Acad. Sci. U. S. A. 111, 13822–13827.

Wu, S.-H., Nilsson, H.R., Chen, C.-T., Yu, S.-Y., Hallenberg, N., 2010. The white-rotting genus *Phanerochaete* is polyphyletic and distributed throughout the phleboid clade of the Polyporales (Basidiomycota). Fungal Divers. 42, 107–118.

Xiao, P., Mori, T., Kamei, I., Kiyota, H., Takagi, K., Kondo, R., 2011a. Novel metabolic pathways of organochlorine pesticides dieldrin and aldrin by the white rot fungi of the genus *Phlebia*. Chemosphere 85, 218–224.

Xiao, P., Mori, T., Kamei, I., Kondo, R., 2011b. A novel metabolic pathway for biodegradation of DDT by the white rot fungi, *Phlebia lindtneri* and *Phlebia brevispora*. Biodegradation 22, 859–867.

Xiao, P., Mori, T., Kamei, I., Kondo, R., 2011c. Metabolism of organochlorine pesticide heptachlor and its metabolite heptachlor epoxide by white rot fungi, belonging to genus *Phlebia*. FEMS Microbiol. Lett. 314, 140–146.

Xu, G., Wang, J., 2014. Biodegradation of decabromodiphenyl ether (BDE-209) by white-rot fungus *Phlebia lindtneri*. Chemosphere 110, 70–77.

Yang, H., Wang, K., Song, X., Xu, F., Sun, R.C., 2012. Enhanced enzymatic hydrolysis of triploid poplar following stepwise acidic pretreatment and alkaline fractionation. Process Biochem. 47, 619–625.

Yeo, S., Kim, M.K., Choi, H.T., 2008. Increased expression of laccase by the addition of phthalates in *Phlebia tremellosa*. FEMS Microbiol. Lett. 278, 72–77.

Zámocký, M., Hofbauer, S., Schaffner, I., Gasselhuber, B., Nicolussi, A., Soudi, M., Pirker, K.F., et al., 2015. Independent evolution of four heme peroxidase superfamilies. Arch. Biochem. Biophys. 574, 108–119.

Zhu, N., Liu, J., Yang, J., Lin, Y., Yang, Y., Ji, L., Li, M., et al., 2016. Comparative analysis of the secretomes of *Schizophyllum commune* and other wood-decay basidiomycetes during solid state fermentation reveals its unique lignocellulose‐degrading enzyme system. Biotechnol. Biofuels 1–22.

I

Kuuskeri et al. BMC Microbiology (2015) 15:217
DOI 10.1186/s12866-015-0538-x

BMC Microbiology

RESEARCH ARTICLE Open Access

Lignocellulose-converting enzyme activity profiles correlate with molecular systematics and phylogeny grouping in the incoherent genus *Phlebia* (Polyporales, Basidiomycota)

Jaana Kuuskeri[1*], Miia R. Mäkelä[1], Jarkko Isotalo[2], Ilona Oksanen[1] and Taina Lundell[1]

Abstract

Background: The fungal genus *Phlebia* consists of a number of species that are significant in wood decay. Biotechnological potential of a few species for enzyme production and degradation of lignin and pollutants has been previously studied, when most of the species of this genus are unknown. Therefore, we carried out a wider study on biochemistry and systematics of *Phlebia* species.

Methods: Isolates belonging to the genus *Phlebia* were subjected to four-gene sequence analysis in order to clarify their phylogenetic placement at species level and evolutionary relationships of the genus among phlebioid Polyporales. rRNA-encoding (5.8S, partial LSU) and two protein-encoding gene (*gapdh*, *rpb2*) sequences were adopted for the evolutionary analysis, and ITS sequences (ITS1 + 5.8S + ITS2) were aligned for in-depth species-level phylogeny. The 49 fungal isolates were cultivated on semi-solid milled spruce wood medium for 21 days in order to follow their production of extracellular lignocellulose-converting oxidoreductases and carbohydrate active enzymes.

Results: Four-gene phylogenetic analysis confirmed the polyphyletic nature of the genus *Phlebia*. Ten species-level subgroups were formed, and their lignocellulose-converting enzyme activity profiles coincided with the phylogenetic grouping. The highest enzyme activities for lignin modification (manganese peroxidase activity) were obtained for *Phlebia radiata* group, which supports our previous studies on the enzymology and gene expression of this species on lignocellulosic substrates.

Conclusions: Our study implies that there is a species-level connection of molecular systematics (genotype) to the efficiency in production of both lignocellulose-converting carbohydrate active enzymes and oxidoreductases (enzyme phenotype) on spruce wood. Thus, we may propose a similar phylogrouping approach for prediction of lignocellulose-converting enzyme phenotypes in new fungal species or genetically and biochemically less-studied isolates of the wood-decay Polyporales.

Keywords: White rot fungus, Wood decay, Lignocellulose, Lignin biodegradation, Oxidoreductases, Carbohydrate active enzymes, Molecular systematics, Multi-locus phylogeny, *Phlebia*, Polyporales, Basidiomycota

* Correspondence: jaana.kuuskeri@helsinki.fi
[1]Department of Food and Environmental Sciences, Division of Microbiology and Biotechnology, University of Helsinki, Viikki Biocenter 1, P.O.B. 56, FIN-00014 Helsinki, Finland
Full list of author information is available at the end of the article

Background

Fungi of the phylum Basidiomycota have an important role in the global carbon cycle due to their ability to decompose plant biomass that is the richest carbon source on earth. Basidiomycota class Agaricomycetes, in particular the order Polyporales, includes species which are efficient decomposers of wood and other plant biomass, and are able to activate and degrade lignin [1, 2]. The ability to decompose polymeric wood components, that is cellulose, hemicellulose and lignin, requires sets of carbohydrate active enzymes (CAZymes), and oxidoreductases such as peroxidases and laccases [3–5].

The fungal genus *Phlebia* includes several lignin-modifying white rot species which have a high potential for forest-based biotechnology, biopulping, production of lignocellulose-active enzymes and conversion of lignin-derived compounds and xenobiotics [6–15]. Taxonomically, the genus *Phlebia* is positioned to the Polyporales phlebioid clade and to the family Meruliaceae [16–20]. The phlebioid clade includes mainly corticioid basidiocarp-forming species, and the clade consists of seven family names including *Phlebiaceae* originally given by Jülich in 1981 [21]. The genus *Phlebia* has a multitude of species [20, 21] with 203 and 220 taxons recorded in MycoBank (http://www.mycobank.org/) and Index Fungorum (http://www.indexfungorum.org), respectively (August 2015). *Phlebia* has several synonym genera - *Merulius, Mycoaciella* and *Mycoacia* [22, 23].

The type species *Phlebia radiata* Fr. [24] is widely distributed in North America and Europe [25] and has been a subject of genetic and biochemical studies [26–30]. *P. radiata* is a white rot fungus which efficiently degrades lignin in softwood and hardwood [31, 32], depolymerizes milled pine wood [33], mineralizes ^{14}C-labelled synthetic lignin (DHP) to carbon dioxide [34, 35], and efficiently produces a versatile set of lignin-modifying oxidoreductases (class II peroxidases and laccase) [26, 28, 30, 35–38]. In addition to *P. radiata*, research has focussed on a few other species of the genus, e.g. *P. tremellosa*, *P. brevispora, P. ochraceofulva* and *P. lindtneri*, in regard to physiology and potential for bioconversion of plant biomass [39–45]. According to genome sequencing of the species *P. brevispora* [2, 4, 21] and *P. radiata* (ongoing) [29], there is a versatile repertoire of genes encoding lignin-modifying and other lignocellulose-converting oxidoreductases, and multiple CAZymes. However, while genomic data may predict the number of genes and potential functions of the extracellular lignocellulose-converting enzymes in fungal species, protein secretion and biochemical enzyme activities need to be verified by proteomics and activity assays, respectively. This is particularly important on natural growth substrates such as wood. Therefore, we performed lignocellulose-converting enzyme activity profiling of 49 *Phlebia* species on wood cultures. The production of lignocellulose-converting enzyme activities were compared with the molecular taxonomy, in order to find out if the enzyme phenotypes of the species groups were determined by their evolutionary proximity and genotype characters.

Our second aim was to deepen the taxonomic knowledge of the phlebioid clade in Polyporales and study the genetic diversity of *Phlebia* by adopting rRNA-encoding (SSU and LSU) and two cellular core protein-encoding genes - glyceraldehyde phosphate dehydrogenase (*gapdh)* and nuclear RNA polymerase II (*rpb2*). The internal transcribed spacer (ITS) sequence has been selected for fungal barcoding and identification [46], giving adequate information for fungal isolate level molecular taxonomy and definition of species. Recently, extensive ITS sequence analysis of phanerochaetoid taxa in the phlebioid clade enlightened the complex phylogeny of this clade [20] and by focusing on the *Phlebia* clade, our study even deepens the understanding of this clade. In our study, statistical and clustering analyses of the *Phlebia* genotype groups with their enzyme activity production profiles demonstrated that the enzyme phenotypes correlated with the species group genotypes. Thus, for the diverse *Phlebia* species, there is a strong connection between the genotype and their CAZyme and lignin-modifying oxidoreductase activity profiles on a natural-like, wood-supplemented growth medium.

Results

Molecular identification of *Phlebia* isolates

Results obtained from ITS1-5.8S-ITS2 PCR and sequencing of the *Phlebia* isolates confirmed their earlier identification results, which were mostly based on their basidiocarp morphological features, with a few exceptions (Additional file 1: Table S1). Most of the FBCC (University of Helsinki Fungal Biotechnology Culture Collection) isolates previously identified to the species *P. radiata* were correctly confirmed including 14 isolates which were 100 % identical according to their complete ITS sequences (Fig. 1). The only exceptions were the isolates FBCC4 and FBCC345, which were over 99 % identical to the species *P. acerina* (Additional file 1: Table S1). In addition, the phylogenetic maximum likelihood analysis strongly supported positioning of the two isolates in the *P. acerina* branch (bootstrap value 97, Fig. 1) and thereby, these isolates were re-named *P. acerina* at the species level in this study.

Also, the isolates FBCC421 and FBCC426 were re-named *P. centrifuga* and *P. subserialis*, respectively, according to their ITS-sequence identity (99.0 % and 99.8 %) in comparison to taxon reference sequences (Additional file 1: Table S1) and support from high node bootstrap values (100 and 100) (Fig. 1 and Additional file 2: Figure S1a). Considering *P. subserialis,* our isolate

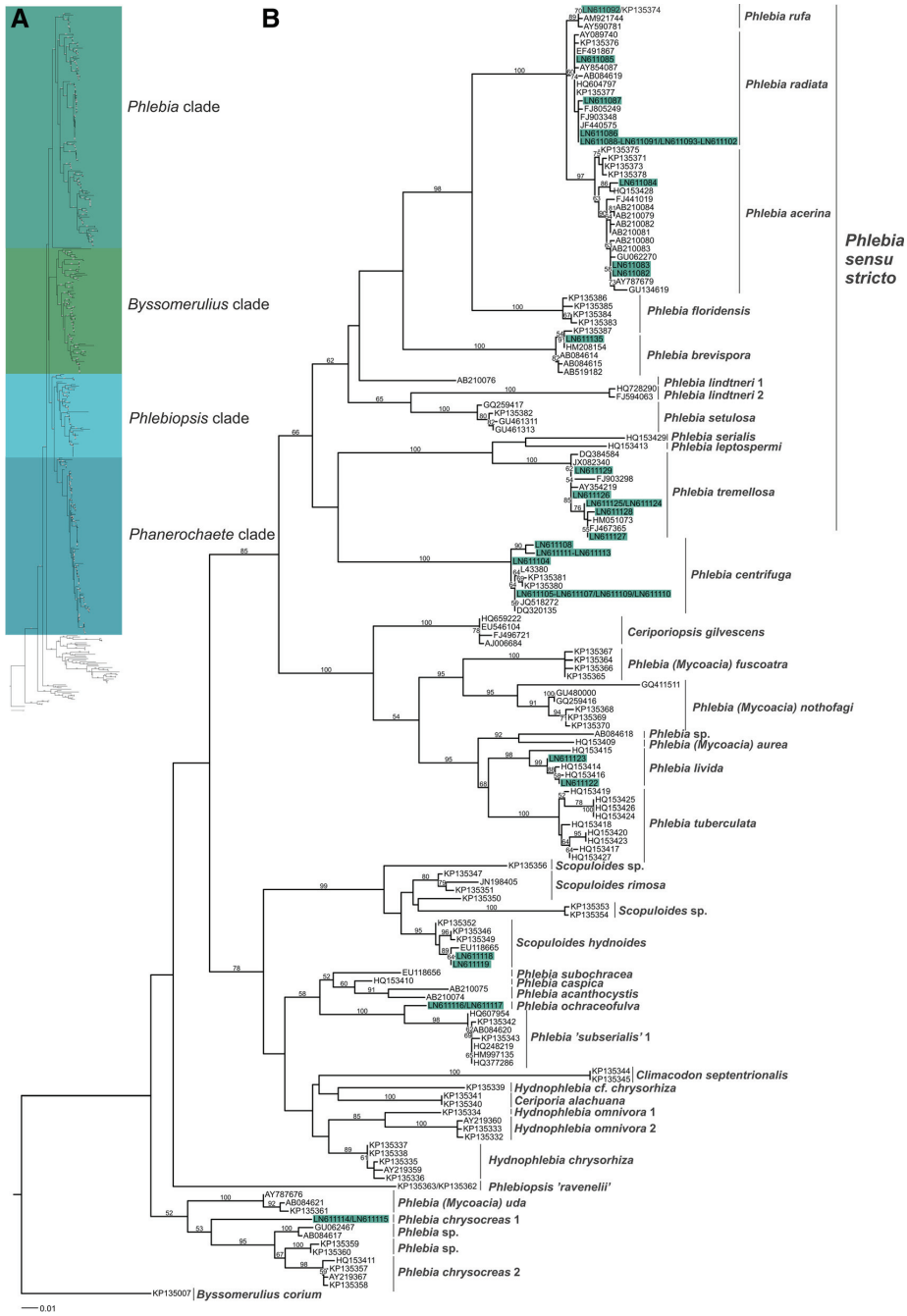

Fig. 1 (See legend on next page.)

(See figure on previous page.)
Fig. 1 Maximum likelihood trees of the phlebioid clade and *Phlebia* clade of Polyporales based on ITS1-5.8S-ITS2 sequences. (**a**) Maximum likelihood tree illustrating the separation of four clades (*Phlebia, Byssomerulius, Phlebiopsis* and *Phanerochaete*) in the phlebioid clade. For the tree, 481 ITS sequences were aligned and phylogenetical analysis was performed using RAxML v. 7.2.8. and 100x bootstrapping. (**b**) Maximum likelihood analysis of ITS1-5.8S-ITS2 sequences from the *Phlebia* clade. Fungi of this study (shaded in green, ITS accession numbers are presented in Table 1) are compared with related taxons with sequences retrieved from NCBI (http://www.ncbi.nlm.nih.gov/) database. Bootstrap values (100 replications) higher than 50 % are indicated for the nodes. Quotation marks represent uncertain identification or provisional names suggested [20]. An ITS sequence of *Byssomerulius corium* was used as an outgroup. Scale bar represents 0.01 nucleotide substitutions per position

FBCC426 and one reference sequence were positioned far away from *Phlebia* species into the *Phanerochaete* clade. Our ITS-sequencing and phylogenetic analyses were unable to confirm the previous identification for three isolates of the 54 studied. Isolate FBCC427 (initially *P. subserialis*) was positioned in the *Phlebiopsis* clade but distant from *Phlebiopsis*, *Rhizochaete* and *Phaeophlebiopsis* (Additional file 2: Figure S1b). Isolate FBCC296 (initially *P. albida*) was distantly related to the *Phlebia* clade and was situated in the *Phanerochaete* clade. However, more information is apparently needed to confirm the species level taxonomy, and therefore, these isolates were not yet given definite identities or taxon names, and are thus depicted *Phlebia* sp. isolates (Additional file 1: Table S1).

ITS phylogeny

An ITS sequence dataset was generated for phylogenetic analyses of the Polyporales phlebioid clade by including reference sequences retrieved from NCBI GenBank and the sequences of this study. Altogether 481 ITS sequences were included in the maximum likelihood (ML) phylogram (Fig. 1a), and 156 sequences were positioned in the *Phlebia* clade (Fig. 1b). The phylogenetic analyses resulted in three major clades in the phlebioid clade, which were named according to Floudas and Hibbet [20] as *Phlebia*, *Byssomerulius* and *Phanerochaete* clades. Similarly as in the recent study [20], the *Phanerochaete* clade was divided into *Phlebiopsis* and *Phanerochaete* clades.

According to the ITS phylogeny, genus *Phlebia* produced no single taxonomic cluster (Fig. 1). While *Phlebia* species are widely distributed in the ITS tree, the *Phlebia sensu stricto* species form one uniform core group, which includes the type species *P. radiata* (Fig. 1b). The three species *P. radiata*, *P. acerina* and *P. rufa* are very closely related forming a distinct branch (bootstrap value 100) in the *Phlebia* clade. In addition, *Phlebia sensu stricto* includes the species *P. floridensis, P. brevispora, P. lindtneri, P. setulosa, P. serialis, P. leptospermi* and *P. tremellosa*. It is noteworthy that the *Phlebia* clade includes a number of isolates that were identified to the genera *Ceriporiopsis, Scopuloides*, *Climacodon, Phlebiopsis, Ceriporia* and *Hydnophlebia* (Fig. 1b).

Furthermore, the species *P. unica, P. firma*, and two isolates of *P. subserialis* were clearly separated from the *Phlebia* clade and were positioned in *Phanerochaete* or *Phlebiopsis* clades (Additional file 2: Figure S1). Three isolates without a previous species-level identity and thus named *Phlebia* sp. were similarly positioned outside the *Phlebia* clade.

Four-gene phylogeny

According to the four-gene multilocus phylogeny analysis, *Phlebia* isolates were divided into ten phylogroups (Fig. 2a, Table 1). Statistical analyses of the enzyme activity data were based on this grouping except for *P. brevispora* due to only one isolate cultivated for enzyme profiling. The first phylogroup included isolates of the species *P. radiata* and *P. rufa* (Fig. 2a). The well-supported sister lineage to this phylogroup was the *P. acerina* branch consisting of three isolates. According to the four-gene phylogeny, *P. tremellosa* clearly deviated from the *P. radiata* and *P. acerina* species groups with 100 % branching support (Fig. 2a). The species *P. brevispora* and *P. livida,* as well as *P. hydnoides, P. chrysocreas* and *P. ochraceofulva* all branched as sister lineages forming distinct species clusters or clades, and were therefore treated as separate phylogroups in the statistical enzyme-phenotype analyses.

Isolates of *P. radiata*, *P. tremellosa*, *P. centrifuga* and *P. subserialis* also diverged at the species level (Fig. 2a). However, the *P. subserialis* group was formed by only two isolates, and more noteworthy, the isolate FBCC426 is the nearest related to species of *Phanerochaete* (*P. chrysosporium* and *P. carnosa*, bootstrap value 100 %). Moreover, the two *Phanerochaete* species, *Phlebia subserialis*, and the isolates *Phlebia* sp. FBCC296 and FBCC427 were positioned far out from the *Phlebia sensu stricto*, and in fact, these isolates were the most related to the species *Phlebiopsis gigantea* and *Bjerkandera adusta* (Fig. 2a).

Presence or absence of introns, intron positioning and intron length varied in *Phlebia gapdh* genes with respect to the species grouping (Fig. 2b). The *P. radiata* and *P. acerina* phylogroups had similar *gapdh* exon-intron structures and length of the sequenced region. *P. tremellosa* and *P. hydnoides* phylogroups were similarly uniform. Other phylogroups showed variable sizes of *gapdh*

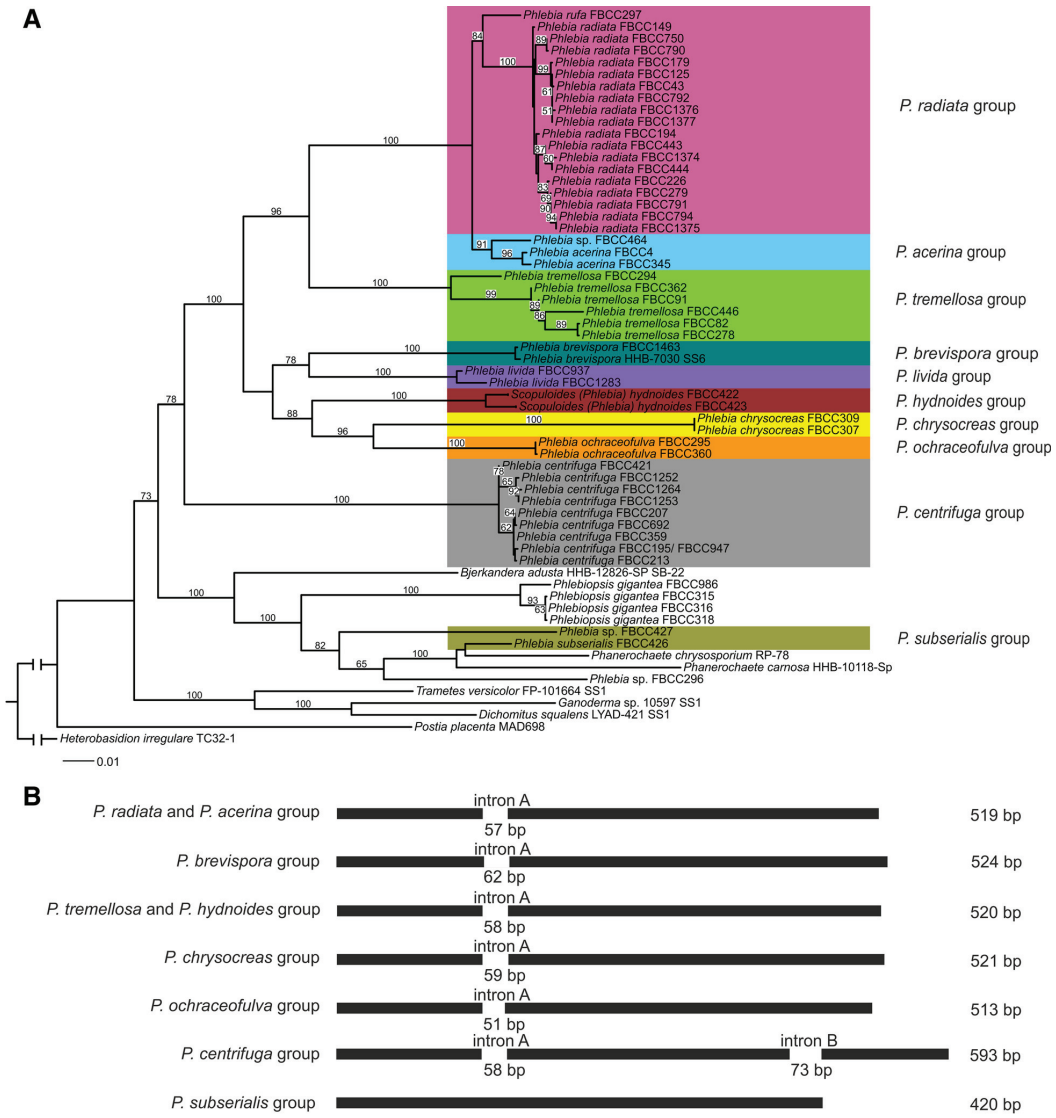

Fig. 2 Maximum likelihood phylogeny and exon-intron structure of partial *gapdh* nucleotide sequences of the *Phlebia* isolates. (**a**) Maximum likelihood phylogeny of the *Phlebia* isolates showing the phylogroups formed. 5.8S, partial LSU, and partial sequences from two protein-encoding genes (*gapdh*, *rpb2*) were concatenated for an alignment, and the phylogenetic analysis was performed using RAxML v. 7.2.8. and 100x bootstrapping. Sequences of related Agaricomycetes species (taxons without FBCC-identifier) were retrieved from JGI MycoCosm database [76] and NCBI (http://www.ncbi.nlm.nih.gov/). Species names are followed by isolate culture collection identifiers. The sequences from species *Heterobasidion irregulare* (Russulales, Basidiomycota) were used as an outgroup. Bootstrap values higher than 50 % are indicated for the nodes. Scale bar represents 0.01 nucleotide substitutions per position. (**b**) Exon-intron structure of partial *gapdh* nucleotide sequences from the *Phlebia* phylogroups studied. Black and white areas indicate exons and introns, respectively

PCR products due to differences in intron length and positioning. All *P. centrifuga gapdh* sequences had a unique intron B, whereas isolate FBCC427 from the *P. subserialis* group as well as *Phlebia* sp. FBCC296 and all *Phlebiopsis gigantea* isolates lacked both introns A and B. With the *gapdh* primers used, no PCR-product was

Table 1 Fungal isolates of this study

Group name[a]	Fungal Biotechnological Culture Collection identifier	Identity[b]	Site of origin	Natural substrate[c]	ITS Accession number	Isolate number used in Figs. 4 and 5
P. radiata group	43	*Phlebia radiata*	Finland; Vantaa	D	LN611085	1
	297	*Phlebia rufa*	Sweden		LN611092	2
	125	*Phlebia radiata*	Finland; Lieksa	D	LN611086	3
	149	*Phlebia radiata*	Finland; Ruovesi	D	LN611087	4
	179	*Phlebia radiata*	Finland; Lammi	D	LN611088	5
	194	*Phlebia radiata*	Finland; Sodankylä	D	LN611089	6
	226	*Phlebia radiata*	Finland; Kolari	D	LN611090	7
	279	*Phlebia radiata*	Sweden		LN611091	8
	443	*Phlebia radiata*	UK	D	LN611093	9
	444	*Phlebia radiata*	France		LN611094	10
	750	*Phlebia radiata*	Finland; Lammi		LN611095	11
	790	*Phlebia radiata*	Finland; Ruovesi	D	LN611096	12
	791	*Phlebia radiata*	Finland; Ruovesi	D	LN611097	13
	792	*Phlebia radiata*	Finland; Ruovesi	D	LN611098	14
	794	*Phlebia radiata*	Finland; Ruovesi	D	LN611099	15
	1374	*Phlebia radiata*	Finland; Lammi	D	LN611100	16
	1375	*Phlebia radiata*	Finland; Ruovesi	D	LN611101	17
	1376	*Phlebia radiata*	unknown		LN611102	18
	1377	*Phlebia radiata*	unknown		LN611103	19
P. acerina group	4	*Phlebia acerina*	unknown		LN611082	20
	345	*Phlebia acerina*	Russia		LN611083	21
	464	*Phlebia* sp.	Argentina; Bariloche	D	LN611084	22
P. brevispora group	1463	*Phlebia brevispora*	USA; Florida		LN611135	23
P. tremellosa group	82	*Phlebia tremellosa*	Finland; Salo	D	LN611124	24
	91	*Phlebia tremellosa*	Finland; Perniö	D	LN611125	25
	294	*Phlebia tremellosa*	Canada	D	LN611127	26
	362	*Phlebia tremellosa*	Russia; Kavalerovo	D	LN611128	27
	446	*Phlebia tremellosa*	Netherlands		LN611129	28
	278	*Phlebia tremellosa*	Sweden		LN611126	29
P. livida group	937	*Phlebia livida*	Finland; Lammi	C	LN611122	30
	1283	*Phlebia livida*	Norway; Telemark	C	LN611123	31
P. hydnoides group	423	*Phlebia (Scopuloides) hydnoides*	Belgium; Bois de Matignolle	D	LN611119	32
	422	*Phlebia (Scopuloides) hydnoides*	France; Haute Savoie		LN611118	33
P. chrysocreas group	307	*Phlebia chrysocreas*	unknown		LN611114	34
	309	*Phlebia chrysocreas*	unknown		LN611115	35
P. ochraceofulva group	295	*Phlebia ochraceofulva*	Sweden		LN611116	36
	360	*Phlebia ochraceofulva*	Sweden		LN611117	37
P. centrifuga group	207	*Phlebia centrifuga*	Finland; Kolari	C	LN611105	38
	213	*Phlebia centrifuga*	Finland; Aakenus	C	LN611106	39
	195	*Phlebia centrifuga*	Finland; Sodankylä	C	LN611104	40

Table 1 Fungal isolates of this study *(Continued)*

	359	*Phlebia centrifuga*	Sweden		LN611107	41
	692	*Phlebia centrifuga*	Finland; Sodankylä	C	LN611109	42
	947	*Phlebia centrifuga*	Finland; Kolari	C	LN611110	43
	1252	*Phlebia centrifuga*	Bulgaria; Rila mountains		LN611111	44
	1253	*Phlebia centrifuga*	Bulgaria; Rila mountains		LN611112	45
	1264	*Phlebia centrifuga*	Bulgaria; Rila mountains		LN611113	46
	421	*Phlebia centrifuga*	USA; Idaho	C	LN611108	47
P. subserialis group	426	*Phlebia subserialis*	France		LN611120	48
	427	*Phlebia* sp.	France; Rhône		LN611121	49
Species included in phylogenetic study	296	*Phlebia* sp.	Sweden		LN611130	
	315	*Phlebiopsis gigantea*	Sweden		LN611131	
	316	*Phlebiopsis gigantea*	Sweden		LN611132	
	318	*Phlebiopsis gigantea*	Sweden		LN611133	
	986	*Phlebiopsis gigantea*	Finland; Kolari	C	LN611134	

[a]Confirmed by ITS1-5.8S-ITS2 and LSU sequence similarity using nBLAST search. See details in Methods
[b]The isolates were grouped based on ITS sequence similarity and phylogrouping based on phylogenetic analyses of concatenated SSU, partial LSU sequences, and partial sequences from two protein-encoding genes (*gapdh, rpb2*)
[c]C = Coniferous wood, D = Deciduous wood

obtained for the *P. livida* isolates, which leaves the question open whether this species group has a more variable *gapdh* gene structure than the other studied species. In general, exon-intron structure of the *gapdh* gene (Fig. 2b) was coherent with the multilocus sequence phylogeny and phylogrouping of *Phlebia* species.

Phylogenetic analyses conducted with either individual or contiguous ITS and partial LSU sequences, and respectively with individual or concatenated *gapdh* and *rpb2* sequences, resulted in evolutionary trees with slightly different topologies than was obtained with the four-gene phylogeny (Additional file 3: Figure S2, Additional file 4: Figure S3). Phylogenetic analyses based on ITS and *gapdh* sequences positioned *P. brevispora* near to *P. radiata - P.acerina* sister species, when the LSU and *rpb2* sequences were not able to confirm its evolutionary placement (Additional file 4: Figure S3). Our four-gene phylogeny also positioned *P. brevispora* closer to *P. livida* than to *P. radiata*. Positioning of *P. livida* as well as *P. hydnoides* was not supported by the protein-encoding sequences (Additional file 3: Figure S2b). Taken together, similar fungal species-based phylogroupings were observed in all evolutionary analyses.

Fungal growth rates and activity normalization

In order to test if the enzyme activities were influenced by the differences in fungal growth rates, we tried to estimate production of mycelium biomass (as mycelium dry weight) for each isolate and each culture flask in the end of cultivation. However, deviation of the dry weight values between the parallel cultures (three parallel culture flasks) was too divergent. This was probably due to wood sawdust particles that were attached to the mycelia. Instead, we measured the hyphal growth rate on malt agar plates for each isolate, and used these values (cm d^{-1}) (Additional file 5: Figure S4f) to adjust the enzyme activity values (μkat l^{-1}) of day 14. This normalization resulted in fairly similar differences between the isolates and species groups that was observed with the non-normalized enzyme activities, except for a few isolates of *P. centrifuga* (see below).

Production of enzyme activities

During the 21 days of cultivation on semi-solid liquid medium with milled spruce as a carbon source, all the 49 *Phlebia* isolates produced lignocellulose-converting enzyme activities periodically (Fig. 3). When the enzyme activity patterns were investigated on the 14th day of cultivation, differences between *Phlebia* phylogroups became apparent (Fig. 4). The *P. radiata* group produced the highest levels of oxidoreductase activities, that is laccase and manganese peroxidase (MnP) (up to 3.0 and 0.9 μkat l^{-1}, respectively) (Fig. 4a, b). The highest laccase activity, 3.0 μkat l^{-1}, was observed in the cultures of *P. radiata* FBCC149, whereas *P. radiata* FBCC125 produced the highest MnP activity (0.9 μkat l^{-1}). Relatively high laccase and MnP activites were

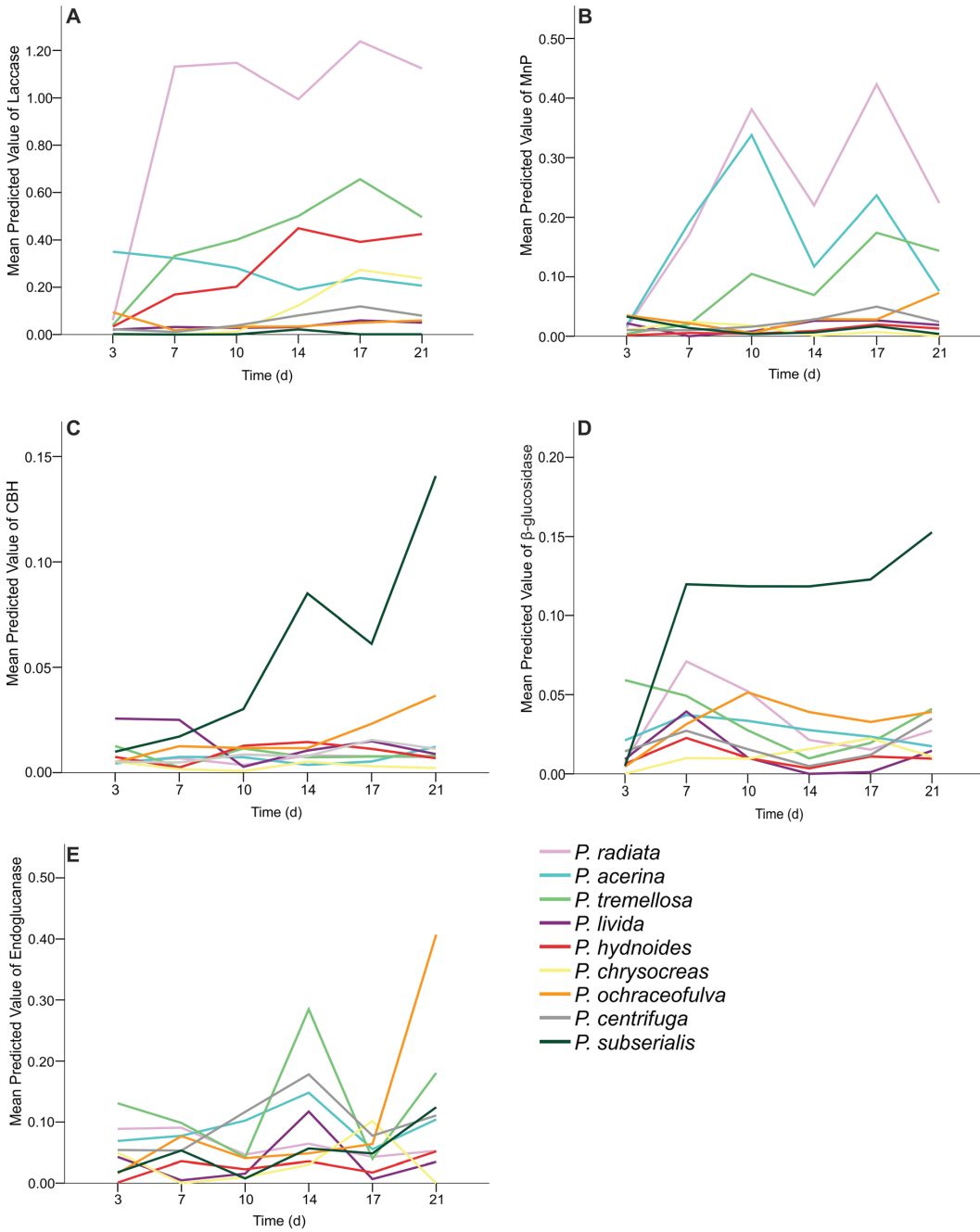

Fig. 3 Fitted values of enzyme activities of each phylogenetic group. Fitted values (mean predicted value) of (**a**) laccase (**b**) MnP (**c**) CBH (**d**) β-glucosidase and (**e**) endoglucanase activities of each phylogenetic group during 21 days of cultivation in semi-solid milled spruce cultures

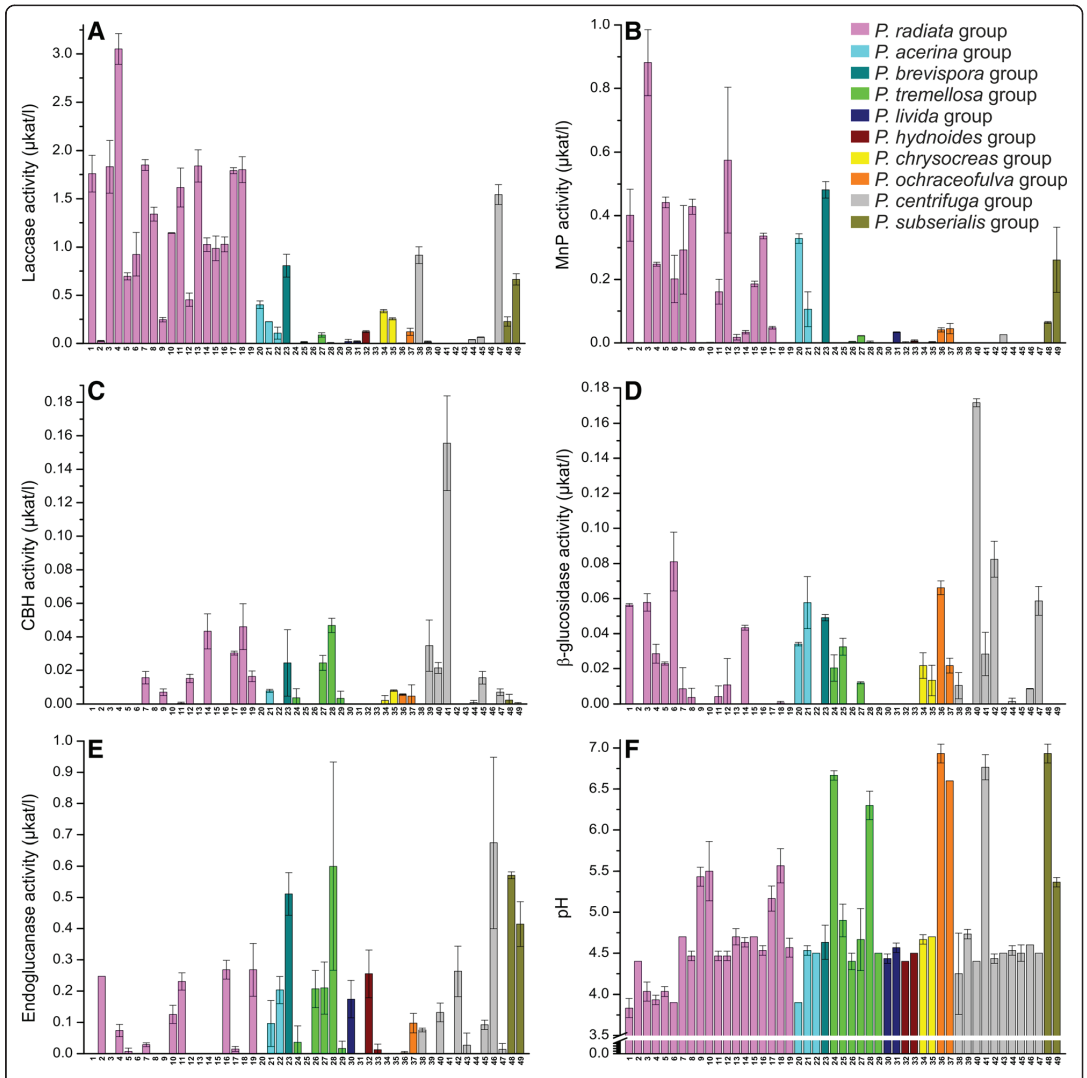

Fig. 4 Enzyme activities and pH values of culture liquids of *Phlebia* isolates. Extracellular (**a**) laccase (**b**) MnP (**c**) CBH (**d**) β-glucosidase and (**e**) endoglucanase activities after 14 days of cultivation in semi-solid milled spruce cultures of *Phlebia* isolates. (**f**) pH values of the semi-solid milled spruce culture liquids after 21 days of cultivation. Initial pH of the culture medium was 4.5. Error bars represent standard deviation of the mean activity value or pH value from two parallel cultivations. The isolates were numbered as listed in Table 1

detected in the cultures of *P. brevispora* FBCC1463. Even though the overall production of laccase in the *P. centrifuga* phylogroup was moderate, one isolate (FBCC421) in this group attained similar activity levels (maximum 1.5 μkat l^{-1}) as obtained in the *P. radiata* – *P. acerina* phylogroups. However, with normalized laccase activities another isolate of *P. centrifuga* (FBCC207) demonstrated the highest production value on the day 14, which is due to its very slow hyphal growth rate (Additional file 5: Figures S4a, S4f). In the case of MnP activity, normalization of the data (on day 14) caused minor differences, with an exceptionally high value for one slow-growing isolate of *P. centrifuga* (FBCC947) (Additional file 5: Figures S4b, S4f).

In contrast to the lignin-modifying oxidoreductases, the activity production profiles of the hydrolytic CAZymes were more coherent within each phylogroup (Fig. 3), and less evident differences were detected in the

CAZyme activity levels between the fungal isolates of each phylogroup (Fig. 4). Concerning cellulose-degrading enzyme activities, the highest level of endoglucanase activity was detected after two weeks for the isolates *P. tremellosa, P. centrifuga* and *P. subserialis* (Fig. 4e), peaking up to 0.7 μkat l^{-1} in the culture liquid of *P. centrifuga* FBCC1264. Cellobiohydrolase (CBH) activities in turn were marginal, and the highest values (0.16 μkat l^{-1}) were observed for the *P. centrifuga* phylogroup (Fig. 4c), which was furthermore obvious with the normalized activity values (Additional file 5: Figure S4c). The highest β-glucosidase activity (0.17 μkat l^{-1}) was also produced in the *P. centrifuga* phylogroup (Fig. 4d). Activities of β-glucosidase in *P. radiata, P. acerina*, *P. brevispora, P. tremellosa* and *P. ochraceofulva* phylogroups were at similar levels but isolate-level differences within each of the phylogroups were detected (Fig. 4d). When CBH activities were studied, the *P. radiata* species group shared similar production patterns as *P. acerina, P. tremellosa* and *P. hydnoides* groups (Fig. 4c), and endoglucanase activities (Fig. 4e) were at the same levels in *P. radiata, P. tremellosa* and *P. subserialis* phylogroup cultures. Isolate-level differences among the species groups were also observed in hyphal growth rates on ME agar (Additional file 5: Figure S4f).

This study utilized generalized estimating equations (GEE) method to analyze differences resulting from enzyme activity values of the samples taken and measured at sequential time points. When the complete cultivation period (21 d) was studied, statistically significant differences in production of lignocellulose-converting oxidoreductases and cellulolytic enzyme activities were detected between the phylogroups (Additional file 6: Table S2). In the statistical calculations, time and species group were the explanatory variables, and also their interaction was statistically significant. When fitted values of enzyme activities of each phylogroup were plotted, the high variation of laccase activity production levels between the phylogroups was observed (Fig. 3). *P. radiata* group produced the highest activities of laccase and MnP during the cultivation period. The second best producer of laccase activity were the *P. tremellosa* and *P. hydnoides* phylogroups which produced increasing amounts of laccase activity within the course of the cultivation. Together with the *P. radiata* phylogroup, the *P. acerina* and *P. tremellosa* groups produced higher amounts of MnP activity compared to the other phylogroups. Fitted values of enzyme activities of each phylogroup showed moderate production of cellulolytic activities. The phylogenetically most distant and incoherent group, the *P. subserialis* group, produced the highest CBH and β-glucosidase activities when compared to the other *Phlebia* phylogroups.

pH values and culture acidity

The pH values of the culture fluids remained stable during the 21 d cultivation period for most of the fungal isolates (Fig. 4f). However, a few of the *P. radiata* isolates (FBCC43, FBCC149, and FBCC194) and *P. acerina* isolate FBCC4 apparently acidified their cultures leading to final pH values below 4.0, which suggests active production of organic acids. On the contrary, final pH values in the cultures of *P. tremellosa* isolates FBCC446 and FBCC82, *P. ochraceofulva* isolates FBCC360 and FBCC295, *P. centrifuga* isolate FBCC359, and *P. subserialis* isolate FBCC426 increased to pH values over 6 (pH 6.3-6.9).

Enzyme phenotype clusters

To further visualize and compare the plant-biomass degrading enzyme production profiles as combinations of the periodical enzyme activity values of the fungal isolates, a double hierarchical clustering calculation method was adopted. Similarities of enzyme activities in the semi-solid milled spruce cultures for each sampling day were calculated to create the data matrix. The normalized enzyme activity values on cultivation day 14 were selected for presentation (Fig. 5).

According to the normalized enzyme activity profiles at this time point, isolates of *Phlebia* demonstrated three enzyme phenotype clusters (Fig. 5). Cluster C contained most of the isolates, including isolates of *P. radiata* and *P. acerina*, and this cluster demonstrated production of both laccase and MnP activities. Cluster B showed high endoglucanase activities and contained sixteen isolates. In Cluster A, enzyme activity production was more scattered but included the highest production of cellulose-degrading CBH activities. Overall, clustering analysis pinpointed two enzyme production patterns: *Phlebia* isolates producing high oxidoreductase (laccase and MnP) activities, and isolates showing high activities of cellulose-degrading enzymes (CBH, endoglucanase, β-glucosidase).

Discussion

In this study, we report on the interdependence of fungal molecular systematics (genotyping) and extracellular enzyme activity profiles (enzyme phenotyping) for isolates of ten species of the largely unknown genus *Phlebia* and other representatives of the phlebioid clade of Polyporales. The 49 fungal isolates were subjected to multilocus gene phylogeny, and cultivated on semi-solid spruce wood medium to follow wood-decay enzyme activities for a three-week period.

Besides enzyme production profiling, our second attempt was to examine molecular systematics of the taxonomically incoherent genus *Phlebia*, and to more accurately position the type species (*P. radiata*) in the

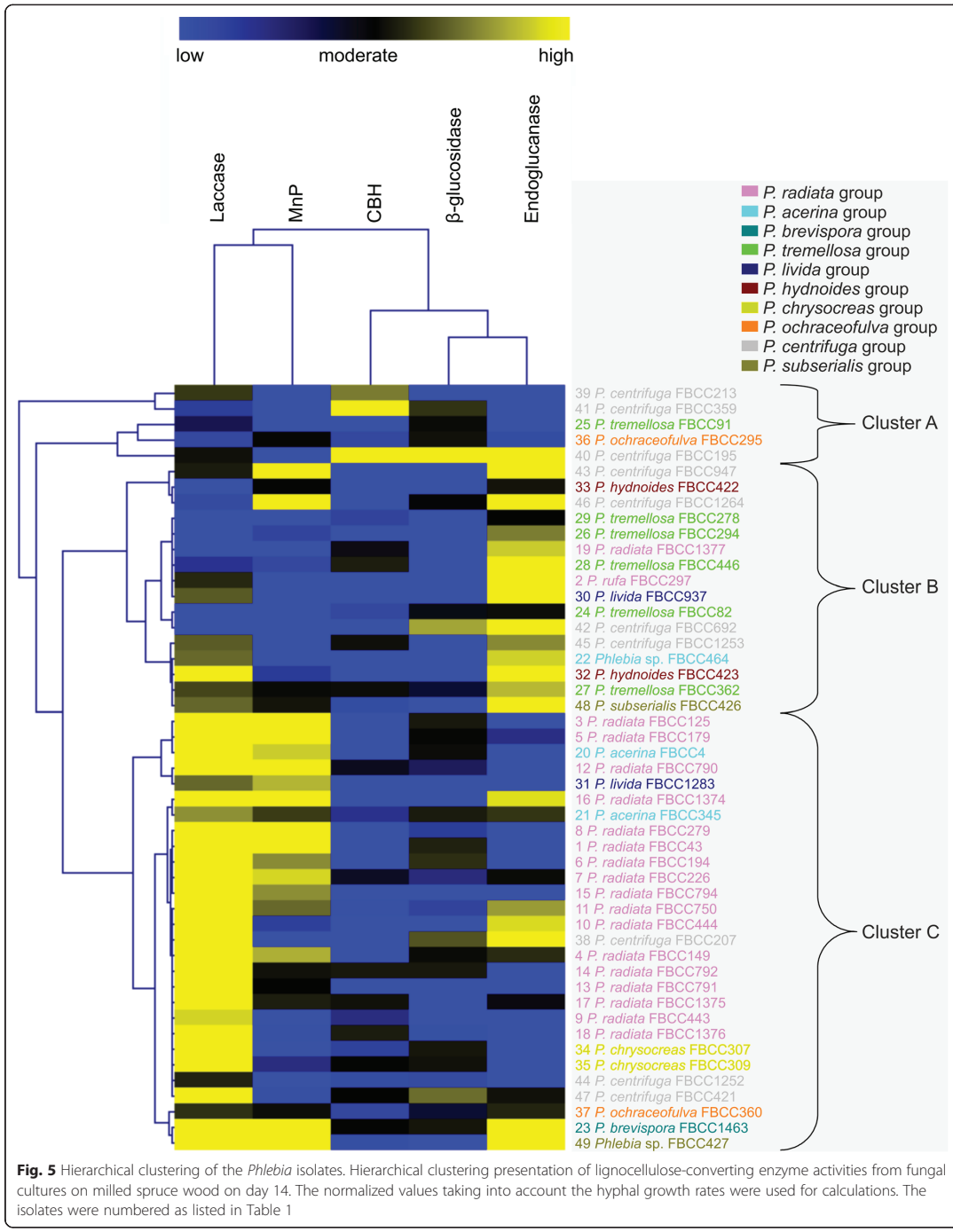

Fig. 5 Hierarchical clustering of the *Phlebia* isolates. Hierarchical clustering presentation of lignocellulose-converting enzyme activities from fungal cultures on milled spruce wood on day 14. The normalized values taking into account the hyphal growth rates were used for calculations. The isolates were numbered as listed in Table 1

genus and phlebioid clade. The genus *Phlebia* has been proposed to be a set of unrelated taxa that have some shared morphological traits [47]. Our sequence-based phylogenetic study was also conducted in order to confirm taxonomic species-level identity of phlebioid and *Phlebia* isolates with previous history of principally morphology-based identification.

Several studies – both traditional and modern molecular systematics applying - have tried to resolve the taxonomy of the multiple genera positioned in the phlebioid clade of Polyporales, but so far without complete success [21, 22, 48–52]. The recent study on phanerochaetoid fungi increased this knowledge but showed the need for reference sequences for some of the species. Our study provided 152 new sequences, and the phylogenetic analyses, both multilocus alignment and single-gene phylogenetic analysis, produced phylograms which point out that fungi with taxon species name *Phlebia* are found in most of the currently recognized lineages of the phlebioid clade (order Polyporales, class Agaricomycetes) [21].

In our study, the barcode marker sequence [46] demonstrated its usefulness for concluding phylogenetic positioning of evolutionarily closely and more distantly related species of *Phlebia*. Although the ITS region is useful to resolve fungal phylogenetic relationships to certain extent, the importance of using other non-protein and protein-encoding genes to resolve the phylogenetic position of certain *Phlebia* species has been demonstrated [47, 49, 50]. For these reasons, we included three genes - rRNA LSU, and protein-encoding *gapdh* and *rpb2* - to improve the outcome of our molecular systematic and evolutionary analyses.

Species named as *Phlebia* can be found in other clades of Polyporales, for example the species *P. bresadolae* and *P. queletii* belong to the 'residual polyporoid clade' [21]. It has been described earlier that the *Phlebia* clade is not uniformly composed of only *Phlebia* species [20]. This study confirmed that the *Phlebia* clade includes also fungal isolates identified to the genera *Ceriporiopsis, Scopuloides*, *Climacodon, Phlebiopsis, Ceriporia* and *Hydnophlebia.* This demonstrates the difficulty to obtain a uniform phylogenetic analysis on *Phlebia* species. For that reason, extensive ITS phylogeny was used as a starting point for generating *Phlebia*, *Phanerochaete* and *Phlebiopsis* clades, wherein our isolates were positioned. After analyzing the *Phlebia* clade, our study confirmed the existence of the *Phlebia sensu stricto* [20]. According to our ITS analysis we propose that at least *P. lindtneri*, *P. serialis* and *P. leptospermi* should be added to this core group. It remains unclear, if *P. centrifuga* belongs to the core group since other phylogenetic analyses of this study and other studies on *P. centrifuga* [20, 49] are not supporting this positioning.

Species-level identity of most of our fungal isolates was confirmed by the four-gene and ITS sequence phylogeny analyses, and taxonomic re-positioning occurred only for a few *Phlebia*-named isolates. Two isolates (FBCC4, FBCC345) previously identified as *P. radiata* were re-classified to *P. acerina* due to their high ITS sequence identity (99.4-99.5 %) to *P. acerina* isolates. Sampling of the reference ITS sequences of *P. radiata*, *P. acerina* and *P. rufa* taxons obtained from NCBI showed that some of these isolates were incorrectly named. Difficulty to identify and discriminate these three species by using traditional methods is not a surprise since *P. rufa*, *P. acerina* and *P. radiata* are very similar in their basidiocarp (basidiomal) and hymenial macro-structure and micro-morphology [25], thus also supporting their genetic similarity and evolutionary close speciation.

P. chrysocreas isolates of this study (FBCC307, FBCC309) were separated from the four reference *P. chrysocreas* isolates according to ITS sequence phylogeny. Four reference sequence isolates without species-level identity (named as *Phlebia* sp.) fall in between this rather scattered branch. *P. ochraceofulva* isolates (FBCC 295 and FBCC 360) produced a separated lineage without reference sequences. Their identity is problematic to confirm without more reference taxons.

Another peculiarity is the positioning of the isolate *P. subserialis* FBCC426 in our phylogenetic analyses, which supported clustering of the isolate far from the *Phlebia* clade to the *Phanerochaete* clade. Different taxonomic positioning of isolates of *P. subserialis* has been observed in earlier studies [21, 47, 49–51, 53]. According to our ITS phylogeny, there is a *Phlebia subserialis* lineage (number 1) in the *Phlebia* clade and a second lineage in the *Phanerochaete* clade (number 2). Recently, a third *P. subserialis* lineage has been demonstrated in the *Phlebia* clade [20]. Six *P. subserialis* ITS sequences were positioned in the *Phanerochaete* clade, but they were separated into two lineages (Additional file 2: Figures S1a, S1b). The first lineage includes our isolate FBCC426. A provisional species name of *Phanerochaete krikophora* was given to the second lineage [20].

We cultivated the phlebioid isolates on semi-solid medium containing milled Norway spruce wood, which is a natural lignocellulose substrate for a multitude of Polyporales wood-decay species in the northern temperate and boreal forests. Most of the *Phlebia* species prefer angiosperm wood for growth but may also colonize dead gymnosperm wood [25, 48]. For instance *P. centrifuga* is usually observed as a saprotroph of Norway spruce [54]. So far, production and activities of wood-decay enzymes has been reported only for a few species of the phlebioid clade. In our study, the wood-containing medium supported production of lignin-modifying oxidoreductase and CAZyme activities in species of *Phlebia*.

In general, moderate levels of cellulolytic endoglucanase activity were produced by all phlebioid isolates, and the highest activities were measured after two weeks of growth. Production of low endoglucanase activities on wood cultures by *P. radiata* and *P. tremellosa* isolates was demonstrated earlier [55], and negligible amounts of other cellulolytic activities have been observed for *P. radiata* cultures on lignocellulose substrates [26]. The type species *P. radiata* produces several cellulolytic enzymes, including β-1,4-endoglucanase, exo-β-1,4-glucanase, aryl-β-1,4-glucosidase, and β-1,4-glucosidase [56], hemicellulolytic enzymes, including β-xylosidase and endo-1,4-β-xylanase [57], and debranching enzymes, such as α-glucuronidase and α-galactosidase, which may cleave the glucosyl side-chains of hemicelluloses and pectin [58, 59]. In this respect, it was expected that production of a wide array of CAZymes acting on wood polysaccharides would be as general as in *P. radiata* at least among the *Phlebia sensu stricto* species. The measured CAZyme activities were reasonably coherent within the species phylogroups, and the few observed differences between fungal isolates (intraspecies variation) may be a consequence of differences in the hyphal growth rates of the isolates.

According to enzyme activity production profiling, *P. subserialis* isolate (FBCC426) and most of the isolates of *P. acerina* and *P. radiata* clustered differently in the double hierarchical clustering calculation analysis. Also statistical analyses showed that the *P. subserialis* phylogroup produced higher cellulolytic enzyme (CBH and β-glucosidase) activities during the cultivation period compared to species that were included in the *Phlebia sensu stricto*. Phenotype similarity of *P. subserialis* to the genus *Phanerochaete* is well supported in this context, since *Phanerochaete* species (*P. chrysosporium*, *P. carnosa*, *P. sordida*) are well known producers of cellulolytic enzymes, with several CAZymes and respective genes characterized [60–62].

Considering the lignin-modifying oxidoreductases, our study reveals that there are significant differences in production of laccase activities among the *Phlebia* species groups. Production of laccase activity was one of the features clearly distinguishing between the enzyme phenotype groups. This is rather surprising since production of laccase has classically categorised wood-decay fungi as white rot and lignin-modifying species [63]. However, in line with the accumulating genomic data and comparative genomics on Basidiomycota and Polyporales species, the role of laccase in decomposition of wood lignin has been questioned [3, 64]. Instead, it is more evident that secreted class II heme peroxidases and in particular, various MnPs are necessary for lignin degradation and white rot type of wood decay [1, 2].

In this respect, it was assumed that all phlebioid isolates studied could actively produce MnP when growing on spruce wood. Convincingly, MnP activities were either at moderate steady levels throughout the cultivation period, or a pattern of cyclic production (MnP activity peaking on 10th and 17th cultivation day) was observed for closely related *P. radiata*, *P. acerina* and *P. tremellosa* strains. Cyclic production of MnP has been reported for *P. radiata* isolate FBCC43 on milled alder wood under similar cultivation conditions [28]. Furthermore, high MnP activities as well as protein properties for MnP enzymes (long- and short-MnPs) and isoenzymes have been reported for several *Phlebia* species (*P. radiata, P. tremellosa, P. brevispora, P. floridensis, P. subserialis*, *Phlebia* sp. MG60, and *Phlebia* sp. b19) [8, 42, 43, 65–67], and divergent *mnp* genes have been cloned from e.g. *P. radiata* [27].

Surprisingly, no lignin peroxidase (LiP) activity was detected in the spruce wood cultures of any of the phlebioid isolates studied, although isolates of *P. radiata, P. tremellosa, P. floridensis, P. brevispora* and *P. ochraceofulva* produced LiP enzymes under variant culture conditions and in cultures including solid lignocellulose supplements [8, 28, 41, 42, 67]. For *P. radiata*, LiP activity has been reported even on similar semi-solid cultures but supplemented with alder sawdust [28, 30], and three LiP-encoding genes have been cloned and characterized in this species [37]. Partial *lip* gene sequences were amplified from isolates of *P. tremellosa* and *P. chrysocreas* [68]. In several previous studies [38, 66, 69] the authors have discussed that LiP activities may not be detectable due to the presence of coloured, apparently phenolic compounds, which are dissolved in the fungal cultures from the wood and plant biomass substrates. These type of compounds may have masked LiP activities also in our study.

Our ITS sequence phylogeny analysis was in agreement with the recent extensive ITS phylogeny study on taxa of *Phanerochaete* and related genera [20]. The protein-encoding gene (*gapdh* and *rpb2*) regions, however, were somewhat less successful in supporting evolutionary positioning of our set of *Phlebia* isolates. The *gapdh* primers designed and applied in this study resulted in a higher frequency of PCR amplification than obtained with *rpb2* primers. Accordingly, *gapdh* intron positioning was one of the genotyping features most conserved among the *Phlebia sensu stricto* species. Presence of a unique second intron in *gapdh* genes of *P. centrifuga* isolates differentiated this species from *Phlebia sensu stricto*. One challenge in using the *gapdh* region for molecular systematics and phylogenetic analyses is yet the lack of reference sequences in nucleotide sequence databases. For this reason, current use of primers targeted to ITS sequences and rRNA encoding genes

together with carefully selected conserved protein-encoding genes promotes coherency for taxonomic comparison and fungal systematics.

Conclusions

Our study on the polyphyletic genus *Phlebia* infers that the fungal phylogroups showed significant differences in lignocellulose-converting enzyme phenotypes according to generalized estimation statistical analysis. These results may reflect different efficiencies of the enzyme-production profiles of *Phlebia* species in their natural habitats, and predict their life-style differences on strategies to degrade various types of wood and lignocellulose. Knowledge of the taxonomy and physiological versatility of genus *Phlebia* has a great importance for more applicative studies on fungal enzyme production and bioconversion abilities. Our study is the first using such approach of combined molecular genotyping and enzyme activity profiling, and may thus be an example for similar research for systematically unknown or biochemically less studied wood-decay fungi, and aid in characterizing new fungal species and isolates.

Methods

Fungal isolates

The fungal isolates (Table 1) were living pure cultures deposited in the University of Helsinki Fungal Biotechnology Culture Collection (FBCC, fbcc@helsinki.fi), of the Division of Microbiology and Biotechnology, Department of Food and Environmental Sciences.

Cultivation of the fungal isolates

Fungal isolates (Table 1) were maintained on 2 % (w/v) malt-extract (Biokar Diagnostics, France) agar (2 % w/v agar-agar, Biokar Diagnostics, France) (MEA) plates at room temperature. For extraction of DNA, fungal isolates were cultivated on 2 % MEA plates for 14 days at 28 °C. For the determination of hyphal growth rates, one mycelium agar plug (7 mm in diameter) was inoculated in the center of each 2 % MEA plate and cultivated for 14 days at 28 °C - except in the case of the fungal isolates FBCC297, FBCC464, FBCC1283, FBCC422, FBCC423, FBCC359 and FBCC421, which were cultivated at 22 °C. For enzyme activity production, *Phlebia* spp. strains were cultivated as semi-solid liquid cultures in three parallel flasks containing 100 ml of low-nitrogen asparagine-succinate medium, pH 4.5 [31, 35], without glucose but supplemented with 1 g (dry weight) of milled Norway spruce (*Picea abies*) wood as the sole carbon source. The semi-solid cultures were inoculated with four mycelial agar plugs (7 mm in diameter) from 7–14 days grown MEA plates, and incubated for 21 days at 28 °C in the dark as stationary cultures.

DNA extraction

Pieces of mycelia were disrupted with acid-washed and sterilized glass beads (1–2 mm) in sterile plastic cryotubes using FastPrep®-24 Instrument (M.P. Biomedicals, USA). DNA was extracted by using CTAB buffer and purified as previously described [27]. Amount and quality of total DNA was determined with NanoDrop 1000 Spectrophotometer (Thermo Scientific, Germany).

PCR amplification

Complete nuclear rDNA ITS region (ITS1 + 5.8S + ITS2), part (1361–1419 bp) of the large rRNA subunit (LSU) coding region, partial (505–636 bp) sequence of the glyceraldehyde phosphate dehydrogenase encoding gene (*gapdh*), and a ca. 1097 bp region of the 140 kDa size subunit of the nuclear RNA polymerase II encoding gene (*rpb2*) were PCR amplified by using genomic DNA as template. The complete ITS region was amplified with ITS1 and ITS4 primers [70], the 5′ region of the LSU with 5.8sr and LR7 primers [71], and the partial *rpb2* region with 7cf and 11bR primers [72]. Primers were designed to amplify the partial *gapdh* region from *Phlebia* isolates (fw: 5′-ATG GTC TAC ATG TTC AAG TAC GAC-3′; rev: 5′-TCG ACG AGG GGA TGA TGT T -3′). PCR reactions were conducted with Dynazyme II or Phusion Hot Start DNA polymerase (Finnzymes, Finland). PCR was performed as previously described [27, 73].

Sequencing

The amplified PCR products were either directly used as templates or cut out of the agarose gels and purified with GeneJET™ Gel Extraction Kit (Fermentas, Lithuania), and used for sequencing (Institute of Biotechnology, University of Helsinki, Finland, and Macrogen Ltd, Republic of Korea) with the initial PCR primer pairs.

Sequence analyses

Nucleotide sequences were edited and assembled with BioEdit software [74]. Regions of ITS1, 5.8S and ITS2 were identified with the ITS extractor software [75]. Introns were excluded manually from the protein-encoding *gapdh* sequences in all analyses. They were confirmed by recognizing the consensus exon/intron splice junction sequences present in reference genes. Reference sequences were obtained from NCBI GenBank (http://www.ncbi.nlm.nih.gov), especially the ITS sequences produced by Floudas and Hibbet [20], and JGI MycoCosm genome portal (http://genome.jgi.doe.gov/programs/fungi/index.jsf, [76], Additional file 7: Table S3). All sequences were aligned using PRANK (http://www.ebi.ac.uk/goldman-srv/webprank/) with the default settings [77]. The alignments were manually trimmed

(overhangs were removed and gaps were corrected) prior to phylogenetic analyses.

After multiple alignment of each trimmed gene, ITS alignment comprising the regions ITS1, 5.8S and ITS2 of 481 DNA sequences from taxa of the phlebioid clade was created and subjected to maximum likelihood (ML) inference by using RAxML v. 7.2.8 (http://phylobench.vital-it.ch/raxml-bb/, [78]). The best-scoring ML tree was searched and the bootstrap analysis was run under the GTRCAT model, using 100 rapid bootstrap replicates. Trees were visualized with the Interactive Tree Of Life (iTOL) online tool [79] and CorelDRAW X3 software (Corel Corporation, Canada). The resulted ML tree helped to divide ITS sequences into four subsets. The ITS sequences of each subset were realigned separately using PRANK and the ML analyses were performed with the same parameters in each case. Multilocus phylogenetic analysis based on 5.8S (SSU) (158 nucleotides), and LSU (1421 nucleotides), *gapdh* (413 nucleotides) and *rpb2* (913 nucleotides) gene coding regions were conducted from the aligned dataset of 62 combined nucleotide sequences containing 2905 positions, of which 810 were variable (including missing data). ITS1 and ITS2 sequences were omitted from the four-gene phylogeny since these were poorly aligned. ML analysis was performed for this alignment with RAxML with GTRCAT model of evolution. Node support was assessed with 100 rapid bootstrap replicates. Individual runs were also performed for each target sequence and for combined ribosomal (ITS + LSU) sequences and combined protein-encoding sequences (*gapdh* + *rpb2*). The ML analyses were performed with the same parameters in each case.

Determination of enzyme activities

Enzyme activities from samples collected on days 3, 7, 10, 14, 17, 21 and 28 after inoculation from three semi-solid culture flasks were measured by using 96-well plates and Tecan Infinite M200 microplate reader spectrophotometer (Tecan, USA) for each fungal isolate. Reaction volume was 250 μl, and three parallel reactions were measured for each sample and each fungal culture flask.

Laccase activity was determined by following the oxidation of 1 mM 2,6-dimethoxyphenol (2,6-DMP, Aldrich, Germany) at 476 nm in 50 mM Na-malonate buffer (pH 4.5) at 25 °C [28, 80]. MnP activity was assayed by detecting the formation of Mn^{3+}-malonate complex at 270 nm in 50 mM Na-malonate buffer (pH 4.5) at 25 °C [81].

Cellulase (cellobiohydrolase I, β-glucosidase and endo-β-1,4-glucanase) reactions were performed in 50 mM Na-citrate buffer (pH 5) at 45 °C [82]. Cellobiohydrolase (CBHI) activity was measured by using 4-methylumbelliferyl-β-D-lactoside (MULac, Biokemis, Russia) as substrate. β-glucosidase activity was assayed by quantification of *p*-nitrophenol released from 1 mM 4-nitrophenyl β-D-glucopyranoside (Applied Chemical Laboratories, USA) at 400 nm. Endo-β-1,4-glucanase activity was determined with 1 % (wt/vol) hydroxyethyl cellulose (HEC, Sigma, USA) as a substrate. Reducing sugars were measured with dinitrosalisylic acid (DNS) at 540 nm [82].

For calculation of the hyphal growth rate, mean data points (measured from three parallel MEA plates) were selected from the linear growth phase. This was presented as cm d^{-1}. Enzyme activity values on cultivation day 14 were divided by this value to obtain the 'normalized' enzyme activity values.

Statistical analyses

The linear models and the method of generalized estimating equations (GEE) were used to analyze differences in the set of enzyme activities between the *Phlebia* phylogroups. The phylogroups were determined by the multigene sequence similarity and evolutionary analysis. In each generalized linear model, time and group were explanatory variables and their interaction terms were also included in all models. The enzyme activities were assumed to follow the Tweedie distribution with link function chosen to be the log link. The working correlation matrix of within-subject repeated measurements was assumed to have a first-order autoregressive structure in each model. In estimation, the index parameter of the Tweedie distribution was first estimated by using the R software 3.1.1 (R Core Team, 2014) with the tweedie package. Then the GEE procedure was performed by using IBM SPSS Statistics 22, release 22.0.0.0 (IBM Corporation, USA). Significance level of 5 % was used in all analyses.

To visualize normalized enzyme activity profiles of the 49 *Phlebia* isolates after 14 days of growth on semi-solid milled spruce medium, hierarchical clustering of the enzyme activities was performed by generating a Pearson correlation matrix with Multiexperiment Viewer (MeV) [83].

Availability of supporting data

The data sets supporting the results of this article are included within the article and its additional files. All nucleotide sequences were deposited in EMBL-EBI European Nucleotide Archive (ENA) under accession numbers presented in Additional file 1: Table S1 [EMBL: LN610995-LN611135 and LN651202-LN651212].

Additional files

Additional file 1: Table S1. Morphological and sequence based identification of isolates and sequenced specimens used in this study. (PDF 152 kb)

Additional file 2: Figure S1. Maximum likelihood analysis of ITS sequences of (a) *Phanerochaete* and (b) *Phlebiopsis* lineages of the phlebioid clade. Description: Bootstrap values (100 replications) higher than 50 % are indicated for the nodes. Fungi of this study (shaded in blue) are compared with related taxons with sequences retrieved from NCBI (http://www.ncbi.nlm.nih.gov/) database. Quotation marks represent uncertain identification or provisional names [20]. Scale bar represents 0.01 nucleotide substitutions per position. (TIFF 4093 kb)

Additional file 3: Figure S2. Maximum likelihood tree of *Phlebia* isolates and related species. Description: Partial nucleotide sequences from (a) rRNA-encoding genes (ITS1-5.8S-ITS2, LSU) and (b) two protein-encoding genes (*gapdh*, *rpb2*) were concatenated for alignment, and the phylogenetic analysis was performed using RAxML v. 7.2.8. and 100x bootstrapping for the nodes. For comparison, sequences from JGI MycoCosm database [76] and NCBI were retrieved. Species names are followed by isolate culture collection identifiers or sequence accessions. Bootstrap values higher than 50 % are indicated for the nodes. Scale bar represents 0.01 nucleotide substitutions per position. (TIFF 3310 kb)

Additional file 4: Figure S3. Phylogenetic trees of phlebioid isolates from maximum likelihood analyses of individual gene datasets. Description: Bootstrap values (100 replications) higher than 50 % are indicated for the nodes. Species names are followed by culture collection identifiers. For comparison, sequences from JGI MycoCosm database [76] were retrieved. Scale bar represents 0.01 nucleotide substitutions per position. (TIFF 6079 kb)

Additional file 5: Figure S4. Normalized enzyme activities of culture liquids and hyphal growth rates of *Phlebia* isolates. Description: Normalized extracellular (a) laccase (b) MnP (c) CBH (d) β-glucosidase and (e) endoglucanase activities on day 14 in semi-solid milled spruce cultures of *Phlebia* isolates. Error bars represent standard deviation of the mean activity value from two parallel cultivations. (f) Hyphal growth rates from three parallel MEA plates. Mean value for each isolate is presented. Error bars represent variance of the growth rates. The isolates were numbered as listed in Table 1. (TIFF 1427 kb)

Additional file 6: Table S2. Statistical tests of model effects and estimates of index parameter in Tweedie distribution. (PDF 155 kb)

Additional file 7: Table S3. Accessions for nucleotide and protein-encoding gene model sequences used for comparison in the four-gene phylogenetic analyses. Description: All the sequences were retrieved from JGI MycoCosm database [76] with minor exception: [a] from NCBI http://www.ncbi.nlm.nih.gov/. (PDF 13 kb)

Abbreviations

CAZymes: carbohydrate active enzymes; CBH: cellobiohydrolase; FBCC: University of Helsinki Fungal Biotechnology Culture Collection; *gapdh*: gene encoding for glyceraldehyde phosphate dehydrogenase; GEE: generalized estimating equations; ITS: internal transcribed spacer; LiP: lignin peroxidase; LSU: large rRNA subunit; MEA: malt extract agar; ML: maximum likelihood; MnP: manganese peroxidase; *rpb2*: gene encoding for a nuclear RNA polymerase II subunit; SSU: small rRNA subunit.

Competing interests

The authors declare that they have no competing interests.

Authors' contributions

JK carried out the experiments, analyzed the data and wrote the manuscript. MRM participated in the design and coordination of the study and contributed to the writing of the manuscript. JI planned and participated in the statistical analyses. IO planned and participated in the bioinformatic analyses. TL conceived the study, participated in its design and contributed to the writing of the manuscript. All authors read and approved the final manuscript.

Acknowledgements

The study was supported by the Academy of Finland Ox-Red research project (grant 138331 to TL). The Microbiology and Biotechnology Doctoral Programme of the University of Helsinki is thanked for the doctoral study position for JK. The authors want to thank the editor and the reviewers for valuable comments on our results and manuscript. Mr Pekka Oivanen is acknowledged for information on the fungal isolates.

Author details

[1]Department of Food and Environmental Sciences, Division of Microbiology and Biotechnology, University of Helsinki, Viikki Biocenter 1, P.O.B. 56, FIN-00014 Helsinki, Finland. [2]Department of Forest Sciences, University of Helsinki, Helsinki, Finland.

Received: 20 January 2015 Accepted: 25 September 2015
Published online: 19 October 2015

References

1. Floudas D, Binder M, Riley R, Barry K, Blanchette RA, Henrissat B, et al. The Paleozoic origin of enzymatic lignin decomposition reconstructed from 31 fungal genomes. Science. 2012;336:1715–9.
2. Ruiz-Dueñas FJ, Lundell T, Floudas D, Nagy LG, Barrasa JM, Hibbett DS, et al. Lignin-degrading peroxidases in Polyporales: an evolutionary survey based on 10 sequenced genomes. Mycologia. 2013;105:1428–44.
3. Lundell TK, Mäkelä MR, de Vries RP, Hildén KS. Genomics, lifestyles and future prospects of wood-decay and litter-decomposing basidiomycota. In: Francis MM, editor. *Advances in Botanical Research*, Vol 70, *Fungi*. London: Academic; 2014. p. 329–70.
4. Hori C, Gaskell J, Igarashi K, Samejima M, Hibbett D, Henrissat B, et al. Genomewide analysis of polysaccharides degrading enzymes in 11 white- and brown-rot Polyporales provides insight into mechanisms of wood decay. Mycologia. 2013;105:1412–27.
5. Riley R, Salamov AA, Brown DW, Nagy LG, Floudas D, Held BW, et al. Extensive sampling of basidiomycete genomes demonstrates inadequacy of the white-rot/brown-rot paradigm for wood decay fungi. Proc Natl Acad Sci U S A. 2014;111:9923–8.
6. Kamei I, Hirota Y, Mori T, Hirai H, Meguro S, Kondo R. Direct ethanol production from cellulosic materials by the hypersaline-tolerant white-rot fungus *Phlebia* sp. MG-60. Bioresour Technol. 2012;112:137–42.
7. Fatehi P, Ates S, Ni Y. Fungal pretreatment of wheat straw and its effect on the soda-AQ pulps. Nord Pulp Pap Res J. 2009;24:193–8.
8. Arora DS, Gill PK. Production of ligninolytic enzymes by *Phlebia floridensis*. World J Microbiol Biotechnol. 2005;21:1021–8.
9. Campoy S, Alvarez-Rodríguez ML, Recio E, Rumbero A, Coque J-JR. Biodegradation of 2,4,6-TCA by the white-rot fungus *Phlebia radiata* is initiated by a phase I (O-demethylation)-phase II (O-conjugation) reactions system: implications for the chlorine cycle. Environ Microbiol. 2009;11:99–110.
10. Kamei I, Suhara H, Kondo R. Phylogenetical approach to isolation of white-rot fungi capable of degrading polychlorinated dibenzo-p-dioxin. Appl Microbiol Biotechnol. 2005;69:358–66.
11. Xiao P, Mori T, Kamei I, Kiyota H, Takagi K, Kondo R. Novel metabolic pathways of organochlorine pesticides dieldrin and aldrin by the white rot fungi of the genus *Phlebia*. Chemosphere. 2011;85:218–24.
12. Xu G, Wang J. Biodegradation of decabromodiphenyl ether (BDE-209) by white-rot fungus *Phlebia lindtneri*. Chemosphere. 2014;110:70–7.
13. Mori T, Kitano S, Kondo R. Biodegradation of chloronaphthalenes and polycyclic aromatic hydrocarbons by the white-rot fungus *Phlebia lindtneri*. Appl Microbiol Biotechnol. 2003;61:380–3.
14. Cho NS, Hatakka AI, Rogalski J, Cho HY, Ohga S. Directional degradation of lignocellulose by *Phlebia radiata*. J Fac Agric Kyushu Univ. 2009;54:73–80.
15. Schüffler A, Wollinsky B, Anke T, Liermann JC, Opatz T. Isolactarane and sterpurane sesquiterpenoids from the basidiomycete *Phlebia uda*. J Nat Prod. 2012;75:1405–8.
16. Hibbett DS, Binder M, Bischoff JF, Blackwell M, Cannon PF, Eriksson OE, et al. A higher-level phylogenetic classification of the Fungi. Mycol Res. 2007;111:509–47.
17. Miettinen O, Larsson E, Sjökvist E, Larsson K-H. Comprehensive taxon sampling reveals unaccounted diversity and morphological plasticity in a group of dimitic polypores (Polyporales, Basidiomycota). Cladistics. 2012;28:251–70.
18. Binder M, Hibbett DS, Larsson K-H, Larsson E, Langer E, Langer G. The phylogenetic distribution of resupinate forms across the major clades of mushroom-forming fungi (Homobasidiomycetes). Syst Biodivers. 2005;3:113–57.

19. McLaughlin DJ, Hibbett DS, Lutzoni F, Spatafora JW, Vilgalys R. The search for the fungal tree of life. Trends Microbiol. 2009;17:488–97.
20. Floudas D, Hibbett DS. Revisiting the taxonomy of *Phanerochaete* (Polyporales, Basidiomycota) using a four gene dataset and extensive ITS sampling. Fungal Biol. 2015;119:679–719.
21. Binder M, Justo A, Riley R, Salamov A, Lopez-Giraldez F, Sjökvist E, et al. Phylogenetic and phylogenomic overview of the Polyporales. Mycologia. 2013;105:1350–73.
22. Moreno G, Blanco M-N, Checa J, Platas G, Peláez F. Taxonomic and phylogenetic revision of three rare irpicoid species within the Meruliaceae. Mycol Prog. 2011;10:481–91.
23. Nakasone KK. Studies in *Phlebia*. Six species with teeth. Sydowia. 1997;49:49–79.
24. Nakasone KK, Burdsall HH. *Merulius*, a synonym of *Phlebia*. Mycotaxon. 1984;21:241–6.
25. Nakasone KK, Sytsma KJ. Biosystematic Studies on *Phlebia acerina*, *P. rufa*, and *P. radiata* in North America. Mycologia. 1993;85:996–1016.
26. Niku-Paavola M-L, Karhunen E, Kantelinen A, Viikari L, Lundell T, Hatakka A. The effect of culture conditions on the production of lignin modifying enzymes by the white-rot fungus *Phlebia radiata*. J Biotechnol. 1990;13:211–21.
27. Hildén K, Martinez AT, Hatakka A, Lundell T. The two manganese peroxidases Pr-MnP2 and Pr-MnP3 of *Phlebia radiata*, a lignin-degrading basidiomycete, are phylogenetically and structurally divergent. Fungal Genet Biol. 2005;42:403–19.
28. Mäkelä MR, Lundell T, Hatakka A, Hildén K. Effect of copper, nutrient nitrogen, and wood-supplement on the production of lignin-modifying enzymes by the white-rot fungus *Phlebia radiata*. Fungal Biol. 2013;117:62–70.
29. Salavirta H, Oksanen I, Kuuskeri J, Mäkelä M, Laine P, Paulin L, et al. Mitochondrial genome of *Phlebia radiata* is the second largest (156 kbp) among fungi and features signs of genome flexibility and recent recombination events. PLoS One. 2014;9:e97141.
30. Mäkelä MR, Hildén KS, Hakala TK, Hatakka A, Lundell TK. Expression and molecular properties of a new laccase of the white rot fungus *Phlebia radiata* grown on wood. Curr Genet. 2006;50:323–33.
31. Hatakka AI, Uusi-Rauva AK. Degradation of ^{14}C-labelled poplar wood lignin by selected white-rot fungi. Appl Microbiol Biotechnol. 1983;17:235–42.
32. Hakala TK, Maijala P, Konn J, Hatakka A. Evaluation of novel wood-rotting polypores and corticioid fungi for the decay and biopulping of Norway spruce (*Picea abies*) wood. Enzyme Microb Technol. 2004;34:255–63.
33. Hofrichter M, Lundell T, Hatakka A. Conversion of milled pine wood by manganese peroxidase from *Phlebia radiata*. Appl Environ Microbiol. 2001;67:4588–93.
34. Lundell T, Leonowicz A, Rogalski J, Hatakka A. Formation and action of lignin-modifying enzymes in cultures of *Phlebia radiata* supplemented with veratric acid. Appl Environ Microbiol. 1990;56:2623–9.
35. Moilanen AM, Lundell T, Vares T, Hatakka A. Manganese and malonate are individual regulators for the production of lignin and manganese peroxidase isozymes and in the degradation of lignin by *Phlebia radiata*. Appl Microbiol Biotechnol. 1996;45:792–9.
36. Lundell T, Hatakka A. Participation of Mn(II) in the catalysis of laccase, manganese peroxidase and lignin peroxidase from *Phlebia radiata*. FEBS Lett. 1994;348:291–6.
37. Hildén KS, Mäkelä MR, Hakala TK, Hatakka A, Lundell T. Expression on wood, molecular cloning and characterization of three lignin peroxidase (LiP) encoding genes of the white rot fungus *Phlebia radiata*. Curr Genet. 2006;49:97–105.
38. Vares T, Kalsi M, Hatakka A. Lignin peroxidases, manganese peroxidases, and other ligninolytic enzymes produced by *Phlebia radiata* during solid-state fermentation of wheat straw. Appl Environ Microbiol. 1995;61:3515–20.
39. Sharma RK, Arora DS. Solid state degradation of paddy straw by *Phlebia floridensis* in the presence of different supplements for improving its nutritive status. Int Biodeterior Biodegradation. 2011;65:990–6.
40. Sulej J, Janusz G, Mazur A, Żuber K, Żebracka A, Rogalski J. Cellobiose dehydrogenase from the ligninolytic basidiomycete *Phlebia lindtneri*. Process Biochem. 2013;48:1715–23.
41. Vares T, Lundell TK, Hatakka AI. Production of multiple lignin peroxidases by the white-rot fungus *Phlebia ochraceofulva*. Enzyme Microb Technol. 1993;15:664–9.
42. Vares T, Niemenmaa O, Hatakka A. Secretion of ligninolytic enzymes and mineralization of ^{14}C-ring-labelled synthetic lignin by three *Phlebia tremellosa* strains. Appl Environ Microbiol. 1994;60:569–75.
43. Kamei I, Daikoku C, Tsutsumi Y, Kondo R. Saline-dependent regulation of manganese peroxidase genes in the hypersaline-tolerant white rot fungus *Phlebia* sp. strain MG-60. Appl Environ Microbiol. 2008;74:2709–16.
44. Hofrichter M, Vares K, Scheibner K, Galkin S, Sipilä J, Hatakka A. Mineralization and solubilization of synthetic lignin by manganese peroxidases from *Nematoloma frowardii* and *Phlebia radiata*. J Biotechnol. 1999;67:217–28.
45. Arora DS, Sharma RK. Effect of different supplements on bioprocessing of wheat straw by *Phlebia brevispora*: changes in its chemical composition, in vitro digestibility and nutritional properties. Bioresour Technol. 2011;102:8085–91.
46. Schoch CL, Seifert KA, Huhndorf S, Robert V, Spouge JL, Levesque CA, et al. Nuclear ribosomal internal transcribed spacer (ITS) region as a universal DNA barcode marker for Fungi. Proc Natl Acad Sci U S A. 2012;109:6241–6.
47. De Koker TH, Nakasone KK, Haarhof J, Burdsall Jr HH, Janse BJH. Phylogenetic relationships of the genus *Phanerochaete* inferred from the internal transcribed spacer region. Mycol Res. 2003;107:1032–40.
48. Ghobad-Nejhad M, Hallenberg N. Multiple evidence for recognition of *Phlebia tuberculata*, a more widespread segregate of *Phlebia livida* (Polyporales, Basidiomycota). Mycol Prog. 2010;11:27–35.
49. Wu S-H, Nilsson HR, Chen C-T, Yu S-Y, Hallenberg N. The white-rotting genus *Phanerochaete* is polyphyletic and distributed throughout the phleboid clade of the *Polyporales* (Basidiomycota). Fungal Divers. 2010;42:107–18.
50. Greslebin A, Nakasone KK, Rajchenberg M. *Rhizochaete*, a new genus of phanerochaetoid fungi. Mycologia. 2004;96:260–71.
51. Parmasto E, Hallenberg N. A taxonomic study of phlebioid fungi (Basidiomycota). Nord J Bot. 2000;20:105–18.
52. Larsson K-H, Larsson E, Kõljalg U. High phylogenetic diversity among corticioid homobasidiomycetes. Mycol Res. 2004;108:983–1002.
53. Suhara H, Sakai K, Kondo R, Maekawa N, Kubayashi T. Identification of the basidiomycetous fungus isolated from butt rot of the Japanese cypress. Mycoscience. 2002;43:477–81.
54. Kotiranta H, Saarenoksa R, Kytövuori I. Aphyllophoroid fungi of Finland. A check-list with ecology, distribution, and threat categories. Norrlinia. 2009;19:1–223.
55. Ander P, Eriksson K-E. Selective degradation of wood components by white-rot fungi. Physiol Plant. 1977;41:239–48.
56. Rogalski J, Hatakka A, Wojtas-Wasilewska M, Leonowicz A. Cellulolytic enzymes of the ligninolytic white-rot fungus *Phlebia radiata*. Acta Biotechnol. 1993;13:41–5.
57. Rogalski J, Oleszek M, Tokarzewska-Zadora J. Purification and characterization of two endo-1,4-β-xylanases and a β-xylosidase from *Phlebia radiata*. Acta Microbiol Pol. 2001;50:117–28.
58. Prendecka M, Szyjka K, Rogalski J. Purification and properties of α-galactosidase isosymes from *Phlebia radiata*. Acta Microbiol Pol. 2003;52:25–33.
59. Mierzwa M, Tokarzewska-Zadora J, Deptuła T, Rogalski J, Szczodrak J. Purification and characterization of an extracellular alpha-D-glucuronidase from *Phlebia radiata*. Prep Biochem Biotechnol. 2005;35:243–56.
60. Diorio L, Galati B, García MA, Papinutti L. Degradation of pruning wastes by *Phanerochaete sordida* growing in SSF: Ultrastructural, chemical, and enzymatic studies. Int Biodeterior Biodegradation. 2009;63:19–23.
61. Vanden Wymelenberg A, Gaskell J, Mozuch M, Kersten P, Sabat G, Martinez D, et al. Transcriptome and secretome analyses of *Phanerochaete chrysosporium* reveal complex patterns of gene expression. Appl Environ Microbiol. 2009;75:4058–68.
62. MacDonald J, Doering M, Canam T, Gong Y, Guttman DS, Campbell MM, et al. Transcriptomic responses of the softwood-degrading white-rot fungus *Phanerochaete carnosa* during growth on coniferous and deciduous wood. Appl Environ Microbiol. 2011;77:3211–8.
63. Hatakka A. Lignin-modifying enzymes from selected white-rot fungi: Production and role in lignin degradation. FEMS Microbiol Rev. 1994;13:125–35.
64. Lundell TK, Mäkelä MR, Hildén K. Lignin-modifying enzymes in filamentous basidiomycetes - ecological, functional and phylogenetic review. J Basic Microbiol. 2010;50:5–20.
65. Bonnarme P, Jeffries TW. Mn(II) regulation of lignin peroxidases and manganese-dependent peroxidases from lignin-degrading white rot fungi. Appl Environ Microbiol. 1990;56:210–7.

66. Hofrichter M, Vares T, Kalsi M, Galkin S, Fritsche W, Hatakka A. Production of manganese peroxidase and organic acids and mineralization of ^{14}C-labelled lignin (^{14}C-DHP) during solid-state fermentation of wheat straw with the white rot fungus *Nematoloma frowardii*. Appl Environ Microbiol. 1999;65:1864–70.
67. Perez J, Jeffries TW. Mineralization of ^{14}C-ring-labeled synthetic lignin correlates with the production of lignin peroxidase, not of manganese peroxidase or laccase. Appl Environ Microbiol. 1990;56:1806–12.
68. Morgenstern I, Klopman S, Hibbett DS. Molecular evolution and diversity of lignin degrading heme peroxidases in the Agaricomycetes. J Mol Evol. 2008;66:243–57.
69. Orth AB, Royse DJ, Tien M. Ubiquity of lignin-degrading peroxidases among various wood-degrading fungi. Appl Environ Microbiol. 1993;59:4017–23.
70. White TJ, Bruns T, Lee S, Taylor JW. Amplification and direct sequencing of fungal ribosomal RNA genes for phylogenetics. In: Innis MA, Gelfand DH, Sninsky JJ, White TJ, editors. PCR Protocols: A Guide to Methods and Applications. New York: Academic Press Inc; 1990. p. 315–22.
71. Hopple JS, Vilgalys R. Phylogenetic relationships in the mushroom genus *Coprinus* and dark-spored allies based on sequence data from the nuclear gene coding for the large ribosomal subunit RNA: divergent domains, outgroups, and monophyly. Mol Phylogenet Evol. 1999;13:1–19.
72. Liu YJ, Whelen S, Hall BD. Phylogenetic relationships among ascomycetes: evidence from an RNA polymerse II subunit. Mol Biol Evol. 1999;16:1799–808.
73. Mäkelä MR, Hildén K, Hatakka A, Lundell TK. Oxalate decarboxylase of the white-rot fungus *Dichomitus squalens* demonstrates a novel enzyme primary structure and non-induced expression on wood and in liquid cultures. Microbiology. 2009;155:2726–38.
74. Hall TA. BioEdit: a user-friendly biological sequence alignment editor and analysis program for Windows 95/98/NT. Nucleic Acids Symp Ser. 1999;41:95–8.
75. Nilsson RH, Veldre V, Hartmann M, Unterseher M, Amend A, Bergsten J, et al. An open source software package for automated extraction of ITS1 and ITS2 from fungal ITS sequences for use in high-throughput community assays and molecular ecology. Fungal Ecol. 2010;3:284–7.
76. Grigoriev IV, Nikitin R, Haridas S, Kuo A, Ohm R, Otillar R, et al. MycoCosm portal: gearing up for 1000 fungal genomes. Nucleic Acids Res. 2014;42:D699–704.
77. Löytynoja A, Goldman N. webPRANK: a phylogeny-aware multiple sequence aligner with interactive alignment browser. BMC Bioinformatics. 2010;11:579.
78. Stamatakis A, Hoover P, Rougemont J. A rapid bootstrap algorithm for the RAxML Web servers. Syst Biol. 2008;57:758–71.
79. Letunic I, Bork P. Interactive Tree Of Life (iTOL): an online tool for phylogenetic tree display and annotation. Bioinformatics. 2007;23:127–8.
80. Slomczynski D, Nakas JP, Tanenbaum SW. Production and characterization of laccase from *Botrytis cinerea* 61–34. Appl Environ Microbiol. 1995;61:907–12.
81. Wariishi H, Valli K, Gold MH. Manganese(II) oxidation by manganese peroxidase from the basidiomycete *Phanerochaete chrysosporium*. Kinetic mechanism and role of chelators. J Biol Chem. 1992;267:23688–95.
82. Rytioja J, Hildén K, Hatakka A, Mäkelä MR. Transcriptional analysis of selected cellulose-acting enzymes encoding genes of the white-rot fungus *Dichomitus squalens* on spruce wood and microcrystalline cellulose. Fungal Genet Biol. 2014;72:91–8.
83. Saeed AI, Sharov V, White J, Li J, Liang W, Bhagabati N, et al. TM4: a free, open-source system for microarray data management and analysis. Biotechniques. 2003;34:374–8.

II

OPEN ACCESS Freely available online

PLOS | ONE

Mitochondrial Genome of *Phlebia radiata* Is the Second Largest (156 kbp) among Fungi and Features Signs of Genome Flexibility and Recent Recombination Events

Heikki Salavirta[1], Ilona Oksanen[1], Jaana Kuuskeri[1], Miia Mäkelä[1], Pia Laine[2], Lars Paulin[2], Taina Lundell[1]*

1 Microbiology and Biotechnology, Department of Food and Environmental Sciences, University of Helsinki, Helsinki, Finland, **2** Institute of Biotechnology, DNA Sequencing and Genomics Laboratory, University of Helsinki, Helsinki, Finland

Abstract

Mitochondria are eukaryotic organelles supporting individual life-style *via* generation of proton motive force and cellular energy, and indispensable metabolic pathways. As part of genome sequencing of the white rot Basidiomycota species *Phlebia radiata*, we first assembled its mitochondrial genome (mtDNA). So far, the 156 348 bp mtDNA is the second largest described for fungi, and of considerable size among eukaryotes. The *P. radiata* mtDNA assembled as single circular dsDNA molecule containing genes for the large and small ribosomal RNAs, 28 transfer RNAs, and over 100 open reading frames encoding the 14 fungal conserved protein subunits of the mitochondrial complexes I, III, IV, and V. Two genes (*atp6* and tRNA-Ile^{GAU}) were duplicated within 6.1 kbp inverted region, which is a unique feature of the genome. The large mtDNA size, however, is explained by the dominance of intronic and intergenic regions (sum 80% of mtDNA sequence). The intergenic DNA stretches harness short (≤200 nt) repetitive, dispersed and overlapping sequence elements in abundance. Long self-splicing introns of types I and II interrupt eleven of the conserved genes (*cox1,2,3; cob; nad1,2,4,4L,5; rnl; rns*). The introns embrace a total of 57 homing endonucleases with LAGLIDADGD and GYI-YIG core motifs, which makes *P. radiata* mtDNA to one of the largest known reservoirs of intron-homing endonucleases. The inverted duplication, intergenic stretches, and intronic features are indications of dynamics and genetic flexibility of the mtDNA, not fully recognized to this extent in fungal mitochondrial genomes previously, thus giving new insights for the evolution of organelle genomes in eukaryotes.

Citation: Salavirta H, Oksanen I, Kuuskeri J, Mäkelä M, Laine P, et al. (2014) Mitochondrial Genome of *Phlebia radiata* Is the Second Largest (156 kbp) among Fungi and Features Signs of Genome Flexibility and Recent Recombination Events. PLoS ONE 9(5): e97141. doi:10.1371/journal.pone.0097141

Editor: Jae-Hyuk Yu, University of Wisconsin - Madison, United States of America

Received November 13, 2013; **Accepted** April 15, 2014; **Published** May 13, 2014

Funding: This study was supported by the Academy of Finland research project grants AF-138331 (Ox-Red) and AF-129869, and a Master's thesis grant from the Department of Food and Environmental Sciences, University of Helsinki. The funders had no role in study design, data collection and analysis, decision to publish, or preparation of the manuscript.

Competing Interests: The authors have declared that no competing interests exist.

* E-mail: taina.lundell@helsinki.fi

Introduction

Phlebia radiata Fr. is a saprobic, wood-colonizing and white-rot type of wood decay causing polypore fungal species of the class Agaricomycetes, phylum Basidiomycota, and is encountered in Eurasian and North-American forests generally on dead angiosperm wood [1,2]. We initiated *de novo* whole genome sequencing of *P. radiata* due to its notable biotechnological abilities in decomposition of wood components and lignocelluloses, and in oxidation and conversion of synthetic and milled wood lignin, and lignin model compounds [3–5]. The fungus is also efficient in degradation of xenobiotics and production of lignin-converting oxidoreductases like lignin peroxidases and manganese peroxidases, and laccase [3–6].

The draft assembly of 454-sequenced *P. radiata* genome resulted first with ca. 300x coverage of a single scaffold and circular dsDNA molecule of over 156 kbp in size, which turned out to be the mitochondrial genome. Mitochondria are cellular organelles of eukaryotes which support individual life-style and generate proton motive force for production of ATP and energy *via* respiration [7–9]. Mitochondria are also known to participate in many other indispensable cellular processes such as calcium homeostasis, cell aging and apoptosis, iron metabolism, and synthesis of iron-sulphur clusters for oxidoreductive enzymes [9–12].

Essence of mitochondria is accepted to arise from endosymbiosis [13,14], most reliably of the SAR11 clade ancestor marine bacterium (pelagibacteria) [15]. Adaptation to the host organism has resulted with co-evolution of the mitochondrial genome and gene flow to the host genome [7,8,16,17]. It was previously considered that mitochondrial genomes are small and compact, according to information mostly achieved from metazoa, such as the only 16 kbp-size human mitochondrial genome [9]. This notion has, together with the retarded mtDNA sizes, previously led to the proposal of the "vanishing mitochondria", especially in fungi [8].

Complete genome sequencing on eukaryotic micro- and macro-organisms has, however, demonstrated a higher degree of mitochondrial genome structural complexity, and variation in the mtDNA size than was previously realized. Complicated network of mini-circle mtDNAs are present in the basal body mitochondrion of the Kinetoplastida protozoa [18], when the

largest mt genomes are described for Embryophyta and Charophyta [19,20], i.e. for land plants and green algae. In angiosperm flowering plants, the mtDNA varies highly in size (200 kbp to 11 Mbp) and may be organized to multiple chromosomes [20–22]. So far, the largest plant mt genomes were recently sequenced for *Silene* species as complex entities with up to 128 circular-mapping chromosomes [22].

Currently, 162 fully sequenced and annotated fungal mtDNA sequences are publicly available. The overwhelming majority (124) of these belong to Ascomycota [19]. Basidiomycota are the second best represented fungal phylum with 21 complete mt genomes [19,23–28]. The other publicly available fungal mtDNAs include a few genomes from species of Blastocladiomycota, Chytridiomycota, Glomeromycota, Monoblepharidomycota, one Cryptomycota (*Rozella allomycis*), and three previous Zygomycota, now *incertae sedis* species [19]. Exceptionally, the Microsporidia and the anaerobic fungi of Neocallimastigomycotina lack traditional mitochondria, which were modified to other cellular organelles such as hydrogenosomes [8]. Most fungal mt genomes are characterized as single circular dsDNA molecules [7,8,23–29], when linear or transiently linear chromosome organization was reported for a few species [7,8,30–32].

Fungal mtDNA generally encloses 14 essential protein-coding genes (*atp6*,*8*,*9*; *cob*, *cox1-3*, *nad1-6*, and *nad4L*) for protein subunits of the mitochondrial complexes I, III, IV, and V required for electron transfer and oxidative phosphorylation. Another common, but more randomly distributed fungal mtDNA-contained gene is *rps3*, which encodes the small ribosomal subunit protein S3. Other typical genes to fungal mtDNA are the small (*rns*) and large (*rnl*) subunit mitochondrial rRNAs, and a tRNA set - generally at least 23 unique anticodons - sufficient to translate the mtDNA-encoded proteome [7,8,10,23–28]. However, exceptions are not unusual. For example, in the Ascomycota budding yeast *Saccharomyces cerevisiae*, the 85.8 kbp mtDNA includes over 40 genes encoding e.g. 24 tRNAs and the two rRNAs, but lacks two of the 14 conserved protein-coding genes (those for Complex I subunits) [29].

Together with our study, recent genome sequencing reports indicate that fungal mitochondrial genomes have a much higher degree of variation in size, gene content, genomic organization and gene order, and gene intron-exon construction than has been realized previously. We acknowledge that the high number of intron-homing endonucleases (HEs) recognized in the *P. radiata* mtDNA may play an editing role, both in genome replication and gene transcription, as well as an integrating role for intron and gene transposition in the mtDNA. Another unique feature is the duplicated "mirror" region in the genome, which together with the repetitive-element dense sections may promote both DNA recombination and gene transcription. We also discuss mtDNA-encoded proteome phylogeny in relation to tRNA evolution and ORF codon usage, in regard to the currently accepted concept of fungal systematics.

Materials and Methods

Fungal Isolate and Cultivation

Phlebia radiata Fr. strain 79 (FBCC0043) was originally isolated from a distinguishable fruiting body found in South Finland on white-rot decayed alder (*Alnus incana*), and maintained in the Fungal Biotechnology Culture Collection at the Department of Food and Environmental Sciences, University of Helsinki, as living mycelium on 2% (wt/vol) malt extract, 1.5% (wt/vol) agar slants under paraffin oil at 12°C. Species identification is based on both macroscopic features of the original fruiting body and mycelium, as well as at molecular level on ribosomal 18S rRNA gene and ITS1-5.8S-ITS2 bar coding sequences [33]. For isolation of total DNA, the fungus was cultivated in liquid 2% (wt/vol) malt extract broth for 10 days at 28°C in the dark. After cultivation, the mycelial mats were harvested and washed with cold ultrapure water, frozen to −20°C, and lyophilized.

DNA Isolation

Dry mycelium was quickly ground in acid-washed and autoclaved mortar. DNA was isolated using a modified version of the hot-CTAB extraction at 65°C [34], followed by phenol-chloroform and 3x chloroform-isoamyl alcohol extractions, and incubation with 0.1 mg/ml Proteinase K (Fermentas) for 30 min at 55°C. Total DNA was precipitated overnight with isopropanol at 4°C, centrifuged at 6500 g 30 min at 4°C, washed twice with 70% ethanol, and subjected to 50 U/ml of RNAseA (Fermentas) treatment at 37°C overnight. After chloroform-isoamyl alcohol extraction, and re-precipitation with ice-cold 94% ethanol overnight at −20°C, DNA was dissolved in sterile TE (10 mM Tris-HCl buffer with 1 mM EDTA, pH 7.5) solution. Integrity an d amount of the isolated total DNA was examined by 1.5% (wt/vol) agarose gel electrophoresis, and using the NanoDrop 1000 Spectrophotometer (Thermo Scientific).

454 Sequencing and mt Genome Assembly

Single-stranded template DNA (sstDNA) was sequenced using the 454 sequencing technology with GS FLX Titanium chemistry (Roche, 454 Life Sciences). Number of obtained reads was 1 876 081 containing 752 Mbp of both genomic DNA (gDNA) and mitochondrial DNA (mtDNA). All reads were assembled using Newbler (Roche, 454 Life Sciences) software. Mitochondrial contigs containing high average sequence coverage (approximately 300x) were placed in proper order, resulting with single scaffold, and a finished mtDNA circular genome was defined being 156 348 bp in length. Circularity and sequence orientation, in particular for the large duplicated region, was verified with genome-walking PCR.

Gene Annotation and Bioinformatic Analyses

The Mold, Protozoan, and Coelenterate Mitochondrial Code and the Mycoplasma/Spiroplasma Code (NCBI translation table 4) was at first assumed for ORF detection. Protein-coding and rRNA genes were annotated by blastp and blastn queries against non-redundant NCBI databases [35–37], and localised and annotated in the mtDNA sequence using Artemis [38] software. Intron-exon boundaries of the conserved genes were adjusted manually on the basis of ClustalX [39] multiple Basidiomycota mt coding sequence alignments. Transfer-RNAs were identified with tRNAscan-SE [40]. HEs were recognized by Pfam 26.0 database [41] queries. Protein domain images were generated with ExPASy PROSITE MyDomains Image Creator (http://prosite.expasy.org/mydomains/) and edited in Inkscape version 0.48.2 (http://inkscape.org/). Intron types were determined with RNAweasel algorithm [42]. Nucleotide sequence repeat elements were identified and analysed with the EMBOSS package Nucleic repeats group tools [43], and by performing a local blastn [35] query of the complete mtDNA sequence against itself. The hits were clustered as a function of similarity in CD-HIT Suite [44], and the h-cd-hit-est algorithm was run with consecutive 0.75, 0.80, and 0.90 cut-off values, using the sequence set that returned <0.001 blastn E-values in the 1 vs. 1 search.

Phylogenetic Analyses

Genome accessions of completely sequenced fungal mtDNAs were retrieved from NCBI Organelle Genome Resources website [19], and linked to corresponding proteomes through GenBank [45] queries. Subsequently, super alignments were generated from USEARCH [46] de-replicated proteomes with the core of Hal pipeline [47], allowing 50% of missing data. Phylogenetic trees were constructed from 44 fungal taxa and 2 019 aa remgaps super alignment first with RAxML 8.0.0 [48] with 100 rapid bootstrap repetitions and automatic model selection (-f a -d -m PROTGAMMAAUTO) using Blastocladiomycota as outgroup (best-scoring aa model was MTZOA), and with PhyloBayes 3.3f [49] using default options, 2 parallel chains were run until maxdiff was <0.1, first 100 trees were discarded as burn-in, and one in ten remaining trees were sampled for posterior consensus. The tree was rooted from mid-point. Nodes receiving ≤ 0.8 posterior consensus (Bayesian) or ≤ 80 bootstrap support (ML) were collapsed to polytomies with TreeCollapseCL4 (http://emmahodcroft.com/TreeCollapseCL.html). The trees were edited in FigTree (http://tree.bio.ed.ac.uk/software/figtree/).

Correlation Analyses

Sequence similarity of the core domain aa-sequences from 57 HEs in the *P. radiata* mtDNA were analyzed by generating aa-sequence pairwise distance matrix of the LAGLIDADG 1 and 2, and GIY-YIG catalytic ORFs using Geneious 5.5.5 software. In addition, pairwise distance matrices of the HE domain loci were calculated using the R environment 2.14.1 package for Windows (http://www.r-project.org/) in order to test correlation of the locus distance to the sequence-similarity based (evolutionary) distance. The data matrices were tested for being parametric or non-parametric. LAGLIDADG 1 aa-sequence similarity scores were normalized with logarithmic transformation. Parametric Pearson correlation in PASW Statistics 18, release 18.0.0 (SPSS Inc., Chicago, IL, USA) was used for LAGLIDADG 1, and GIY-YIG type HE domains, when the non-parametric Spearman's correlation test was applied to LAGLIDADG 2.

Results

P. radiata mtDNA Genome Structure and Conserved Genes

The mitochondrial genome (mtDNA) of *Phlebia radiata* isolate 79 was achieved by *de novo* 454 sequencing of total DNA using Titanium chemistry, and the final assembly resulted in a single 156 348 bp scaffold with a sequence coverage of over 300x, representing one circular dsDNA molecule (Figure 1) with a GC percentage of 31.1. The genome contains the 14 protein-coding genes typical to fungal mtDNA, which are related to the mitochondrial inner membrane Complexes I, III, IV and V of the respiratory chain, i.e. *cox1, atp6, cox2, cox3, nad4L, nad5, atp8, nad2, nad3, atp9, cob, nad4, nad6, nad1*, in clockwise order of the mtDNA (Figure 1). Additionally, 31 conserved genes related to information transfer (28 tRNAs, *rnl*, *rns*, and *rps3*) were identified (Tables 1, 2).

Identified protein (sum 68 953 bp), rRNA (sum 13 606 bp), and tRNA (sum 2 070 bp) genes including introns cover 55% of the *P. radiata* mtDNA. However, only about 15% (25 045 bp) of the genome refers to conserved coding sequences, when intergenic regions (in total 44% of the genome) and coding-sequence splicing introns (sum 59 584 bp, 38%) dominate the sequence space (Figure 2). The majority of the conserved protein-coding genes were split by long introns into multiple short exons (Figure 1, Table 1). The highest number of introns (13) was in the *cox1* gene, which covered ca. 21 kbp (14%) of the genome.

Notably, the genes encoding *atp6*, tRNA-Ile^{GAU} and tRNA-Phe^{GAA} were present in two identical copies. The duplicate *atp6* and tRNA-Ile^{GAU} genes were identified in the "mirror" region, which comprised an inverted and almost identical 6.1 kbp region in the genome (Figure 1). On the basis of multiple sequence alignments, *cob* and *nad6* ORFs had C-terminal fused extensions. Moreover, alternative 3′-ends were found for *atp6* and *cox2* (Figure 3 A, B).

Open Reading Frames with Unknown or Non-conserved Function

In total, 108 ORFs in addition to the conserved genes met our initial search criteria (Table S1). From these, 39 produced significant (E-value ≤ 0.001) blastp hits against the nr database, with a Codon Adaptation Index (CAI) range of 0.299–0.800 in reference to the conserved protein-coding genes. The majority of these ORFs were intronic and were associated with HE domains (Table 3). A notable exception was ORF793 within the long group II intron in the middle of *cob* gene (Figure 1). This intronic ORF was associated with identified RNA-dependent DNA polymerase domain (annotated locus PRA_mt0165, reverse transcriptase) and had particularly low CAI-value of 0.299 (Table S1), which indicates relatively recent horizontal gene transfer from a genetically distant source, most probably of viral origin.

Due to annotated genome sequence submission requirements, ORFs that continued from undisrupted exon reading frames into putative intronic regions were 5′-truncated to their first Met codons, which shortened eight annotated ORFs, and excluded five ORFs that returned significant E-values (Table S2). These ORFs may represent inteins ("protein introns").

Freestanding *P. radiata* mtDNA ORFs that returned significant blastp hits were ORF588, ORF319, ORF314, ORF273 and ORF90, with respective CAI values of 0.624, 0.577, 0.747, 0.633, and 0.515 (Table S1), indicative of fungal mitochondrial origin. Two of these, ORF588 (PRA_mt0150) and ORF273 (PRA_mt0076), were the most similar to putative DNA polymerases of *Pleurotus ostreatus* mt genome (Table S1). Two coding sequences, ORF319 and ORF314, were the most similar to hypothetical proteins annotated in *Moniliophthora roreri* mtDNA as orf2 and hyp11, respectively. Notably, the 5′-end of ORF319 is similar to that of the *P. radiata* mt *nad6* gene (36/37 nt identities), as it is located at the edge of the mirror region (Figure 1). The best hit for ORF90 in turn was a hypothetical protein annotated in the mtDNA of the Ascomycota species *Ajellomyces dermatitidis*.

Transfer RNAs and Codon Usage

The tRNAscan-SE algorithm identified 28 tRNAs (Table 2). This tRNA set is likely able to sense all the codons of the *P. radiata* mtDNA-encoded proteome. With the exception of anticodons of Trp and Ile tRNAs, where possible, U was always the anticodon wobble position base. In the remaining tRNAs, G was always used over A at the anticodon wobble position. For the tRNA-Cys, the tRNAscan-SE Cove algorithm predicted probability for a gene match score below the threshold value of 20.0. However, Cove scores were low as well for other Basidiomycota tRNA-Cys genes, e.g. in *Phakopsora meibomiae* (cove: 19.75), *P. ostreatus* (cove: 19.67), and *Schizophyllum commune* (cove: 22.36). This indicates that the *P.radiata* mtDNA tRNA-Cys gene is real despite the low Cove score obtained.

The GC-content of *P. radiata* mtDNA ORFs was 26.83% (1st letter GC: 34.14%, 2nd letter GC: 33.33%, 3rd letter GC: 13.00%), with no obvious bias observed in codon usage between

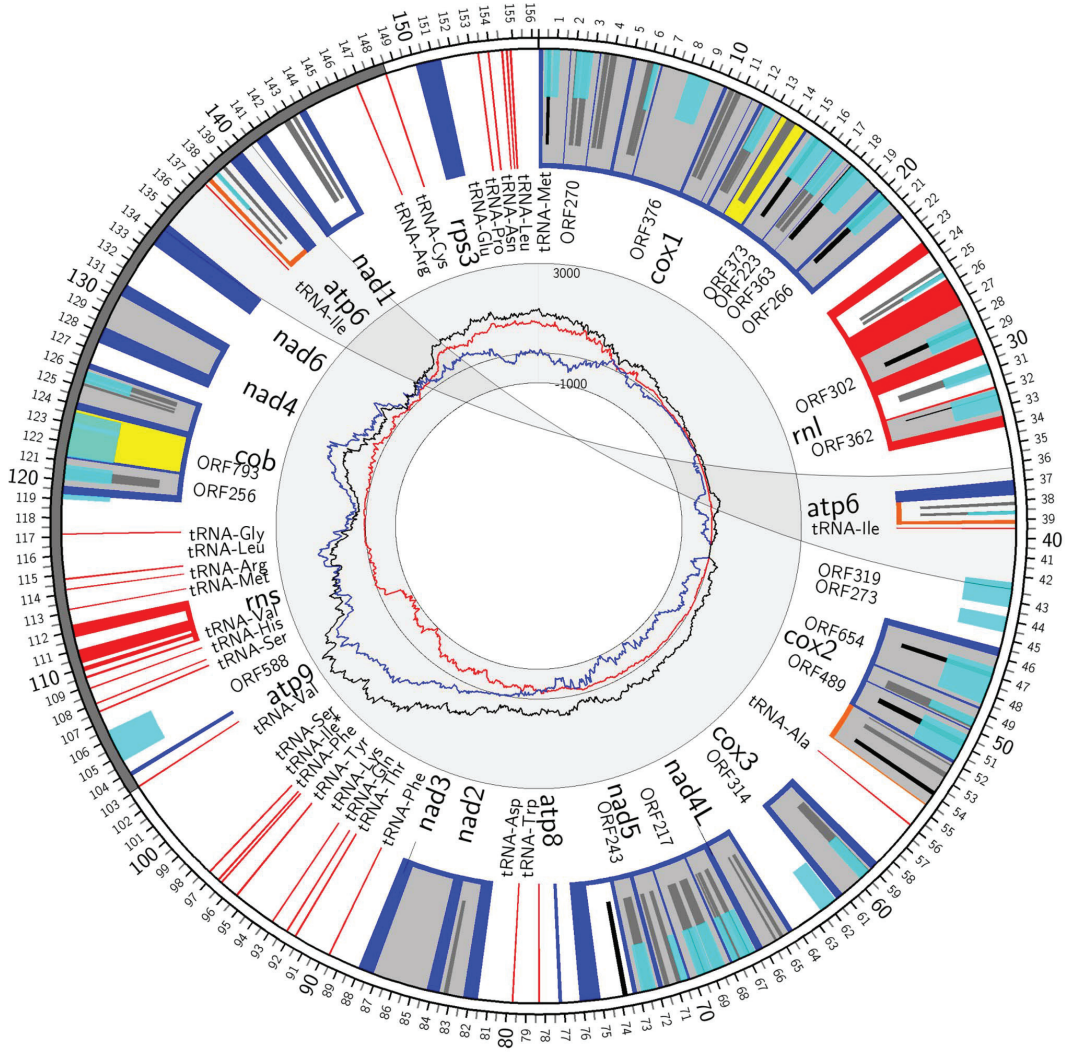

Figure 1. Gene map of *Phlebia radiata* mtDNA. Colour of the scale (kb) bar indicates orientation of transcription: clockwise (CW, white), counter-clockwise (CCW, grey). Bars mark protein-coding (blue) and RNA (red) genes, and alternative C-termini in *atp6* and *cox2* are depicted (orange). Intron type is indicated in colour: group I (light grey), group II (yellow), and uncertain (white). Within introns, the hypothetical and identified ORFs are indicated: over >200 amino-acid long ORFs (turquoise), and homing endonuclease domains GIY-YIG (black) and LAGLIDADG (dark grey). The transparent ribbon illustrates location of the 6,076 bp inversion-duplication. Asterisk indicates putative tRNA-Ile^{CAU}. The inner circle (scale at 12 o'clock in linear units) plots nucleotide bias (G/C skew) up to hexamers along each mtDNA position; G/C (red), A/T (blue), total strand bias (black), placing *oriC* around 11:30 o'clock as the largest bias of G over C.
doi:10.1371/journal.pone.0097141.g001

the leading and the lagging strand encoded ORFs. With the exception of Trp, W-base (A or T/U) ending codons were preferred over S-ending (C or G) codons across all codon families. Cys codons showed the smallest bias with 72% UGU over 28% UGC. For Ala, Phe, His, Ile, Asn, Pro and Tyr the same percentage was ≥80%, and for the rest ≥90%. Some codons UGA (1), AAG (9), CGC (1), AGG (5), and CGG (2) may be unassigned, as they were only present in non-conserved regions, mainly in the putative non-translated C-terminal fused extensions of *cob* and *nad6*.

Phylogeny

The first phylogenetic analysis was established on the similarity and variations of codon usage in fungal mtDNA-protein coding sequence ORFs (Figure 4). The restricted amount of species included in the analysis, however, already grouped *P. radiata*

Table 1. Annotated conserved protein-coding and rRNA genes, their characteristics, location and intron types in *P. radiata* mtDNA.

Gene	Start	End	Strand	Length bp	Coding sequence length (bp)	Protein length (aa)	Introns			Average intron length (bp)	Coding sequence density	Stop codon
							group I	group II	un-certain			
cox1	1	21743	+	21743	1590	529	12	1		1550	7.3%	TAA
rnl	23389	34087	+	10699	3624		2		2	1769	33.9%	
atp6	36924	37700	+	777	777	258					100.0%	TAA
cox2	45480	52022	+	6543	756	251	3			1929	11.6%	TAA
cox3	58610	61439	+	2830	813	270	1			2017	28.7%	TAA
nad4L	64304	66152	+	1849	273	90	1			1576	14.8%	TAA
nad5[1]	66153	76178	+	10026	2007	668	4		1	1604	20.0%	TAA
atp8	77128	77286	+	159	159	52					100.0%	TAA
nad2	81572	87656	+	6085	1812	603	2			2137	29.8%	TAA
nad3[2]	87656	88030	+	375	375	124					100.0%	TAA
atp9	103782	104003	−	222	222	73					100.0%	TAA
rns	109435	112341	−	2907	1711				3	399	58.9%	
cob [3]	119244	126306	−	7063	1272	423	2	1		1930	18.0%	TAA
nad4	127498	130848	−	3351	1473	490	1			1878	44.0%	TAA
nad6[4]	133402	134382	−	981	981	326					100.0%	TAA
atp6	139006	139782	−	777	777	258					100.0%	TAA
nad1[5]	140738	143807	−	3070	1017	338			1	2053	33.1%	TAG
rps3	150069	151403	+	1335	1335	444					100.0%	TAA

[1]*nad5* starts from the adjacent in frame codon to *nad4L* stop.
[2]*nad3* uses the last A of *nad2* stop codon for initiation Met's first nt.
[3]Based on multiple sequence alignment of *Basidiomycota cob* genes the last conserved aa of *P. radiata cob* is 43 aa before the stop codon.
[4]Based on multiple sequence alignment of *Basidiomycota nad6* genes the last conserved aa of *P. radiata nad6* is 122 aa before the stop codon.
[5]The codon after the putative TAG stop codon is TAA.
Empty cell, not present or observed, or unable to calculate.
doi:10.1371/journal.pone.0097141.t001

Table 2. Transfer RNA genes in *P. radiata* mtDNA.

Transfer RNA[1]	Anticodon	Start	End	Strand	Length (bp)
Ile	GAU	39443	39514	+	72
Ala	UGC	55927	55999	+	73
Trp	CCA	78296	78369	+	74
Asp	GUC	79686	79758	+	73
Phe	GAA	89697	89767	+	71
Thr	UGU	91722	91793	+	72
Gln	UUG	92238	92311	+	74
Lys	UUU	93159	93231	+	73
Tyr	GUA	95474	95557	+	84
Phe	GAA	96533	96603	+	71
Ile[2]	CAU	96632	96704	+	73
Ser	UGA	97243	97328	+	86
Val	UAC	103081	103151	−	71
Ser	GCU	107528	107609	−	82
His	GUG	107979	108050	−	72
Val	UAC	108850	108920	−	71
Met	CAU	113144	113216	−	73
Arg	UCG	114191	114261	−	71
Leu	UAG	114743	114816	−	74
Gly	UCC	117118	117188	−	71
Ile	GAU	137192	137263	−	72
Arg	UCU	146748	146818	−	71
Cys[3]	GCA	148390	148461	−	72
Pro	UGG	153357	153429	+	73
Asn	GUU	153900	153972	+	73
Leu	UAA	154617	154701	+	85
Met	CAU	154736	154807	+	72
Glu	UUC	154832	154902	+	71

[1]tRNAscan predicts the tRNA type from the anticodon.
[2]This tRNA was determined to be Ile through comparative means (see below).
[3]The bit score of tRNA-Cys was below 20, which is a typical cut-off value for a pseudogene. The gene was predicted with exceptionally low score from all Basidiomycota mtDNAs.
doi:10.1371/journal.pone.0097141.t002

mtDNA-proteome with Agaricomycotina. Exceptional was the positioning of *C. neoformans* far out from the other Agaricomycotina species.

Our protein phylogenetic approaches, the maximum-likelihood based RAxML, and the Bayesian Monte Carlo Markov Chain sampler PhyloBayes, reconstructed the recognized fungal phyla as monophyletic clades. However, in RAxML the branching of Chytridiomycota, Glomeromycota, and Dikarya (Ascomycota and Basidiomycota) was polytomic, whereas in the PhyloBayes derived tree, Chytridiomycota and Monoblepharidomycota were a sister lineage to Glomeromycota and Dikarya, and Glomeromycota were a sister lineage to Dikarya (Figure 5). Further, in the Bayesian phylogeny, the *incertae sedis* species (previous Zygomycota) *R. oryzae* and *M. verticillata* were within the Glomeromycota/Dikarya branch.

Basidiomycota subphyla were resolved by both methods to current fungal taxonomy with the single exception of the Agaricomycotina classified *C. neoformans* node (two strains, Figure 5). As with higher-level taxonomy, PhyloBayes seemingly solved Basidiomycota subphylum level phylogeny with less polytomies, placing Agaricomycotina as a sister lineage to the Pucciniomycotina/Ustilaginomycotina group. *P. radiata* positioned nearest to *Trametes cingulata* and two *Ganoderma* species (Figure 5).

Introns and Intron Homing Endonucleases

Nine of the 16 fungal mitochondrial conserved genes in *P. radiata* mtDNA were interrupted by over 1 000 bp long introns (Table 3). RNAweasel [42] algorithm detected 29 group I and two group II intron structures, out of which all but one were located within regions that were determined to be intronic also by our manual approach (blastp, blastn, Pfam queries, ClustalX alignments). Our semi-manual approach (blastp, blastn, Pfam queries, ClustalX alignments) predicted seven additional introns. Four of these were associated with core catalytic HE domains within the *nad1*, *nad2* and *rnl* gene regions. Despite the lack of sequence homology, three shorter introns were inferred to reside within the *rns* gene (Table 3). In total, 29 introns were associated with HE domains. Introns varied in length from 201 bp (intron 2 in *rns*) to 3 420 bp (intron 5 in *cox1*), with an average length of about 1.5 kbp for the protein-coding gene splicing introns (Table 3).

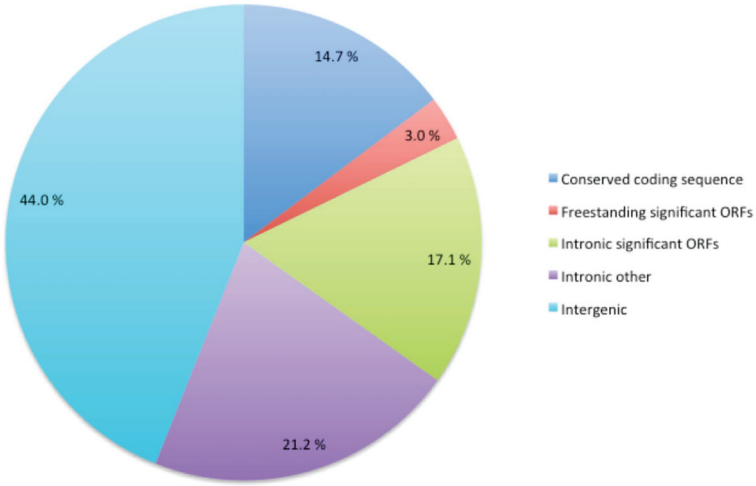

Figure 2. Contribution of the various features of *P. radiata* mtDNA to genome size. Conserved coding sequence refers to the conserved fungal mitochondrial proteome ORFs, rRNAs and tRNAs. Significant ORFs refer to additional identified and hypothetical protein coding sequences with E-value<0.001 obtained by BLASTp queries. Freestanding refers to intronless. Intronic significant ORFs include homing endonucleases, also exon-to-exon-fused ORFs, excluding intergenic ORF HEGs (see text).
doi:10.1371/journal.pone.0097141.g002

Based on Pfam queries, the *P. radiata* mtDNA contained 57 characteristic protein domains encoded by HE genes (HEGs, Pfam family PF05204; Table 4) belonging to three different structural families: LAGLIDADG (47) with subtypes 1 (28) and 2 (19), and GIY-YIG (10). The catalytic HE domains expanded from 21 to 181 aa (59 to 542 bp), and their aa pairwise sequence similarities varied from 3.2% to 32% for LAGLIDADG 1, from no identity to 67% similarity for LAGLIDADG 2, and from 12% to 52% for GIY-YIG type of domains (Table 4, Table S5). The HE motifs were predominantly (45/57) situated within group I type introns. One single GIY-YIG domain located within a group II intron, and 10 motifs located in regions of unrecognized intron type (Table 3).

Eight of the HE catalytic domains were exceptional in appearing as free-standing after the last putative coding sequence exon and stop codon in the genes *atp6* and *cox2*. Notably, alternative C-termini were annotated for both of these genes (Figure 3A, B). The parametric Pearson's correlation test of pairwise aa-similarity and locus distance for the identified HE domain types (Table S1, S2, S5) resulted in correlation value of −0,166 with a statistically significant p-value (0.031) for LAGLIDADG type 1, and correlation value of −0.256 with, however, a statistically insignificant p-value (0.089) for GIY-YIG type. The non-parametric Spearman's correlation test for LAGLIDADG type 2 (19) resulted in a test value of −0.040 but with statistically insignificant p-value (0.607). These results infer

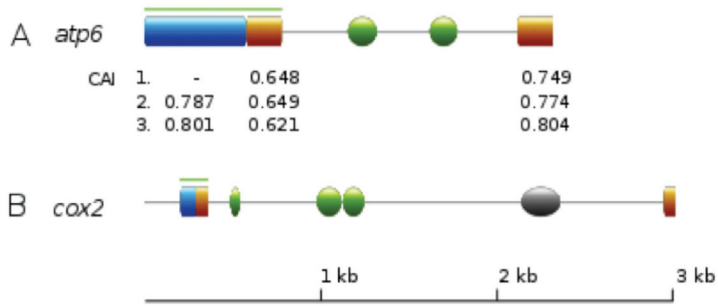

Figure 3. Schematic view of the C-termini regions of *P. radiata* mtDNA *atp6* and *cox2* genes. Green lines denote *atp6* coding sequence region and the last exon of *cox2*. Spheres/ovals represent LAGLIDADG 1 (green) and GIY-YIG (grey) homing endonuclease domains. **A)** Region of 201 bp (orange) with high 1 vs. 1 sequence similarity, corresponding to the 3′-end of the *atp6* gene. Codon Adaptation Index (CAI) values are shown for the *atp6* N-terminal region (blue) and for the regions of high sequence similarity. Reference codon usage is from: 1) *atp6* N-terminus, 2) *atp6* N-terminus and *atp8-9*, 3) *atp6* N-terminus, *atp8-9*, *cox1-3*, *nad1-5* and *nad4L*. **B)** Separated by three LAGLIDADG 1 domains and a GIY-YIG domain, two regions of high 1 vs. 1 sequence similarity (orange) exist for the last 66 bp of the *cox2* gene. Image was generated with ExPASy PROSITE MyDomains Image Creator (http://prosite.expasy.org/mydomains/) and edited in Inkscape version 0.48.2 (http://inkscape.org/).
doi:10.1371/journal.pone.0097141.g003

Table 3. Introns, their lengths and types in the conserved *P. radiata* mtDNA-encoded genes.

Gene	Intron 1	Intron 2	Intron 3	Intron 4	Intron 5	Intron 6	Intron 7	Intron 8	Intron 9	Intron 10	Intron 11	Intron 12	Intron 13	Total length (bp)	Average length (bp)
cox1	1463 G	1540 L1	1680 L1	1356 L2	3420	1447 L1	432	1144 L2	1410 L2	1649 G	1076 L1	2004 G	1532 G	20153	1550
nad5	1413 L1	2278 L2	1405 L1	1186 L2	1737 G									8019	1604
rnl	1675 L2	1912 G	1756 L2	1732 G										7075	1769
cox2	2849 G	1152 L2	1786 G											5787	1929
rns	704	201	291											1196	399
cob	1864 L1	2452 R	1475 L2											5791	1930
nad2	1306 L2	2967												4273	2137
cox3	2017 L2													2017	2017
nad4L	1576 L1													1576	1576
nad4	1878													1878	1878
nad1	2053 L1													2053	2053

Homing endonuclease associations: G, GIY-YIG; L1, LAGLIDADG 1; L2, LAGLIDADG 2; R, reverse-transcriptase ORF including.
Underlined, group II intron type.
doi:10.1371/journal.pone.0097141.t003

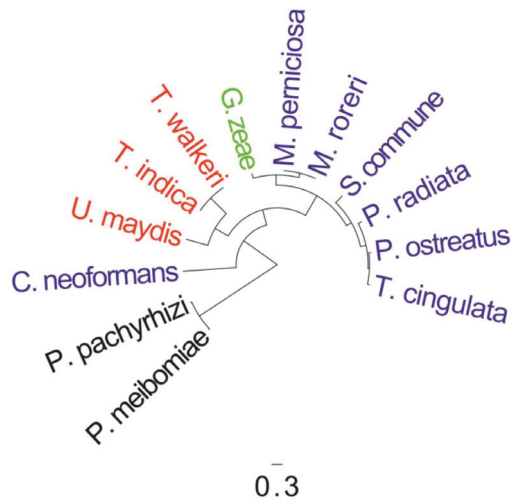

Figure 4. Codon usage of the *P. radiata* mitochondrial genome protein-coding gene open reading frames in comparison to selected Basidiomycota and Ascomycota species. Neighbor-joining tree with topology derived from codon on codon root mean squared difference distance matrix (Table S3, Table S4). Agaricomycotina, blue; Ustilaginomycotina, red; Pucciniomycotina, black; Ascomycota species *Gibberella zeae* = *Fusarium graminearum*, green, as outgroup. Scale bar indicates nucleotide changes per site.
doi:10.1371/journal.pone.0097141.g004

that genome (intron) location is to some extent related to the degree of HE sequence similarity, at least for the LAGLIDADG 1 HEs. However, it may also be concluded that HE motif transposition to more distant locations are equally allowed, as is observed for LAGLIDADG 2 and GIY-YG domains.

Inverted Duplication and Other Repeated Elements

A distinguishing feature was the inverted duplication region of 6 075 bp in size that accounted for 3.9% of the *P. radiata* mtDNA. One region (ID1) expanded from nt position 140 421 to 134 346 and the other (ID2) from nt position 36 285 to 42 360 (Figure 1), which is named "mirror region" in our EMBL submitted and annotated *P. radiata* mt genome. Both regions harboured the two genes *atp6* and tRNA-Ile^{GAU}, and differed only by 3 nt –in the plus DNA strand at nt position 40 066 with an additional A, at nucleotide position 41 338 with absence of T, and at position 42 353, T instead of G.

A major difference between the ID1 and ID2 regions was the start of the coding sequence of the single-copy gene *nad6* within the 3′ end of the ID1 region (Figure 1). Another difference was the occurrence of a single-copy, functionally unknown ORF319 (PRA_mt0074) that was only recognized in ID2. However, the ORF was only 1-nt different in the 5′ end sequence (first 37 nt) compared to *nad6* in ID1. In addition to the mirror region, the *P. radiata* mtDNA is frequent with short (≤200 nt), dispersed, and partially overlapping tandem repeat sequence motifs (Figure 6A, B), in particular between positions 85 000 to 100 000 nt, where also tRNA encoding genes were clustered (Figure 1). The most abundant repeat sequence types were dispersed and inverted repeat sequences, which were almost exclusively localized into intronic, and especially into intergenic regions (Figure 6A). These repeats were often overlapping, and covered as much as 15% of

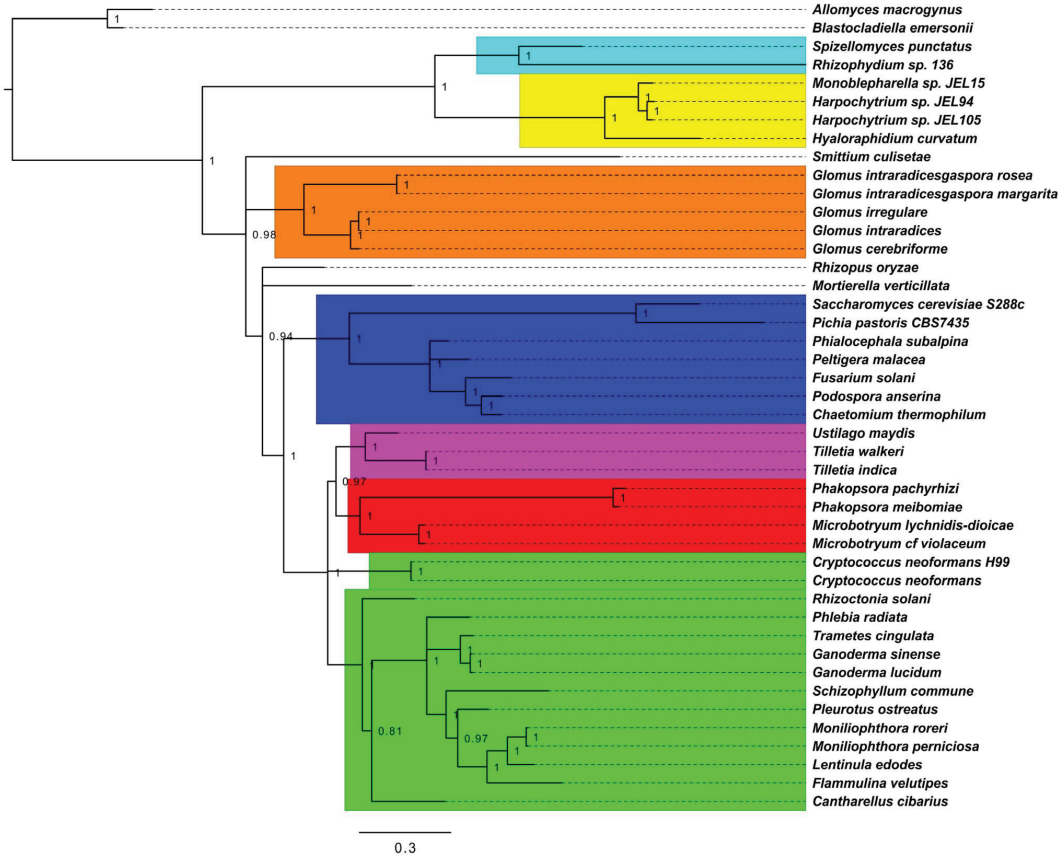

Figure 5. Phylogeny of fungal mitochondrial proteomes. The statistically most likely tree was derived by Bayesian inference from a multi-gene superalignment of mtDNA-encoded proteins (2 019 aa positions, 44 taxa). Posterior consensus support values are depicted for branching, and nodes receiving ≤0.8 support were collapsed into polytomies. The tree was rooted from mid-point. Colours refer to phyla or sub-phyla: turquoise, Chytridiomycota; yellow, Monoblepharidomycota; orange brown, Glomeromycota; dark blue, Ascomycota; pink, Ustilaginomycotina (Basidiomycota); red, Pucciniomycotina (Basidiomycota); bright green, Agaricomycotina (Basidiomycota); Blastocladiomycota node as outgroup. Scale bar indicates amino-acid substitutions per site. For species and mtDNA accession, see Table 5.
doi:10.1371/journal.pone.0097141.g005

the *P. radiata* mtDNA. Subsets of these sequences shared high sequence similarity (Figure 6B).

Origin of Replication

According to G/C skew analysis, origin of replication (*oriC*) of the *P. radiata* mtDNA may be located around 11:30 to 00:30 o'clock (position 153 000 to position 7 nt) regarding to the largest bias of G over C (Figure 1). The lowest G/C skew ratio in turn is located around 7:00 to 8:30 o'clock (positions 88 000 to 109 000 nt), in the about 21 kb size intergenic region indicative of a putative mtDNA replication termination site, which is supported by switching of the coding strand (orientation of transcription) at this site, around position 103 000 nt.

Sequence Accession

The complete and annotated *Phlebia radiata* 79 mitochondrial genome sequence is available under the accession codes [EMBL: HE613568] and [NCBI: NC_020148].

Discussion

mtDNA Size and Genome Organization

To our knowledge, at 156 348 bp, the mitochondrial genome of *P. radiata* described in our current study is the second largest completely sequenced, gene annotated and located mtDNA among fungi, and presents specific features as signs of genetic flexibility, recombination history and active editing process of the genome. Our findings on the size and original features of the *P. radiata* mtDNA, together with other recent Basidiomycota mitochondrial genome studies are thereby not explicitly supporting the previous conclusions for the rather small sized and disappearing fungal mitochondrial genomes.

On the contrary, fungal mt genomes apparently vary greatly in size, from ca. 12 kb kbp of the Cryptomycota parasite species *Rozella allomycis* [19] to over 235 kbp (165 kbp main mtDNA [50]) of the Basidiomycota Agaricomycotina species *Rhizoctonia solani* strain AG3 Rhs1AP (Table 5). Evidence of large variations in the

Table 4. Intron-homing endonuclease domains and their location in the *P. radiata* mtDNA.

Homing endonuclease			Length (aa)			Similarity (aa% identity)			Locus distance (bp)		
Catalytic domain	Pfam	Sum	Min	Max	Mean	Min	Max	Mean	Min	Max	Mean
LAGLIDADG-1	CL0324	28	29	115	69	3.2	32	11	408	141 226	56 490
LAGLIDADG-2	CL0324	19	34	181	102	0	67	16	106	114 830	34 171
GIY-YIG	CL0418	10	21	112	80	12	52	26	2 214	73 172	26 106
All		57	28	136	84						

doi:10.1371/journal.pone.0097141.t004

genome size and a high degree of mtDNA structural complexity between eukaryotic organism lineages and species is currently accumulating through sequencing projects. For fungi, such extreme variations in the mtDNA size or multi-chromosomal organization have not, however, been noticed than is updated for plant (from 0.2 to 10 Mbp mtDNAs), algae and protozoa mitochondria [18–22]. Fungal mitochondrial genomes are usually mapped as single circular dsDNA molecules [7,8,23–29]. We likewise assume a similar configuration for the *P. radiata* mtDNA on the basis of our sequence assembly, bioinformatic analyses and PCR. Reports on more linear than circular chromosomal structure of the mtDNA in the Chytridiomycota species *Hyaloraphidium curvatum* [30], in the Ascomycota yeasts *Candida albicans* [31] and *Saccharomyces cerevisiae* [32,51,52] indicate that the possibility for a partial linear or linear-circular chromosomal organization for the *P. radiata* mtDNA cannot be completely ruled out, despite the convincing circular assembly which was obtained from the careful study of our sequence data.

With fungal mt genomes of less than 30 kb in size, usually all the 14 fungal mtDNA-conserved, mitochondrial inner-membrane protein complex I, III, IV and V protein subunit-coding genes are present. Examples of these compact mt genomes within Basidiomycota are species of the animal-pathogenic genus *Cryptococcus*, with some variation of the mtDNA size (24–34.7 kb), gene order and intronic and ORF coding sequence between species and variants [53,54]. The large fungal mitochondrial genomes, alike *P. radiata* mtDNA, expand over 100 kb in size and may include over 50 protein-coding ORFs (Table 5). The tendency for larger fungal mt genomes (over 90 kbp) in the Basidiomycota subphylum Agaricomycotina is pinpointed by recent reports on *Moniliopthora perniciosa* and *M. roreri* [24,28], *T. cingulata* (over 90 kb) [26], *A. bisporus* (135 kbp) [23] and *R. solani* (165 kbp/235 kbp) [50]. This tendency is furthermore confirmed by our study on the 156 kbp *P. radiata* mtDNA showing up to 126 predicted protein-coding ORFs and 30 RNA genes, which are the second highest numbers reported for the fungal mitochondrial genomes.

The largest mtDNAs within Ascomycota are those of the filamentous species *Podospora anserina* (over 100 kbp) and *Chaetomium thermophilum* var. *thermophilum* (over 120 kbp), similar to many of the Agaricomycotina basidiomycete mtDNAs, when the smallest (from Ascomycota yeasts) mt genomes are reduced to about 20 kbp in size (Table 5) with only 10 protein-coding genes [19]. Among Ascomycota fungi, however, there are yet large variations at the genus level – between species - of both mtDNA size and gene content. In the yeast *S. cerevisiae*, the 85.8 kbp mtDNA harnesses 19 protein-coding genes when only the mitochondrial Complex I NADH dehydrogenase subunit encoding genes are absent [19,29,51]. In another species of *Saccharomyces*, *S. castellii*, the mtDNA is reduced to 1/3 in size (25.7 kb) and contains only 9 protein-coding genes [51].

Only slight differences, however, in mtDNA size, gene number and organisation have been observed in the Basidiomycota genera *Moniliophthora* (Agaricomycotina) [24,28], *Tilletia* (Ustilaginomycotina) [19], *Phakopsora* (Pucciniomycotina) [27], and *Cryptococcus* (Agaricomycotina) [53,54], thus indicating genus-level conservation of the mitochondrial genomes in the phylum Basidiomycota. The large differences in gene order and location (loss of synteny) between the Basidiomycota mitochondrial genomes at higher taxon levels, as was reported for *Ganoderma lucidum* (Agaricomycotina) mtDNA [55], and is observed in this study for *P. radiata* mtDNA, may thus indicate frequent recombination events and flexibility of fungal organelle genomes.

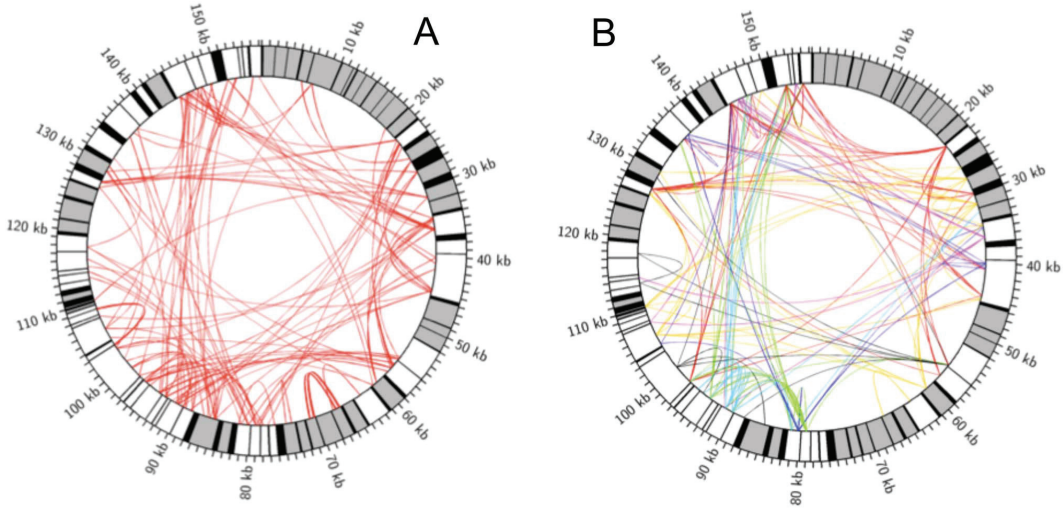

Figure 6. Dispersed and inverted repeat sequences in *P. radiata* mtDNA. Colors: black, conserved protein-coding, rRNA and tRNA genes; grey, introns; white, intergenic regions. The large 6.2 kb duplication-inversion is excluded from the figures. **A)** Red ribbons connect regions of significant (E-value $<1\times10^{-7}$) nucleotide sequence similarity. **B)** Coloured ribbons connect similar sequence regions. Only clusters with at least 6 similar repeat members are shown. The sequences were clustered as a function of similarity in CD-HIT Suite [44] (h-cd-hit-est run with consecutive 0.75, 0.80, and 0.90 cut-off values) from a sequence set that returned <0.001 1 vs. 1 blastn values.
doi:10.1371/journal.pone.0097141.g006

Intergenic and Repetitive Sequences

In the large angiosperm plant mt genomes, the genome size is mainly due to long intergenic regions and non-coding sequence (gene spacers, introns, and pseudogenes) [20,22]. Accordingly in the large *P. radiata* mtDNA, over 80% of the mt genome is either intergenic or intronic sequence (Figure 2). Our analyses show that most of the intergenic sequence space in the *P. radiata* mtDNA is filled with repeated sequences, in particular between genome nt positions from 90 000 to 110 000 surrounding several tRNA-coding gene loci. Accumulation of polymorphic microsatellite repeated elements (1–6 nt in length) were reported for species of the Agaricomycotina genus *Agrocybe* [56], and already in *S. cerevisiae* mtDNA, long AT rich stretches were identified [29]. Putative roles in splicing of mitochondrial polycistronic transcripts may be proposed for the intergenic regions, as well as action as potential promoters with regulative element motifs.

Surprisingly, the mtDNA of *P. radiata* contains a large (6.1 kbp) inverted duplication segment. This is another similar feature to the angiosperm plant mitochondrial genomes, where large duplicated sequences in the mtDNA apparently function as co-linear recombination sites to aid genome organization [21,22]. In the Ascomycota species *C. albicans*, the very similar in size (7 kbp) inverted repeat regions in the apparently linear mtDNA are directing genome replication *via* homologous recombination at the site [31]. Interestingly, the *C. albicans* mtDNA inverted repeat harnesses duplication of the gene *cox3*, whereas in the *P. radiata* mtDNA mirror site, we recognized duplication of the genes *atp6* and tRNA-Ile^{GAU}. Two inverted repeats of over 4 kbp in size were reported for another Agaricomycotina species, *A. bisporus*, devoid of protein-coding ORFs but containing duplicated sets of tRNA genes [23]. At the moment, we may suggest a replication-directing recombination function for the inverted duplication in the *P. radiata* mt genome, similar to that observed in *C. albicans* mtDNA [31].

Introns and Homing Endonucleases

Together with the high portion of the intergenic regions, notable in *P. radiata* mtDNA is the degree of invasion by mobile DNA-elements, which were recognized as long type I and II self-splicing introns (in total over 30 long introns), and including up to 57 HE domain-encoding ORFs. Nine of the 15 conserved protein-coding genes, and the *rnl* gene in *P. radiata* mtDNA are invaded by long introns carrying HE motifs of LAGLIDADG types I and II, when the ten recognized GIY-YIG motifs correspond a minority of the HE domain types.

Homing endonuclease genes were previously identified within mtDNAs of other Basidiomycota species, such as *M. perniciosa* and *M. roreri* [24,28] and *A. bisporus* [23]. However, only four of the protein-coding genes (*cob*, *cox1*,*2*, and *nad5*), and the *rns* and *rnl* genes were previously reported to contain self-splicing introns with HE motifs in these fungal mtDNAs, when in the *P. radiata* mtDNA, nine of the 11 intron-containing conserved genes contained intronic HE domains. In the elongated *cox1* gene of *P. radiata*, eleven LAGLIDADG and four GIY-YIG motifs were recognized in 13 long, self-splicing type I (12) and type II (1) introns. In regard to this, even up to 18 introns, both type I and II, were recognized in the almost 30 kb-size *cox1* gene of *A. bisporus* [57].

A few reports enlighten the enzymatic and molecular functions of intronic HEs in the fungal mtDNAs. In gene transcription, the HE domains are apparently removed from the transcribed pre-mRNA resulting in a contiguous RNA transcript [58–60]. It is likely that existence of intron-homing endonucleases within fungal mtDNA genes is one apparatus for promoting genetic diversity and adaptive response for the mitochondrial genome, when the allelic recombination events may be impossible or rare due to the mainly uniparental nature of mtDNA inheritance in fungi [10,17].

In the Ascomycota species *Aspergillus nidulans*, C-terminal fragment of the mtDNA *cob* gene intron-homing translated LAGLIDADG type endonuclease (I-AniI) is involved in splicing

Table 5. Fungal mitochondrial genomes, representatives of Basidiomycota and other phyla. *Phlebia radiata* mtDNA, this study; **R. solani* 162 751 kbp [50], 235 849 kbp [19].

Fungal phylum	Species	Subphylum or class	mtDNA sequence accession	mtDNA size (bp)
Basidiomycota				
	Rhizoctonia solani	Agaricomycotina	NC_021436	*162 751
	Phlebia radiata	Agaricomycotina	**NC_020148**	156 348
	Agaricus bisporus	Agaricomycotina	JX271275	135 005
	Lentinula edodes	Agaricomycotina	NC_018365	121 394
	Moniliophthora perniciosa	Agaricomycotina	NC_005927	109 103
	Moniliophthora roreri	Agaricomycotina	NC_015400	93 722
	Trametes cingulata	Agaricomycotina	NC_013933	91 500
	Flammulina velutipes	Agaricomycotina	NC_021373	88 508
	Ganoderma sinense	Agaricomycotina	NC_022933	86 451
	Pleurotus ostreatus	Agaricomycotina	NC_009905	73 242
	Ganoderma lucidum	Agaricomycotina	NC_021750	60 630
	Cantharellus cibarius	Agaricomycotina	NC_020368	58 656
	Schizophyllum commune	Agaricomycotina	NC_003049	49 704
	Cryptococcus neoformans var. grubii H99	Agaricomycotina	NC_018792	24 919
	Cryptococcus neoformans var. grubii	Agaricomycotina	NC_004336	24 874
	Tilletia indica	Ustilaginomycotina	NC_009880	65 147
	Tilletia walkeri	Ustilaginomycotina	NC_010651	59 352
	Ustilago maydis	Ustilaginomycotina	NC_008368	56 814
	Microbotryum lychnidis-dioicae	Pucciniomycotina	NC_020353	107 808
	Microbotryum cf. violaceum	Pucciniomycotina	NC_020354	92 107
	Phakopsora meibomiae	Pucciniomycotina	NC_014352	32 520
	Phakopsora pachyrhizi	Pucciniomycotina	NC_014344	31 825
Ascomycota				
	Chaetomium thermophilum var. thermophilum	Pezizomycotina	NC_015893	127 206
	Podospora anserina	Pezizomycotina	NC_001329	100 314
	Fusarium graminearum (Gibberella zeae)	Pezizomycotina	NC_009493	95 676
	Peltigera malacea	Pezizomycotina	NC_016955	63 363
	Fusarium solani	Pezizomycotina	NC_016680	62 978
	Phialocephala subalpina	Pezizomycotina	NC_015789	43 742
	Nakaseomyces bacillisporus	Saccharomycotina	NC_012621	107 123
	Saccharomyces cerevisiae	Saccharomycotina	NC_001224	85 779
	Komagataella (Pichia) pastoris	Saccharomycotina	NC_015384	35 683
Glomeromycota				
	Gigaspora rosea	Glomeromycetes	NC_016985	97 350
	Gigaspora margarita	Glomeromycetes	NC_016684	96 998
	Glomus irregulare	Glomeromycetes	NC_014489	70 800
	Glomus (Rhizophagus) intraradices	Glomeromycetes	NC_012056	70 606
	Glomus cerebriforme	Glomeromycetes	NC_022144	59 633
Chytridiomycota				
	Spizellomyces punctatus	Chytridiomycetes	NC_003052	61 347
	Rhizophydium sp. 136	Chytridiomycetes	NC_003053	68 834
Monoblepharidomycota				
	Monoblepharella sp.	Monoblepharidomycetes	NC_004624	60 432
	Hyaloraphidium curvatum	Monoblepharidomycetes	NC_003048	29 593
	Harpochytrium sp.	Monoblepharidomycetes	NC_004623	24 169
	Harpochytrium sp.	Monoblepharidomycetes	NC_004760	19 473
Blastocladiomycota				
	Allomyces macrogynus	Blastocladiomycetes	NC_001715	57 473

Table 5. Cont.

Fungal phylum	Species	Subphylum or class	mtDNA sequence accession	mtDNA size (bp)
	Blastocladiella emersonii	Blastocladiomycetes	NC_011360	36 503
Cryptomycota				
	Rozella allomycis		NC_021611	12 055

doi:10.1371/journal.pone.0097141.t005

of the intronic pre-mRNA, while the second, N-terminal endonuclease motif was not essential for intron splicing [58]. Instead, the N-terminal motif functioned in cleavage of the DNA target site to initiate the HE intron mobilization. These reports on well-ordered and bi-functional effects of the intronic HEs imply their active involvement in supporting genetic flexibility in the fungal mitochondrial genomes.

The HEs recognize longer DNA target regions (14–40 bp) than common DNA-endonucleases and tolerate more sequence variation, which assists in interrupting and introducing new genetic elements (usually introns) and ORFs (mainly intronic HE domains) in their target sites [59,60]. In *P. radiata* mtDNA, two potential examples (genes *atp6* and *cox2*) of HE-transmitted introns and alternative coding sequences, both C-terminal, are observed (Figure 3A, B). Unusual splicing of the mtDNA *atp6* C-terminus was early on reported for the Blastocladiomycota species *Allomyces macrogynus* [61]. Additional intron with HE was found as an insertion including foreign C-terminal *atp6* sequence fused in-frame, which was explained by horizontal gene transfer [61]. However, a more likely explanation is that intronic HEs may have transposed to a new site downstream of the stop codon, as has apparently occurred in *P. radiata atp6* leading to alternative C-termini, but in the case of *A. macrogynus atp6*, introducing somewhat altered homolog of the new C-terminus.

Additional C-terminal coding sequence was likewise inserted into the mitochondrial intronic *rps3* gene of the Ascomycota *Ophiostoma novo-ulmi* subsp. *americana* [62]. In the latter case, the HE insertion apparently shifted a small portion of the *rps3* coding region downstream and disrupted the ORF with a premature stop codon. Accordingly, in the *P. radiata cox2* gene, the duplicated C-terminus is intervened by a 2.5 kb sequence containing catalytic HE domains, and is fused after a premature stop codon in the first C-terminus.

The group I and II type self-splicing introns and HEs are interlinked since the self-splicing introns need endonuclease activity to assist splicing of the transcribed intronic RNA [58–60]. If the numerous HE motifs in the *P. radiata* mtDNA are active, the homing processes may modify their target genes, and even the genome size and structure considerably - in the course of either a long or short evolutionary time period - as is seen in the mt genomes of the animal-pathogenic *Cryptococcus* spp. [53,54]. Another function for the multiple HE domains could be regulation of transcription of their target genes, which is observed for bacterial viruses [60].

Considering the density of group I type introns (26) and their high frequency of HE domains in the core genes of *P. radiata* mtDNA, it is well established to expect that if functional, the HEs could assist in intronic RNA splicing and thereby affect transcription of their target genes, with a possibility for alternative intron splicing. The mitochondrial Complex IV cytochrome oxidase subunit 1 encoding *cox1* gene of *P. radiata* is particularly interrupted by long self-splicing introns (13) containing multiple HEs, as seemingly is general in Agaricomycota mtDNAs [24–28,57]. In *P. radiata* mtDNA, *cox1* is apparently the first replicated and transcribed gene in sense (leading strand) orientation (Figure 1). Whether regulation of *P. radiata* mtDNA gene expression is mediated by the multiple introns and their identified HEs will be of our future concern.

Plasmid-originating Features

Although mitochondrial plasmids have been sequenced, and plasmid-originating genes are identified in fungal mtDNAs [8,23–28,50,63,64], our sequence analyses supported no individual plasmid dsDNA features in the *P. radiata* mtDNA. We were also unable to detect integrated-plasmid like sequence regions with inverted repeat ends as has been reported for other Agaricomycota species, i.e. *A. bisporus* [23], *M. perniciosa* [24] and *A. aegerita* [64]. However, putative and degenerative plasmid and viral-originating features, such as the *cob* gene intron-located reverse transcriptase (RT, RNA-directed DNA polymerase), and DNA polymerase B encoding *dpob* genes were identified in the *P. radiata* mtDNA, thereby possibly indicating previous plasmid-transmitted DNA integration events. The mitochondrial type II intron-homing and retrovirus-related reverse transcriptase [65,66] may function in plasmid integration to the mtDNA, and due to template-switching capacity, intron loss and gain to the mitochondrial genomes may occur.

tRNA Assembly, Codon Usage and Phylogeny

Fungal and animal mitochondrial genomes generally have a single tRNA gene for each synonymous protein-coding codon [67]. This also applies to the mitochondria of Basidiomycota, and implies extensive codon third nucleotide (wobble) pairing, similar to that observed for the tRNAs of the bacterium *Mycoplasma capricolum* [68], i.e. the tRNA anticodon first nucleotide (anticodon wobble) U pairs with all four third position nucleotides, and the first anticodon G pairs with third codon position C or U nucleotides.

Assuming that these codon/anticodon recognition rules apply, the predicted tRNA set of *P. radiata* mtDNA is sufficient to translate its conserved mitochondrial proteome, except for the codons Ile AUA (274) and Trp UGA (1), which would require unusual A•G and A•C wobble-pairing to their respected tRNA anticodons. However, we infer from Basidiomycota tRNA-Met and tRNA-Ile multiple sequence alignments that one of the *P. radiata* mtDNA tRNAs with CAU anticodon is in fact a tRNA-Ile gene, and the predicted anticodon is likely edited. Likewise, based on the lack of UGA codons in *P. radiata* mtDNA conserved ORFs, presence of the canonical CCA anticodon in tRNA-Trp, and the high bias towards low GC-content, we infer that *P. radiata* mitochondrial genome does not utilize the Mold, Protozoan, and Coelenterate Mitochondrial Code (NCBI translation table 4) in which UGA encodes Trp.

From the frequency of UGA codons in fungal mtDNA-encoded proteomes, we infer that UGA has been assigned to Trp multiple times in the evolution of Basidiomycota mitochondrial genomes,

i.e. in the lineage leading to the Pucciniomycotina genus *Phakopsora*, and in the lineage leading to the Agaricomycotina genus *Moniliopthora*, but not in the lineage leading to *Phlebia*. Likewise, we infer from sequence alignments of Basidiomycota *cox3* genes that in *C. neoformans*, UGA induces a +1 nt frameshift, which restores sequence homology for the last 16 codons of the gene in reference to other Basidiomycota *cox3* genes. We conclude that with this repertoire of mtDNA-encoded tRNAs, the mitochondria of *P. radiata* do not require tRNA import from the cytosol.

mtDNA Proteome Phylogeny

Maximum-likelihood and Bayesian inference approaches of the Basidiomycota mtDNA-encoded proteomes resulted with well-supported and systematically consistent evolutionary trees in line with current multigene-based fungal taxonomies [69,70], both in respect to fungal phyla (-mycota) and within subphyla (-mycotina) (Figure 5). *P. radiata* mt proteome grouped together with other Agaricomycotina species, nearest to *Ganoderma* spp. and *T. cingulata*, which also belong to the same taxonomic class (Agaricomycetes) and share similar, wood-decaying white-rot saprobic lifestyle with *P. radiata*. The opportunistic pathogen *C. neoformans* was the only exception in protein phylogeny by falling outside the subphylum Agaricomycotina, which is consistent with our mtDNA proteome ORF codon usage evolutionary analysis (Figure 4). Multi-protein Bayesian evolutionary analysis positioned the yet *insertae sedis* subphyla Kixcellomycotina (*Zancudomyces (Smittium) culisetae*) nearest to Glomeromycota, and Mucoromycotina (*Rhizopus oryzae*) and Mortierellomycotina (*Mortierella verticillata*) together between Glomeromycota and Dikarya (Figure 5). Otherwise the relationships between extant taxons were well resolved, thus indicating a strong signal for a single common origin of the Basidiomycota and fungal mt genomes.

Conclusions

Mitochondria are numerous in eukaryotic cells and thereby, mitochondrial genomes as well have high cellular copy numbers. Our study confirms the high degree of variety of fungal mtDNAs in genome structure and size, gene order and location, and exon-intron structure of the protein-coding genes. This indicates that for mtDNA, continuous and adaptive modifications are allowed, including mobile genetic elements and signs of recombination events. Several features in the *P. radiata* mtDNA support such genetic flexibility and repair mechanisms, and regulation of transcription. Existence of the long inverted-duplicated region, frequency of repetitive sequence motifs, and especially the abundance of intron-homing endonucleases support these conclusions. Surprisingly, these features of *P. radiata* mtDNA, together with the large genome size, are shared with fungal, plant and algae mtDNAs.

Accurately characterized reference genomes including the mtDNAs are currently needed to aid in *de novo* sequencing and evolutionary studies of fungi. The novel *P. radiata* mtDNA features observed in our research indicate a general phenomenon for evolutionary pressure and genome diversity in mitochondrial genomes, not being as stable and compact integrities as previously considered. The fungal mtDNAs could thus serve as sources for evolutionary and biochemical studies of genetic mobile elements, intron loss and gain, virulence and adaptation, and targeted genetic engineering by the use of homing endonucleases.

Supporting Information

Table S1 Intronic and additional ORFs annotated in the *P. radiata* mtDNA.
(XLSX)

Table S2 ORFs continuing from coding sequence exons into putative intronic regions.
(XLSX)

Table S3 Root mean squared difference distance matrix of Basidiomycota conserved codons in the protein-coding ORFs.
(XLSX)

Table S4 Sum squared difference distance matrix of Basidiomycota conserved codons in the protein-coding ORFs.
(XLSX)

Table S5 Intronic homing endonuclease (HE) domains in the *P. radiata* mtDNA.
(XLSX)

Acknowledgments

The help of Ms Elina Kokkonen with statistical analyses is warmly thanked.

Author Contributions

Conceived and designed the experiments: TL LP. Performed the experiments: PL JK MM. Analyzed the data: HS IO PL. Contributed reagents/materials/analysis tools: TL LP. Wrote the paper: TL HS.

References

1. Nakasone KK, Sytsma KJ (1993) Biosystematic studies on *Phlebia acerina*, *P. rufa*, and *P. radiata* in North America. Mycologia 85: 996–1016.
2. Miettinen O, Larsson E, Sjökvist E, Larsson KH (2012) Comprehensive taxon sampling reveals unaccounted diversity and morphological plasticity in a group of dimitic polypores (Polyporales, Basidiomycota). Cladistics 28: 251–270.
3. Lundell T, Leonowicz A, Rogalski J, Hatakka A (1990) Formation and action of lignin-modifying enzymes in cultures of *Phlebia radiata* supplemented with veratric acid. Appl Environ Microbiol 56: 2623–2629.
4. Moilanen AM, Lundell T, Vares T, Hatakka A (1996) Manganese and malonate are individual regulators for the production of lignin and manganese peroxidase isozymes and in the degradation of lignin by *Phlebia radiata*. Appl Microbiol Biotechnol 45: 792–799.
5. Lundell TK, Mäkelä MR, Hildén K (2010) Lignin-modifying enzymes in filamentous basidiomycetes - ecological, functional and phylogenetic review. J Basic Microbiol 50: 5–20.
6. Mäkelä MR, Lundell T, Hatakka A, Hildén K (2013) Effect of copper, nutrient nitrogen and wood-supplement on the production of lignin-modifying enzymes by the white-rot fungus *Phlebia radiata*. Fungal Biol 117: 62–70.
7. Lang BF, Gray MW, Burger G (1999) Mitochondrial genome evolution and the origin of eukaryotes. Annu Rev Genet 33: 351–397.
8. Bullerwell CE, Lang BF (2005) Fungal evolution: the case of the vanishing mitochondrion. Curr Opin Microbiol 8: 362–369.
9. Chan DC (2006) Mitochondria: dynamic organelles in disease, aging, and development. Cell 125: 1241–1252.
10. Basse CW (2010) Mitochondrial inheritance in fungi. Curr Opin Microbiol 13: 712–719.
11. Contreras L, Drago I, Zampese E, Pozzan T (2010) Mitochondria: the calcium connection. Biochim Biophys Acta 1797: 607–618.
12. Richardson DR, Lane DJR, Becker EM, Huang MLH, Whitnall M, et al. (2010) Mitochondrial iron trafficking and the integration of iron metabolism between the mitochondrion and cytosol. Proc Natl Acad Sci U S A 107: 10775–10782.
13. Sagan L (1967) On the origin of mitosing cells. J Theor Biol 14: 225–274.
14. Margulis L (1970) Origin of eukaryotic cells: evidence and research implications for a theory of the origin and evolution of microbial, plant, and animal cells on the Precambrian earth. New Haven-London: Yale University Press. 349 p.
15. Thrash JC, Boyd A, Huggett MJ, Grote J, Carini P, et al. (2011) Phylogenomic evidence for a common ancestor of mitochondria and the SAR11 clade. Sci Rep 1: 13. doi:10.1038/srep00013.

16. Timmis JN, Ayliffe MA, Huang CY, Martin W (2004) Endosymbiotic gene transfer: organelle genomes forge eukaryotic chromosomes. Nat Rev Genet 5: 123–135.
17. Barr CM, Neiman M, Taylor DR (2005) Inheritance and recombination of mitochondrial genomes in plants, fungi and animals. New Phytol 168: 39–50.
18. Lukes J, Guilbride DL, Votypka J, Zikova A, Benne R, et al. (2002) Kinetoplast DNA network: evolution of an improbable structure. Eukaryot Cell 1: 495–502.
19. NCBI Organelle Genome Resources. National Center of Biotechnology Information. http://www.ncbi.nlm.nih.gov/genomes/GenomesHome.cgi?taxid = 2759&hopt = stat&opt = organelle (23 December 2013, last accessed).
20. Kitazaki K, Kubo T (2010) Cost of having the largest mitochondrial genome: evolutionary mechanism of plant mitochondrial genome. J Bot 2010: article ID 620137, 12 p. doi:10.1155/2010/620137.
21. Alverson AJ, Rice DW, Dickinson S, Barry K, Palmer JD (2011) Origins and recombination of the bacterial-sized multichromosomal mitochondrial genome of cucumber. Plant Cell 23: 2499–2513.
22. Sloan DB, Alverson AJ, Chuckalovcak JP, Wu M, McCauley DE, et al. (2012) Rapid evolution of enormous, multichromosomal genomes in flowering plant mitochondria with exceptionally high mutation rates. PLOS Biol 10: e1001241. doi:10.1371/journal.pbio.1001241.
23. Férandon C, Xu J, Barroso G (2013) The 135 kbp mitochondrial genome of *Agaricus bisporus* is the largest known eukaryotic reservoir of group I introns and plasmid-related sequences. Fung Gen Biol 53: 85–91.
24. Formighieri EF, Tiburcio R, Armas E, Medrano FJ, Shimo H, et al. (2008) The mitochondrial genome of the phytopathogenic basidiomycete *Moniliophthora perniciosa* is 109 kb in size and contains a stable integrated plasmid. Mycol Res 112: 1136–1152.
25. Wang Y, Zeng F, Hon CC, Zhang Y, Leung FCC (2008) The mitochondrial genome of the Basidiomycete fungus *Pleurotus ostreatus* (oyster mushroom). FEMS Microbiol Lett 280: 34–41.
26. Haridas S, Gantt JS (2010) The mitochondrial genome of the wood-degrading basidiomycete *Trametes cingulata*. FEMS Microbiol Lett 308: 29–34.
27. Stone CL, Buitrago ML, Boore JL, Frederick RD (2010) Analysis of the complete mitochondrial genome sequences of the soybean rust pathogens *Phakopsora pachyrhizi* and *P. meibomiae*. Mycologia 102: 887–897.
28. Costa GGL, Cabrera OG, Tiburcio RA, Medrano FJ, Carazzolle MF, et al. (2012) The mitochondrial genome of *Moniliophthora roreri*, the frosty pod rot pathogen of cacao. Fungal Biol 116: 551–562.
29. Foury F, Roganti T, Lecrenier N, Purnelle B (1998) The complete sequence of the mitochondrial genome of *Saccharomyces cerevisiae*. FEBS Lett 440: 325–331.
30. Forget L, Ustinova J, Wang Z, Huss V, Lang B (2002) *Hyaloraphidium curvatum*: A linear mitochondrial genome, tRNA editing, and an evolutionary link to lower fungi. Mol Biol Evol 19: 310–319.
31. Gerhold JM, Aun A, Sedman T, Jõers P, Sedman J (2010) Strand invasion structures in the inverted repeat of *Candida albicans* mitochondrial DNA reveal a role for homologous recombination in replication. Mol Cell 39: 851–861.
32. Bendich AJ (2010) The end of the circle for yeast mitochondrial DNA. Mol Cell 39: 831–832.
33. Hildén KS, Bortfeldt R, Hofrichter M, Hatakka A, Lundell TK (2008) Molecular characterization of the basidiomycete isolate *Nematoloma frowardii* b19 and its manganese peroxidase places the fungus in the corticioid genus *Phlebia*, Microbiol-SGM 154: 2371–2379.
34. Hildén K, Martinez A, Hatakka A, Lundell T (2005) The two manganese peroxidases Pr-MnP2 and Pr-MnP3 of *Phlebia radiata*, a lignin-degrading basidiomycete, are phylogenetically and structurally divergent. Fungal Gen Biol 42: 403–419.
35. Zhang Z, Schwartz S, Wagner L, Miller W (2000) A greedy algorithm for aligning DNA sequences. J Comput Biol 7: 203–214.
36. Altschul SF, Madden TL, Schaffer AA, Zhang J, Zhang Z, et al. (1997) Gapped BLAST and PSI-BLAST: a new generation of protein database search programs. Nucleic Acids Res 25: 3389–3402.
37. Altschul SF, Wootton JC, Gertz EM, Agarwala R, Morgulis A, et al. (2005) Protein database searches using compositionally adjusted substitution matrices. FEBS J 272: 5101–5109.
38. Rutherford K, Parkhill J, Crook J, Horsnell T, Rice P, et al. (2000) Artemis: sequence visualization and annotation. Bioinformatics 16: 944–945.
39. Larkin MA, Blackshields G, Brown NP, Chenna R, McGettigan PA, et al. (2007) Clustal W and Clustal X version 2.0. Bioinformatics 23: 2947–2948.
40. Schattner P, Brooks AN, Lowe TM (2005) The tRNAscan-SE, snoscan and snoGPS web servers for the detection of tRNAs and snoRNAs. Nucleic Acids Res 33(Web Server issue): W686–689.
41. Finn RD, Mistry J, Tate J, Coggill P, Heger A, et al. (2010) The Pfam protein families database. Nucleic Acids Res 38(Database issue): D211–222.
42. Lang BF, Laforest M, Burger G (2007) Mitochondrial introns: a critical view. Trends Genet 23: 119–125.
43. Rice P, Longden I, Bleasby A (2000) EMBOSS: the European molecular biology open software suite. Trends Genet 16: 276–277.
44. Huang Y, Niu B, Gao Y, Fu L, Li W (2010) CD-HIT Suite: a web server for clustering and comparing biological sequences. Bioinformatics 26: 680–682.
45. Benson DA, Cavanaugh M, Clark K, Karsch-Mizrachi I, Lipman DJ, et al. (2013) GenBank. Nucleic Acids Res 41(D1): D36–D42. doi: 10.1093/nar/gks1195.
46. Edgar RC (2010) Search and clustering orders of magnitude faster than BLAST. Bioinformatics 26: 2460–2461.
47. Robbertse B, Yoder RJ, Boyd A, Reevers J, Spatafora JW (2011) Hal: an automated pipeline for phylogenetic analyses of genomic data. PLOS currents 3: RRN1213 p. doi:10.1371/currents.RRN1213.
48. Stamatakis A (2008) RAxML-VI-HPC: maximum likelihood-based phylogenetic analyses with thousands of taxa and mixed models. Bioinformatics 22: 2688–2690.
49. Lartillot N, Lepage T, Blanquart S (2009) PhyloBayes 3: a Bayesian software package for phylogenetic reconstruction and molecular dating. Bioinformatics 25: 2286–2288.
50. Wibberg D, Jelonek L, Rupp O, Hennig M, Eikmeyer F, et al. (2013) Establishment and interpretation of the genome sequence of the phytopathogenic fungus *Rhizoctonia solani* AG1-IB isolate 7/3/14. J Biotechnol 167: 142–155.
51. Petersen RF, Langkjaer RB, Hvidtfeldt J, Gartner J, Palmen W, et al. (2002) Inheritance and organisation of the mitochondrial genome differ between two *Saccharomyces* yeasts. J Mol Biol 318: 627–636.
52. Willamson D (2002) The curious history of yeast mitochondrial DNA. Nature Rev Gen 3: 1–7.
53. Litter J, Keszthelyi A, Hamari Z, Pfeiffer I, Kucsera J (2005) Differences in mitochondrial genome organization of *Cryptococcus neoformans* strains. Ant Van Leeuw 88: 249–255.
54. Ma H, Hagen F, Stekel DJ, Johnston SA, Sionov E, et al. (2009) The fatal fungal outbreak on Vancouver Island is characterized by enhanced intracellular parasitism driven by mitochondrial regulation. Proc Natl Acad Sci U S A 106: 12980–12985.
55. Li J, Zhang J, Chen H, Chen X, Lan J, et al. (2013) Complete mitochondrial genome of the medicinal mushroom *Ganoderma lucidum*. PLOS ONE 8: e72038. doi: 10.1371/journal.pone.0072038.
56. Mouhamadou B, Ferandon C, Chazoule S, Barroso G (2007) Unusual accumulation of polymorphic microsatellite loci in a specific region of the mitochondrial genome of two mushroom-forming *Agrocybe* species. FEMS Microbiol Lett 272: 276–281.
57. Férandon C, Moukha S, Callac P, Benedetto J-P, Castroviejo M, et al. (2010) The *Agaricus bisporus cox1* gene: the longest mitochondrial gene and the largest reservoir of mitochondrial group I introns. PLOS ONE 5: e14048. doi: 10.1371/journal.pone.0014048.
58. Caprara MG, Chatterjee P, Solem A, Brady-Passerini K, Kaspar B (2007) An allosteric-feedback mechanism for protein-assisted group I intron splicing. RNA 13: 211–222.
59. Taylor GK, Stoddard BL (2012) Structural, functional and evolutionary relationships between homing endonucleases and proteins from their host organisms. Nucleic Acids Res 40: 5189–5200.
60. Stoddard BL (2011) Homing endonucleases: from microbial genetic invaders to reagents for targeted DNA modification. Structure 19: 7–15.
61. Paquin B, Laforest M-J, Lang BF (1994) Interspecific transfer of mitochondrial genes in fungi and creation of a homologous hybrid gene. Proc Natl Acad Sci U S A 91: 11807–11810.
62. Sethuraman J, Majer A, Friedrich NC, Edgell DR (2009) Genes within genes: multiple LAGLIDADG homing endonucleases target the ribosomal protein S3 gene encoded within an *rnl* group I intron of *Ophiostoma* and related taxa. Mol Biol Evol 26: 2299–2315.
63. Kim EK, Jeong JH, Youn HS, Koo YB, Roe JH (2000) The terminal protein of a linear mitochondrial plasmid is encoded in the N-terminus of the DNA polymerase gene in white-rot fungus *Pleurotus ostreatus*. Curr Genet 38: 283–290.
64. Férandon C, Chatel Sel K, Castandet B, Castroviejo M, Barroso G (2008) The *Agrocybe aegerita* mitochondrial genome contains two inverted repeats of the *nad4* gene arisen by duplication on both sides of a linear plasmid integration site. Fungal Genet Biol 45: 292–301.
65. Gu S, Cui X, Mou S, Mohr S, Yao J, et al. (2010) Genetic identification of potential RNA-binding regions in a group II intron-encoded reverse transcriptase. RNA 16: 732–747.
66. Michel FF, Lang B (1985) Mitochondrial class II introns encode proteins related to the reverse transcriptases of retroviruses. Nature 316: 641–643.
67. Xia X (2008) The cost of wobble translation in fungal mitochondrial genomes: integration of two traditional hypotheses. BMC Evol Biol 8: 211. doi:10.1186/1471-2148-8-211.
68. Inagaki Y, Kojima A, Bessho Y, Hori H, Ohama T, et al. (1995) Translation of synonymous codons in family boxes by *Mycoplasma capricolum* tRNAs with unmodified uridine or adenosine at the first anticodon position. J Mol Biol 251: 486–492.
69. Hibbett D, Binder M, Bischoff JF, Blackwell M, Cannon PF, et al. (2007) A higher-level phylogenetic classification of the fungi. Mycol Res 111: 509–547.
70. Jones MDM, Forn I, Gadelha C, Egan MJ, Bass D, et al. (2011) Discovery of novel intermediate forms redefines the fungal tree of life. Nature 474: 200–205.

III

Kuuskeri *et al. Biotechnol Biofuels (2016) 9:192*
DOI 10.1186/s13068-016-0608-9

Biotechnology for Biofuels

RESEARCH Open Access

Time-scale dynamics of proteome and transcriptome of the white-rot fungus *Phlebia radiata*: growth on spruce wood and decay effect on lignocellulose

Jaana Kuuskeri[1], Mari Häkkinen[1], Pia Laine[2], Olli-Pekka Smolander[2], Fitsum Tamene[3], Sini Miettinen[3], Paula Nousiainen[4], Marianna Kemell[5], Petri Auvinen[2] and Taina Lundell[1*]

Abstract

Background: The white-rot Agaricomycetes species *Phlebia radiata* is an efficient wood-decaying fungus degrading all wood components, including cellulose, hemicellulose, and lignin. We cultivated *P. radiata* in solid state cultures on spruce wood, and extended the experiment to 6 weeks to gain more knowledge on the time-scale dynamics of protein expression upon growth and wood decay. Total proteome and transcriptome of *P. radiata* were analyzed by peptide LC–MS/MS and RNA sequencing at specific time points to study the enzymatic machinery on the fungus' natural growth substrate.

Results: According to proteomics analyses, several CAZy oxidoreductase class-II peroxidases with glyoxal and alcohol oxidases were the most abundant proteins produced on wood together with enzymes important for cellulose utilization, such as GH7 and GH6 cellobiohydrolases. Transcriptome additionally displayed expression of multiple AA9 lytic polysaccharide monooxygenases indicative of oxidative cleavage of wood carbohydrate polymers. Large differences were observed for individual protein quantities at specific time points, with a tendency of enhanced production of specific peroxidases on the first 2 weeks of growth on wood. Among the 10 class-II peroxidases, new MnP1-long, characterized MnP2-long and LiP3 were produced in high protein abundances, while LiP2 and LiP1 were upregulated at highest level as transcripts on wood together with the oxidases and one acetyl xylan esterase, implying their necessity as primary enzymes to function against coniferous wood lignin to gain carbohydrate accessibility and fungal growth. Majority of the CAZy encoding transcripts upregulated on spruce wood represented activities against plant cell wall and were identified in the proteome, comprising main activities of white-rot decay.

Conclusions: Our data indicate significant changes in carbohydrate-active enzyme expression during the six-week surveillance of *P. radiata* growing on wood. Response to wood substrate is seen already during the first weeks. The immediate oxidative enzyme action on lignin and wood cell walls is supported by detected lignin substructure side-chain cleavages, release of phenolic units, and visual changes in xylem cell wall ultrastructure. This study contributes to increasing knowledge on fungal genetics and lignocellulose bioconversion pathways, allowing us to head for systems biology, development of biofuel production, and industrial applications on plant biomass utilizing wood-decay fungi.

Keywords: Wood decay, White-rot, Proteomics, Transcriptomics, *Phlebia radiata*, Phlebioid, Lignin biodegradation, Lignin-modifying enzymes, Carbohydrate-active enzymes, Peroxidases

*Correspondence: taina.lundell@helsinki.fi
[1] Microbiology and Biotechnology, Department of Food and Environmental Sciences, University of Helsinki, P.O.Box 56, Viikki Biocenter 1, 00014 Helsinki, Finland
Full list of author information is available at the end of the article

Background

Lignocellulosic biomass is a large renewable resource of carbon that can be used as a substrate in the production of biofuels and biochemicals contrary to the polluting and diminishing fossil hydrocarbon sources. In nature, the carbon from lignocellulosic substrates including wood is utilized and recycled by fungi, most belonging to wood-colonizing and litter-decomposing Basidiomycota of the class Agaricomycetes [1–3]. The wood-decaying Polyporales species have been divided into white-rot and brown-rot fungi based on their visually observable decay types and differences in carbohydrate-active enzyme (CAZyme) encoding gene repertoires [1, 4]. Especially, the white-rot fungi are interesting due to their ability to degrade all components of wood, including the recalcitrant, aromatic, and heterogeneous lignin polymers [2, 5].

Lignin degradation is an important step prior to industrial use of plant biomass and lignocellulose raw materials [6]. In the white-rot fungal lifestyle—before gaining access to the carbohydrate storages of cellulose and hemicelluloses—lignin barrier is attacked to facilitate utilization of these carbon and energy sources [2, 7]. Lignin modification is possible because of a wide array of extracellular oxidoreductases produced by white-rot fungi. These oxidoreductases are enzymes of CAZy auxiliary activity family 2 (AA2) [8] fungal class-II lignin-modifying peroxidases including lignin peroxidases (LiPs), manganese peroxidases (MnPs), and versatile peroxidases (VPs) that are important in lignin modification [2, 9, 10]. Class-II peroxidases require hydrogen peroxide which may be generated by other CAZy auxiliary activity enzymes belonging to copper radical oxidases (CROs, AA5) and glucose–methanol–choline superfamily (GMCs, AA3) oxidoreductases [11, 12]. Lignin-converting enzyme set also includes the dye-decolorizing peroxidases (DyPs) [10, 13] and laccases. Laccases are phenol-oxidizing multicopper oxidases (MCOs, CAZy class AA1) which may thereby potentially act on lignin substructures by the aid of aromatic mediator compounds [2, 5].

Crystalline cellulose is utilized by the white-rot fungi with the help of cellobiohydrolases belonging to CAZy glycoside hydrolase (GH) families GH6 and GH7 [1, 3]. For complete enzymatic degradation of cellulose chains, endoglucanases of several GH families (GH5, GH9, GH12, GH44, and GH45), family AA9 (GH61) lytic polysaccharide monooxygenases (LPMO), and β-glucosidases of families GH1 and GH3 are needed [2, 14]. In addition, Basidiomycota genomes encode a wide array of other carbohydrate-active enzymes such as carbohydrate esterases (CEs) and polysaccharide lyases (PLs) for degradation of wood components including hemicelluloses and pectins [14]. The genes expressed and proteins produced during growth on plant biomass material reflect specific lifestyle of each fungal species and its strategy utilized for lignocellulose conversion [2, 15–17].

Phlebia radiata is a saprobic, wood-colonizing white-rot species of Agaricomycetes order Polyporales and phlebioid clade, and it is the taxonomic type species of the genus *Phlebia* [18, 19]. In nature, *Phlebia* species are mainly found colonizing deciduous wood and to some extent, also on coniferous wood [20, 21]. *P. radiata* and other *Phlebia* species are able to grow on Norway spruce (*Picea abies*) wood, producing wood-decaying enzymes [18, 22]. Spruce and coniferous wood from northern temperate and boreal forests are significant renewable feedstocks for forest-based industry [23]. To investigate the applicability of *P. radiata* isolate 79 for wood pretreatment and lignocellulose bioconversions, we selected Norway spruce as its growth substrate for the proteomic and transcriptomic analyses.

Several lignin-modifying enzymes of *P. radiata* 79 were previously cloned and characterized, including three LiPs [24], two divergent MnPs [25], and two laccases [26, 27]. Especially, the lignin-modifying peroxidases (LiPs and MnPs) of *P. radiata* and near-related *Phlebia* isolates have demonstrated high activity and efficiency in oxidoreductive reactions, conversion and degradation of lignin-like molecules, and potential in biotechnological applications [28–31]. However, no complete proteomic or transcriptomic study of the fungus on its natural lignocellulose wood substrate has been conducted before.

Our aim was to analyze the time-dependent changes in protein and enzyme expression of *P. radiata* during 6 weeks of growth on wood under conditions mimicking the natural fungal habitat. Transcriptome analysis from two cultivation time points served as a support for the proteomics study and also provided additional information on gene expression during growth on wood. The genome assembly of *P. radiata* (to be discussed elsewhere) was functionally annotated and searched for CAZyme encoding genes which were upregulated and produced as proteins on spruce wood.

Results

Genome sequencing of *P. radiata* wild-type dikaryon isolate 79 resulted with 40.92-Mb haploid size genome assembly including 14,113 predicted gene models (to be discussed elsewhere). To study the proteome of *P. radiata*, to recognize as many proteins as possible, and to identify time-dependent expression of lignocellulose degrading CAZymes on coniferous wood, total proteins from six time points (0, 7, 14, 21, 28, 42 days of growth) were extracted from solid-state spruce wood cultivations. In addition to proteomics, transcriptome on wood at growth time points of 14 and 28 days was compiled by

RNA sequencing to facilitate analysis of differential gene expression by using the 14-day malt extract medium grown mycelia as reference.

Characteristics of *P. radiata* proteome and transcriptome on wood

In total, 1356 proteins were identified by peptide LC–MS/MS proteomics and mapping the peptide sequences against translated coding sequences of the gene models of *P. radiata* genome assembly (with at least two unique peptides mapping per protein, Additional file 1: Table S1). For each protein at each time point, the mean abundance value with standard deviation was calculated from the three biological replicate culture values (Additional file 1: Table S1). The biological replicate protein abundances had high coherence according to principal component analysis (Additional file 2: Figure S1a). The number of identified proteins increased up to 28 days then slightly decreased on day 42 (Table 1). This was in accordance with total protein concentrations measured from protein extracts of each time point (Additional file 3: Figure S2).

To estimate the number of secreted proteins in the total proteome, Phobius analysis [32] was performed. N-terminal signal peptide was predicted for 15 % (210) of the proteins (Fig. 1). This percentage was higher than the number of secreted proteins according to the in silico analysis of *P. radiata* gene models (10 %, Fig. 1). The number of secreted proteins may be an underestimation due to difficulties in recognition of the true 5' initiation site (start Met codon) of gene model ORFs by computational methods. However, in silico analysis gave a rough estimation of the ratio of the number of theoretically predicted versus proteomics-obtained number of secreted proteins.

Overall, composition of *P. radiata* proteome was relatively constant in the course of spruce wood solid-state cultivation (Fig. 2b, c). In total, 823 (61 %) proteins were shared at each time point from day 7 to 42. As expected, we identified some proteins (89) at time point zero representing those introduced to the solid wood substrate within the fungal inoculum (cultivated on malt extract liquid medium for 14 days). Blast2GO searches showed that the identified proteins were divided into various functional categories (Fig. 2a). Based on the preliminary annotation of the gene models, proteins were divided into eight different categories: AA2 (class-II peroxidases), other AAs, CEs, GHs, peptidases, PLs, proteins with other functions, and proteins of unknown function. The majority of identified proteins (77 %) were classified as proteins with other functions that include an array of intracellular proteins involved in translation and in metabolic processes.

Table 1 Number of identified proteins in the proteome, and proteins with N-terminal secretion signal sequence at the six time points of *P. radiata* cultivation on spruce wood

Time (d)	Number of identified proteins[a]	Number of secreted proteins[b] (percentage of identified proteins)
0	89	31 (35 %)
7	1009	150 (15 %)
14	1077	163 (15 %)
21	1149	170 (15 %)
28	1151	170 (15 %)
42	1035	157 (15 %)

The proteins were analyzed by peptide LC–MS/MS and identified by searching against translated gene models of *P. radiata* genome. The secreted proteins were recognized with Phobius prediction analysis [32]

[a] Proteins were identified from peptide LC–MS/MS analysis

[b] Secreted proteins were identified with Phobius prediction

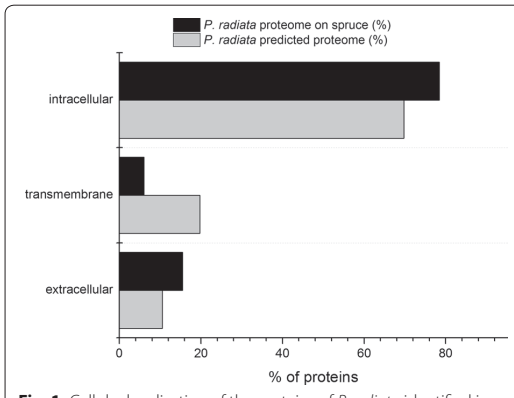

Fig. 1 Cellular localization of the proteins of *P. radiata* identified in the proteome on spruce wood and predicted from the translated protein models annotated on the genome assembly. Analysis was performed computationally

The transcriptomes of two biological replicate cultures on spruce wood at two time points (14 and 28 days) and from one time point (14 days) on malt extract reference medium, respectively, were analyzed by RNA-sequencing (Additional file 2: Figure S1b, c). According to the transcriptome analysis, 2 162 of the predicted *P. radiata* transcripts had significantly higher expression level ($p < 0.05$ and log2-fold change ≥ 1) and 1 820 had significantly lower ($p < 0.05$ and log2-fold change ≤ -1) expression level at both or one of the time points on wood as compared with the malt extract cultivation. For specific transcripts, also more stringent p value and fold change threshold ($p < 0.01$ and log2-fold change ≥ 2)

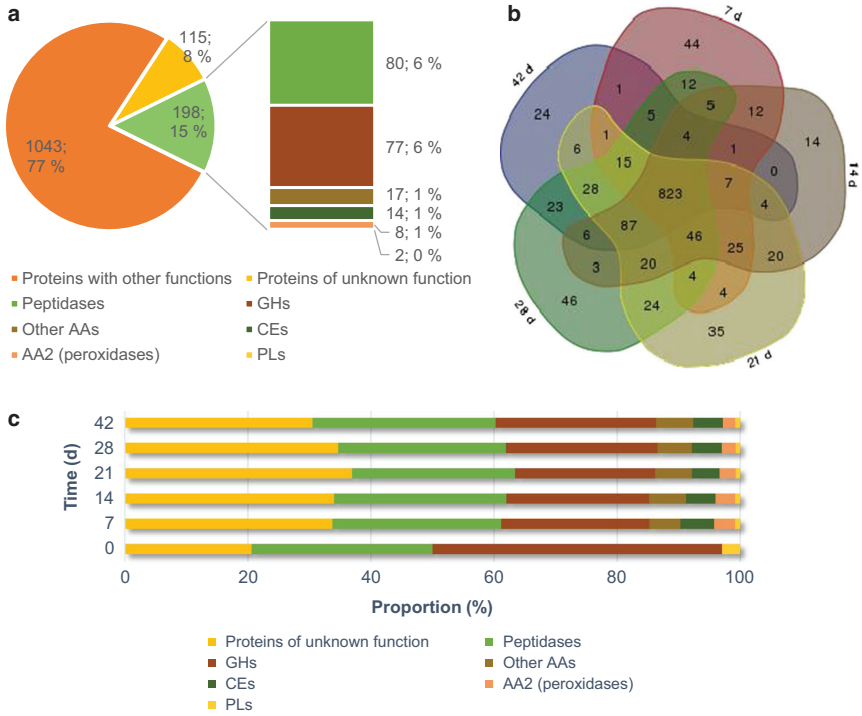

Fig. 2 Functional distribution of proteins identified in *P. radiata* proteome on spruce wood by LC–MS/MS peptide analysis. **a** Distribution of the total identified proteins (1356) into functional classes. **b** Venn diagram of distribution of identified proteins (1349) in the fungal proteomes on wood extracted from five weekly time points. **c** Distribution in percentage of wood-decay CAZy and other proteins at the six time points. Proteins with equal or more than two unique peptides were included in the analyses

were applied to test for highly significant differences of gene expression between growth on wood and malt extract medium. The most highly upregulated transcripts on wood were recognized to encode candidate transporter proteins, hydrophobins, and candidate proteases together with various CAZymes (Table 2).

Wood-decay enzyme set of *P. radiata*

The emphasis of this study was on CAZyme encoding genes and especially on those identified as proteins and with known functions in degradation of plant cell wall components. The proportion of CAZymes, including GHs and CEs, was 7 % of the total proteome (Fig. 2). The auxiliary oxidoreductase activities covered 2 % of the total proteome with the AA2 family class-II peroxidases representing 32 % of this protein pool, that is 1 % of the total proteome. The proportion of GH proteins of the total proteome was relatively high (18 % of total proteome) at time point zero indicating active enzymatic carbohydrate utilization occurring by the fungal hyphae already in the malt extract inoculum cultivation. Overall distribution of proteins according to their CAZy families showed a large variety of functions (Additional file 4: Figure S3).

The number of upregulated transcripts and the number of detected proteins functionally annotated to correspond to plant cell wall degrading enzymes were compared, and the proportions were shown to be consistent (Fig. 3). Large proportion of the genes was upregulated and translated to proteins indicating active degradation of lignocellulose. In general, from the approximately 300 transcripts predicted to encode CAZymes belonging to different GH, CE, PL, and cellulose-binding module (CBM) families (excluding glycosyltransferases, GTs) together with AA9 lytic polysaccharide monooxygenases, AA2 class-II lignin-modifying peroxidases, and AA1 laccases, 141 were expressed on a significantly higher level on both or one of the transcriptome time points (14 and 28 days) on wood as compared with the 14-day malt extract cultivation. 107

Table 2 Fifty most highly upregulated transcripts on 2 and/or 4 week time points of spruce wood cultivations of *P. radiata*

Gene id	Top 50 day 14	Top 50 day 28	Log2fc day 14	Log2fc day 28	Protein abundance (% of total MS intensity)					Function	Family
					7 days	14 days	21 days	28 days	42 days		
Minus.g6827	x		10.72	4.49	1.03	1.08	0.26	0.01	0.00	Lignin peroxidase (LiP2)	AA2
Minus.g11349	x	x	10.32	8.74	0.79	0.61	0.46	0.39	0.37	Alcohol oxidase	AA3
Plus.g9320	x	x	10.16	9.36	0.03	0.06	0.05	0.07	0.06	Lytic polysaccharide monooxygenase	AA9
Plus.g11539	x	x	9.96	8.43	0.02	0.07	0.10	0.14	0.07	Lytic polysaccharide monooxygenase	AA9
Plus.g2118	x	x	9.7	9.59						Oligopeptide transporter	
Minus.g10274	x	x	9.24	7.95						Lytic polysaccharide monooxygenase	AA9
Minus.g3073	x		8.71	1.72	0.91	0.32	0.10	0.00	0.00	Lignin peroxidase 1 (LiP1)	AA2
Plus.g1419	x	x	8.55	7.25	8.33	3.86	3.76	3.08	3.81	Manganese peroxidase (MnP1-long)	AA2
Plus.g1442	x	x	8.52	7.86	0.00	0.03	0.03	0.06	0.07	Acid protease, family A01A	
Minus.g10376	x	x	8.46	6.4						Hypothetical protein	
Minus.g3552	x	x	8.46	5.49	0.03	0.06	0.05	0.03	0.01	Lytic polysaccharide monooxygenase	AA9
Plus.g12321	x	x	8.43	7.48	0.01	0.01	0.03	0.01	0.01	Acetyl xylan esterase	CE1
Plus.g10527	x	x	8.07	8.37	0.00	0.05	0.14	0.06	0.04	Copper radical oxidase	AA5
Minus.g8138	x		8.07	5.16						Hypothetical protein	
Plus.g10872	x	x	7.62	6.5	0.29	0.39	0.23	0.45	0.68	Tripeptidyl peptidase, family S53	
Minus.g4805	x		7.62	4.5	0.15	0.15	0.11	0.06	0.02	Glutathione transferase	
Plus.g6944	x	x	7.61	7.75	0.00	0.00	0.01	0.02	0.03	Carboxypeptidase, family S10	
Minus.g2657	x	x	7.59	5.73						MFS general substrate transporter	
Minus.g3349	x	x	7.32	6.01						Carbohydrate-binding module family 1 protein	CBM1
Plus.g4342	x	x	7.2	7.32	0.20	0.32	0.22	0.23	0.10	Cellobiohydrolase	GH6
Minus.g4996	x	x	7.19	7.06						Sugar transporter	
Plus.g8760	x		7.19	3.71	0.15	0.22	0.10	0.01	0.00	S-adenosyl-L-methionine-dependent methyltransferase	
Minus.g11037	x		7.18	0.36	0.00	0.02	0.00	0.00	0.00	β-1,4-endoxylanase	GH10
Plus.g12778	x	x	7.12	7.36	0.06	0.14	0.28	0.70	1.29	GDSL-like lipase acylhydrolase	
Minus.g8600	x	x	7.08	6.33	0.00	0.01	0.02	0.15	0.16	Oxalate decarboxylase	
Minus.g3792	x	x	7.07	6.02						Hypothetical protein	
Plus.g3697	x		7.02	4.94	0.01	0.04	0.04	0.02	0.01	β-1,4-endoxylanase	GH11
Minus.g3846	x		6.96	5.43						Hypothetical protein	
Plus.g6610	x	x	6.89	5.87						Hexose transporter	
Minus.g10273	x	x	6.86	5.93						Lytic polysaccharide monooxygenase	AA9
Minus.g927	x	x	6.83	6.58	0.14	0.19	0.22	0.21	0.21	Tripeptidyl peptidase, family S53	
Plus.g6929	x	x	6.83	6.5						Hydrophobin	
Minus.g7795	x	x	6.73	6.38	0.05	0.07	0.11	0.08	0.05	Clavaminate synthase	
Minus.g3957	x	x	6.7	6.6	0.02	0.04	0.05	0.09	0.13	Acetylesterase	CE16
Plus.g11538	x		6.59	3.44	0.02	0.12	0.08	0.04	0.01	Lytic polysaccharide monooxygenase	AA9

Table 2 continued

Gene id	Top 50 day 14	Top 50 day 28	Log2fc day 14	Log2fc day 28	Protein abundance (% of total MS intensity)					Function	Family
					7 days	14 days	21 days	28 days	42 days		
Plus.g5095	x		6.58	2.97	0.00	0.04	0.03	0.01	0.01	NAD-binding oxidoreductase	
Minus.g2367	x		6.55	3.09	0.50	0.46	0.26	0.06	0.01	S-adenosyl-L-methionine-dependent methyltransferase	
Plus.g8273	x		6.5	5.14						Grp1/Fun34/YaaH domain transporter protein	
Plus.g13374	x		6.48	5.25	0.02	0.07	0.06	0.05	0.02	Lytic polysaccharide monooxygenase	AA9
Plus.g11441	x		6.46	3.65	1.65	2.24	1.93	1.23	1.09	NAD-dependent formate dehydrogenase	
Minus.g3726	x		6.36	4.61	0.00	0.01	0.02	0.01	0.01	Dihydrodipicolinate synthetase	
Plus.g917	x	x	6.33	6.17						Hydrophobin	
Plus.g3219	x	x	6.29	7.06	0.00	0.00	0.00	0.01	0.01	Carboxylesterase	
Plus.g4436	x		6.27	3.9						Hypothetical protein	
Minus.g9081	x		6.26	5.03	0.02	0.06	0.08	0.11	0.05	Exo-β-1,3/1,6-glucanase	GH131
Minus.g12191	x	x	6.23	5.7	0.07	0.11	0.07	0.09	0.03	β-1,4-endoxylanase	GH10
Plus.g4845	x		6.19	4.84	0.35	0.42	0.53	0.58	0.50	Short-chain dehydrogenase/reductase SDR	
Minus.g11036	x		6.18	4.12	0.03	0.03	0.02	0.02	0.01	β-1,4-endoxylanase	GH10
Minus.g9727	x	x	6.16	5.67						MFS general substrate transporter	
Minus.g9590	x	x	6.14	5.76	0.03	0.09	0.15	0.27	0.21	Peptidase, family G1	
Minus.g8467		x	6.13	5.61	0.04	0.05	0.08	0.07	0.09	Homoserine O-acetyltransferase	
Minus.g5595		x	6.07	5.55	0.16	0.54	0.34	0.18	0.04	Cellobiohydrolase	GH7
Minus.g10025		x	6.04	5.58	0.02	0.01	0.01	0.02	0.01	Acetylesterase	CE16
Minus.g9239		x	5.92	5.93	0.00	0.01	0.06	0.03	0.06	Unknown protein	
Plus.g4481		x	5.74	5.57						Cupredoxin domain protein	
Plus.g5796		x	5.7	6.17	0.02	0.01	0.02	0.01	0.02	Exo-β-1,3/1,6-glucanase	GH131
Plus.g8890		x	5.7	5.6						Hydrophobin	
Minus.g5364		x	5.57	5.65	0.00	0.02	0.06	0.11	0.27	α-glucuronidase	GH115
Minus.g7830		x	5.46	5.71	0.20	0.37	0.57	0.82	1.14	Alpha/beta-hydrolase	
Plus.g8163		x	5.4	6.73	0.01	0.05	0.13	0.39	0.53	Cellobiohydrolase	GH7
Plus.g4813		x	5.37	7.76	0.09	0.44	0.64	1.21	1.65	GMC oxidoreductase	AA3
Plus.g7451		x	5.36	5.51	0.09	0.22	0.16	0.18	0.09	β-1,4-endoglucanase	GH5_5
Minus.g3151		x	5.23	6.27	0.01	0.05	0.08	0.17	0.13	Mannosyl-oligosaccharide 1,2-α-mannosidase	GH47
Plus.g8155		x	5.22	6.2						WSC-domain-containing protein	
Plus.g6787		x	5.2	5.47						APC amino acid permease	
Minus.g4639		x	5.06	5.73						Glycoside hydrolase family 92 protein	GH92
Minus.g1646		x	4.95	5.72						Oligopeptide transporter	
Minus.g10423		x	4.07	5.49						Oligopeptide transporter	
Plus.g4812		x	3.24	5.79						Hypothetical protein	

Abundance values are given for proteins identified by peptide LC–MS/MS

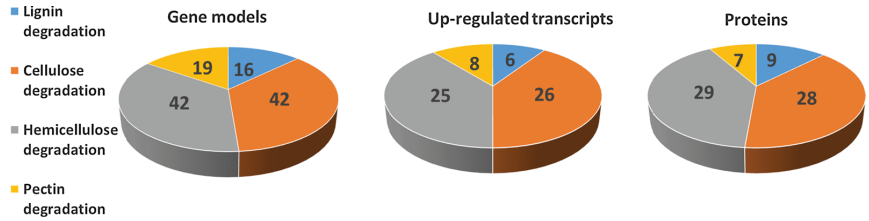

Fig. 3 Comparison of functional distribution of plant cell wall degradation involved proteins in *P. radiata*, according to the annotated and translated gene models, upregulated transcripts in the wood transcriptome, and identified proteins from the wood proteome. Upregulated transcripts: transcripts having significantly ($p < 0.05$ and log2-fold change ≥ 1) higher level of expression at the specific time point on spruce wood relative to the malt extract cultivation

of the transcripts were upregulated at both time points on wood (Fig. 4a). Majority (61 %) of these putatively encode activities against the plant cell wall (Fig. 4b). Moreover, majority of the transcripts upregulated at both time points on wood and coding for plant cell wall degrading activities were present in the proteome (85 %) (Fig. 4c).

Upregulated transcripts involved in attack on lignin were encoding several class-II lignin modifying peroxidases, both LiPs and MnPs, upregulation being apparent at both time points on wood and being in agreement with the proteome data at the same time points (Fig. 5). The 20 most abundant CAZy proteins identified in the proteome samples included the most upregulated class-II peroxidases (Table 3). Moreover, transcripts for LiP2, LiP3, MnP1-long, and MnP3-short were highly significantly accumulated ($p < 0.01$, log2-fold change ≥ 2) during the wood cultivations.

The single dye-decolorizing peroxide encoding gene (DyP) which was annotated in the genome was transcriptionally up-regulated only at the earlier time point (14 days) on wood. Quite surprisingly, the respective protein was not detected in the proteome at any of the studied time points, from 0 to 42 days of wood colonization. Contrary to the DyP transcription response, a novel class-II peroxidase MnP6-long together with the previously cloned LiP4 was identified in the proteomes, although not observed being upregulated in the wood transcriptomes. In fact, both corresponding genes were downregulated at the later time point (28 days) on wood as compared with the malt extract reference transcriptome. On the contrary to the peroxidases, none of the five annotated laccase-encoding genes were regulated on wood, and Lacc1 protein was the only laccase enzyme present in the proteomes, taking into account all the time points analyzed. Noticeable is, however, that

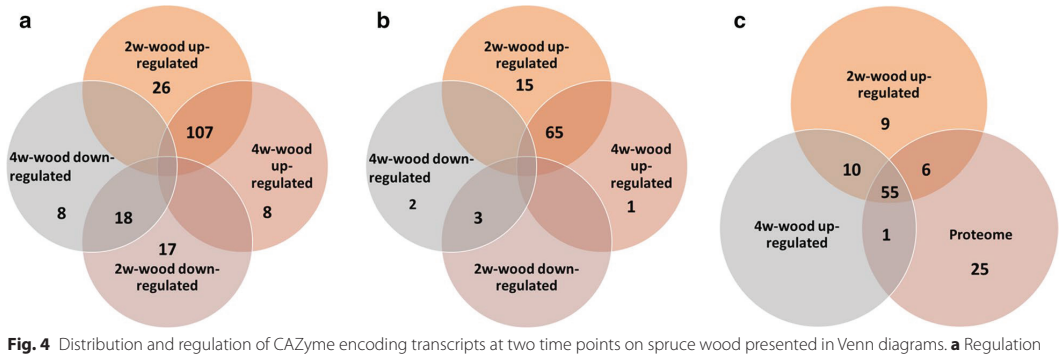

Fig. 4 Distribution and regulation of CAZyme encoding transcripts at two time points on spruce wood presented in Venn diagrams. **a** Regulation of expression of all identified CAZy protein encoding transcripts. **b** Regulation of expression of plant cell wall degrading CAZy activities encoding transcripts. **c** Overlap of wood upregulated transcriptomes and total wood proteome of *P. radiata* for the plant cell wall degrading activities encoding transcripts and corresponding proteins. Upregulated and downregulated: transcripts having significantly ($p < 0.05$ and log2-fold change ≥ 1 or ≤ -1) higher or lower level of expression at specific time points on spruce wood relative to malt extract cultivations. *2w* 2 week time point of cultivation; *4w* 4 week time point of cultivation

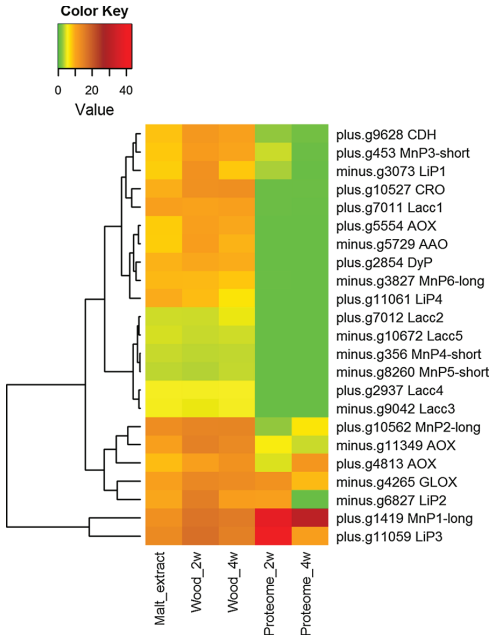

Fig. 5 Heatmap presenting correspondence and clustering of expression of lignin-modifying and accessory oxidoreductase wood-decay CAZyme encoding transcripts and the corresponding protein production as identified in the proteome, at two time points during growth of *P. radiata* on spruce wood. *Columns* represent the culture conditions (Wood, Malt extract) and *rows* the transcripts and proteins (Proteome; total proteome on wood). *2w* 2 weeks; *4w* 4 weeks; growth on wood. *Color key* illustrates the rlog normalized expression values and the normalized abundance values for the transcripts and peptides, respectively. Gene model ids and annotated gene names are presented (right). *CDH* cellobiose dehydrogenase; *MnP* manganese peroxidase; *LiP* lignin peroxidase; *CRO* copper radical oxidase; *Lacc* laccase; *AOX* alcohol oxidase; *AAO* aryl-alcohol oxidase; *DyP* dye-decolorizing peroxidase; *GLOX* glyoxal oxidase

laccase activity was detected at every time point in the protein extracts of wood cultures (Additional file 3: Figure S2).

A large number of additional AA accessory oxidoreductases were found in the proteomes including alcohol oxidases, copper radical oxidases, one glyoxal oxidase (GLOX), GMC oxidoreductases, alcohol and aryl-alcohol dehydrogenases, one cellobiose dehydrogenase (CDH), and one benzoquinone reductase. Of this pool of H_2O_2 producing and other important oxidoreductive activities possessing enzymes, 11 were upregulated as transcripts at both time points on wood, with one alcohol oxidase gene transcript having the highest fold change. Transcripts for two alcohol oxidases, an aryl-alcohol oxidase, a GMC oxidoreductase, a GLOX, a copper radical oxidase, and a cellobiose dehydrogenase were highly significantly accumulated during the wood cultivations (Fig. 5).

Transcripts from a number of different CAZy families, including activities against cellulose (Fig. 6) and hemicelluloses (Fig. 7), were upregulated independent of the time point on wood, and encode enzyme candidates, for example, AA9 LPMOs, cellobiohydrolases, β-1,4-glucosidases, β-xylosidases, β-1,4-endoglucanases, exo-β-1,3/1,6-glucanases, β-1,4-endomannanases, β-mannosidases, an acetyl xylan esterase, glucuronoyl esterases, acetylesterases, β-1,4-endoxylanases, an α-glucuronidase, an arabinofuranosidase, β-galactosidases, and xyloglucanases. Several of these genes, including seven genes encoding the AA9 LPMOs, were significantly differentially expressed on wood. These CAZy families were also present in the proteomes at least by one representative, and several of them were detected as being the most abundant CAZymes produced (Table 3).

A number of pectin-degrading CAZy genes, both lyases and hydrolases were expressed as transcripts on wood encoding for activities against polygalacturonan and rhamnogalacturonan, ester linkages (pectinesterase) and galactan. Many of these genes were upregulated at both time points on wood (Fig. 7). From these, three GH28 polygalacturonases, one CE8 pectinesterase, and the only PL4 rhamnogalacturonan lyase identified were highly significantly differentially expressed as transcripts. All of these—except one polygalacturonase enzyme—were also found as proteins in the proteome on wood. In addition, a candidate GH43 galactan 1,3-β-D-galactosidase possibly involved in degradation of arabinogalactan and transcripts encoding CBM1 modules and one cytochrome b562 iron reductase with a CBM1 domain were upregulated at both time points on wood (also when more stringent p-value and fold change were applied). From these, only the GH43 protein was present in the proteome.

In total, a portion (7.3–8.6 %) of the proteins identified in the total proteome on wood was classified as proteins with unknown function. Although none of these were among the 20 most abundant proteins produced on wood (Additional file 1: Table S1), they may include a few candidates that are important for fungal wood decay, thus presenting interesting targets for future studies. One of these is the transcriptionally highly upregulated *P. radiata* gene model minus.g9239 with unknown function but with the corresponding peptides discovered in the wood proteome (Table 2).

Dynamics of plant cell wall degrading enzymes

When time-dependency of protein expression was studied, it was noticed that despite the fact that protein numbers within each functional category were somewhat

Table 3 Twenty most abundant CAZymes in the proteome of *P. radiata*

Gene ID	Predicted function	Protein abundances						Average abundance on days 7–42	Transcripts up-regulated on wood
		Cultivation time (days)							
		0	7	14	21	28	42		
Plus.g1419	AA2: MnP1-Long	0.00	8.33	3.86	3.76	3.08	3.81	4.57	x
Plus.g11059	AA2: LiP3	0.00	5.37	4.32	2.58	1.10	0.70	2.81	x
Minus.g4265	AA5_1; glyoxal oxidase	0.00	2.32	1.25	0.75	0.88	2.10	1.46	x
Plus.g4813	AA3: GMC oxidoreductase	0.00	0.09	0.44	0.64	1.21	1.65	0.81	x
Plus.g10562	AA2: MnP2-Long	0.00	0.45	0.25	0.41	0.65	1.30	0.61	x
Minus.g11349	AA3: GMC oxidoreductase	0.00	0.79	0.61	0.46	0.39	0.37	0.52	x
Minus.g6827	AA2: LiP2	0.00	1.03	1.08	0.26	0.01	0.00	0.48	x
Minus.g7380	CE1	0.00	0.39	0.28	0.33	0.30	0.49	0.36	x
Plus.g453	AA2: MnP3-short	0.00	1.13	0.40	0.10	0.06	0.06	0.35	x
Minus.g2306	GH3	2.80	0.33	0.38	0.35	0.27	0.29	0.32	
Minus.g3073	AA2: LiP1	0.00	0.91	0.32	0.10	0.00	0.00	0.27	x
Minus.g5595	GH7	0.00	0.16	0.54	0.34	0.18	0.04	0.25	x
Plus.g8163	GH7	0.00	0.01	0.05	0.13	0.39	0.53	0.22	x
Minus.g6399	GH3	0.01	0.11	0.15	0.20	0.25	0.40	0.22	x
Plus.g4342	GH6	0.00	0.20	0.32	0.22	0.23	0.10	0.22	x
Plus.g637	CE16	0.00	0.18	0.13	0.15	0.27	0.33	0.21	x
Minus.g12190	GH10	0.00	0.24	0.23	0.21	0.22	0.08	0.19	x
Minus.g11677	GH28	0.76	0.53	0.16	0.04	0.02	0.01	0.15	
Plus.g7451	GH5	0.00	0.09	0.22	0.16	0.18	0.09	0.15	x
Plus.g9628	AA8-AA3_1: CDH	0.00	0.18	0.24	0.10	0.11	0.04	0.14	x
	Proportion (%) of total proteome	3.57	22.84	15.22	11.27	9.81	12.38	14.30	

Gene ID corresponds to annotated gene locus on the *P. radiata* genome assembly. Protein abundances are calculated based on mass spectrometric signal intensity values per each time point. Up-regulated transcripts refer to transcripts with significantly higher level of expression ($p < 0.05$ and log2-fold change ≥ 1) on wood as compared to the malt extract cultivations at both time points

MnP manganese peroxidase; *LiP* lignin peroxidase; *CE* carbohydrate esterase; *CDH* cellobiose dehydrogenase; *GH* glycoside hydrolase; *GLOX* glyoxal oxidase

constant during the cultivation (Fig. 2), differences in relative abundances of the proteins were observed (Fig. 8). When fungal proteins predicted to be important for wood decay were analyzed at every time point, the largest expansion seemingly occurred in the pool of identified proteins (of the overall protein production) during the first cultivation week. The abundances of the lignin-attack associated proteins peaked at growth day 7, and as the cultivation time advanced, abundances of these proteins started to decline. The only exception was the class-II peroxidase MnP2-long, the abundance of which started to increase again on cultivation day 17 (Additional file 5: Table S2).

Especially, the LiP abundance was decreasing, whereas MnP proteins were either constantly produced or demonstrating a less dramatic decline in protein abundances during the cultivation. This phenomenon was also observed in the transcriptome with the expression of especially LiP transcripts decreasing after 14 days on spruce wood. The MnP enzyme activities were constant on wood and detected also from the last time point (Additional file 3: Figure S2). Accessory oxidoreductase enzymes demonstrated likewise constant protein production during the cultivation. The abundancy of one GLOX protein (encoded by the gene model minus.g4265) of family AA5_1 declined between days 21 and 28 then increasing again until the end of the cultivation on wood (day 42). In addition, various dehydrogenases belonging to GMC oxidoreductases were produced with low protein abundances.

Cellulose degrading enzymes peaked in the proteomes on wood on cultivation day 14 (Fig. 8). Of the CAZy family GH7 cellobiohydrolases, relative abundance of one protein (encoded by the gene model minus.g5595) was clearly decreasing during the cultivation whereas the abundance of another GH7 protein (encoded by the gene plus.g8163) increased. The transcriptome data indicated corresponding differences in gene expression indicating that these two GH7 cellobiohydrolase encoding genes are under differential regulation. Relatively

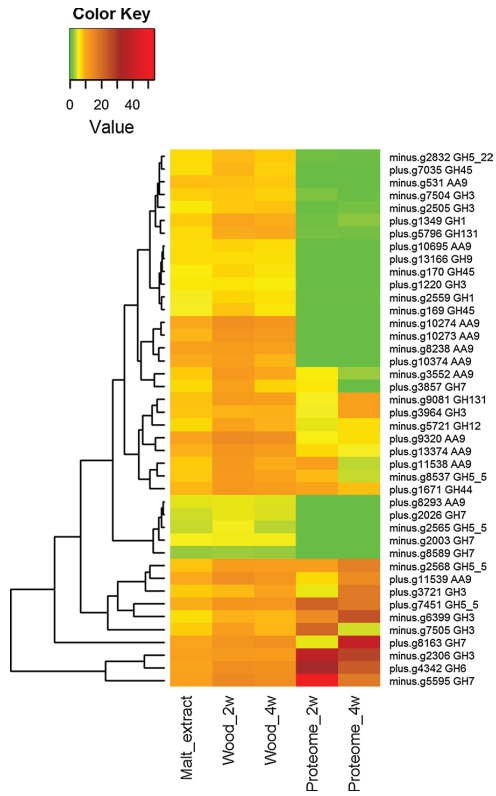

Fig. 6 Heatmap presenting correspondence of expression of CAZy cellulose degrading enzyme encoding transcripts and respective protein production during growth of *P. radiata* on spruce wood. *Columns* represent the culture conditions and *rows* the transcripts/proteins. *Color key* shows the rlog normalized expression values and the normalized abundance values for the transcripts and peptides, respectively. Gene model ids and functional CAZy family annotations are presented (right). *GH* glycoside hydrolase; *AA* auxiliary activities. For other explanations, see Fig. 5

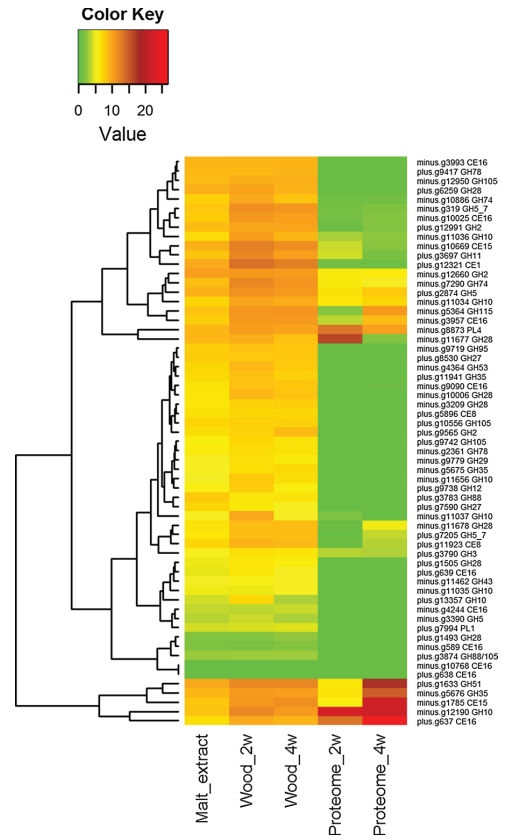

Fig. 7 Heatmap presenting correspondence of expression of CAZy hemicellulose and pectin degrading enzyme encoding transcripts and respective protein production during growth of *P. radiata* on spruce wood. *Columns* represent the culture conditions and *rows* the transcripts/proteins. *Color key* shows the rlog normalized expression values and the normalized abundance values for the transcripts and peptides, respectively. Gene model ids and functional CAZy family annotations are presented (right). *CE* carbohydrate esterase; *GH* glycoside hydrolase; *PL* polysaccharide lyase. For other explanations, see Fig. 5

low cellobiohydrolase activities were, however, measured after the third week of cultivation on wood (Additional file 3: Figure S2). The highest abundance of β-glucosidases was detected for proteins of CAZy family GH3 while family GH1 proteins remained low in abundance. β-glucosidase activities in turn were measured throughout the cultivation (Additional file 3: Figure S2). Relative abundances of hemicellulose degrading enzymes increased in the proteome on wood during the active growth of *P. radiata*, and xylanase activity was detected at time points 7, 28 and 42 (Fig. 8; Additional file 3: Figure S2). Production of CAZy family GH35 β-1,4-galactosidase, a GH51 α-arabinofuranosidase and a GH115 α-glucuronidase proteins increased during the cultivation. The total abundance of pectin degrading proteins was quite low during the cultivation on wood.

To follow the dynamics of fungal cell wall degradation and hyphal autolysis, abundances of twelve chitinase and β-glucanase proteins belonging to GH families 5, 13, 16, 18, 20, 55, 72, and 92 were followed. Abundances of these proteins were increasing up to day 28 of the wood cultivation (Fig. 8). It is of interest that the abundance of peptidases (protease activity

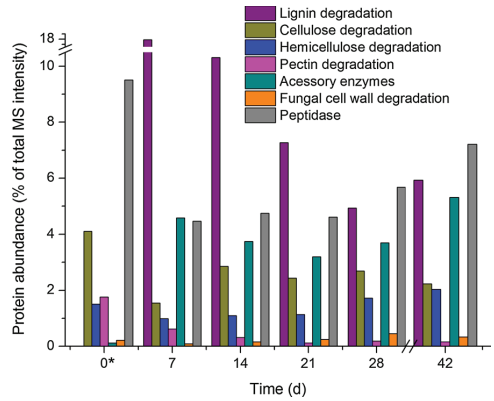

Fig. 8 Net abundances for CAZy plant and fungal cell wall degrading and accessory enzymes of *P. radiata* at each week and studied time point on spruce wood cultivations. *The total proteome at time point zero was the malt extract inoculum culture mycelium which contained approximately 1/10 of the number of identified proteins detected at the other time points (Table 1)

proteins) followed a similar pattern although the protein numbers (number of individual gene products) and their abundances were higher. Identified peptidases represented 27 different MEROPS peptidase families. Majority of the peptidases were assigned to A01A and T01A subfamilies. The top three most abundant peptidases included a family M28 metalloprotease, an A01 aspartyl peptidase and an S53 tripeptidyl peptidase.

Decay of spruce wood by *P. radiata*

Vertical and transverse sections of spruce wood samples were observed by field-emission scanning electron microscopy. Intact xylem and wood cell wall ultrastructure with tracheid bordered pits were observable in non-inoculated spruce wood (Fig. 9a, b). After 42 days of growth, *P. radiata* hyphae were visible particularly inside the tracheids (in tracheid lumen) and attached to secondary cell walls (Fig. 9e, f). In fungal colonized wood samples, a few enlarged bordered pits and thinning of tracheid cell walls were noticeable (Fig. 9c, d).

Supporting results were obtained by lignin analyses at first determining the gravimetric Klason lignin content and by more accurate analytical methods (Table 4). Klason lignin content and total yield of aromatic compounds detected by pyrolysis–GC/MS analyses were relatively constant in the fungal decayed wood samples compared to non-inoculated wood but some changes were, however, observed in lignin structure and polymerization stage. By pyrolysis–GC/MS analyses, in total, 20 compounds originating from lignin substructure units were tentatively identified according to MS spectra and reference compounds (Table 4). Increase in the abundance of monomeric phenolic compounds such as methylated phenols and guaiacol was probably caused by attack on lignin moieties resulting with decrease in the molecular size of polymeric lignin and release of oligomeric and monomeric substructures during fungal decay. This was also observed as an increase in the content of acid soluble lignin. The ratio of phenylmethane and phenylethane units to phenylpropane units (Ph-C1,C2/Ph-C3 ratio) increased after fungal cultivation indicating that a part of the side chain linkages of lignin substructures were cleaved. Lignin oxidative and degradative activity was also observed as increment of the amount of phenolic compounds, such as vanillin and coniferyl aldehyde (Table 4).

Discussion

White-rot fungal secretomes on various lignocelluloses have been investigated largely concentrating on the model white-rot fungus, Agaricomycetes Polyporales species *Phanerochaete chrysosporium* [16, 33, 34]. Similar studies on phlebioid clade fungi, including *Phanerochaete carnosa* [35], *Phlebiopsis gigantea* [36] and *Irpex lacteus* [37], as well as on the other white-rot Polyporales species *Ganoderma lucidum* [38], *Ceriporiopsis subvermispora* [39, 40], *Pycnoporus cinnabarinus* [41], *Pycnoporus coccineus* [42], and *Trametes trogii* [43], were conducted recently. In addition, lignocellulose-decay proteomics and transcriptomics of the order Agaricales white-rot species *Pleurotus ostreatus* have been elucidated [44, 45]. With these data and the accumulating genomic knowledge on fungi, however, it is evident that there are some differences in gene numbers but larger variations in gene expression and CAZy protein production between the white-rot fungal species. Moreover, these differences seem to be more fungal species and isolate dependent than influenced by, e.g., the type of wood and lignocellulose used as growth substrate [35, 42, 45].

Regarding this, we aimed at characterisation of the CAZy proteins in the total proteome on wood of an efficient lignin-degrading white rot species, *P. radiata*, isolate 79, not fully investigated by omics approach before but with a recently sequenced and annotated genome available. This allowed us to perform an extensive and deep time point study on the proteome and transcriptome while the fungus is colonizing wood. Moreover, the time point study allowed us to observe dynamic changes in the abundances of *P. radiata* proteins expressed on wood, and to gain insight into regulation of CAZy gene expression by transcriptome analyses.

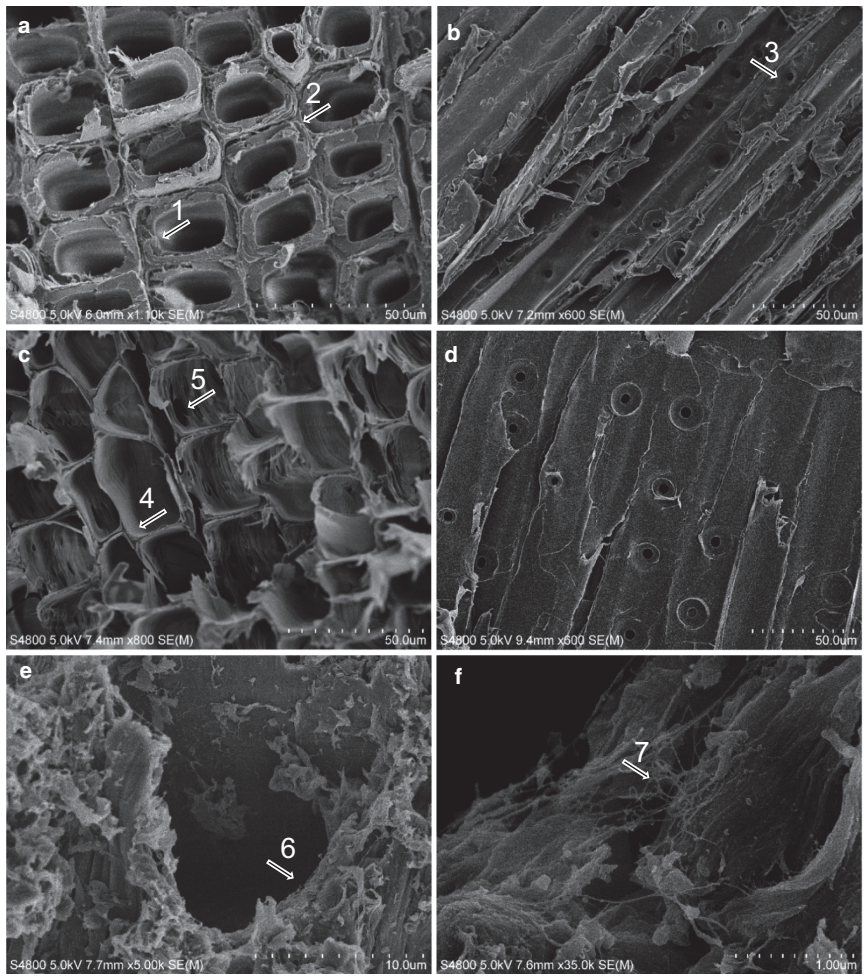

Fig. 9 Field emission scanning electron microscope images of Norway spruce xylem after 42 days of solid-state growth and decay of spruce sticks by *P. radiata*. Transverse (**a**) and longitudinal (**b**) sections of non-inoculated wood. The *arrows* indicate *1* intact spruce wood cell secondary wall, *2* middle lamella, *3* bordered pits at the tracheid walls. **c** Transverse section of spruce xylem after decay by *P. radiata* demonstrating enlargement of the tracheid lumen volume and apparent thinning of secondary cell wall. The *arrows* indicate *4* thinned remains of secondary cell wall, *5* enlarged bordered pit. Notice detachment of the tracheids due to erosion of primary cell walls and middle lamellae. **d** Vertical section of fungal decomposed spruce xylem. Tracheids are flattened and detached due to secondary cell wall thinning and erosion of middle lamellae. **e**, **f** Transverse sections of fungal colonization of xylem observed with higher magnification (5000 and 35,000x) demonstrating the hyphae *6*, *7* as threads inside the tracheids. Notice glucan deposits (**e**) and release of tracheid cell wall layers. *Scale bars* are in (**a**, **b**) 50 µm, (**e**) 10 µm and (**f**) 1 µm

Our results confirm that the wood-decaying enzyme repertoire of *P. radiata* is functional and composed of a variety of CAZy families including the auxiliary oxidoreductases, a set of lignin-modifying peroxidases accompanied by H_2O_2 producing enzymes and LPMOs, and a selection of hydrolases, esterases and lyases, all needed for complete degradation of the polymeric lignocellulose components.

The wood-decay machinery of *P. radiata* is typical for a traditional white-rot fungus (including various class-II lignin-modifying peroxidases, laccase, CDH, GMC oxidoreductases, GLOXs, LPMOs, cellulases of GH5, GH6,

Table 4 Lignin composition analysis of Norway spruce wood after 6 weeks of colonization by *P. radiata*

RT	Peak name	Spruce wood (%)	After 6 weeks of fungal growth (%)	Change (%)
		Mean	Mean	
7.126	Phenol (hydroxybenzene)	0.29 ± 0.08	0.50 ± 0.09	+72
8.401	2-methylphenol	0.11 ± 0.03	0.16 ± 0.03	+45
8.753	4-methylphenol, (4-methylguaiacol)	0.25 ± 0.06	0.33 ± 0.05	+32
9.01	2-methoxyphenol, (Guaiacol)	3.33 ± 0.24	4.69 ± 0.30	+41
10.437	2-methoxy-3-methylphenol	0.76 ± 1.22	1.24 ± 0.99	+63
10.64	2-methoxy-4-methylphenol	3.19 ± 0.47	2.44 ± 0.47	−24
11.89	2-methoxy-4-ethylphenol, (ethylguaiacol)	0.83 ± 0.10	0.73 ± 0.08	−18
12.428	4-vinylguaiacol	3.17 ± 0.29	3.22 ± 0.39	+2
12.994	Eugenol, 4-allylguaiacol	0.57 ± 0.05	0.45 ± 0.02	−21
13.129	2-methoxy-4-propylphenol, (4-propylguaiacol)	0.31 ± 0.03	0.26 ± 0.04	−16
13.626	Vanillin	1.27 ± 0.56	1.45 ± 0.71	+14
13.692	2-methoxy-4-(1-propenyl)phenol, (isoeugenol, *cis*)	0.27 ± 0.02	0.23 ± 0.02	−15
14.274	2-methoxy-4-(1-propenyl)phenol, (isoeugenol, *trans*)	1.78 ± 0.18	1.47 ± 0.25	−17
14.355	1-(4-hydroxy-3-methoxyphenyl)ethanone, (guaiacylacetone)	1.06 ± 0.65	0.86 ± 0.65	−19
14.733	1-(4-hydroxy-3-methoxyphenyl)ethanone (acetovanillone)	0.98 ± 0.46	0.54 ± 0.47	−45
15.201	Phenol, 2-methoxy-4-propan-1-ol, (dihydroconiferyl alcohol)	0.81 ± 0.54	0.35 ± 0.27	−57
15.749	Coniferyl alcohol, *cis*	0.47 ± 0.25	0.24 ± 0.17	−49
15.867	1-(4-hydroxy-3-methoxyphenyl)propanone, (propiovanillone)	0.58 ± 0.27	0.35 ± 0.30	−40
16.657	Coniferyl alcohol, *trans*	0.60 ± 0.46	0.35 ± 0.46	−42
17.673	Coniferyl aldehyde	0.51 ± 0.35	0.52 ± 0.59	+2
Pyrolysis lignin (area aromatics/total)		21.3 ± 0.7	20.4 ± 2.0	−4
Gravimetric (Klason) lignin		25.8 ± 0.33	26.1 ± 0.51	+1
Acid soluble lignin		0.30 ± 0.04	0.68 ± 0.23	+127
Pch-C1,2/Pch-C3 ratio[a]		0.03	0.08	+167

Relative peak areas (%) of lignin-derived pyrolysis product compounds identified with pyrolysis–GC/MS. Gravimetric and acid soluble lignin contents are also shown. The values are calculated from two biological replicates where 3–4 technical replicates were taken for pyrolysis samples, and from three biological replicates each of which with two technical replicate samples for Klason lignin determination

[a] Ratio of phenylmethane and phenylethane to phenylpropane type compounds

GH7 families) [1–3, 46]. However, some unique features like high expression of several LiPs and both long- and short-MnPs but low expression of laccase differentiate *P. radiata* from many other white-rot species of Polyporales. Strong expression of multiple lignin-modifying LiP and MnP class-II peroxidases, together with H_2O_2 producing oxidoreductases (GLOX, GMCs) and GH6 and GH7 cellobiohydrolases is more similar to the spectrum of CAZymes expressed by *P. chrysosporium* [7, 47]. In another phlebioid clade species, *Phlebiopsis gigantea*, ten genes codifying for class-II peroxidases were identified, but none of these were detected as secreted proteins in pine wood containing cultures [36]. Instead, one DyP (dye-decolorizing peroxidase) was identified in the *P. gigantea* secretome [36]. In our study, the only DyP encoding gene annotated in *P. radiata* genome was detected in the wood transcriptome but not identified in the proteome. These findings pinpoint that each phlebioid species expresses a unique array of CAZy and oxidoreductase enzymes and have an exquisite strategy for colonization and decay of wood.

Preliminary annotation of the *P. radiata* genome assembly revealed ten genes for class-II lignin-modifying peroxidases. Of the four LiPs, the well-characterized LiP3 enzyme [30] was the most abundant protein in the proteome with high expression level on wood, although transcriptionally not as strongly upregulated as LiP2 and LiP1 encoding genes. Three of the *P. radiata* LiP encoding genes (LiP1, LiP3, and LiP4) have been cloned and characterized with the respective transcripts shown to be

expressed by the fungus on milled spruce and alder wood supplemented cultures [24]. Furthermore, LiP1 protein was previously detected in Norway spruce shavings containing bioreactor cultivations of *P. radiata* [48].

Similar to LiP production, variations were observed in this study for expression of the six MnP encoding genes as transcripts and proteins on spruce wood. A novel *P. radiata* long-MnP1 encoding gene was observed as highly upregulated on spruce wood and correspondingly produced in high protein amounts throughout the cultivation. In contrast, of the two previously cloned and characterized *P. radiata* MnPs [25], expression of the long-MnP2 showed an increasing tendency, while the short-MnP3 demonstrated protein decline during the six-week surveillance on wood. This indicates that the multiple class-II lignin-modifying peroxidase encoding genes are differentially regulated in fungi, with some genes being quickly responsive to the wood substrate while transcription of the others may be more subjected to time and fungal growth-dependent regulation.

Previously on solid-state wheat straw lignocellulose cultures of *P. radiata* 79, LiP2 enzyme was detected as one of the major extracellular proteins produced by the fungus together with a few GLOXs [49]. Moreover, LiP and GLOX activities were observed to decline between cultivation days 14 and 28 [49], accordingly as is observed in our present study for the several LiPs indicating a decline in protein abundances in the later stages of the six-week cultivation on spruce wood. Taken together, our results confirm the previous observations for *P. radiata* and indicate synergistic action of GLOXs and LiPs when the fungus is growing on lignocelluloses likewise is reported for *P. chrysosporium* [7, 50, 51].

Together with the CRO glyoxal oxidases of the CAZy family AA5, GMC aryl-alcohol oxidases from CAZy family AA3 may also supply extracellular hydrogen peroxide for the fungal wood decay and class-II peroxidases, and AA3 oxidoreductases may also act as coupled activities to aryl-alcohol dehydrogenases [52]. Both AA3 and AA5 proteins were detected on *P. radiata* spruce wood cultivations together with various other alcohol oxidases and dehydrogenases possibly working as accessory oxidoreductive enzymes and having a role in enhancing attack on wood lignin. Expression of the latter transcripts may be a result of active intracellular modification of lignin metabolites as is reported for *P. chrysosporium* [47].

Laccase activities were measured in our spruce wood cultivation and in previous studies on wood-containing cultures of *P. radiata* [18, 53]. Five laccase encoding genes are recognized in the *P. radiata* genome. However, only one laccase protein, that is the well characterized *P. radiata* Lacc1 [26, 27], was identified in constant but low amounts in the wood proteomes at the time points studied. Lacc1 protein has been repeatedly detected in liquid media and solid lignocellulose cultures of the fungus [49, 53–56] emphasizing its main role in *P. radiata* secretome regardless of the growth substrate and carbon source. The transcriptome revealed that several laccase encoding genes were expressed on wood although *lacc1* gene had clearly the highest transcript abundances. None of the laccase encoding genes, however, was significantly upregulated on wood, which indicates constant expression in particular for *lacc1*.

The constant expression of laccase encoding genes with only one secreted protein may reflect the evolutionary relationship of *P. radiata* and systematic placement in the phlebioid clade of Polyporales. Phlebioid clade includes fungal species completely lacking laccase encoding genes in their genomes, such as *Phanerochaete chrysosporium, Phanerochaete carnosa,* and *Phlebiopsis gigantea* [36, 57, 58]. On the contrary, lignocellulose secretomes of more far-related white-rot fungal species from other systematic clades and orders of Agaricomycetes demonstrate a wider array of laccase proteins, e.g., in *C. subvermispora* (three detected laccases on lignocellulose), *Pleurotus eryngii* (four detected laccases), and *Pleurotus ostreatus* (four detected laccases) [39, 43, 45, 59]. In this respect, the phlebioid white-rot fungi demonstrate their own type of (less or non-laccase dependent) strategies of wood-decay.

In addition to lignin attack, cellulose degradation by white-rot fungi occurs via the combination of several divergent protein families, that is by cellobiohydrolases, LPMOs and CDH [60]. LPMOs from CAZy family AA9 are important in cellulose and hemicellulose degradation [61–63], and they may utilize various electron donors including CDH, haem proteins fused to cellulose-binding module (cytochrome b562-CBM1), or lignocellulose-derived and fungal produced di-phenols [63–65]. In addition, the GMC oxidoreductases, such as glucose oxidase and pyranose dehydrogenase, may participate in the redox system [63]. Transcripts of *P. radiata* encoding LPMOs and the assisting activities were identified on wood. Seven of the twelve annotated LPMO encoding genes were highly expressed and significantly upregulated on wood, and five of these were accordingly identified as peptides in the proteome. Moreover, supporting the oxidative and electron transfer oxidoreductive protein attack on wood generated by fungal produced LPMOs, CDH protein— having variable suggested catalytic roles [66]—was one of the most abundant CAZymes identified in the *P. radiata* wood proteome and was accordingly upregulated in the transcriptome.

Additional enzymes important in fungal carbohydrate metabolism and connected to wood-decay are aldose-1-epimerases (ALE) [67] that generate cellobiose β-anomers, which in turn are reducing substrates

of CDH enzymes. Three putative ALEs were found in the wood proteome of *P. radiata*. One *ale* (gene model minus.g8594) was upregulated in the wood transcriptome. ALE encoding genes are apparently general in wood-decay fungi and identified in white-rot and brown-rot Polyporales genomes [67]. Corresponding peptides were supportively detected in secretomes of *Phanerochaete chrysosporium* but not in *Phlebiopsis gigantea* [13, 33, 63].

To study the effects of hyphal growth on wood on the fungal cell wall reorganization and degradation, the abundances of fungal cell wall degrading proteins during the cultivation were followed together with peptidases. Abundances of these proteins increased over time, thus indicating the need of *P. radiata* to recycle essential nutrients and reorganize the fungal hyphae and cell wall upon growth and colonization of wood. It has been suggested that protease expression is connected to nitrogen acquisition from fungal produced and lignin-linked proteins in the nitrogen-limited wood environment [68–70]. Several other nitrogen metabolism associated transcripts were also upregulated in *P. radiata* on wood including oligopeptide transporters similar to as is observed in *P. chrysosporium* [7], although the corresponding proteins were absent from our proteome samples.

In addition to nutrient cycling and degradation of intracellular proteins, fungal proteases have been suggested to be important for β-1,4-endoglucanase activation [71] and cleavage of the CDH flavin-containing protein domain [72]. Proteases have previously been connected to the decline of extracellular LiP activities in fungal cultures [73, 74]. In this study, the initially very high and upregulated LiP abundances were slowly decreasing as protease abundances were increasing in the *P. radiata* wood proteome, thus indicating that some part of the highly secreted and produced enzymes may be degraded by the fungus' own proteases to recycle the otherwise scarce organic nitrogen pool in the high C/N ratio wood environment. Overall, high peptidase abundances in secretomes of plant biomass-degrading saprotrophic Basidiomycota have been observed [75].

Differences between the abundances of expressed transcripts and detected proteins, and their relation to enzyme activity values at specific time points of the wood cultivation reflect differential and perhaps time-dependent regulation of fungal genes. Alternating processes of gene regulation occurring during (transcriptional regulation) and after transcription (post-transcriptional regulation) may affect the outcome of transcriptomics and proteomics studies. Distinct isoenzyme proteins that are products of individual genes may in turn be active only at certain phase of wood degradation or under specific environmental conditions such as ambient pH [76, 77]. Thus, gene expression analyses, protein detection, and enzymatic activity measurements are not always directly comparable. Moreover, low-molecular-weight proteins, proteins without trypsin cleavage sites or those left intact and attached to the wood matrix, as well as quickly degraded proteins are usually underestimated or lost entirely by peptide LC–MS/MS [39]. However, the clear correlation in time-dependent (higher at the earlier time points) production of proteins with transcript level expression of *P. radiata* genes encoding the various class-II peroxidases indicates strong transcriptional activation of the genes when the fungus is in contact with wood, a natural lignocellulose substrate for hyphal colonization and growth.

After 42 days of wood colonization, it appears that *P. radiata* causes simultaneous decay of spruce xylem components proceeding from the wood cell empty lumen side to secondary cell walls towards primary cell wall and tracheid middle lamellae. This is seen as evident thinning and erosion of the secondary cell walls, together with some erosion of middle lamellae and release of the tracheids. Similar wood-decay pattern is observed for other white-rot Polyporales species on gymnosperm wood [78]. Clear indication of degradation of lignin moieties and release of phenolic compounds during the cultivation period (42 days) was demonstrated by pyrolysis–GC/MS although the gravimetric Klason total lignin content (in relation to wood dry weight) demonstrated a slight increase. This may be explained by the apparent simultaneous degradation of wood cell wall cellulose and other polysaccharides at this stage, thus affecting the ratio of lignin content versus content of wood carbohydrates. Coinciding results were obtained in *P. chrysosporium* cultivations on softwood after 21 days [79].

In a previous study, up to 22 % decrease in Klason lignin content was obtained with the same fungus *P. radiata* 79 after 70 days of cultivation on Norway spruce wood chips [22]. In our study, spruce wood lignin was attacked and degraded during 42 days by *P. radiata* to some extent. Pyrolysis–GC/MS analysis demonstrated decrease in the amount of spruce wood phenylpropane units with concomitant increase in the number of smaller fragmented products from these lignin units, suggesting that especially the upregulated lignin peroxidases were actively attacking and converting the predominant non-phenolic structures of the spruce wood coniferous lignin. Lignin peroxidase LiP3 of *P. radiata* is an efficient oxidizer and degrader of non-phenolic lignin β-O-4 dimeric structures [30, 55]. *P. radiata* short-MnP3 is active against phenolic lignin compounds [29] and in decomposition of pine wood lignin [28]. Increment of phenolic units after fungal growth on lignocellulose was likewise observed in *P. chrysosporium* on pre-treated

biomass [80]. Although chemical and structural evidence of spruce wood lignin decay was obtained with *P. radiata*, it appears that a somewhat longer cultivation time (than 6 weeks) is needed to observe a decrease in total lignin content as well as more dramatic wood ultrastructural changes leading to complete tracheid (wood fiber) separation by degradation of middle lamellae.

Conclusions

It appears that *P. radiata* initiates a strong oxidoreductase and lignin-attacking enzyme expression in contact with wood, which is seen in high transcription upregulation and protein production already during the first weeks upon wood colonization. After this, together with the lignin-attacking and auxiliary oxidoreductases, an array of cellulose and hemicellulose acting GH and CE enzymes is produced, with some changes in protein abundances in the course of the 6 week surveillance and growth on wood. Thus, after the initial lignin-attacking reactivity, at the second stage of wood decay, the *P. radiata* CAZyme repertoire is more targeted against the wood polysaccharides. The change of strategy is most likely to support supply of readily metabolized carbohydrates (sugars) for energy and biosynthetic metabolic processes. After 42 days of wood colonization, the fungal decay is seen as erosion of the wood cell walls with some release of the tracheids, with evident attack on the lignin subunits leading to release of phenolic and lignin-derived fragmented compounds.

In general, transcriptome analysis supported the proteomic results, thus confirming that majority of the identified CAZy encoding transcripts which were upregulated on wood were also present in the proteome. The transcriptome data indicated a pronounced role especially for a few lignin peroxidases (LiP2, LiP3) and manganese peroxidases (MnP1-long, MnP2-long, MnP3-short), various hydrogen peroxidase generating accessory enzymes (GLOX, AA3 AOX), CE acetyl xylan esterase, and lytic polysaccharide monooxygenases (LPMOs), when *P. radiata* is actively colonizing and degrading coniferous spruce wood. In addition, various CAZymes against cellulose, and both glucomannan and xylan type of hemicellulose together with constant expression of pectin-degrading enzymes were detected, all adding up to the impressive repertoire of lignocellulose-attacking enzymes expressed by *P. radiata* upon colonization of spruce wood.

Methods

Fungal strain

Phlebia radiata Fr. (isolate 79, FBCC0043), previously collected in South Finland and isolated from decayed gray alder (*Alnus incana*) wood, was obtained from the HAMBI Fungal Biotechnology Culture Collection (HAMBI-FBCC, fbcc@helsinki.fi) of the University of Helsinki, and cultivated and maintained on 2 % (w/v) malt extract agar plates at 25 °C and in the dark.

Cultivation conditions

For fungal inoculum, *P. radiata* was cultivated in 75 ml liquid 2 % (w/v) malt extract broth, which was inoculated with four mycelium-covered plugs (7 mm in diameter) from malt agar plates, and incubated for 7 days at 25 °C. The inoculum culture was homogenized using Waring blender to initiate either 100 ml portions of liquid 2 % (w/v) malt extract medium or spruce wood cultures by using 2 ml of the homogenized fungal mycelium. The solid wood cultivations contained 2 g (dry weight) of autoclaved Norway spruce (*Picea abies*) wood sticks (dimensions about 25 × 3 × 2 mm) on a 1 % (w/v) water agar with a total moisture content of 60 %. All cultivations were incubated under stationary conditions at 25 °C in the dark for 7–42 days. After cultivation, the fungal colonized wood pieces, and the mycelial mats from the liquid malt extract cultivations were separately harvested and immediately frozen with liquid nitrogen, and stored at −80 °C prior to RNA and protein extractions.

RNA extraction and purification

The frozen samples from two biological replicate wood cultivations (2 and 4 weeks of growth) and mycelial mats (2 weeks of growth on malt extract medium) were used for RNA extraction. The 2-g wood samples were ground under liquid nitrogen with A11 Basic analytical mill (IKA), and total RNA was extracted by CsCl gradient centrifugation method [81]. The quantity and quality of the dialyzed RNA fractions were estimated by using Agilent 2100 Bioanalyzer (Agilent Technologies) with the RNA6000 Nano Assay. Poly-A mRNA was further purified from the RNA fractions of accepted quality using Dynabeads mRNA Purification Kit (Invitrogen) by following manufacturer's instructions. The purified mRNA fractions were quantified by using NanoDrop1000 Spectrophotometer (Thermo Scientific) and Qubit Fluorometer (Thermo Fisher Scientific).

Illumina RNA sequencing and data treatments

From each mRNA fraction, a library was constructed using a TruSeq Stranded mRNA Library Prep Kit according to the manufacturer's instructions (Illumina, Inc.). The libraries were paired-end sequenced using MiSeq (326 + 286 bp) and NextSeq 500 (86 + 74 bp) sequencers (Illumina, Inc.). Pre-processing of the reads was performed with Cutadapt version 1.7.1. Adapters were removed and reads were quality trimmed from the 3′

ends. Only reads that fulfilled the pairing criteria (both R1 and R2 reads present) and were >50 bp in length were included in the analysis.

In average, approximately 93 % of the raw reads were left in each sample after data filtering and cleaning. RNA-seq reads were mapped against gene models of the genomic assembly of *P. radiata* (to be published elsewhere) by STAR aligner version 2.4.1b [82]. Alignments were guided by an annotation file containing the genomic coordinates of gene models predicted by the BRAKER1 software [83]. Resulting alignment files were cleaned using Bamtools.

Aligned reads were counted using HTSeq software [84] guided by the annotation file. Read counts were transformed by variance stabilizing transformation (VST) method after which principal component analysis (PCA) and hierarchical clustering of the samples were performed using DESeq2 package [85]. Differential expression was as well analyzed in DESeq2 package [85]. Significantly differentially expressed genes were identified using thresholds of Benjamini–Hochberg adjusted $p < 0.05$ and log2-fold change ≥ 1 or ≤ -1. HTSeq and DESeq2 analyses as well as construction of the PCA and heatmap were performed in the Chipster platform [86].

Transcripts were functionally annotated by PANNZER software [87] and Blastp (version 2.2.30) searches against the NCBI non-redundant protein sequences database [88]. For visualization and clustering purposes, read counts were transformed by regularized log transformation (rlog) method of the DESeq2 package [85, 86]. Hierarchical clustering and visualization was performed using heatmap.2 function within gplots package of the R environment [89, 90].

Protein extraction and purification

Three parallel fungal cultivations on spruce wood after 7, 14, 21, 28, and 42 days were used for studying the total proteome of *P. radiata*. Spruce wood after adding the inoculum (0 day cultivation) and without the inoculum were used as controls. Spruce sticks from one culture flask (2 g) were ground with A11 Basic analytical mill (IKA) under liquid nitrogen. The milled wood was transferred to 40 ml of 25 mM potassium phosphate buffer (pH 7) containing 0.01 % (v/v) Tween80 and 0.2 mM phenylmethane sulfonyl fluoride (PMSF) as protease inhibitor. This mixture was incubated on a magnetic stirrer for 4 h at 4 °C, and the liquid was separated by filtering through glass fiber filters (GF/C, Whatman) under suction.

After filtration the samples were stored at −20 °C overnight. Thawed samples were precipitated by direct addition of solid trichloroacetic acid (TCA) to 10 % (w/v). Following overnight storage at −20 °C, the precipitate was centrifuged at 5000 g for 15 min at 4 °C, and the pellet was washed three times with cold acetone. To solubilize the air-dried protein pellet, 8.0 M urea was added, followed by overnight mixing and sonication (two times for 1 h). This suspension was centrifuged two times at 21,000 *g* for 15 min, and the supernatant was collected and diluted to a final concentration of 1.5 M urea. The cystein–cystein covalent bonds of the proteins in the samples were reduced with 0.05 M dithiothreitol (Sigma-Aldrich, USA) for 20 min at 37 °C, and then alkylated with 0.15 M iodoacetamide (Fluka, Sigma-Aldrich, USA) at room temperature. Samples were digested by adding 0.75 µg sequencing grade trypsin (Promega, USA), and incubated for overnight at 37 °C. Resulting peptides were purified two times with C18 Microspin columns (Harvard Apparatus) according to the protocol of the manufacturer, and redissolved in 50 µl of A-buffer (0.1 % m/vol TFA (trifluoroacetic acid) in 1 % vol/vol acetonitrile solution in HPLC grade water).

Protein identification by peptide LC–MS/MS

Liquid chromatography coupled to tandem mass spectrometry (LC–MS/MS) analysis was carried out on an EASY-n1000 HPLC (Thermo Fisher Scientific, Germany) connected to a Q Exactive hybrid quadrupole orbitrap mass spectrometer (Thermo Fisher Scientific, Germany) with nano-electrospray ion source (Thermo Fisher Scientific, Germany). The LC–MS/MS samples were separated using a two-column set-up consisting of an Acclaim PepMap 100 pre-column C18, 3 µm, 100 Å; ID 75 µm × 2 cm) and separated with an Acclaim PepMap RSLC analytical column (C18, 2 µm, 100 Å; ID 55 µm × 15 cm (Thermo Fisher Scientific, Germany). The linear separation gradient consisted of 5 % buffer B in 5 min, 35 % buffer B in 60 min, 80 % buffer B in 5 min and 100 % buffer B in 10 min at a flow rate of 0.3 µl/min (buffer A: 0.1 % FA (fluoroacetic acid), 0.01 % TFA in 1 % acetonitrile; buffer B: 0.1 % FA, 0.01 % TFA in 98 % acetonitrile). Peptide samples (100-fold diluted, 2 µl volume) were injected for each LC–MS/MS run and analyzed. Full MS scan was acquired with a resolution of 60,000 at normal mass range in the orbitrap analyzer. The method was set to fragment the 10 most intense precursor ions with higher energy collisional dissociation (energy 28). Data were acquired using Q Exactive Tune software (Thermo Fisher Scientific, Germany).

Proteins were identified and quantified using Andromeda search engine combined with MaxQuant proteomics software [91, 92]. Raw data were searched against the translated coding sequence gene models of *P. radiata* complemented with trypsin and tag sequences. Database searches were limited to fully tryptic peptides with a maximum of two missed cleavages. Cysteine

carbamidomethylation and methionine oxidation were set as fixed and variable modifications, respectively. Error tolerances on the precursor and fragment ions were ± 4.5 ppm and ± 0.5 Da, respectively. Results were filtered to a maximum false discovery rate (FDR) of 0.05. For each spectrum, a propensity score matching (PSM) with high score was retained and these PSMs were further filtered with the cutoff of Andromeda score (>40) and delta score (>8). The peptide FDR was set to <0.01.

Protein quantitation and functional prediction of the proteome

For abundance calculation, mass spectrometric signal intensities (MaxQuant) of peptide precursor ions belonging to each protein were divided by the total abundance of all detected proteins at each time point and for each wood culture. Protein abundance values and their standard deviation were calculated from the normalized values of the three biological replicate cultures. In addition, consistency of the biological replicates was studied by PCA. The abundance values were subjected to arcsin transformation, and PCA was performed with stats package of the R environment and visualized with ggbiplot package [89, 93]. Cellular locations of LC–MS/MS identified proteins being transmembrane, intracellular or extracellular, were analyzed with Phobius predictor [32] together with in silico-predicted secretome, the latter being based on identification of potential secretion signals in the translated protein models corresponding to respective gene models in *P. radiata* genome. Gene ontology (GO) annotations for LC–MS/MS identified proteins were assigned using Blast2GO software [94] and annotations of CAZy-encoding genes were subjected to manual quality control. Peptidases were classified according to Blastp searches against the MEROPS database (http://merops.sanger.ac.uk/ [95]).

Enzyme activity and protein concentration measurements

Enzyme activities and protein concentrations were measured from the solution phase (filtered phosphate buffer with solutes) from above-mentioned proteome samples in which the ground wood samples were incubated before TCA precipitation. Measurements of laccase, manganese peroxidase, xylanase, β-glucosidase, and cellobiohydrolase activities were performed as previously described [18]. Protein concentrations were measured by the BCA Protein Assay (Pierce, Thermo Fisher Scientific, Rockford, USA) according manufacturer's instructions and using bovine serum albumin as reference protein.

Lignin composition analysis of fungal-colonized spruce wood

Similar to the transcriptome and proteome experiments, the solid spruce wood cultures were harvested after 42 days of cultivation, together with reference wood samples (non-inoculated wood sticks without fungus were similarly incubated for 42 days) and dried at 90 °C for 72 h. After this, the dried wood pieces were ground with A11 Basic analytical mill (IKA, Germany) and sieved through a 1-mm particle size metal screen for homogeneity.

Gravimetric (Klason) lignin and acid soluble lignin were analyzed from three biological cultivation and two technical replicate 0.1-g samples. The ground wood samples were mixed with 2 ml of 72 % sulfuric acid (Sigma-Aldrich, Germany) using a magnetic stirrer for 2 h at room temperature. After mixing, the total volume was adjusted to 50 ml with deionized water, and the mixtures were autoclaved at 121 °C, 1 atm, for 30 min. The cooled samples were filtered through 30-ml glass filter crucible (porosity 4, ROBU Glasfilter-Geraete GmbH, Germany) with vacuum suction. The insoluble residue was washed with 35 ml of deionized water and dried in an oven overnight at 90 °C. Filtrates were adjusted to 100 ml with deionized water. The acid soluble lignin was determined spectrophotometrically at 205 nm (absorption coefficient 128 g cm^{-1} l^{-1}, [96]) with Shimadzu Pharma-Spec UV-1700 spectrophotometer. The dry mass of solids was weighted for obtaining the Klason lignin content of the samples.

The same fractions (0.2 g of each) were further ground in a planetary ball mill (Fritsch Planetary Mono Mill Pulverisette, Fritsch GmbH, Germany) using tungsten-carbide cup (29 ml) with four balls. The milling time was 25 min with milling frequency 350 rpm, after which a 20 min pause was introduced to prevent overheating. The cycle was repeated seven times with overall milling time of 5 h. The analytical scale Py–GC/MS equipment Pyrolab2000 (Pyrolab, Sweden) was adopted, and three to four different runs were performed on each sample using a platinum foil pulse pyrolyzer and 580 °C isothermal pyrolysis temperature [97]. The system was directly connected to Bruker Scion SQ 456-GC/MS equipped with Agilent DB-5MS UI (5 %-phenyl)-methylpolysiloxane, 30 m × 0.250 mm × 0.25 μm film) capillary column. The injector temperature was 250 °C, ion source 250 °C with electron ionization of 70 eV, the MS scan range m/z 40–400 and helium as carrier gas at the flow rate of 1 mL/min and 1:20 split ratio. From the base line corrected GC/MS total ion count (TIC) chromatograms, the amount of aromatic degradation products as area was compared to the total area (relative peak areas). The products used in calculations were measured between retention time of 3.04–20 min, and 78 peaks were included in quantification. The samples were treated equally, and the pyrolysis was performed under the same conditions. Products were identified by selected reference compounds with

their retention times and mass spectra, and by comparison with National Institute of Standards and Technology (NIST) library and with literature [97–100].

Electron microscopy of wood decay

Spruce wood sticks from 42 days cultivated solid-state cultures of *P. radiata* were inspected with field emission scanning electron microscopy (FE-SEM) to visually study the fungal hyphal growth in wood, and wood decay processing. Vertical and transverse sections of wood sticks were cut with a sharp blade and fixed according to Ji et al. [43] except that the dehydration was performed with an increasing series of ethanol (from 20 to 98 %, v/v) and acetone (30 to 90 %, v/v). After freeze-drying, the samples were coated with a few nm layer of Au/Pd alloy using a Cressington 208 HR high-resolution sputter coater (Cressington, UK) before imaging with Hitachi S-4800 FE-SEM (Hitachi, Japan).

Additional files

Additional file 1: Table S1. Complete list of gene models, their locations in the genome assembly, transcript counts and normalized abundances, peptide and protein abundances, and functional annotations, of the transcriptome and proteome of *P. radiata* cultivated on spruce wood.

Additional file 2: Figure S1. Principal component analysis A) for the normalized protein abundance values of three biological replicates extracted at the weekly time points (0–6 weeks) from wood cultivations, B) for normalized transcript count values of two RNA-sequencing biological replicates from 2 week time point (2 weeks) of malt extract cultivations and 2 and 4 week (4 weeks) time points of wood cultivations, C) hierarchical clustering of the transcriptome samples according to normalized count values. Ellipses in A) represent general trend of the groups with 68 % confidence interval.

Additional file 3: Figure S2. Protein production and CAZyme activities from protein extracts of the solid-state cultures of *P. radiata* during 6 weeks of growth on spruce wood. Mean values with standard deviations of three biological replicate cultures are presented.

Additional file 4: Figure S3. Number of *P. radiata* CAZy and AA enzyme encoding transcripts, and detected as proteins in the proteome analyses, and upregulated on spruce wood cultivations. Values include all proteins identified in the wood cultivation proteomes by peptide LC–MS/MS analysis. Only proteins with equal or more than two unique peptides were included. Upregulated transcripts: $p < 0.05$ and log2-fold change ≥ 1 at both (2-week and 4-week) time points.

Additional file 5: Table S2. Summary of lignocellulose acting proteins identified in the spruce wood cultivation proteomes of *P. radiata* by peptide LC–MS/MS analysis.

Abbreviations

AA: auxiliary activity enzyme; ALE: aldose-1-epimerase; AOX: alcohol oxidase; CAZy, CAZyme: carbohydrate-active enzyme; CBM: carbohydrate binding module; CDH: cellobiose dehydrogenase; CE: carbohydrate esterase; CRO: copper radical oxidase; DyP: dye-decolorizing peroxidase; FE-SEM: field emission scanning electron microscopy; GC/MS: gas chromatography/mass spectrometry detection; GH: glycoside hydrolase; GLOX: glyoxal oxidase; GMC: glucose–methanol–choline; GO: gene ontology; GT: glycosyltransferase; Lacc: laccase; LPMO: lytic polysaccharide monooxygenase; LiP: lignin peroxidase; MnP: manganese peroxidase; ORF: open reading frame; Ph: phenyl; PL: polysaccharide lyase; TCA: trichloroacetic acid.

Authors' contributions

TL, JK, PA, designed the study. JK, SM, PN, MK, carried out the experiments. OPS, PL, MH, JK, FT, analyzed the data. JK, MH, TL, PN, OPS, PL, PA, interpreted the data. JK, MH, TL, wrote the manuscript. All authors read and approved the final manuscript.

Author details

[1] Microbiology and Biotechnology, Department of Food and Environmental Sciences, University of Helsinki, P.O.Box 56, Viikki Biocenter 1, 00014 Helsinki, Finland. [2] DNA Sequencing and Genomics Laboratory, Institute of Biotechnology, University of Helsinki, Helsinki, Finland. [3] Proteomics Unit, Institute of Biotechnology, University of Helsinki, Helsinki, Finland. [4] Laboratory of Organic Chemistry, Department of Chemistry, University of Helsinki, Helsinki, Finland. [5] Laboratory of Inorganic Chemistry, Department of Chemistry, University of Helsinki, Helsinki, Finland.

Acknowledgements

Ilkka Fagerlund is especially thanked for helping in the RNA extractions, Lars Paulin for expertise in RNA-sequencing, and Markku Varjosalo for valuable advice in proteomics and data analyses.

Competing interests

The authors declare that they have no competing interests.

Availability of supporting data

The datasets supporting the conclusions of this article are included within the article and its additional files.

Consent for publication

Consent was obtained from all the authors of the manuscript for publication.

Funding

This study was financed by the Academy of Finland project Grants No. 138331 (Ox-Red) and 285676 (Fungcolife) to TL. The YEB doctoral school of the University of Helsinki, Doctoral Programme in Microbiology and Biotechnology study position, and Niemi Foundation support for JK are acknowledged.

Received: 11 July 2016 Accepted: 30 August 2016
Published online: 05 September 2016

References

1. Floudas D, Binder M, Riley R, Barry K, Blanchette RA, Henrissat B, et al. The Paleozoic origin of enzymatic lignin decomposition reconstructed from 31 fungal genomes. Science. 2012;336:1715–9.
2. Lundell TK, Mäkelä MR, de Vries RP, Hildén KS. Genomics, lifestyles and future prospects of wood-decay and litter-decomposing Basidiomycota. In: Francis MM, editor. Advances in botanical research. Fungi, vol. 70. London: Academic; 2014. p. 329–70.
3. Riley R, Salamov AA, Brown DW, Nagy LG, Floudas D, Held BW, et al. Extensive sampling of basidiomycete genomes demonstrates inadequacy of the white-rot/brown-rot paradigm for wood decay fungi. Proc Natl Acad Sci USA. 2014;111:9923–8.
4. Eastwood DC, Floudas D, Binder M, Majcherczyk A, Schneider P, Aerts A, et al. The plant cell wall-decomposing machinery underlies the functional diversity of forest fungi. Science. 2011;333:762–5.
5. Hatakka A, Hammel KE. Fungal biodegradation of lignocelluloses. In: Hofrichter M, editor. Industrial applications, the mycota X. 2nd ed. Berlin: Springer; 2010. p. 319–40.
6. Martínez ÁT, Ruiz-Dueñas FJ, Martínez MJ, del Río JC, Gutiérrez A. Enzymatic delignification of plant cell wall: from nature to mill. Curr Opin Biotechnol. 2009;20:348–57.
7. Vanden Wymelenberg A, Gaskell J, Mozuch M, Kersten P, Sabat G, Martinez D, et al. Transcriptome and secretome analyses of *Phanerochaete chrysosporium* reveal complex patterns of gene expression. Appl Environ Microbiol. 2009;75:4058–68.
8. Levasseur A, Drula E, Lombard V, Coutinho PM, Henrissat B. Expansion of the enzymatic repertoire of the CAZy database to integrate auxiliary redox enzymes. Biotechnol Biofuels. 2013;6:41.

9. Ruiz-Dueñas FJ, Lundell T, Floudas D, Nagy LG, Barrasa JM, Hibbett DS, et al. Lignin-degrading peroxidases in Polyporales: an evolutionary survey based on 10 sequenced genomes. Mycologia. 2013;105:1428–44.
10. Hofrichter M, Ullrich R, Pecyna MJ, Liers C, Lundell T. New and classic families of secreted fungal heme peroxidases. Appl Microbiol Biotechnol. 2010;87:871–97.
11. Kersten P, Cullen D. Copper radical oxidases and related extracellular oxidoreductases of wood-decay agaricomycetes. Fungal Genet Biol. 2014;72:124–30.
12. Ferreira P, Carro J, Serrano A, Martínez AT. A survey of genes encoding H_2O_2-producing GMC oxidoreductases in 10 Polyporales genomes. Mycologia. 2015;107:1105–19.
13. Sugano Y. DyP-type peroxidases comprise a novel heme peroxidase family. Cell Mol Life Sci. 2009;66:1387–403.
14. Rytioja J, Hildén K, Yuzon J, Hatakka A, de Vries RP, Mäkelä MR. Plant-polysaccharide-degrading enzymes from Basidiomycetes. Microbiol Mol Biol Rev. 2014;78:614–49.
15. Fernández-Fueyo E, Ruiz-Dueñas FJ, Miki Y, Martínez MJ, Hammel KE, Martínez AT. Lignin-degrading peroxidases from genome of selective ligninolytic fungus *Ceriporiopsis subvermispora*. J Biol Chem. 2012;287:16903–16.
16. Vanden Wymelenberg A, Gaskell J, Mozuch M, BonDurant SS, Sabat G, Ralph J, et al. Significant alteration of gene expression in wood decay fungi *Postia placenta* and *Phanerochaete chrysosporium* by plant species. Appl Environ Microbiol. 2011;77:4499–507.
17. Skyba O, Cullen D, Douglas CJ, Mansfield D. Gene expression patterns of wood decay fungi *Postia placenta* and *Phanerochaete chrysosporium* are influenced by wood substrate composition during degradation. Appl Environ Microbiol. 2016;82:4387–400.
18. Kuuskeri J, Mäkelä MR, Isotalo J, Oksanen I, Lundell T. Lignocellulose-converting enzyme activity profiles correlate with molecular systematics and phylogeny grouping in the incoherent genus *Phlebia* (Polyporales, Basidiomycota). BMC Microbiol. 2015;15:217.
19. Binder M, Justo A, Riley R, Salamov A, Lopez-Giraldez F, Sjökvist E, et al. Phylogenetic and phylogenomic overview of the Polyporales. Mycologia. 2013;105:1350–73.
20. Nakasone KK, Sytsma KJ. Biosystematic studies on *Phlebia acerina*, *P. rufa*, and *P. radiata* in North America. Mycologia. 1993;85:996–1016.
21. Ghobad-Nejhad M, Hallenberg N. Multiple evidence for recognition of *Phlebia tuberculata*, a more widespread segregate of *Phlebia livida* (Polyporales, Basidiomycota). Mycol Prog. 2010;11:27–35.
22. Hakala TK, Maijala P, Konn J, Hatakka A. Evaluation of novel wood-rotting polypores and corticioid fungi for the decay and biopulping of Norway spruce (*Picea abies*) wood. Enzyme Microb Technol. 2004;34:255–63.
23. Peltola A. Finnish statistical yearbook of forestry. Finnish forest research institute. Tampere: Tammerprint Oy; 2014. p. 426.
24. Hildén KS, Mäkelä MR, Hakala TK, Hatakka A, Lundell T. Expression on wood, molecular cloning and characterization of three lignin peroxidase (LiP) encoding genes of the white rot fungus *Phlebia radiata*. Curr Genet. 2006;49:97–105.
25. Hildén K, Martinez AT, Hatakka A, Lundell T. The two manganese peroxidases Pr-MnP2 and Pr-MnP3 of *Phlebia radiata*, a lignin-degrading basidiomycete, are phylogenetically and structurally divergent. Fungal Genet Biol. 2005;42:403–19.
26. Saloheimo M, Niku-Paavola ML, Knowles JK. Isolation and structural analysis of the laccase gene from the lignin-degrading fungus *Phlebia radiata*. J Gen Microbiol. 1991;137:1537–44.
27. Mäkelä MR, Hildén KS, Hakala TK, Hatakka A, Lundell TK. Expression and molecular properties of a new laccase of the white rot fungus *Phlebia radiata* grown on wood. Curr Genet. 2006;50:323–33.
28. Hofrichter M, Lundell T, Hatakka A. Conversion of milled pine wood by manganese peroxidase from *Phlebia radiata*. Appl Environ Microbiol. 2001;67:4588–93.
29. Lundell T, Bentley E, Hildén K, Rytioja J, Kuuskeri J, Ufot UF, et al. Engineering towards catalytic use of fungal class-II peroxidases for dye-decolorizing and conversion of lignin model compounds. Curr Biotechnol. 2016. doi:10.2174/2211550105666160520120101.
30. Lundell T, Wever R, Floris R, Harvey P, Hatakka A, Brunow G, et al. Lignin peroxidase L3 from *Phlebia radiata*. Pre-steady-state and steady-state studies with veratryl alcohol and a non-phenolic lignin model compound 1-(3,4-dimethoxyphenyl)-2-(2-methoxyphenoxy)propane-1,3-diol. Eur J Biochem. 1993;211:391–402.
31. Hildén KS, Bortfeldt R, Hofrichter M, Hatakka A, Lundell TK. Molecular characterization of the basidiomycete isolate *Nematoloma frowardii* b19 and its manganese peroxidase places the fungus in the corticioid genus *Phlebia*. Microbiology. 2008;154:2371–9.
32. Käll L, Krogh A, Sonnhammer ELL. A combined transmembrane topology and signal peptide prediction method. J Mol Biol. 2004;338:1027–36.
33. Manavalan A, Adav SS, Sze SK. ITRAQ-based quantitative secretome analysis of *Phanerochaete chrysosporium*. J Proteomics. 2011;75:642–54.
34. Gaskell J, Marty A, Mozuch M, Kersten PJ, Splinter BonDurant S, Sabat G, et al. Influence of *Populus* genotype on gene expression by the wood decay fungus *Phanerochaete chrysosporium*. Appl Environ Microbiol. 2014;80:5828–35.
35. Mahajan S, Master ER. Proteomic characterization of lignocellulose-degrading enzymes secreted by *Phanerochaete carnosa* grown on spruce and microcrystalline cellulose. Appl Microbiol Biotechnol. 2010;86:1903–14.
36. Hori C, Ishida T, Igarashi K, Samejima M, Suzuki H, Master E, et al. Analysis of the *Phlebiopsis gigantea* genome, transcriptome and secretome provides insight into its pioneer colonization strategies of wood. PLoS Genet. 2014;10:e1004759.
37. Salvachúa D, Martínez AT, Tien M, López-Lucendo MF, García F, de Los Ríos V, et al. Differential proteomic analysis of the secretome of *Irpex lacteus* and other white-rot fungi during wheat straw pretreatment. Biotechnol Biofuels. 2013;6:115.
38. Manavalan T, Manavalan A, Thangavelu KP, Heese K. Secretome analysis of *Ganoderma lucidum* cultivated in sugarcane bagasse. J Proteomics. 2012;77:298–309.
39. Hori C, Gaskell J, Igarashi K, Kersten P, Mozuch M, Samejima M, et al. Temporal alterations in the secretome of the selective ligninolytic fungus *Ceriporiopsis subvermispora* during growth on aspen wood reveal this organism's strategy for degrading lignocellulose. Appl Environ Microbiol. 2014;80:2062–70.
40. Zhu N, Liu J, Yang J, Lin Y, Yang Y, Ji L, et al. Comparative analysis of the secretomes of *Schizophyllum commune* and other wood-decay basidiomycetes during solid–state fermentation reveals its unique lignocellulose–degrading enzyme system. Biotechnol Biofuels. 2016;9:42.
41. Levasseur A, Lomascolo A, Chabrol O, Ruiz-Dueñas FJ, Boukhris-Uzan E, Piumi F, et al. The genome of the white-rot fungus *Pycnoporus cinnabarinus*: a basidiomycete model with a versatile arsenal for lignocellulosic biomass breakdown. BMC Genomics. 2014;15:486.
42. Couturier M, Navarro D, Chevret D, Henrissat B, Piumi F, Ruiz-Dueñas FJ, et al. Enhanced degradation of softwood versus hardwood by the white-rot fungus *Pycnoporus coccineus*. Biotechnol Biofuels. 2015;8:216.
43. Ji XL, Zhang WT, Gai YP, Lu BY, Yuan CZ, Liu QX, et al. Patterns of lignocellulose degradation and secretome analysis of *Trametes trogii* MT. Int Biodeterior Biodegrad. 2012;75:55–62.
44. Alfaro M, Castanera R, Lavín JL, Grigoriev IV, Oguiza JA, Ramírez L, et al. Comparative and transcriptional analysis of the predicted secretome in the lignocellulose-degrading basidiomycete fungus *Pleurotus ostreatus*. Environ Microbiol. 2016. doi:10.1111/1462-2920.13360.
45. Fernández-Fueyo E, Ruiz-Dueñas FJ, López-Lucendo MF, Pérez-Boada M, Rencoret J, Gutiérrez A, et al. A secretomic view of woody and non-woody lignocellulose degradation by *Pleurotus ostreatus*. Biotechnol Biofuels. 2016;9:49.
46. Floudas D, Held BW, Riley R, Nagy LG, Koehler G, Ransdell AS, et al. Evolution of novel wood decay mechanisms in Agaricales revealed by the genome sequences of *Fistulina hepatica* and *Cylindrobasidium torrendii*. Fungal Genet Biol. 2015;76:78–92.
47. Korripally P, Hunt CG, Houtman CJ, Jones DC, Kitin PJ, Cullen D, et al. Regulation of gene expression during the onset of ligninolytic oxidation by *Phanerochaete chrysosporium* on spruce wood. Appl Environ Microbiol. 2015;81:7802–12.
48. Niku-Paavola M-L, Karhunen E, Kantelinen A, Viikari L, Lundell T, Hatakka A. The effect of culture conditions on the production of lignin modifying enzymes by the white-rot fungus *Phlebia radiata*. J Biotechnol. 1990;13:211–21.

49. Vares T, Kalsi M, Hatakka A. Lignin peroxidases, manganese peroxidases, and other ligninolytic enzymes produced by *Phlebia radiata* during solid-state fermentation of wheat straw. Appl Environ Microbiol. 1995;61:3515–20.
50. Kersten PJ. Glyoxal oxidase of *Phanerochaete chrysosporium*: its characterization and activation by lignin peroxidase. Proc Natl Acad Sci USA. 1990;87:2936–40.
51. Hammel K, Mozuch MD, Jensen KA, Kersten PJ. Recycling during oxidation of the arylglycerol p-aryl ether lignin structure. Biochemistry. 1994;33:13349–54.
52. Hernández-Ortega A, Ferreira P, Martínez AT. Fungal aryl-alcohol oxidase: a peroxide-producing flavoenzyme involved in lignin degradation. Appl Microbiol Biotechnol. 2012;93:1395–410.
53. Mäkelä MR, Lundell T, Hatakka A, Hildén K. Effect of copper, nutrient nitrogen, and wood-supplement on the production of lignin-modifying enzymes by the white-rot fungus *Phlebia radiata*. Fungal Biol. 2013;117:62–70.
54. Niku-Paavola ML, Karhunen E, Salola P, Raunio V. Ligninolytic enzymes of the white-rot fungus *Phlebia radiata*. Biochem J. 1988;254:877–83.
55. Lundell T, Hatakka A. Participation of Mn(II) in the catalysis of laccase, manganese peroxidase and lignin peroxidase from *Phlebia radiata*. FEBS Lett. 1994;348:291–6.
56. Lundell T, Leonowicz A, Rogalski J, Hatakka A. Formation and action of lignin-modifying enzymes in cultures of *Phlebia radiata* supplemented with veratric acid. Appl Environ Microbiol. 1990;56:2623–9.
57. Martinez D, Larrondo LF, Putnam N, Gelpke MDS, Huang K, Chapman J, et al. Genome sequence of the lignocellulose degrading fungus *Phanerochaete chrysosporium* strain RP78. Nat Biotechnol. 2004;22:695–700.
58. Suzuki H, MacDonald J, Syed K, Salamov A, Hori C, Aerts A, et al. Comparative genomics of the white-rot fungi, *Phanerochaete carnosa* and *P. chrysosporium*, to elucidate the genetic basis of the distinct wood types they colonize. BMC Genomics. 2012;13:444.
59. Xie C, Luo W, Li Z, Yan L, Zhu Z, Wang J, et al. Secretome analysis of *Pleurotus eryngii* reveals enzymatic composition for ramie stalk degradation. Electrophoresis. 2016;37:310–20.
60. Langston JA, Shaghasi T, Abbate E, Xu F, Vlasenko E, Sweeney MD. Oxidoreductive cellulose depolymerization by the enzymes cellobiose dehydrogenase and glycoside hydrolase 61. Appl Environ Microbiol. 2011;77:7007–15.
61. Vaaje-Kolstad G, Westereng B, Horn SJ, Liu Z, Zhai H, Sørlie M, et al. An Oxidative enzyme boosting the enzymatic conversion of recalcitrant polysaccharides. Science. 2010;330:219–22.
62. Agger JW, Isaksen T, Várnai A, Vidal-Melgosa S, Willats WGT, Ludwig R, et al. Discovery of LPMO activity on hemicelluloses shows the importance of oxidative processes in plant cell wall degradation. Proc Natl Acad Sci USA. 2014;111:6287–92.
63. Kracher D, Scheiblbrandner S, Felice AKG, Breslmayr E, Preims M, Haltrich D, et al. Extracellular electron transfer systems fuel cellulose oxidative degradation. Science. 2016;3165:1–13.
64. Courtade G, Wimmer R, Røhr ÅK, Preims M, Felice AKG, Dimarogona M, et al. Interactions of a fungal lytic polysaccharide monooxygenase with β-glucan substrates and cellobiose dehydrogenase. Proc Natl Acad Sci USA. 2016;113:5922–7.
65. Yoshida M, Igarashi K, Wada M, Kaneko S, Suzuki N, Matsumura H, et al. Characterization of carbohydrate-binding cytochrome b 562 from the white-rot fungus *Phanerochaete chrysosporium*. Appl Environ Microbiol. 2005;71:4548–55.
66. Henriksson G, Johansson G, Pettersson G. A critical review of cellobiose dehydrogenases. J Biotechnol. 2000;78:93–113.
67. Hori C, Gaskell J, Igarashi K, Samejima M, Hibbett D, Henrissat B, et al. Genomewide analysis of polysaccharides degrading enzymes in 11 white- and brown-rot Polyporales provides insight into mechanisms of wood decay. Mycologia. 2013;105:1412–27.
68. Vanden Wymelenberg A, Sabat G, Martinez D, Rajangam AS, Teeri TT, Gaskell J, et al. The *Phanerochaete chrysosporium* secretome: database predictions and initial mass spectrometry peptide identifications in cellulose-grown medium. J Biotechnol. 2005;118:17–34.
69. Sato S, Liu F, Koc H, Tien M. Expression analysis of extracellular proteins from *Phanerochaete chrysosporium* grown on different liquid and solid substrates. Microbiology. 2007;153:3023–33.
70. Keller B, Templeton MD, Lamb CJ. Specific localization of a plant cell wall glycine-rich protein in protoxylem cells of the vascular system. Proc Natl Acad Sci USA. 1989;86:1529–33.
71. Eriksson KE, Pettersson B. Purification and partial characterization of two acidic proteases from the white-rot fungus *Sporotrichum pulverulentum*. Eur J Biochem. 1982;124:635–42.
72. Habu N, Samejima M, Dean JFD, Eriksson KEL. Release of the FAD domain from cellobiose oxidase by proteases from cellulolytic cultures of *Phanerochaete chrysosporium*. FEBS Lett. 1993;327:161–4.
73. Dosoretz CG, Chen H, Grethlein HE. Effect of environmental conditions on extracellular protease activity in ligninolytic cultures of *Phanerochaete chrysosporium*. Appl Environ Microbiol. 1990;56:395–400.
74. Dosoretz CG, Dass SB, Reddy CA, Grethlein HE. Protease-mediated degradation of lignin peroxidase in liquid cultures of *Phanerochaete chrysosporium*. Appl Environ Microbiol. 1990;56:3429–34.
75. Alfaro M, Oguiza JA, Ramírez L, Pisabarro AG. Comparative analysis of secretomes in basidiomycete fungi. J Proteomics. 2014;102:28–43.
76. Adav SS, Ravindran A, Chao LT, Tan L, Singh S, Sze SK. Proteomic analysis of pH and strains dependent protein secretion of *Trichoderma reesei*. J Proteome Res. 2011;10:4579–96.
77. Häkkinen M, Sivasiddarthan D, Aro N, Saloheimo M, Pakula TM. The effects of extracellular pH and of the transcriptional regulator PACI on the transcriptome of *Trichoderma reesei*. Microb Cell Fact. 2015;14:63.
78. Eriksson KE, Blanchette RA, Ander P. Microbial and enzymatic degradation of wood and wood components. Berlin: Springer-Verlag; 1990. p. 407.
79. Ravalason H, Jan G, Mollé D, Pasco M, Coutinho PM, Lapierre C, et al. Secretome analysis of *Phanerochaete chrysosporium* strain CIRM-BRFM41 grown on softwood. Appl Microbiol Biotechnol. 2008;80:719–33.
80. Singh D, Zeng J, Laskar DD, Deobald L, Hiscox WC, Chen S. Investigation of wheat straw biodegradation by *Phanerochaete chrysosporium*. Biomass Bioenergy. 2011;35:1030–40.
81. Patyshakuliyeva A, Mäkelä MR, Sietiö O-M, de Vries RP, Hildén KS. An improved and reproducible protocol for the extraction of high quality fungal RNA from plant biomass substrates. Fungal Genet Biol. 2014;72:201–6.
82. Dobin A, Davis CA, Schlesinger F, Drenkow J, Zaleski C, Jha S, et al. STAR: ultrafast universal RNA-seq aligner. Bioinformatics. 2013;29:15–21.
83. Hoff KJ, Lange S, Lomsadze A, Borodovsky M, Stanke M. BRAKER1: unsupervised RNA-Seq-based genome annotation with GeneMark-ET and AUGUSTUS. Bioinformatics. 2015;32:767–9.
84. Anders S, Pyl PT, Huber W. HTSeq-A Python framework to work with high-throughput sequencing data. Bioinformatics. 2015;31:166–9.
85. Love MI, Huber W, Anders S. Moderated estimation of fold change and dispersion for RNA-seq data with DESeq2. Genome Biol. 2014;15:550.
86. Kallio MA, Tuimala JT, Hupponen T, Klemelä P, Gentile M, Scheinin I, et al. Chipster: user-friendly analysis software for microarray and other high-throughput data. BMC Genomics. 2011;12:507.
87. Koskinen P, Törönen P, Nokso-Koivisto J, Holm L. PANNZER: high-throughput functional annotation of uncharacterized proteins in an error-prone environment. Bioinformatics. 2014;31:1544–52.
88. Altschul SF, Madden TL, Schaffer AA, Zhang J, Zhang Z, Miller W, et al. Gapped BLAST and PSI-BLAST: a new generation of protein database search programs. Nucleic Acids Res. 1997;25:3389–402.
89. R Core Team. R: a language and environment for statistical computing. Vienna: R foundation for statistical computing; 2015. http://www.r-project.org/. Accessed 18 Aug 2016.
90. Warnes GR, Bolker B, Bonebakker L, Gentleman R, Liaw WHA, Lumley T, et al. gplots: various R programming tools for plotting data. 2015. https://www.cran.r-project.org/package=gplots. Accessed 18 Aug 2016.
91. Cox J, Mann M. MaxQuant enables high peptide identification rates, individualized p.p.b.-range mass accuracies and proteome-wide protein quantification. Nat Biotechnol. 2008;26:1367–72.
92. Cox J, Neuhauser N, Michalski A, Scheltema RA, Olsen JV, Mann M. Andromeda: a peptide search engine integrated into the MaxQuant environment. J Proteome Res. 2011;10:1794–805.
93. Vu VQ. Ggbiplot: A ggplot2 based biplot. R package version 0.55. 2011. http://www.github.com/vqv/ggbiplot. Accessed 18 Aug 2016.

94. Conesa A, Götz S, García-Gómez JM, Terol J, Talón M, Robles M. Blast2GO: a universal tool for annotation, visualization and analysis in functional genomics research. Bioinformatics. 2005;21:3674–6.
95. Rawlings ND, Barrett AJ, Finn R. Twenty years of the MEROPS database of proteolytic enzymes, their substrates and inhibitors. Nucleic Acids Res. 2016;44:343–50.
96. Iakovlev M, van Heiningen A. SO_2-ethanol-water (SEW) pulping: I. Lignin determination in pulps and liquors. J Wood Chem Technol. 2011;31:233–49.
97. Ohra-Aho T, Tenkanen M, Tamminen T. Direct analysis of lignin and lignin-like components from softwood kraft pulp by Py-GC/MS techniques. J Anal Appl Pyrolysis. 2005;74:123–8.
98. Alves A, Schwanninger M, Pereira H, Rodrigues J. Analytical pyrolysis as a direct method to determine the lignin content in wood: Part 1: Comparison of pyrolysis lignin with Klason lignin. J Anal Appl Pyrolysis. 2006;76:209–13.
99. Gu X, Ma X, Li L, Liu C, Cheng K, Li Z. Pyrolysis of poplar wood sawdust by TG-FTIR and Py-GC/MS. J Anal Appl Pyrolysis. 2013;102:16–23.
100. Lupoi JS, Singh S, Parthasarathi R, Simmons BA, Henry RJ. Recent innovations in analytical methods for the qualitative and quantitative assessment of lignin. Renew Sustain Energ Rev. 2015;49:871–906.

Recent Publications in this Series

3/2016 Stiina Rasimus-Sahari
Effects of Microbial Mitochondriotoxins from Food and Indoor Air on Mammalian Cells
4/2016 Hany S.M. EL Sayed Bashandy
Flavonoid Metabolomics in *Gerbera hybrida* and Elucidation of Complexity in the Flavonoid Biosynthetic Pathway
5/2016 Erja Koivunen
Home-Grown Grain Legumes in Poultry Diets
6/2016 Paul Mathijssen
Holocene Carbon Dynamics and Atmospheric Radiative Forcing of Different Types of Peatlands in Finland
7/2016 Seyed Abdollah Mousavi
Revised Taxonomy of the Family *Rhizobiaceae*, and Phylogeny of Mesorhizobia Nodulating *Glycyrrhiza spp*.
8/2016 Sedeer El-Showk
Auxin and Cytokinin Interactions Regulate Primary Vascular Patterning During Root Development in *Arabidopsis thaliana*
9/2016 Satu Olkkola
Antimicrobial Resistance and Its Mechanisms among *Campylobacter coli* and *Campylobacter upsaliensis* with a Special Focus on Streptomycin
10/2016 Windi Indra Muziasari
Impact of Fish Farming on Antibiotic Resistome and Mobile Elements in Baltic Sea Sediment
11/2016 Kari Kylä-Nikkilä
Genetic Engineering of Lactic Acid Bacteria to Produce Optically Pure Lactic Acid and to Develop a Novel Cell Immobilization Method Suitable for Industrial Fermentations
12/2016 Jane Etegeneng Besong epse Ndika
Molecular Insights into a Putative Potyvirus RNA Encapsidation Pathway and Potyvirus Particles as Enzyme Nano-Carriers
13/2016 Lijuan Yan
Bacterial Community Dynamics and Perennial Crop Growth in Motor Oil-Contaminated Soil in a Boreal Climate
14/2016 Pia Rasinkangas
New Insights into the Biogenesis of *Lactobacillus rhamnosus GG* Pili and the *in vivo* Effects of Pili
15/2016 Johanna Rytioja
Enzymatic Plant Cell Wall Degradation by the White Rot Fungus *Dichomitus squalens*
16/2016 Elli Koskela
Genetic and Environmental Control of Flowering in Wild and Cultivated Strawberries
17/2016 Riikka Kylväjä
Staphylococcus aureus and *Lactobacillus crispatus*: Adhesive Characteristics of Two Gram-Positive Bacterial Species
18/2016 Hanna Aarnos
Photochemical Transformation of Dissolved Organic Matter in Aquatic Environment – From a Boreal Lake and Baltic Sea to Global Coastal Ocean
19/2016 Riikka Puntila
Trophic Interactions and Impacts of Non-Indigenous Species in the Baltic Sea Coastal Ecosystems

Helsinki 2016 **ISSN 2342-5423** **ISBN 978-951-51-2419-7**